

AD-A205 318

IDA PAPER P-2004

**IDA GAMMA-RAY LASER
ANNUAL SUMMARY REPORT (1986)
INVESTIGATION OF THE FEASIBILITY OF
DEVELOPING A LASER USING NUCLEAR TRANSITIONS**

***Bohdan Balko
Leslie Cohen
David A. Sparrow
Editors***

December 1988

***Prepared for
Strategic Defense Initiative Organization
Innovative Science and Technology Office***

***James Ionson, Director
Dwight Duston, Deputy Director***

**DTIC
ELECTE
MAR 13 1989
S H D**

DISTRIBUTION STATEMENT A

**Approved for public release;
Distribution Unlimited**



**INSTITUTE FOR DEFENSE ANALYSES
1801 N. Beauregard Street, Alexandria, Virginia 22311-1772**

89 3 10 005

DEFINITIONS

IDA publishes the following documents to report the results of its work.

Reports

Reports are the most authoritative and most carefully considered products IDA publishes. They normally embody results of major projects which (a) have a direct bearing on decisions affecting major programs, or (b) address issues of significant concern to the Executive Branch, the Congress and/or the public, or (c) address issues that have significant economic implications. IDA Reports are reviewed by outside panels of experts to ensure their high quality and relevance to the problems studied, and they are released by the President of IDA.

Papers

Papers normally address relatively restricted technical or policy issues. They communicate the results of special analyses, interim reports or phases of a task, ad hoc or quick reaction work. Papers are reviewed to ensure that they meet standards similar to those expected of refereed papers in professional journals.

Memorandum Reports

IDA Memorandum Reports are used for the convenience of the sponsors or the analysts to record substantive work done in quick reaction studies and major interactive technical support activities; to make available preliminary and tentative results of analyses or of working group and panel activities; to forward information that is essentially unanalyzed and unevaluated; or to make a record of conferences, meetings, or briefings, or of data developed in the course of an investigation. Review of Memorandum Reports is suited to their content and intended use.

The results of IDA work are also conveyed by briefings and informal memoranda to sponsors and others designated by the sponsors, when appropriate.

The work reported in this document was conducted under contract MDA 963 84 C 8831 for the Department of Defense. The publication of this IDA document does not indicate endorsement by the Department of Defense, nor should the contents be construed as reflecting the official position of that agency.

This paper has been reviewed by IDA to assure that it meets high standards of thoroughness, objectivity, and sound analytical methodology and that the conclusions stem from the methodology.

Approved for public release: distribution unlimited.

UNCLASSIFIED

SECURITY CLASSIFICATION OF THIS PAGE

REPORT DOCUMENTATION PAGE

1a. REPORT SECURITY CLASSIFICATION UNCLASSIFIED			1b. RESTRICTIVE MARKINGS		
2a. SECURITY CLASSIFICATION AUTHORITY NA			3. DISTRIBUTION/AVAILABILITY OF REPORT Approved for public release; distribution unlimited.		
2b. DECLASSIFICATION/DOWNGRADING SCHEDULE NA					
4. PERFORMING ORGANIZATION REPORT NUMBER(S) IDA Paper P-2004			5. MONITORING ORGANIZATION REPORT NUMBER(S)		
6a. NAME OF PERFORMING ORGANIZATION Institute for Defense Analyses		6b. OFFICE SYMBOL (if applicable) STD	7a. NAME OF MONITORING ORGANIZATION DoD-IDA Management Office, OUSD(A)		
6c. ADDRESS (City, State, and Zip Code) 1801 N. Beauregard Street Alexandria, VA 22311			7b. ADDRESS (CITY, STATE, AND ZIP CODE) 1801 N. Beauregard Street Alexandria, VA 22311		
8a. NAME OF FUNDING/SPONSORING ORGANIZATION Strategic Defense Initiative Organization		8b. OFFICE SYMBOL (if applicable)	9. PROCUREMENT INSTRUMENT IDENTIFICATION NUMBER MDA 903 84 C 0031		
8c. ADDRESS (City, State, and Zip Code) The Pentagon Washington, DC 20301-7100			10. SOURCE OF FUNDING NUMBERS		
			PROGRAM ELEMENT	PROJECT NO.	TASK NO. T-R2-316
					WORK UNIT ACCESSION NO.
11. TITLE (Include Security Classification) IDA Gamma-Ray Laser Annual Summary Report (1986): Investigation of the Feasibility of Developing a Laser Using Nuclear Transitions					
12. PERSONAL AUTHOR(S) Bohdan Balko, Leslie Cohen, and David Sparrow, Editors					
13. TYPE OF REPORT Final		13b. TIME COVERED FROM 10/1/85 TO 9/30/86		14. DATE OF REPORT (Year, Month, Day) December 1988	
15. PAGE COUNT 256					
16. SUPPLEMENTARY NOTATION					
17. COSATI CODES			18. SUBJECT TERMS (Continue on reverse if necessary and identify by block number)		
FIELD	GROUP	SUB-GROUP	Nuclear Laser, Gamma-ray laser, Graser, Superradiance, Mössbauer effect, Borrmann effect, Dressed nuclear states, Nuclear isomers, Nuclear data, Nuclear structure, Multiphoton excitation, Atomic shielding of nuclei, Electron nucleon energy transfer.		
19. ABSTRACT (Continue on reverse if necessary and identify by block number)					
This report summarizes the IDA research effort in FY 1986 in investigating the feasibility of developing a Y-ray laser.					
20. DISTRIBUTION/AVAILABILITY OF ABSTRACT <input type="checkbox"/> UNCLASSIFIED/UNLIMITED <input checked="" type="checkbox"/> SAME AS RPT. <input type="checkbox"/> DTIC USERS			21. ABSTRACT SECURITY CLASSIFICATION UNCLASSIFIED		
22a. NAME OF RESPONSIBLE INDIVIDUAL Bohdan Balko			22b. TELEPHONE (Include Area Code) (703) 578-2991		22c. OFFICE SYMBOL

IDA PAPER P-2004

***IDA GAMMA-RAY LASER
ANNUAL SUMMARY REPORT (1986)
INVESTIGATION OF THE FEASIBILITY OF
DEVELOPING A LASER USING NUCLEAR TRANSITIONS***

*Bohdan Balko
Leslie Cohen
David A. Sparrow
Editors*

December 1988



INSTITUTE FOR DEFENSE ANALYSES

*Contract MDA 903 84 C 0031
Task T-R2-316*

PREFACE

In January 1985, Dr. James A. Ionson, then Director of the Science and Technology Directorate of SDIO, asked the research staff at IDA to investigate the feasibility of developing a gamma-ray laser. The staff responded first by determining what work had been done, who was currently working in the field, and what work should be encouraged or supported. This was accomplished by convening a workshop for research workers directly involved in gamma-ray laser work and others involved in ancillary fields such as nuclear structure, radiation propagation in crystals, Mössbauer Effect, and optical lasers. The proceedings of the workshop are presented in IDA Report M-162 (Ref. 1).

Next, a study was undertaken to clarify critical issues concerning the various pumping schemes proposed at the workshop as well as systems questions about the gamma-ray laser as a working device. The work completed in 1985 is presented in IDA Report P-2021 (Ref. 2).

The development of a γ -ray laser is viewed as a high-risk/high-payoff undertaking. IDA's involvement focuses on minimizing that risk and on striving to redirect the effort when proposed schemes are shown not to be feasible.

Most recently, work has focused on extending the data base, on exploring the nature of superradiance in the gamma-ray laser context, and on undertaking a detailed investigation of the upconversion pumping scheme. A study of nuclear systematics, an investigation of electron-nuclear driven pumping, and a discussion of the uncertainty principle lifetime measurement and its impact on the long lifetime concept round out the effort and are discussed in this report.

This report does not have an overall introduction. Each of the seven chapters is an independent study containing its own introduction.

ABSTRACT

This report summarizes the IDA research effort in FY 1986 in investigating the feasibility of developing a γ -ray laser.

Accession For	
NTIS GRA&I	<input checked="checked" type="checkbox"/>
DTIC TAB	<input type="checkbox"/>
Unannounced	<input type="checkbox"/>
Justification	
By	
Distribution/	
Availability Codes	
Dist	Avail and/or Special
A-1	



CONTENTS

Preface	iii
Abstract	v
List of Figures	xi
List of Tables	xvii
Summary	S-1
I. SEARCH FOR NUCLEAR LEVELS FOR GAMMA-RAY LASERS:	
Table of Selected Nuclear Transitions (Isomers with Closely-Spaced Levels)-- Agda Artna-Cohen	1
A. Introduction	1
B. Scope	1
C. Sources	1
D. Explanation of Table	1
1. The Isomer	2
2. Upconversion	2
3. Deexciting Transitions	2
4. Upper Level	3
5. Lower Level	3
II. SYMMETRY APPROACH TO ENHANCED SPONTANEOUS DECAY OF NUCLEI--Francis X. Hartmann	
A. Introduction	17
B. Group Approach to Dicke Superradiance	19
1. Objectives	19
2. Summary of the Theory and Aspects of Mixed-Symmetry States	20
C. Dicke Superradiance for the Case of the Totally Symmetric Multiplet-- Statistical Models	24
1. Characteristics of Pulses	24
2. Expressions for the Pulse Duration Time	28
3. Empirical Estimates for Practical Values of the Cooperation Number	30
D. Enhanced Spontaneous Decay in the Presence of External or Self-Created Radiation Fields	30
1. Background for Dicke Superradiator Models	31
2. The Simple Superradiance Limit	31

3. Simple Superradiator in a Cavity	31
4. Simple Superradiance in Fields Which Emit--Markovian Model	33
5. Simple Superradiance in Fields Which Emit--non-Markovian Model	34
E. Conditions for Gamma-Ray Enhanced Decay Rates	39
1. Effective Gain	40
2. Condition for Gamma-Ray Superradiance.....	41
3. Size of a Gamma-Ray Superradiator	42
F. Comment on Cooperation, Causality and Violation of Microscopic Causality	43
G. Conclusions.....	45
III. EVALUATION AND COMPARISON OF SUPERRADIANT MODELS-- Irvin W. Kay, Bohdan Balko, John Neuberger	47
A. Introduction	47
B. The Bonifacio-Lugiato Model for Superradiance.....	49
1. General Characteristics of the Model	49
2. Comparison with the Feld-McGillivray Model.....	52
3. Validity of the Semi-Classical Approximation	53
C. Calculated Results.....	57
D. Conclusions.....	73
Acknowledgments	73
IV. MULTIPHOTON DEEXCITATION OF ISOMERIC LEVELS-- Bohdan Balko, David A. Sparrow, S. Dixit	75
A. Introduction	75
B. Comparison of Atomic and Nuclear Electromagnetic Transitions	77
C. Multiphoton Effects on Atomic and Nuclear Systems	84
D. Conclusions.....	97
V. AN INVESTIGATION INTO SOME PROBLEMS IN THE DEVELOPMENT OF GAMMA-RAY LASERS: ATOMIC SHIELDING OF NUCLEI AND UPCONVERSION BY MASSIVE PARTICLES-- K.A. Brueckner.....	99
A. Introduction	99
B. Isomer Decay	99
C. Pumping Transition	100
D. Pumping Requirements.....	101
E. Search for Candidate Isomers	102
1. Isomer Excitation in Collisions.....	102
2. Isomer Decay Induced by Atomic Electrons	105

VI. INVESTIGATION OF ENERGY TRANSFER TO NUCLEI THROUGH ELECTRON NUCLEAR COUPLING-- Donald W. Noid, Francis X. Hartmann, Leslie Cohen, Bohdan Balko	109
A. Introduction	109
B. The Semi-Classical Method	110
C. Results	113
D. Conclusions	118
VII. A NUCLEAR LIFETIME MEASUREMENT--AN UNCERTAINTY PRINCIPLE--Leslie Cohen	119
References	123
APPENDIX A-- Symmetry in Spontaneous Decay--Background Information	A-1
APPENDIX B-- Introduction to Enhanced Spontaneous Decay Theory	B-1
APPENDIX C-- Brief Overview of Semiclassical Approximations to the Group Theoretical Approach to Superradiance	C-1
APPENDIX D-- Resonances in the Approximate Bonifacio-Lugiato Model	D-1
APPENDIX E-- The Code SR1.FOR	E-1
APPENDIX F-- The Code SR2.FOR	F-1
APPENDIX G-- Codes SR3.FOR and SR4.FOR	G-1
APPENDIX H-- Equivalence of the Semiclassical and the Dressed State Approaches to the Treatment and Interaction of Atomic and Nuclear Systems	H-1
APPENDIX I-- Enhancement of γ -Emission Using Long-Wavelength Radiation	I-1
APPENDIX J-- Listing of Multiphoton Upconversion Code GAMMAP	J-1
APPENDIX K-- Program PNP (Name List and Code Listing)	K-1
APPENDIX L-- Program NP2 (Name List and Code Listing)	L-1
APPENDIX M-- Program NEC (Name List and Code Listing)	M-1

FIGURES

Figure 1.	The eight states of the three-particle system illustrate the classification of states according to the permutation group tableaux, the cooperation number (r), and the inversion (m). The symmetric multiplet is associated with Dicke superradiance. Mixed symmetry states would have subradiant or reduced decay rates corresponding to a Bloch vector of diminished length	21
Figure 2.	Decay rates for the multiplets illustrated in Fig. 1 according to Dicke's theory. The rates are listed as multiples of the spontaneous decay rate (e.g., 3X means three-times faster, etc.)	21
Figure 3.	Detrimental effects in pumping. Realistic effects, as discussed in the text, can mix r -multiplets (ruining the ideal symmetry) and thus allow some transitions between multiplets. Some of those transitions are illustrated here where the system is being pumped up. The same intra-band transitions also occur in deexcitation	23
Figure 4.	Three statistical pulses and one most probable pulse are based on a computer simulation for a small value of r	25
Figure 5.	A typical pulse shape for $r = 8192$	26
Figure 6.	Pulse duration as function of r from the statistical simulations, assuming a spontaneous lifetime of 1 s	26
Figure 7.	The $1/r$ dependence of the pulse duration (assuming a spontaneous lifetime of 1 s) shows the crude $1/N$ dependence inherent in superradiance	27
Figure 8.	A blowup of the high r region on Fig. 7 depicting the near-linear behavior for larger values of the cooperation number	27
Figure 9.	Behavior of the scaling factor from the statistical simulations	29
Figure 10.	Basic pulse characteristics and associated Bloch vector angles for the statistically simulated $r = 8192$ pulse	29
Figure 11.	Net decay rate, including stimulated absorption and emission	31
Figure 12.	A simple superradiant pulse for the case of $r = 10^6$ calculated using the simple Dicke model. The pulse appears symmetrical, with the delay time comparable to the inverse of r as expected from the previous sections. Moreover, the area under the pulse is also comparable to r	32

Figure 13.	The intensity of photon emission into an ideal closed box for the case of $r = 10^6$ reveals characteristics similar to that of the previous figure, except the pulse width is severely shortened. The Bloch vector has hung up at about 110° , just past superradiant emission (see next figure), since stimulated absorption is now overcoming the emission rate. This simple limit provides a check on the trivial dynamical equations	32
Figure 14.	In the ideal cavity, the population of excited states decays quite rapidly, but then hangs up just past the $m = 0$ level. The m -component corresponds to an approximate Bloch vector angle near 110° , which is easily derived to be a rough constant angle, regardless of cooperation number. This provides a limiting case of the more complicated simple models.....	33
Figure 15.	Views a through f depict pulses calculated according to a simple Markovian radiator for the case $r = 10^6$ and varying values of the length and spontaneous decay rates listed in Table 3. The sequence of pulses from a to e indicates a trend towards a long exponential-like decay roughly following the ringing in the non-Markovian model of the next subsection. Pulse f is from a radiator of length shorter than the radiator in a, thus depicting less of a tail and closer behavior to the simple Dicke superradiator	35
Figure 16.	The (a) quantities dn/dt corresponding to the emitted intensity; (b) $n(t)$ corresponding to the running sum number of emitted photons; (c) $m(t)$ z-component of the cooperation number; and (d) $p(t)$ the photons in the "cavity" are depicted for the case of $r = 1.5 \times 10^6$ and $k = 1.0 \times 10^6$. The example shows the rise and fall of p-field intensity as the simple radiator dumps its photons from $m(t)$ to $n(t)$	36
Figure 17.	Views a through e depict pulses calculated according to a simple non-Markovian radiator for the case $r = 10^6$ and varying the length of the radiator and spontaneous decay rates as was done in Figs. 15(a) through 15(e). For conditions where the p-field plays an increasing role, ringing is observed to increase in scope	37
Figure 18.	The (a) quantities dn/dt corresponding to the emitted intensity; (b) $n(t)$ corresponding to the running sum of emitted photons; (c) $m(t)$ z-component of the cooperation number; and (d) $p(t)$ the photons in the "cavity" are depicted for the case of $r=1.5 \times 10^6$ and $k=1.0 \times 10^6$. Ringing effects are indicated in oscillations of $p(t)$	38
Figure 19.	Superradiating Operating Region. The operating region is illustrated for the conditions and assumptions discussed in the text with $p = 1$. The power and total energy out are for the case of one cooperation length. The cooperation lengths are indicated on the curves for a given lifetime and transition energy	44
Figure 20.	Geometry of the Superradiator Showing the Two Possible Modes of Emission	58

Figure 21.	Dicke Superradiant Model Showing the Various Multiplets of $2N$ two-level Resonators	58
Figure 22.	The Bloch Sphere	59
Figure 23.	Characteristics of a pure superradiant pulse calculated from the diffusion equation of Narducci et al. (program SR1 in Appendix E) for different values of the cooperation number and variance σ of the initial distribution of states on the Bloch sphere	62
Figure 24.	Variation in the superradiant pulse shape as a function of $k_1 = (c/2L) \tau_c$ for $N = 100$ and $k_2 = 10^{-7}$. The initial conditions are $P(m) = 0$ for $m = 5$, $P(5) = 1$ and with $k_1 = 1.5, 0.26, 10^{-20}$ for (a), (b), and (c), respectively.	64
Figure 25.	Variation in the superradiant pulse as a function of the coupling constant g_0' , with $n = 4.4 \times 10^{-24} \text{ cm}^3$, $N = 2$ and initial conditions $P(1) = P(3) = 0$, $P(2) = 1$	65
Figure 26.	A study of the effect on the superradiant lineshape of the initial photon field distribution or $Q(m')$ for the case $N = 100$, $P(m') = 0$, $m' = 5$, $P(5) = 1$, $k_1 = 0.0269$, $k_2 = 2 \times 10^{-20}$ in.....	66
Figure 27.	Calculated superradiant pulses for $N = 2$ and different initial conditions, (a) $P(1) = P(2) = 0$, $P(3) = 1$, (b) $P(1) = 0$, $P(2) = P(3) = 1$, and (c) $P(1) = P(3) = 0$, $P(2) = 1$	68
Figure 28.	Radiative pulse and quantum fluctuations (variance) for different initial conditions. The initial distribution for $P(m')$ is Poisson with $P_c = 10^{-5}$ and $N(m) = 0$. The k values are 0.0269 in (a), 0.269 in (b), 0.8 in (c), and 2.69 in (d).....	69
Figure 29.	Pulse and variance for the initial conditions $P(5) = 1$, $P(m') = 0$, $m' = 5$, $N = 100$, and $k_1 = 0.0269$	70
Figure 30.	Pulse and variance for the initial conditions $P(5) = 1$, $P(m') = 0$, $m' = 5$, $N = 100$, and $k_1 = 2.69$	71
Figure 31.	Quantum mechanical calculation (a) and semiclassical calculation (b) for the case $N = 2$, $k_1 = 0.03$. In Fig. (b) it was assumed $P(m') = 0$, $m' = 2$, $P(2) = 1$	72
Figure 32.	Quantum mechanical calculation (a) and semiclassical calculation (b) for the case $N = 2$, $k_1 = 0.3$. In Fig. (b) it was assumed $P(m') = 0$, $m' = 2$, $P(2) = 1$	72

Figure 33.	A three-state system showing the isomeric level, or initial state $ a\rangle$, the upper lasing level $ c\rangle$ and the ground state $ b\rangle$. In the subsequent analysis we keep E_{ba} and γ_a constant and vary E_{ca} , ω , n_ω , I , and γ_c . Process 1 in the figure shows a single photon off-resonance excitation, process 2 a multiphoton on-resonance excitation, and process 3 a multiphoton off-resonance excitation	76
Figure 34.	Relative cross section as a function of photon energy is shown for the nuclear case proposed by Arad, Eliezer, and Paiss, for the naive Breit-Wigner case, and for a case with the correct threshold behavior	82
Figure 35.	Comparison of naive and correct Breit-Wigner expressions for typical nuclear cases of interest	82
Figure 36.	The effect of the correct threshold behavior on the atomic physics experiment of Cooper and Ringler, with their photon energy indicated by the arrow. Because their photon energy was an appreciable fraction of the resonance energy, the threshold effect was not fatal to their experiment	83
Figure 37.	Multiphoton pumping of the isomeric level as a function of the detuning parameter in units of γ_c . The ordinate is the population of the ground level b . These results are for typical atomic transitions. For typical nuclear transitions the power requirements would have to be increased by a factor of 10^{10}	88
Figure 38.	Multiphoton pumping of the isomeric level $ a\rangle$. The abscissa gives the number of photons used in the process and the ordinate the population of the ground level $ b\rangle$ when $\omega_{ca} = 100$ eV and $\omega = 10$ eV. Since an odd number of photons is required for excitation, this process cannot be on-resonance	89
Figure 39.	Multiphoton pumping of the isomeric level $ a\rangle$. The abscissa gives the number of photons used in the process and the ordinate the population of the ground level $ b\rangle$ when $\omega_{ca} = 90$ eV and $\omega = 10$ eV. This process is on resonance for $n_\omega = 9$	90
Figure 40.	The effect of photon field intensity on pumping of the isomeric level a . The nine photon transitions are used in the calculation with $\omega_{ca} = 100$ eV and $\omega = 10$ eV	90
Figure 41.	On-resonance, single-photon depopulation of isomeric level $ a\rangle$, as a function of photon field intensity, I	91
Figure 42.	Single-photon depopulation of the isomeric level $ a\rangle$ as a function of photon energy for various photon field intensities with $\hbar\omega_{ca} = 100$ eV	91
Figure 43.	Single-photon depopulation of isomeric level $ a\rangle$ as a function of photon field intensity, I , for various photon energies with $\hbar\omega_{ca} = 100$ eV	92

Figure 44.	Off-resonance depopulation of the isomeric level $ a\rangle$ as a function of photon number n_ω for 1 eV photons	93
Figure 45.	Off-resonance depopulation of isomeric level $ a\rangle$, as a function of photon field intensity for different detuning parameters and number of photons participating in the process	94
Figure 46.	Effect of upper level decay rate γ_c (or linewidth) on the off-resonance depopulation of the isomeric level $ a\rangle$, as a function of photon number n_ω	95
Figure 47.	Effect of upper level decay rate γ_c on the off-resonance and on-resonance depopulation of the isomeric level $ a\rangle$	95
Figure 48.	Level populations for the three-state system as a function of the pulse length of the exciting photon beam	96
Figure 49.	Transition rates for electric and magnetic multipoles for a nuclear dimension of 10^{-12} cm.....	100
Figure 50.	Uncoupled electron and nuclear trajectories (upper left). Magnified nuclear trajectory (upper right). Coupled trajectories (lower half). In the uncoupled case the maximum electron $r = 1188$ fm and the maximum nucleon $r = 8.66$ fm.....	112
Figure 51.	Coupled electron and nuclear orbits for three nuclei consisting of a closed shell plus one proton. Nuclear core, one proton, and one electron are interacting. In the figure, Z is the atomic number and l_n the nucleon orbital angular momentum. The distances X, Y are given in femtometers	115
Figure 52.	The dipole moment as a function of time for both coupled (C) and uncoupled (U) cases	116
Figure 53.	Spectral intensities derived from magnetic moment autocorrelation functions for atoms near closed nuclear shells. The uncoupled case is on the left; the coupled on the right. In the figure, Z is the atomic number and l_n the nucleon angular momentum. The energies are given in MeV	117

TABLES

Table 1	Selected Low Energy Nuclear Transitions.....	4
Table 2	Cooperation Number and Pulse Duration.....	25
Table 3	Parameters for Illustrated Pulses.....	36
Table 4	Parameters for Illustrated Pulses.....	38
Table 5	Table of Parameters Describing Superradiance	61
Table 6	Atomic and Nuclear Decay Rates	77

SUMMARY

This report represents the 1986 effort of the IDA staff in the field of gamma-ray lasers. The work is part of a continuing task that supports the Innovative Science and Technology Office (IST) of the Strategic Defense Initiative Organization (SDIO). The development of a γ -ray laser is viewed as a high-risk/high-payoff undertaking. IDA's involvement focuses on minimizing that risk and on striving to redirect the effort when proposed schemes are shown not to be possible. In laying out its work, the IDA staff strives to complement and support the various efforts of the IST contractors who make up the gamma-ray laser community. Thus, although the seven chapters of this report are all independent studies, each supports either a proposed pumping scheme or the general theoretical underpinning of the laser. Three chapters are concerned with aspects of the Upconversion Schemes; one chapter each relates to the Electron-Nuclear Coupling Scheme and the Long Lifetime Scheme; and two chapters focus on theoretical aspects of superradiance which underlies all the proposed schemes.

Chapters I, IV, and V involve the Upconversion Schemes. In these schemes, a nucleus in an isomeric state is excited to a nearby state by absorbing electromagnetic energy. Deexcitation of the nearby state leads to the lasing transition. Chapters II and III discuss various aspects of superradiance (or superfluorescence) phenomena; Chapter VI deals with electron nuclear coupling and its effect on energy transfer; and Chapter VII, lifetime measurement and the uncertainty principle.

Chapter I presents in tabular form the results of a thorough search for nuclear levels in the Nuclear Data Sheets; these are for levels which could be suitable for a laser. The search located 80 isomers in 75 nuclei with 130 levels within 50 keV of the isomer. The data is presented in a form useful for researchers in the field. Work is in progress to produce such information for other pumping schemes.

It is generally believed that if a gamma-ray laser is developed it will probably emit in a superradiant mode instead of a stimulated emission mode. Thus, superradiance is of prime importance to all pumping concepts. In Chapters II and III various aspects of superradiant emission are discussed from the standpoint of adapting the techniques of atomic and molecular superradiance to nuclear systems. In Chapter II, Dicke superradiance

is presented in terms of a group theoretical approach. Various simple models have been devised in the framework of this approach. The use of Young tableaux techniques for describing symmetry properties of the states of a Dicke superradiant system is discussed.

In Chapter III, the quantum mechanical Bonifacio-Lugiato (B-L) theory of superradiance under various conditions is investigated, using numerical calculations. A thorough analysis is provided of some of the assumptions of the theory and for the first time the observation of real instabilities in the superradiance dynamics are pointed out and the source of the instabilities identified. It was determined that for the investigation of certain features of nuclear superradiance the B-L theory can be used to advantage. Effects of coherent excitation, relaxation, and inhomogeneous and homogeneous broadening in nuclear superradiance could be studied with the B-L theory. To take into account incoherent excitation (inversion), competing transitions, and transport effects, all of which are important to the γ -ray laser feasibility study, other theories have to be considered.

Among the many pumping concepts introduced over the years, the upconversion by photons of a nuclear level from an isomeric level to achieve inversion is the one most vigorously pursued by researchers at present. The idea is to pump the isomeric level by a short burst of electromagnetic radiation from a powerful optical laser or x-ray source to a nearby short-lived level. The lifetime of the upper lasing level should be short enough to provide a large cross section for the stimulated emission but not so short that it would introduce pumping problems with large power requirements.

In Chapter IV the requirements imposed by nuclear properties on the realization of those processes are discussed. First, we examine a proposed single-photon Raman scattering experiment and compare requirements set by atomic and nuclear systems. Second, we discuss multiphoton processes and examine the requirements for pumping out isomeric levels and preparing an inverted population for lasing. A number of specific results were obtained in this investigation. We have derived the correct expressions for the off-resonance cross sections and power requirements for single-photon excitations. Previously used expressions have overestimated the cross sections and underestimated power requirements by as much as six orders of magnitude.

A parametric study of multiphoton upconversion for both atomic and nuclear systems underscores the difficulty of working with nuclear systems as compared to atomic systems due to the ten orders of magnitude greater power requirements. Upconversion by photons does not seem to be a good way to produce inversion.

Chapter V considers a set of three nuclear levels and the electromagnetic transitions that must take place among them to upconvert from isomeric nearby state and to go from the latter state to the lasing transition. The nuclear quantum numbers and the level spacings are varied to optimize the lasing problem. It is shown that severe problems occur when upconverting by using a photon beam because of the screening effect of the nucleus by the atomic electrons. The use of the coulomb fields of proton and electron beams for excitation of the isomer is also considered.

Chapter VI considers the possibility that the electronic cloud surrounding the nucleus can actually be used to mediate the transfer of electromagnetic energy to that nucleus. A semiclassical approach has been used to describe the interaction of one or more valence nucleons and one or more valence atomic electrons with each other and with the nuclear core. A Hamiltonian is set up for the problem; it uses a Saxon-Woods potential to describe the interaction of the valence nucleon with the nuclear core. The autocorrelation function of the dipole moment is calculated and used to obtain the power spectrum for one valence proton interacting with one inner electron. The results are encouraging and, it is hoped, will lead to the use of more realistic nuclear potentials.

Chapter VII considers the uncertainty principle to determine whether there is an inherent limitation in the measurement time required to determine the lifetime or width of an isomer. The answer in the example used is no. The strength of the source is the relevant limitation. The discussion is relevant to criticisms about attempts to get rid of inhomogeneous broadening in the long lifetime scheme. The result is that there is no reason to deny the validity of the scheme.

I. SEARCH FOR NUCLEAR LEVELS FOR GAMMA-RAY LASERS

A. INTRODUCTION

This chapter presents the results of the search for candidate nuclei for the upconversion, level mixing, and electron-nuclear energy transfer lasing schemes discussed in IDA Memorandum Report M-162 (Ref. 1). These lasing schemes are described in Chapter I of that report (c.f. Fig. 1). In these schemes the nucleus in an isomeric state is "pumped" to a close-lying level of higher energy from which the lasing radiation is emitted.

B. SCOPE

This compilation includes isomers which have:

1. A half-life (isomeric state) ≥ 1 min.,
2. A known level within 50 keV above the isomeric state (i.e., $E(\text{IS}) < E(\text{level}) \leq E(\text{IS} + 50)$, and
3. For which there exists at least one gamma-ray deexciting this level with energy ≤ 300 keV.

C. SOURCES

References 4 through 7 were used as sources for the compilation presented in Table 1.

D. EXPLANATION OF TABLE

Table 1 lists 80 isomers in 75 nuclei with 130 levels within the 50 keV range of the isomeric state. The basic source of information is the latest edition of "Nuclear Data Sheets," and the policies and conventions of that document are followed throughout.

For clarity, the properties for the isomer, for upconversion and for the upper level are not repeated if the data refers to the same level as in the preceding line. Thus, for the 41.5 m isomer of $^{74}_{35}\text{Br}$ there are two levels known within the 50 keV limit. One, 18 keV

above the isomer (at 212.9 keV) is deexcited by four gamma-transitions, and the other, 44 keV above the isomer (at 239.3 keV) is deexcited by five gammas.

For uncertainties and powers of tens, the following shorthand is used in the table:

- Uncertainty: 28.30 ± 0.15 is given as 28.30 15
- Power of ten: 9.2×10^{-3} is given as 9.2 E-3

Also, because the personal computer used to prepare the table lacked the Greek alphabet, the customary $\pi \rightarrow$ pi and μ appears as u.

The information in the table is listed in 5 groups referring to: 1. The Isomer, 2. The Pumping Radiation, 3. The Potential Lasing Radiation, and 4. The Upper Level--the level reached by the upconversion which is the potential lasing level, and 5. The Lower Level of the lasing radiation.

1. The Isomer: A, Z, T1/2 define the nucleus and the isomeric state.

If two isomers are listed for one nucleus, these are indicated by superscripts: $^{124}_{51}\text{Sb}^1$ and $^{124}_{51}\text{Sb}^2$.

2. Upconversion:

E(keV) Energy required to excite the nucleus to this potential lasing level from the isomeric state. Calculated from measured level energies.

L π Angular momentum and parity change needed in this upconversion. Deduced from level properties.

3. Deexciting Transitions: All gamma-transitions deexciting this potential lasing level are listed.

E(keV) Energy of the transition. If the gamma-ray (photon) has not been observed, but the transition has been deduced from intensity balance in the level scheme, or from observed conversion electrons, this is indicated in a footnote.

IT(%) Transition intensity ($I_{\text{gamma}} + I_{\text{I.C.}}$) in percent of total level decay. In all levels listed in this compilation, gamma-transitions (photons + conversion electrons) are the only competing methods of decay. Thus, all $I_{\text{T}}(\%)$ for a single level (upconversion), should add up to 100 percent. This intensity is generally derived from experimentally measured relative intensities and conversion coefficients. If the multipolarity of the transition or the relative

intensities are uncertain, the absolute intensity is given in parentheses. No uncertainties are given for these quantities.

- Mult. Multipolarity of the deexciting transition. If the multipolarity has not been uniquely determined, but has been deduced from the level scheme, it is given in parentheses.
- ICC Total internal conversion coefficient of the transition for the multipolarity indicated. In general, it is the adopted value given in "Nuclear Data Sheets," either theoretical or experimental (the experimental values are shown here with an experimental uncertainty). If the "Nuclear Data Sheets" do not give an adopted conversion coefficient for the transition, then the theoretical value from the current Nuclear Data Group (NDG) program for theoretical conversion coefficients has been given. If the transition is shown as a mixture of multipolarities, i.e., $M1 + E2$, then the conversion coefficient for the predominant multipolarity is given and is indicated by a subscript (e.g., 2.15_{m1}).
- Iph(%) Photon intensity in percent of level decay. If the absolute value of the intensity cannot be derived because of lack of information, the experimental relative intensities of the deexciting transition are given and are so indicated with a footnote.

4. Upper Level: The level reached by upconversion.

5. Lower Level: The state in which the nucleus is left after emitting the lasing transition.

E(keV) Energy of the level.

J^P_i Spin and parity of the level. The parentheses here indicate weak arguments in the spin assignment as outlined in the "Nuclear Data Sheets."

T_{1/2} Half-life of the level.

TABLE OF SELECTED LOW ENERGY NUCLEAR TRANSITIONS - page 1

ISOMER		PUMPING RAD.			DE-EXCITING TRANSITIONS				UPPER LEVEL			LOWER LEVEL		
A Z	T _{1/2}	E(kev)	L ^π	E(kev)	I _γ (%)	Mult.	ICC	I _{ee} (%)	E(kev)	J ^π	T _{1/2}	E(kev)	J ^π	T _{1/2}
56 _g Co	9.15h 10	27.9 1	1 ⁻	28.30 15 52.96 13 88	12 88	(M1) (E2)	1.421 6.18	5 12	52.8 1	4 ⁻	10.4us 3	24.89 2 0	5 ⁻ 2 ⁻	9.15h 10 70.82d 3
73 _g Se	39.8m 13	0.61 12	(1)	(0.61) ^a (26.32) ^a	7 7				26.32 11	(5/2)		25.71 4 0	3/2 ⁻ 9/2 ⁻	39.8m 13 7.15h 8
79 _g Se	3.91m 5	32 5	1 ⁻	(32) ^a (128) ^a	7 7	(M1) (E3)	2.61 2.56		128 5	1/2 ⁻		95.73 3 0	1/2 ⁻ 7/2 ⁻	3.91m 5 56.5E+4y
		41.32 9	4 ⁻	137.1 2	100	(M1)	0.0436	96	137.05 9	9/2 ⁻		0	7/2 ⁻	56.5E+4y
74 _g Br	41.5m 15	18 60	3 ⁺	123.4 1 140.3 1 203.0 1 212.8 3 26.4 2 149.7 2 166.8 3 229.4 5 238.4 15 89.7 10 179.1 4	(25) (23) (49) (2,3) (22) (58) (8,6) (17,5) (4,8) (77) (23)	(M1) (E1) (E1) (E1) (E1) (E1) (E1) (E1) (E1) (E1) (E1)	0.065 9.2E-3 2.3 ^a 2.3 ^a 4 ^a 56 ^a 8 ^a 6 ^a 4 ^a 67 ^a 23 ^a	23 ^a 23 ^a 49 ^a 2.3 ^a 4 ^a 56 ^a 8 ^a 6 ^a 4 ^a 67 ^a 23 ^a	212.9 1 239.3 1	1 ⁻ (1,2)		89.6 1 72.6 1 9.85 4 0 212.9 1 89.6 1 72.6 1 9.85 4 0 89.6 0	1 ⁻ (0 ⁻ ,1 ⁻) 1 ⁻ 1 ⁻ (0 ⁻ ,1 ⁻) 1 ⁻ (0 ⁻ ,1 ⁻) (0 ⁻ ,1 ⁻) (0 ⁻ ,1 ⁻) (0 ⁻ ,1 ⁻) (0 ⁻ ,1 ⁻)	89.6 1 72.6 1 9.85 4 0 212.9 1 89.6 1 72.6 1 9.85 4 0 89.6 0
77 _g Br	4.28m 10	8 24.0 2	2 ⁻ ,1 ⁻ 2 ⁻	(114) ^a 24.2 2 129.7 1	7 ~13 ~87	(M1,E2) (E2) (E1)	150.6 0.039	0.1 84	114 129.72 9	5/2 ⁻ ,7/2 ⁻ 5/2 ⁻	9.3ns 3	105.68 15 0	3/2 ⁻ 9/2 ⁻ 3/2 ⁻	57.036h 6 4.28m 10 57.036h 6
82 _g Br	6.13m 8	29.113	0,1 ⁻	29.113	100	E1	3.10	24	75.062	(1,2) ⁻		45.949	2 ⁻	6.13m 8
83 _g Kr	1.83h 2	-32.17 2	3 ⁻	9.396 7	100	M1+E2	17.09 5	5.5	9.396 7	7/2 ⁻	147ns 4	0	9/2 ⁻	STABLE
84 _g Rb	20.5m 2	<12	1 ⁻	Decay not known					<476	(5 ⁻)				
90 _g Rb	4.30m 8	14.9		121.82 3	(100)				121.81			0	(1 ⁻)	2.55m 5
94 _g Nb	6.26m 1	17.77 3	(1) ⁻	(17.77) ^a (58.72) ^a	7 ?	(M1) (E2)	4.46 7.96		58.723 11	(4) ⁻		40.95 2 0	3 ⁻ (6) ⁻	6.26m 1 2.0E+4y 2
		37.72 2	(4) ⁻	78.675 3	100	(M1)	0.445	69	78.675 3	(7) ⁻		0	(6) ⁻	2.0E+4y 2
94 _g Tc	52.0m 10	23 3	(1) ⁻	(23) ^a	(100?)	(M1)	20.05	4.87	98 2	(3) ⁻		75.5 19 0	(2) ⁻	52.0m 10
	26 2	(4) ⁻	(4) ⁻	101.9 2	100	(M1+E2)	0.27 4	79	101.9 2	(6) ⁻			7 ⁻	4.88h 2

^a-Gamma-ray not observed
^a-Relative photon intensity

^aGamma-ray not observed
^bRelative photon intensity

TABLE OF SELECTED LOW ENERGY NUCLEAR TRANSITIONS - page 2

ISOMER		PUMPING FAD.		DE-EXCITING TRANSITIONS				UPPER LEVEL			LOWER LEVEL		
A Z	T _{1/2}	E (keV)	L ^π	E (keV)	I _γ (%)	Mult.	ICC	I _γ (%)	J ^π	E (keV)	T _{1/2}	J ^π	T _{1/2}
96 _g Tc	51.5m 10	0.74 9 11.5 2 14.96 9	(1) ⁻ (2) ⁻	(34.9) ⁻ (45.43) ⁻ 49.10 10	7 (100) 100	(E4) M1(E2)	1.17E+5 2.15 ₁₁	32	(3) ⁻ (6) ⁻	34.91 8 45.43 13 49.13 8	0 0 0	7 ⁻ 7 ⁻ 7 ⁻	4.28d 7 4.28d 7 4.28d 7
99 _g Tc	6.01h 1	38.411 2 -2.1725 15	2 ⁻ 3 ⁻	40.584 2 181.063 8 140.5110 10	42 58 100	M1+E2 E2 M1+E2	3.759 4 0.1486 50 0.114 3 90	8.8	5/2 ⁻ 7/2 ⁻	181.094 2 140.5106 10	0 0 0	7/2 ⁻ 9/2 ⁻ 9/2 ⁻	0.19ns 2 2.11E+5y 1 2.11E+5y 1
101 _g Rh	4.34d 1	24.46 7	(1) ⁻	24.46 1	100	M1+E2	20.8 1	4.4	(7/2) ⁻	181.78 6	157.32 4	9/2 ⁻	4.34d 1
104 _g Rh	4.34m 5	-31.84 1	3 ⁻	97.114 3	100	M1	0.37	73	2 ⁻	97.114 3	0	1 ⁻	42.3s 4
111 _g Pd	5.5h 1	20		Decay not known						192 ⁺			
105 _g Ag	7.2m 2	27.47 2	1 ⁻	27.47 1	100	(M1+E2)	18.0 1	5.3	9/2 ⁻	53.142 14	25.472 12	7/2 ⁻	7.2m 2
106 _g Ag	8.46d 10	21.03 11	(4) ⁻	110.46 5	100	(M1)	0.318	76	(2) ⁻	110.46 6	0	1 ⁻	24.0m 1
108 _g Ag	127y 21	44.430 9 -30.332 7	0,1 ⁻ 4 ⁻	44.435 3 79.138 3	100 100	M1+E2 E1	4.9 12 0.313 76	13 76	5,6,7 ⁻ 2 ⁻	155.902 6 79.140 2	109.472 7 0	4 ⁻ 1 ⁻	127y 21 2.37m 1
110 _g Ag	249.76d 4	1.13	3 ⁻	117.607 100 118.716 1 Cascading Gamma-rays (1.113) ⁻ 100	100 <1 100	E1+E2 E2 (E1)	0.10 ₁₁ 0.789 <0.6	90 <0.6	3 ⁻ 2 ⁻	118.718 7 1.113	1.113 0	2 ⁻ 1 ⁻	0.66us 4 24.6s 2 24.6s 2
111 _g Cd	48.6m 3	20.48 10	2 ⁻	171.28 3	100	M1+E2	0.1074	90	7/2 ⁻	416.70 10	245.42 1	5/2 ⁻	85.0ns 7
117 _g Cd	3.36h 5	-1.0 2	(4) ⁻	135.4 1	100	M1	0.200	83	3/2 ⁻	135.4 1	0	1/2 ⁻	2.49h 4
112 _g In	20.9m 2	4.4 1	(1) ⁻	(6.4) ⁻	(100)	(M1)	Large		(5) ⁻	162.9 1	156.5 1	4 ⁻	20.9m 2
114 _g In	49.51d 1	30.77 8	(2 ⁺ ,1,0)	30.73 2	100				(3 ⁺ ,4,5)	221.11 6	190.34 6	5 ⁻	49.51d 1
116 _g Sn	60.3m 6	13 56 28 56 -9 56 -24 56 -34 56	3 5 5,4 5,4 4	92.2 2 424.4 3 518.2 3 480.77 343.3 3 444.2 3 352.3 3 455.9 3	100 80 3 20 3 1007 89 3 11 3 82 2 18 2				5 3 3,4 3,4 4	503.0 3 518.1 3 480.7 2 466.2 2 455.7 5	410.9 2 93.99 5 0 103.0 1 103.0 1 0	4 1 ⁻ 3 ⁻ 2 ⁻ 3 ⁻ 2 ⁻ 3 ⁻	>200ns >200ns 15.8m 8 15.8m 8 <1ns 15.8m 8 <1ns 15.8m 8
				Cascading Gamma-rays 308.2 3 410.0 2 102.9 3 93.7 2	19 3 81 3 100 100				4	410.9 2 103.0 1 103.0 1 93.99 5	103.0 1 0 0 0	2 ⁻ 3 ⁻ 3 ⁻ 1 ⁻	<1ns 15.8m 8 15.8m 8 >200ns

*Gamma-ray not observed
-Probably a doublet

TABLE OF SELECTED LOW ENERGY NUCLEAR TRANSITIONS - page 3

A Z	ISOMER	PUMPING RAD.		DE-EXCITING TRANSITIONS				UPPER LEVEL		LOWER LEVEL	
		E (kev)	L ^a	E (kev)	1- γ Mult.	ICC	I _{rel} (%)	E (kev)	J ^a	E (kev)	J ^a
122 _a Sb	4.21m 2	3.670 2	(6) ⁻	45.7325 9 89.137 2 105.8160 7 Decay not known	37 1.1 62 MI	6.02 0.262 0.533 40	5.3 0.9	167.2293 6	(2) ⁻	<0.28ns	(1) ⁻
		15.07 4		114.8674 9 29.400 2 44.092 2	100 4 4	0.423 1.593 0.7	70 81	178.67 4	4 ⁻	<0.1ns <0.15ns	3 ⁻
		-26.087 2	3 ⁻	148.2376 4 76.0595 7 -42.062 2	98 100 (7) ⁻	0.2074 4.41 0.1093	81 18 90	192.9591 10 137.4724 9 121.4966 9	4 ⁻ 5 ⁻ (1) ⁻	0.53ns 3 6.3ns 3	3 ⁻
				Cascading Gamma-rays:				137.4724 9	5 ⁻	0.53ns 3	3 ⁻
				78.0918 7 41.4127 5	100 100	1.268 0.743	44 57	121.4966 9	(1) ⁻	6.3ns 3	2 ⁻
								78.0914 6	3 ⁻	1.86ns 8	2 ⁻
								61.4130 5	3 ⁻	1.86ns 8	2 ⁻
124 _a Sb ^a	1.55m 8	25.982 2 29.941 2	3 ⁻ 2 ⁻ , 1 ⁻	25.981 3 29.940 1 40.8041 10 39.9601 5 80.7646 15	100 45 55 100 W	3.23E-4 138.0 2.281 8.92 0.366	3E-3 16.9 16.9 100 ^b 7 ^b	36.8465 15 40.8040 8	8 ⁻ 3 ⁻ , 4 ⁻	20.2m 2 3.2us 3	5 ⁻
124 _a Sb ^b	20.2m 2	3.958 2	5 ⁻ , 4 ⁻	29.940 1 40.8041 10 39.9601 5 80.7646 15	45 55 100 W	138.0 2.281 8.92 0.366	0.32 16.9 100 ^b 7 ^b	40.8040 8	3 ⁻ , 4 ⁻	3.2us 3	5 ⁻
126 _a Sb	19.0m 3	22.7 4	(2) ⁻	22.70 7	100	M2	744	40.4 3	(3) ⁻	~11s	(5) ⁻
128 _a Sb	10.4m 2	45.7 2	1 ⁻	45.7 2	100	M1	6.03	18.45.7	4 ⁻	18<20	5 ⁻
119 _a Te	4.69d 4	20		63.0 1 320.6 1			3 ^b 10 ^b	320.56 8		257.51 7 0	(3/2) ⁻
127 _a Te	109d 2	-27.14 13	5 ⁻	61.1 1	100	(M1)	2.84	61.12 10	1/2 ⁻	0	3/2 ⁻
132 _a I	1.39h 3	41	(6) ⁻	111.76 Cascading Gamma-rays: 49.72	100 100	M1(E2) M1	0.59 5.71	161.48 8 49.72 1	2 ⁻ 3 ⁻	49.72 1 0.93ns 4	3 ⁻
127 _a Ie	1.15m 2	24.3 2	(1) ⁻ (4 ⁻ , 3 ⁻)	176.0 5 321.5 2 Cascading Gamma-rays: 124.7 2	16 84 100	M1(E2) M1(E2) M1(E2)	0.127 ^a 0.0343 ^a 0.448 2	297.1 ^a 321.39 14 124.81 12	(11/2) ⁻ (11/2 ⁻ , 3/2 ⁻) (11/2) ⁻	297.1 124.81 12 0	(9/2) ⁻ (13/2) ⁻ (11/2) ⁻
134 _a Ce	2.91h 1	35.048 4	(6, 5, 4) ⁻	113.764 3 173.794 10 116.373 2 176.403 2 116.612 1 60.030 1	99 1 62 38 100	M1 (M1, E2) (E1) E1 E2 M1	0.632 0.194 ^a 0.144 0.046 1.09 3.97	173.795 3 176.4031 15 176.4024 13 60.0304 9	(2, 3, 4) ⁻ (3) ⁻ (3) ⁻ (1) ⁻ (3) ⁻	60.0304 9 0 0 60.0304 9 0	(3) ⁻ 4 ⁻ (3) ⁻ 4 ⁻ (3) ⁻
		37.656 3	(5) ⁻							49.7ns 8	4 ⁻
		37.895 3	(7) ⁻							60.0304 9	4 ⁻
										2.06y 5	4 ⁻

^aGamma-ray not observed^bRelative photon intensity

TABLE OF SELECTED LOW ENERGY NUCLEAR TRANSITIONS - page 4

ISOMER	T _{1/2}	PUMPING RAD.		DE-EXCITING TRANSITIONS				UPPER LEVEL		LOWER LEVEL	
		E(keV)	L ^a	E(keV)	I _r (%)	Mult.	ICC	J ^a	T _{1/2}	E(keV)	J ^a
135 _m La	38.9h 1	2.927 13 (3) ⁻		278.84 2	85	M1(+E2)	0.0595 ⁻	80		291.174 9 (5/2) ⁻	3/2 ⁻
		14.119 11 4 ⁻		291.17 5	15	E2	0.0499	14		0	1/2 ⁻
				290.04 5		M1-E2	0.0534 ⁻	43 ⁻		12.322 5	3/2 ⁻
				302.353 8		M1	0.0481	50 ⁻		0	1/2 ⁻
				Cascading Gamma-rays							
				12.327 4 100	M1	70.3	1.4	3/2 ⁻	7.0ns 3	0	1/2 ⁻
132 _m La	24.3m 5	28.0 14 5 ⁻ , 4 ⁻		41.4	20	(M1)	4.49	3.4		155.4 10	1 ⁻ , 2 ⁻
				216.7 10	80	E1	0.0282	78		0	4.8h 2
				-4.6 14 5 ⁻	100	E1	0.045	94		0	4.8h 2
				-33.3 14 5 ⁻ , 4 ⁻	100	E1	0.070	93		0	4.8h 2
138 _m Pr	2.1h 1	26 23 (6) ⁻		42.6 2	100	(M1)	5.09	14		326.96 5	(⁻)
		-37 23 (1) ⁻		132.73 5		M1-E2		7 ⁻		194.22 5	(⁻)
				326.9 5				1 ⁻		0	1 ⁻
				126.14 5		M1(+E2)		4 ⁻		199.52 5	1 ⁻
				325.76 5		M1(+E2)		96 ⁻		0	1 ⁻
				Cascading Gamma-rays							
				199.50 5 100	M1-E2					0	1 ⁻
				194.21 5 100	M1-E2					0	1 ⁻
142 _m Pr	14.6m 5	14.057 6 2 ⁻		(14.057) ⁻	7	(E2)	1.29E+4			3.683 4	5 ⁻
				(17.740) ⁻	7	(M1)	32.1			0	2 ⁻
144 _m Pr	7.2m 3	21.09 4 2 ⁻		80.104 5 100	M1	2.49	29			80.12 3	1 ⁻
		40.93 4 1 ⁻		40.89 5 92	M1(+E2)	2.79 11 24				99.96 3	2 ⁻
				99.96 2 8	E2	2.144	2.4			0	0 ⁻
148 _m Pr	2.0m 1	28 (3,4)		98.166 3 100	E2	2.302	30			98.166 3	1 ⁻
		29 (3,4)		98.99 3 100	(M1)	1.356	42			98.99 3	1 ⁻ , 0 ⁻
		215 (3,4)		105.20 3 100	(M1)	1.138	47			105.20 3	1 ⁻ , 0 ⁻
		231 (3,4)		121.169 3 100	(M1)	0.761	57			121.169 3	1 ⁻ , 0 ⁻
140 _m Pm	5.95m 5	15 2		76.1 7				9 ⁻		415.3 8	(2) ⁻
				414.9 5				3 ⁻		0	1 ⁻
				Cascading Gamma-rays							
				114.1 5 50	M1	1.080	24			225.5 5	1 ⁻
				200.0 5 15	E1	0.0408	14			139.6 5	(2) ⁻
				339.8 5 35	E2(+M1)		35			0	1 ⁻
				225.5 5 100	M1	0.1622	86			0	1 ⁻
				139.6 5 100	E1	0.1081	90			0	1 ⁻
150 _m Eu	12.8h 1	1 (1) ⁻		(-1) ⁻	(100?)	(M1)	Large			43	0 ⁻ , 1 ⁻
		28 (2) ⁻		26.5 ⁻	7	(M1)	14.0			43	(1) ⁻
				26.5 ⁻	7	(E2)	7.4E+2			42.1	0 ⁻ , 1 ⁻

^a-Gamma-ray not observed
^b-Relative photon intensity
^c-26.5 gamma-ray is probably a doublet

TABLE OF SELECTED LOW ENERGY NUCLEAR TRANSITIONS - page 5

ISOMER		PUMPING RAD.		DE-EXCITING TRANSITIONS				UPPER LEVEL		LOWER LEVEL	
A Z	T _{1/2}	E (keV)	L ^π	E (keV)	I _γ (%)	Mult.	ICC	E (keV)	J ^π	E (keV)	J ^π
132₅₄Eu⁺											
	9.32h	19.4972 5	1 ⁻	19.495 7	91	M1	34.9	65.2966 3	1 ⁻	45.5994 4	0 ⁻
				65.2965 5	9	E2	12.34	0		0	3 ⁻
		31.4394 5	(3) ⁻	77.2583 4	100	M1	3.94	77.2588 3	(3) ⁻	0	3 ⁻
		32.4341 6	1 ⁻	12.965 15	(44)	(E1)	14.02	78.2335 4	1 ⁻	65.2966 3	1 ⁻
				32.4341 3	(56)	E1	1.080	45.5994 4	0 ⁻	45.5994 4	0 ⁻
		44.0136 6	(4) ⁻	89.6128 6	100	M1	2.57	89.6130 4	(4) ⁻	0	3 ⁻
		44.2494 5	(4) ⁻	12.598 15	(4,4)	(E1)	15.17	89.6488 3	(4) ⁻	77.2588 3	(3) ⁻
				89.6492 7	(95)	E1	0.381	0		0	3 ⁻
132₅₄Eu⁰											
	96ns	0.93 11	(4,3,2) ⁻	40.4218 5	100	M1	4.06	148.7364 4	(4,5,6) ⁻	108.1148 4	(5) ⁻
		2.88 11	(4) ⁻	42.5730 8	(0,6)	(E1)	0.511	150.6869 3	(4) ⁻	108.1148 4	(5) ⁻
				61.0727 12	(0,6)	(M1)	7.84	0		89.6130 4	(4) ⁻
				73.4280 7	(97)	M1	4.60	77.2588 3	(3) ⁻	77.2588 3	(3) ⁻
		10.24 11	(7) ⁻	150.6883 15	(2)	M1,E2	0.587 ^{ns}	158.0548 4	1 ⁻	0	3 ⁻
				37.2171 12	(15)	(M1,E2)	5.5 ^{ns}	120.8384 3	(2) ⁻	120.8384 3	(2) ⁻
				79.8216 5	(64)	M1	3.60	78.2335 4	1 ⁻	78.2335 4	1 ⁻
				92.7575 6	(10)	(E1)	0.343	65.2966 3	1 ⁻	65.2966 3	1 ⁻
				112.4557 8	(11)	(E1)	0.2074	45.5994 4	0 ⁻	45.5994 4	0 ⁻
		13.07 11	(5,4,3) ⁻	52.7664 5	(7,4)	(M1,E2)	11.8 ^{ns}	108.1148 4	(5) ⁻	108.1148 4	(5) ⁻
				71.0323 5	(92)	M1	5.05	89.6130 4	(4) ⁻	89.6130 4	(4) ⁻
		27.13 11	(6,5) ⁻	54.0986 6	(1)	(E1)	1.472	120.8384 3	(2) ⁻	120.8384 3	(2) ⁻
				56.7715 5	(54)	M1	9.71	118.1660 3	(2) ⁻	118.1660 3	(2) ⁻
				60.9689 8	(0,5)	(E1)	1.074	113.9696 3	(3) ⁻	113.9696 3	(3) ⁻
				63.4902 4	(39)	M1	7.00	109.0892 6	(1) ⁻	109.0892 6	(1) ⁻
				65.8478 9	(3)	(M1,E2)	6.4 ^{ns}	89.6130 4	(4) ⁻	89.6130 4	(4) ⁻
				85.326 3	(0,3)	(M1,E2)	3.00 ^{ns}	65.2966 3	1 ⁻	65.2966 3	1 ⁻
		29.88 11	(25) ⁻	109.6429 12	(2)	(M1,E2)	1.38 ^{ns}	120.8384 3	(2) ⁻	120.8384 3	(2) ⁻
				56.8466 12	(35)	(M1)	9.67	78.2335 4	1 ⁻	78.2335 4	1 ⁻
				97.4533 8	(65)	M1,E2	1.90 ^{ns}	148.7364 4	(4,5,6) ⁻	148.7364 4	(4,5,6) ⁻
		31.12 11	(5,4) ⁻	30.17 4	(14)	(M1,E2)	9.6 ^{ns}	146.0853 3	(3) ⁻	146.0853 3	(3) ⁻
				32.8457 5	(8,7)	(M1)	7.63	124.5343 3	(3,4) ⁻	124.5343 3	(3,4) ⁻
				54.3964 8	(29)	M1	10.99	113.5596 3	(3) ⁻	113.5596 3	(3) ⁻
				64.9619 5	(38)	M1	6.43	108.1148 4	(5) ⁻	108.1148 4	(5) ⁻
				70.8170 10	(1,7)	(M1,E2)	5.10 ^{ns}	89.6130 4	(4) ⁻	89.6130 4	(4) ⁻
				89.082 2	(0,5)	(M1)	2.62	77.2588 3	(3) ⁻	77.2588 3	(3) ⁻
				89.3182 15	(0,2)	(E1)	0.387	0		0	3 ⁻
				101.6733 7	(7,1)	E1	0.273	150.6869 3	(4) ⁻	150.6869 3	(4) ⁻
		32.82 11	(4) ⁻	178.928 3	(0,6)	(E1)	0.0592	148.7364 4	(4,5,6) ⁻	148.7364 4	(4,5,6) ⁻
				29.934 11	(46)	M1	10.05	141.8253	(4) ⁻	141.8253	(4) ⁻
				31.8962 5	(2,0)	(E1,M2)	1.13 ^{ns}	124.5343 3	(3,4) ⁻	124.5343 3	(3,4) ⁻
				38.8068 5	(17)	M1	4.65	108.1148 4	(5) ⁻	108.1148 4	(5) ⁻
				56.0978 5	(2,1)	(E1)	1.339	89.6130 4	(4) ⁻	89.6130 4	(4) ⁻
				72.5190 6	(22)	E1	0.679	77.2588 3	(3) ⁻	77.2588 3	(3) ⁻
				90.7834 6	(9)	E1	0.371	0		0	3 ⁻
				91.0192 7	(1,6)	(M1)	2.461	150.6869 3	(4) ⁻	150.6869 3	(4) ⁻
				103.3722 10	(1,0)	(M1)	1.707	148.7364 4	(4,5,6) ⁻	148.7364 4	(4,5,6) ⁻
				180.632 5	(0,1)	(M1)	0.355	124.5343 3	(3,4) ⁻	124.5343 3	(3,4) ⁻
		44.7 5		Decay not known				108.1148 4	(5) ⁻	108.1148 4	(5) ⁻
								192.5 5		0	3 ⁻

continued

TABLE OF SELECTED LOW ENERGY NUCLEAR TRANSITIONS - page 4

ISOMER		PUMPING RAD.		DE-EXCITING TRANSITIONS							UPPER LEVEL		LOWER LEVEL	
A	Z	T _{1/2}	E(keV)	L ⁺	E(keV)	I _γ (%)	Mult.	ICC	I _{ex} (%)	E(keV)	J ^π	E(keV)	J ^π	T _{1/2}
152 _g Eu														
Continued														
			49.10 11	(4) ⁻	36.0325 9 (16)		M1	5.80	2.3	196.9135 4	(4) ⁻	160.8808 4 (3,4,5) ⁻	(3) ⁻	2.3ns 6
					50.8284 4 (32)		(M1)	13.0	2.3			146.0853 3 (3) ⁻	(3) ⁻	
					53.084 3 (1)		(E1)	1.48	0.6			141.8253 3 (4) ⁻	(4) ⁻	2.6ns 7
					72.3796 6 (7)		(M1)	4.83	1.2			124.5343 3 (3,4) ⁻	(3) ⁻	
					82.9451 9 (2)		(M1)	3.26	0.4			113.9696 3 (3) ⁻	(3) ⁻	
					88.7982 6 (32)		M1	2.67	8.7			108.1148 4 (3) ⁻	(3) ⁻	≤20ns
					107.0642 10 (9)		M1, E2	1.4 ⁺	3.6			89.8488 3 (4) ⁻	(4) ⁻	384ns 10
					119.6544 12 (1)		(E1)	0.18	1.0			77.2588 3 (3) ⁻	(3) ⁻	38ns 4
		-1.72 11	(5) ⁻		21.354 12 (16)		M1(E2)7	25.0 ⁺	0.6	146.0853 3 (3) ⁻	(3) ⁻	124.5343 3 (3,4) ⁻	(3) ⁻	
					32.1158 5 (45)		M1	8.0	5.0			113.9696 3 (3) ⁻	(3) ⁻	
					56.2362 5 (30)		M1	10.0	2.7			89.8488 3 (4) ⁻	(4) ⁻	384ns 10
					56.4712 15 (0.4)		(E1)	1.30	0.2			89.6130 4 (4) ⁻	(4) ⁻	
					67.8516 5 (8)		E27	10.7	0.7			78.2335 4 (4) ⁻	(4) ⁻	145ns 10
					146.086 2 (0.1)		E1	0.100	0.1			0 3 ⁻	3 ⁻	13.33y 4
		-5.98 11	(4) ⁻		33.7100 7 (0.9)		(E1)	0.76	0.5	141.8253 3 (4) ⁻	(4) ⁻	108.1148 4 (3) ⁻	(3) ⁻	≤20ns
					51.9769 4 (74)		E1	1.80	26.4			89.8488 3 (4) ⁻	(4) ⁻	384ns 10
					52.2145 12 (3.5)		(M1)	12.0	0.3			89.6130 4 (4) ⁻	(4) ⁻	
					64.5670 5 (20)		M1	6.7	2.5			77.2588 3 (3) ⁻	(3) ⁻	38ns 4
		-23.28 11	(5,4) ⁻		141.8253 15 (1.9)		(M1)	0.60	1.2	124.5343 3 (3,4) ⁻	(3,4) ⁻	113.9696 3 (3) ⁻	(3) ⁻	13.33y 4
					10.563 14 (90)		(M1)	230	0.4			89.8488 3 (4) ⁻	(4) ⁻	384ns 10
		-26.97 11	(6) ⁻		34.6853 4 (10)		M1	6.5	1.3	120.8384 3 (2) ⁻	(2) ⁻	78.2335 4 (1) ⁻	(1) ⁻	145ns 10
					42.6051 5 (77)		M1	3.5	17.4			65.2966 3 (1) ⁻	(1) ⁻	940ns 80
		-29.64 11	(6) ⁻		55.5419 5 (23)		(E1)	1.42	9.5	118.1660 3 (2) ⁻	(2) ⁻	78.2335 4 (1) ⁻	(1) ⁻	145ns 10
					39.9319 5 (12.4)		(E1)	0.60	1.5			65.2966 3 (1) ⁻	(1) ⁻	940ns 80
					52.8693 4 (95)		M1	11.7	7.5			45.5994 4 (0) ⁻	(0) ⁻	9.32h 1
					72.5663 7 (2.1)		(E2)	7.8	0.2			0 3 ⁻	3 ⁻	13.33y 4
		-33.84 11	(5) ⁻		118.1666 12 (0.3)		(M1)	1.13	0.1	113.9696 3 (3) ⁻	(3) ⁻	89.8488 3 (4) ⁻	(4) ⁻	384ns 10
					24.110 10 100		M1	18.0	5.3			0 3 ⁻	3 ⁻	13.33y 4
		-36.36 11	(6) ⁻		113.9694 12 (0.06)		(E1)	0.202	0.05	111.4472 4 (2) ⁻	(2) ⁻	65.2966 3 (1) ⁻	(1) ⁻	940ns 80
					46.1504 6 (95)		M1	2.72	26			45.5994 4 (0) ⁻	(0) ⁻	9.32h 1
					65.8478 9 (4.6)		(E2)	12.1	0.35			0 3 ⁻	3 ⁻	13.33y 4
					111.444 7 (0.09)		(M1)	1.30	0.04			0 3 ⁻	3 ⁻	13.33y 4
		-38.72 11	(7) ⁻		43.7926 6 27		M1	3.60	5.8	109.0892 6 (1) ⁻	(1) ⁻	65.2966 3 (1) ⁻	(1) ⁻	940ns 80
					63.4902 4 73		M1	7.0	9.2			45.5994 4 (0) ⁻	(0) ⁻	9.32h 1
		-39.70 11	(3) ⁻		18.265 7 100		M1	43.0	2.3	108.1148 4 (5) ⁻	(5) ⁻	89.8488 3 (4) ⁻	(4) ⁻	384ns 10
154 _g Eu														
		46.0e 3	~16	(5) ⁻	50.61 2 (94)		(M1)	13.6	6.4	173.13 4 (3) ⁻	(3) ⁻	122.54 3 (2) ⁻	(2) ⁻	2.4us 4
			~25	(5,4) ⁻	104.93 2 (6)		(E1)	0.25	5.0			68.167 9 (2) ⁻	(2) ⁻	55ns 4
					80.749 10 (78)		(E1)	0.51	52	181.62 3 (3,4) ⁻	(3,4) ⁻	100.859 13 (4) ⁻	(4) ⁻	55ns 4
					181.60 5 (22)		(M1)	0.35	14			0 3 ⁻	3 ⁻	8.8y 1
		~47	(5,4) ⁻		74.119 11 (15)		(E1)	0.64	9	203.81 2 (3,4) ⁻	(3,4) ⁻	129.68 2 (4,5) ⁻	(4,5) ⁻	≤10ns
					76.40 4 (6)		(M1)	4.09	1.1			127.43 3 (3,4) ⁻	(3,4) ⁻	≤10ns
					102.941 11 (68)		M1	1.73	25			100.859 13 (4) ⁻	(4) ⁻	55ns 4
					203.82 5 (11)		E1	0.042	11			0 3 ⁻	3 ⁻	8.8y 1
		~14	(3) ⁻		(6.777)					143.5 3 (5) ⁻	(5) ⁻	136.77 3 (4,5) ⁻	(4,5) ⁻	≤10ns
					13.9		(E1)	11.59				129.68 2 (4) ⁻	(4) ⁻	≤10ns
		~20			35.818 10		M1+E2	7.4		136.77 3 (4) ⁻	(4) ⁻	107.6 3 (4) ⁻	(4) ⁻	55ns 4
					(35.8027)		(E1)	(0.9)		100.859 13 (4) ⁻	(4) ⁻	0 3 ⁻	3 ⁻	8.8y 1
		~27	(4,3) ⁻		136.8 3		(M1)	0.771				107.6 3 (4) ⁻	(4) ⁻	55ns 4
					21.9 2		(E1)	3.38		129.68 2 (4,5) ⁻	(4,5) ⁻	100.859 13 (4) ⁻	(4) ⁻	55ns 4
		~30	(5,4) ⁻		28.814 9		E1	1.53				99.95 2 (3) ⁻	(3) ⁻	91ns 10
		~34	(6) ⁻		27.469 11 100		M1	13.0	7	127.43 3 (3,4) ⁻	(3,4) ⁻	122.54 3 (2) ⁻	(2) ⁻	20ns 5
		~49	(4) ⁻		39.78 2 100		M1	4.3	19	122.54 3 (4) ⁻	(4) ⁻	100.859 13 (4) ⁻	(4) ⁻	55ns 4
					(6.777)					107.6 3 (4) ⁻	(4) ⁻	99.95 2 (3) ⁻	(3) ⁻	91ns 10
					7.70		(M1)	129						

TABLE OF SELECTED LOW ENERGY NUCLEAR TRANSITIONS - page 7

TABLE OF SELECTED LOW ENERGY NUCLEAR TRANSITIONS															
ISOMER		PUMPING RAD.		DE-EXCITING TRANSITIONS					UPPER LEVEL			LOWER LEVEL			
A	Z	T _{1/2}	E(keV)	L ^π	E(keV)	I _γ (%)	Mult.	ICC	I _{ex} (%)	E(keV)	J ^π	T _{1/2}	E(keV)	J ^π	T _{1/2}
154 _{sm} Eu continued															
Cascading Gamma-ray															
32.71 5 35 E2 271 0.13 100.859 13 (4) ⁻ 55ns 4 68.169 9 (2) ⁻ 2.4us 4															
100.859 10 65 E1 0.28 51 99.95 2 (3) ⁻ 91ns 10 68.169 9 (2) ⁻ 2.4us 4															
31.776 14 100 M1 8.4 11 92.77 2 (1) ⁻ 20ns 5 68.169 9 (2) ⁻ 2.4us 4															
14.43 2 100 E1 10.1 9 68.169 9 (2) ⁻ 2.4us 4															
68.169 9 100 E1 0.80 56 100 109.7 5 ⁻ 49ns 7 0 5.35d 10															
Decay not known (M1) 10.0 9.0 87.0 4 ⁻ 49ns 7 0 5.35d 10															
Decay not known (E1) 0.357 74 49.630 4 ⁻ 49ns 7 0 5.35d 10															
49.630 100 83.397 4 9/2 ⁻ <35ps 0 2.334h 4															
163 _{sm} Dy		1.258m 4	-24.763 5	4 ⁻	83.397 4 100	M1+E2	4.26	19	83.397 4	9/2 ⁻	7/2 ⁻	<35ps	0	7/2 ⁻	2.334h 4
160 _{sm} Ho ¹		5.02h 5	51.5 47.2 7	(1 ⁻) 4 ⁻	(51.5) ⁻ 107.3 100	(E1) M1	Large	2.179	31.5	51.57 107.2 7	(1 ⁻) 6 ⁻	<2m	59.98 3 0	2 ⁻ 5 ⁻	5.02h 5 25.6m 3
160 _{sm} Ho ²		<2m	~45.7	(5 ⁻)	107.3 100	M1		2.179	31.5	107.2 7	6 ⁻		0	5 ⁻	25.6m 3
162 _{sm} Ho		47.0m 10	-10	3 ⁻	37.8 1 100	M1+E2	13.1 1	7.1	96.1 1	3 ⁻	2 ⁻	1.2ns 2	38.3 1	2 ⁻	1.2ns 2
Cascading Gamma-ray															
38.3 1 100 M1 7.14 12 38.3 1 2 ⁻ 1.2ns 2 0 1 ⁻ 15m 1															
164 _{sm} Ho		37.5m 15	26 1	(2 ⁻)	(72) ⁻ (128.7) ⁻	(M1,E2) (E2)	6.9m 1.14			166 1	(4 ⁻)		94.0 1 37.34 5	3 ⁻ 2 ⁻	<2.8ns <2.8ns 29m 1
		-46	-46	3 ⁻	58.64 5 94	M1		13.9	6.3	94.0 1	3 ⁻		37.34 5 0	2 ⁻ 1 ⁻	<2.8ns 29m 1
Cascading Gamma-ray															
37.34 5 100 M1 7.69 11.5 37.34 5 2 ⁻ <2.8ns 0 1 ⁻ 29m 1															
166 _{sm} Ho		1.2E+3y 2	49 2	(5 ⁻)	54.2392 7 100	E2		32.0	3.0	54.239 2	2 ⁻	3.44ns 12	0	0 ⁻	26.80h 2
160 _{sm} Tm		1.24m 3	40	(5,4,3)	140.33 5 100	E1		0.1372 88		140.33 5	0 ⁻ ,1 ⁻ ,2 ⁻		0	1 ⁻	9.4m 3
166 _{sm} Lu ¹		1.41m 10	8.5 22.8	(3 ⁻) (2 ⁻)	(8.5) ⁻ (14.3) ⁻	(M3) (M1)	Large			42.9 57.2	(0 ⁻) (1 ⁻)	2.12m 10	34.37 42.9	(3 ⁻) (0 ⁻)	1.41m 10 2.12m 10
					(26.1) ⁻	(E2) (E1)	3.19E+3 2.62	0.02 28		60.5	(3 ⁻)		34.37	(3 ⁻)	1.41m 10
166 _{sm} Lu ²		2.12m 10	14.3 17.6	(1 ⁻) (3 ⁻)	(14.3) ⁻ (26.1) ⁻	(M1) (E2)	196.4 3.19E+3	0.2 0.02		57.2 60.5	(1 ⁻) (3 ⁻)		42.9 34.37	(0 ⁻) (3 ⁻)	2.12m 10 1.41m 10
						(E1)	2.62	28		60.5	(3 ⁻)		34.37	(3 ⁻)	1.41m 10
171 _{sm} Lu		1.32m 3	(1.6 4)	2 ⁻	(1.6) ⁻	(E2)	Large			(72.9 2)	5/2 ⁻		71.3 2	1/2 ⁻	1.32m 3
172 _{sm} Lu		3.7m 5	24.0 11 26	(1 ⁻)	23.99 2 100	E1		3.30	23	65.86 10 68 ⁻	(1 ⁻)	0.33us 2	41.86 4	(1 ⁻)	3.7m 5

-Gamma-ray not observed

-Probably a doublet

TABLE OF SELECTED LOW ENERGY NUCLEAR TRANSITIONS - page 8

ISOMER		PUMPING RAD.		DE-EXCITING TRANSITIONS					UPPER LEVEL		LOWER LEVEL				
A	Z	T _{1/2}	E(kev)	L ^π	E(kev)	I _γ (%)	Mult.	ICC	I _{ex} (%)	E(kev)	J ^π	T _{1/2}	E(kev)	J ^π	T _{1/2}
174 _g	Lu	142d 2	29.3 9	(2 ⁻)	88.525 10	100	(M1)	5.37	16	200.2 9	(4 ⁻)		111.78 4	(3 ⁻)	
					Cascading Gamma-rays										
					67.08 2	99	M1+E2	12.0	7.6	111.78 4	(3 ⁻)		44.70 3	(2 ⁻)	
					111.7 1	0.9	E2	2.23	0.3			0	(1 ⁻)	3.31v 5	
177 _g	Lu	160.9d 3	9.99 8 15.09 6	6 ⁻ 5 ⁻	44.71 3	100	M1+E2	6.9	13	44.70 3	(2 ⁻)		0	(1 ⁻)	3.31v 5
					259.399	100	E2	0.1208	89	980.14 4	11/2 ⁻		720.74 5	7/2 ⁻	
					148.607	(71)	M1(+E2)	0.855	38	985.24 4	13/2 ⁻		816.64 3	11/2 ⁻	
					313.33	(15)	(E2)	0.0678	14			671.90 3	9/2 ⁻		
					544.35	(7)	M1(+E2)	0.0368	7			440.656 10	13/2 ⁻		
					716.89	(7)	(M1)	0.0183	6			268.787 4	11/2 ⁻		
					145.870	100	E2	0.85	54	957.26 4	13/2 ⁻		811.39 4	9/2 ⁻	
					235.898	(87)	(M1)	0.335	45	956.61 4	9/2 ⁻		720.74 5	7/2 ⁻	
					247.258	(13)	(E2)	0.140	11	709.35 3	5/2 ⁻				
					Cascading Gamma-rays										
					144.746	(76)	M1(+E2)	1.36	32	816.64 3	11/2 ⁻		671.90 3	9/2 ⁻	
					244.582	(9)	E2	0.0112	9				552.06 3	7/2 ⁻	
					547.81	(8)	(M1)	0.036	7				268.787 6	11/2 ⁻	
					695.26	(7)	M1+E2	0.020	6				121.620 3	9/2 ⁻	0.12ns 1
					49.740	(100)	E2	0.48	1.4	811.39 4	9/2 ⁻		761.65 4	5/2 ⁻	35ns 3
					90.66	(0.2)	(E1)	0.45	0.1				720.74 5	7/2 ⁻	
					52.085	(0.7)	(E1)	0.39	0.5	761.65 4	5/2 ⁻	35ns 3	709.35 3	5/2 ⁻	3.5ns 10
					188.080	(30)	(E1)	0.067	28				573.57 4	7/2 ⁻	0.8ns
					209.584	(9)	(E1)	0.051	8.5				552.06 3	7/2 ⁻	6.71d 1
					303.5	(0.6)	(E1)	0.0203	0.6				457.92 3	5/2 ⁻	3.5ns 10
					761.66 7	(60)	E1	0.0027	60				0	5/2 ⁻	0.8ns
					147.165 5	(1)	(E2)	0.82	55	720.74 5	7/2 ⁻		573.57 4	3/2 ⁻	6.71d 1
					135.783	(89)	M1+E2	1.62	34	709.35 3	5/2 ⁻		573.57 4	3/2 ⁻	3.5ns 10
					139.721	(8)	(E2)	0.98	4				569.62 3	1/2 ⁻	150us 10
					251.43	(2.4)	(M1)	0.285	2				457.92 3	5/2 ⁻	0.8ns
					119.836	(83)	M1(+E2)	0.27	25	671.90 3	9/2 ⁻		552.06 3	7/2 ⁻	0.8ns
					213.965	(4)	(E2)	0.27	3				457.92 3	5/2 ⁻	0.8ns
					403.1	(1)	(M1+E2)	0.080	1				268.787 6	11/2 ⁻	0.12ns 1
					550.36	(9)	M1+E2	0.036	9				121.620 3	9/2 ⁻	6.71d 1
					471.86	(3)	M1+E2	0.022	3	573.57 4	3/2 ⁻	3.5ns 10	0	5/3 ⁻	0.8ns
					115.653	(92)	(M1)	2.50	26				0	7/2 ⁻	0.8ns
					573.6	(8)	(E2)	0.0134	8	559.62 3	1/2 ⁻	150us 10	457.92 3	5/2 ⁻	0.8ns
					111.703	100	E2	2.20	31	552.06 3	7/2 ⁻		457.92 3	5/2 ⁻	0.8ns
					94.131	(84)	(M1)	4.55	15				121.620 3	9/2 ⁻	0.12ns 1
					430.52	(3)	M1+E2	0.067	3				0	7/2 ⁻	6.71d 1
					552.07	(13)	(M1+E2)	0.036	12	457.92 3	5/2 ⁻	0.8ns	121.620 3	9/2 ⁻	0.12ns 1
					336.33	(2)	(E2)	0.056	2				0	7/2 ⁻	6.71d 1
					457.90	(98)	M1	0.057	93	440.656 10	13/2 ⁻		268.787 6	11/2 ⁻	0.12ns 1
					171.868	(47)	M1+E2	0.83	26				121.620 3	9/2 ⁻	0.12ns 1
					319.04	(33)	E2	0.064	50	268.787 6	11/2 ⁻		121.620 3	9/2 ⁻	0.12ns 1
					147.165	(49)	M1+E2	1.30	30				0	7/2 ⁻	6.71d 1
					268.801	(31)	E2	0.109	28	121.620 3	9/2 ⁻	0.12ns 1	0	7/2 ⁻	6.71d 1
					121.620	100	M1+E2	2.43	29				0	7/2 ⁻	6.71d 1

TABLE OF SELECTED LOW ENERGY NUCLEAR TRANSITIONS - page 9

ISOMER		PUMPING RAD.		DE-EXCITING TRANSITIONS					UPPER LEVEL		LOWER LEVEL					
A	Z	T _{1/2}	E(kev)	L ^π	E(kev)	I _r (%)	Mult.	ICC	E(kev)	J ^π	E(kev)	J ^π	T _{1/2}			
179 _g Hf	72	25.1d 3	0.2	(9 ⁻ , 8)	891.5	5				1105.9	7/2 ⁻ , 9/2	214.3	(7/2) ⁻	1.86ns 5		
					983.2	23					122.7		0	11/2 ⁻	37ps 3	
					1105.9	72							0	9/2 ⁻	STABLE	
					999.1	24					1120.8		122.7	11/2 ⁻	37ps 3	
					15.1	76							0	9/2 ⁻	STABLE	
					-32.2	(10, 9, 8)					1073.5	(5/2, 7/2, 9/2)	337.7	(9/2) ⁻	1.86ns 5	
						16					214.3		214.3	(7/2) ⁻	1.86ns 5	
						84					337.7		122.7	11/2 ⁻	37ps 3	
180 _g Hf	72	5.5h 1	15	41.6 2	Decay not known				1157		93.324 2	2 ⁻	1.51ns 2			
					1089.9 2 100				1183.2 2		0	0 ⁻	STABLE			
					Cascading Gamma-rays											
					93.324 2 100				4.7	18		93.324 2	2 ⁻	1.51ns 2	0	0 ⁻
182 _g Ta	73	15.84m 10	27.4 5	(7) ⁻	Decay not known				547.1 2	(3) ⁻						
					39				559	(1 ⁻)						
					46.0				565.7	3, 4 ⁻						
					-14.3 5				505.4 2	(5) ⁻						
					-27.9 5				491.8 3	2, 5 ⁻						
					-32				488	(6 ⁻)	292.97 3	5 ⁻				
					-39.9 4				479.8 2	(4) ⁻	360.53 3	(3) ⁻				
											237.27 4	4 ⁻				
											97.80 2	3 ⁻	115.0d 2			
											0					
179 _g M	71	6.7m 3	42.7	(5) ⁻	Decay not known				474.4 7	(3) ⁻						
									360.53 3	(3) ⁻	270.41 3	2 ⁻				
											114.33 2	(4) ⁻				
											0	3 ⁻	115.0d 2			
									292.97 3	5 ⁻	114.33 2	(4) ⁻				
									270.41 3	2 ⁻	114.33 2	(4) ⁻				
											0	3 ⁻	115.0d 2			
									237.27 4	5 ⁻	114.33 2	(4) ⁻				
											97.80 2	4 ⁻				
											0	3 ⁻	115.0d 2			
179 _g M	71	6.7m 3	42.7	(5) ⁻	144.48 7	24	E2 (M1)	0.974m	264.6	(11/2) ⁻	119.9	(9/2) ⁻	37.3m 5			
					264.44 7	74	E2	0.126	0		0	(7/2) ⁻	37.3m 5			
					Cascading Gamma-rays											
					120.02 8	100	(M1, E2)		119.9	(9/2) ⁻	0	(7/2) ⁻	37.3m 5			

TABLE OF SELECTED LOW ENERGY NUCLEAR TRANSITIONS - page 10

ISOMER		PUMPING RAD.		DE-EXCITING TRANSITIONS					UPPER LEVEL			LOWER LEVEL		
A	Z	T _{1/2}	E(keV)	L _π	E(keV)	I _γ (%)	Mult.	ICC	I _π (%)	E(keV)	J _π	E(keV)	J _π	T _{1/2}
185	Re	1.67m	46.04 11	(2) ⁻	69.7 3 150.37 2 177.59 8 243.7 4	37 0.3 58 5	M1+E2 (E2) M1+E2 (E2)	14.3 3 0.814 0.92 12 0.163 4	2.4 0.2 30 4	243.45 10	(7/2) ⁻	173.68 2 93.30 5 65.86 3 0	7/2 ⁻ (3/2) ⁻ 5/2 ⁻ 3/2 ⁻	<1.5ns 75.1d 3
			-9.53 5	(3) ⁻	94.59 4 122.05 7 164.33 2 187.88 2	(21) (10) (29) (40)	(M1+E2) (M1+E2) (E2) (M1+E2)	5.4 4 2.3 5 0.614 18 0.6 2 25	3.3 3.1 18 25	187.88 2	(5/2) ⁻	93.30 5 65.86 3 23.54 5 0	(3/2) ⁻ 5/2 ⁻ (11/2) ⁻ 3/2 ⁻	75.1d 3
			-23.73 5	(2) ⁻	107.85 2 173.68 2	24 74	M1+E2 E2	3.4 2 0.506 49	6.0 49	173.68 2	7/2 ⁻	65.86 3 0	5/2 ⁻ 3/2 ⁻	75.1d 3
					Cascading Gamma-rays									
					69.7 93.30 5 42.29 5 65.86 3 23.54 5		(M1+E2) (M1+E2) E2 M1+E2 (M1+E2)			93.30 5 65.86 3 23.54 5	(3/2) ⁻ 5/2 ⁻ (11/2) ⁻ 3/2 ⁻	23.54 5 0 23.54 5 0	(11/2) ⁻ 3/2 ⁻ (11/2) ⁻ 3/2 ⁻	75.1d 3 75.1d 3 75.1d 3 75.1d 3
182	Re	64.0h	15	(4) ⁻	55.56 5	100	M1	5.12	16	55.54 4	(3) ⁻	0	2 ⁺	12.7h 2
184	Re	165d	48 -46 3 -46 3	(3) ⁻ (5) ⁻ (6) ⁻	Decay not known Decay not known Decay not known					236 142 3 142 3	(5) ⁻ (3) ⁻ (2) ⁻			
186	Re	2E+5y	24 36 -4	(4) ⁻ (2) ⁻ (5) ⁻	74.568 3 Decay not known 87.266 4 (98) 146.273 12	100 Decay not known (12) (2)	(M1) (M1) (E2)	12.50 8.0 0.96	7.4 11 0.9	173.929 6 1857 146.275 6	(4) ⁻ (6) ⁻ (3) ⁻	99.361 3 59.009 4 0	(3) ⁻ (2) ⁻ (1) ⁻	90.64h 9
					Cascading Gamma-rays									
					40.350 3 (89) 97.362 4 (11) 59.009 4 100	(89) (11) 100	M1+E2 E2 M1	13.844 4.20 4.35	(6) (2) 19	99.361 3 59.009 4	(3) ⁻ (2) ⁻	59.009 4 0	(2) ⁻ (1) ⁻ (1) ⁻	90.64h 9
188	Re	18.6m	10.674 11 33.273 11	(4) ⁻	(13.3) ⁻ 141.758 5 205.349 8	88 12	M1+E2 (M1+E2)	1.84 11 0.654 7	31	182.743 6 205.342 5	(2) ⁻	169.443 4 63.582 3 0	(3) ⁻ (2) ⁻ 1 ⁻	54ps 7 16.98h 2 16.98h 2
			35.786 10 (6,5) ⁻ -2.626 10 (3) ⁻		207.849 5 105.87 2 169.53 2	100 99 1	E1 M1+E2 (E2)	0.059 94 4.4 2 18 0.572 0.6		207.855 4 169.443 4	(0,1) ⁻ (3) ⁻	63.582 3 0	1 ⁻ 1 ⁻	54ps 7 16.98h 2
			-16.022 10 (3) ⁻		92.461 7 156.01 5 63.582 3	78 2 100	M1+E2 (E2) M1+E2	6.68 4 13 0.768 1		156.047 4	(3) ⁻	63.582 3 0	(2) ⁻ 1 ⁻	54ps 7 16.98h 2
190	Re	3.2h	~11	(4) ⁻	162.1 1	100	M1+E2	3.56 4	22	63.582 3	(2) ⁻	0	1 ⁻	16.98h 2
193	Os	9.9h	48.4	(4) ⁻	122.8 3 219.3 3 96.5	(90) (10) 100	(M1+E2) (E2) (M1+E2)	3.234 0.247 8	21	219.3	(13/2) ⁻	96.5 0	(11/2) ⁻ (9/2) ⁻	13.0h 5 13.0h 5
					Cascading Gamma-rays									
					96.5	100	(M1+E2)			96.5	(11/2) ⁻	0	(9/2) ⁻	13.0h 5

-Gamma-ray not observed

TABLE OF SELECTED LOW ENERGY NUCLEAR TRANSITIONS - page 11

ISOMER		PUMPING RAD.		DE-EXCITING TRANSITIONS					UPPER LEVEL		LOWER LEVEL		
A Z	T _{1/2}	E(kev)	L ^a	E(kev)	1 _γ (%)	Mult.	ICC	I _γ (%)	E(kev)	J ^π	T _{1/2}	J ^π	T _{1/2}
189 _g Os	5.8h 1	5.34 4 38.71 4	4 ⁻ 2 ⁻	36.20 2 33.32 4 69.54 2	100 14 86	M1+E2 E2 M1+E2	21.1 5 0.02 7.2 2	4.5 0.02 10	36.19 2 69.54 2 0	1/2 ⁻ 5/2 ⁻ 0	0.52ns 2 1.64ns 3 0	3/2 ⁻ 1/2 ⁻ 3/2 ⁻	STABLE 0.52ns 2 STABLE
191 _g Os	13.10h 5	10.0 2	(1 ⁻)	(10) ⁻		(M1)	Large		84.4 2	(1/2 ⁻)		3/2 ⁻	13.10h 5
192 _g Ir ^a	1.45m 5	11.07 16 48.1 4		7 48.0568 8 100					69.07 15 106.0570 7			1 ⁻	1.45m 5
192 _g Ir ^a	241y 9	39.63 12		77.9466 8 88.7335 8 134.792 2					194.7906 8			1 ⁻	1.45m 5
		49.4 11 -12.2 8 -38.32 2 -49.10 12		Decay not known Decay not known 58.8438 10 100 48.0568 8 100					204.6 11 143.0 8 116.8439 8 106.0570 7			1 ⁻ 1 ⁻	1.45m 5 1.45m 5
193 _g Ir	10.40d 11	-7.22 4	5 ⁻	73.012 7	100	M1+E2	6.8 2	13	73.017 7	1/2 ⁻	6.09ns 15	3/2 ⁻	STABLE
185 _g Pt	33.0m 8	-34.3	(5 ⁻)	94.7 3	100	M1+E2	0.83m	55	94.7 3	(11/2 ⁻)		(9/2 ⁻)	71m 2
193 _g Pt	4.33d 3	38.03 5	(5 ⁻)	73.62 3 173.52 5 186.17 3 187.83 4	1.4 23 71 ~5	(M1) M1+E2 M1+E2 E2+M1	2.99 1.34 2 1.10 2 ~0.55	0.4 9.8 34 ~3	187.81 2 14.28 1 1.642 2	(3/2 ⁻) (5/2 ⁻) (3/2 ⁻) (1/2 ⁻)	114.16 1 14.28 1 0	(3/2 ⁻) (5/2 ⁻) (3/2 ⁻) (1/2 ⁻)	2.52ns 3 9.7ns 3 50y 9
		49.2 2 -28.50 5 -35.62 4	(1 ⁻) - (5 ⁻)	49.2 2 119.64 3 99.88 4 112.515 10 114.155 13	100 5 70 25	(M1) M1+E2 M1+E2 M1+E2 M1+E2	9.8 3.7 4 6.12 4 4.72 3 4.39 6	9 21 12 12 4.6	199.0 2 121.28 3 114.16 1	(11/2 ⁻) - (3/2 ⁻) (3/2 ⁻) (3/2 ⁻)	149.78 4 1.642 2 14.28 1 1.642 2 0	(13/2 ⁻) (3/2 ⁻) (5/2 ⁻) (3/2 ⁻) (1/2 ⁻)	4.33d 3 9.7ns 3 2.52ns 5 9.7ns 3 50y 9
				Cascading Gamma-rays: 12.634 8 1.642 2	100 100	M1+E2 (M1)	149 10 1.35E+4	0.7 7E-3	14.28 1 1.642 2	(5/2 ⁻) (3/2 ⁻)	2.52ns 5 9.7ns 3	(3/2 ⁻) (1/2 ⁻)	9.7ns 3 50y 9
195 _g Pt	4.02d 1	-20.0 4	4 ⁻	(28.1) ⁻ 140.6 239.5 3 211.4 3	28 45 27 100	(M1) M1+E2 E2 M1+E2	51.4 2.57 13 0.20 0.76	0.5 13 22.5 57	239.4 3 0 211.35 3	5/2 ⁻	80ps 4 0 67ps 5	3/2 ⁻ 3/2 ⁻ 1/2 ⁻	67ps 5 0.163ns 2 STABLE
		-48.0 4	5 ⁻	98.90 2	100	M1+E2	7.12	12	98.881 15	3/2 ⁻	0.163ns 2	1/2 ⁻	STABLE
				Cascading Gamma-rays: 98.90 2	100	M1+E2	7.12	12	98.881 15	3/2 ⁻	0.163ns 2	1/2 ⁻	STABLE
197 _g Pt	1.573h 13	26.17 3 -29 6		Decay not known Decay not known					425.77 2 371 6				
189 _g Au	4.59m 11	1.2 2	3 ⁻	44.7 3 238.6 2 248.5 2 194.0 3 203.8 2	<5 52 43 47 >93	(M1) M1+E2 (E2) (M1) M1	14.29 0.34 7 0.185 1.143 1.00	0.3 39 36 3 47	248.5 1 0 9.9 2 203.8 1	5/2 ⁻ - 3/2 ⁻ 3/2 ⁻	203.8 1 9.9 2 0 9.9 2	3/2 ⁻ 3/2 ⁻ 1/2 ⁻ 3/2 ⁻	30ns 4 28.7m 3 30ns 4 28.7m 3
		-45.3 2	4 ⁻	Cascading Gamma-rays: 9.9 2	100	(M1, E2)			9.9 2	3/2 ⁻	30ns 4	1/2 ⁻	28.7m 3

^aGamma-ray not observed

TABLE OF SELECTED LOW ENERGY NUCLEAR TRANSITIONS - page 12

ISOMER		PUMPING RAD.		DE-EXCITING TRANSITIONS					UPPER LEVEL		LOWER LEVEL							
A	Z	T _{1/2}	E(keV)	L ^π	E(keV)	I _γ (%)	Mult.	ICC	I _γ (%)	E(keV)	J ^π	T _{1/2}	E(keV)	J ^π	T _{1/2}			
198Au	2.30d	4	20.9 15 (10 ⁻⁹) -10.4 15 (10 ⁻⁹)	571.38 2	100		M1	0.0615	94	832.64 2	2 ⁻ , 3 ⁻		261.253 3	2 ⁻				
				539.992 15	69					69	801.245 18	2 ⁻		261.253 3	2 ⁻			
				542.06 3	18					18				1 ⁻	259.194 3			
				801.35 10	13					13				2 ⁻	0	2.696d 2		
				418.588 9	100		(M1)	0.1406	88	799.566 12	(3 ⁻ , 4 ⁻)		380.978 4	3 ⁻ , 4 ⁻		380.978 4	3 ⁻ , 4 ⁻	
				383.084 8	31				31	788.82 2	1 ⁻ , 2 ⁻		405.775 4	1 ⁻ , 2 ⁻		405.775 4	1 ⁻ , 2 ⁻	
				527.57 4	10				10				261.253 3	2 ⁻		261.253 3	2 ⁻	
				529.624 15	43				43				259.194 3	1 ⁻		259.194 3	1 ⁻	
				552.68 15	2				2				235.914 3	(2) ⁻		235.914 3	(2) ⁻	
				497.82 8	10				10				90.953 2	0 ⁻		90.953 2	0 ⁻	
				733.4 3	4				4				55.151 5	1 ⁻		55.151 5	1 ⁻	
				314.736 4	100					764.048 8			449.312 4	3 ⁻		449.312 4	3 ⁻	
			Cascading Gamma-rays															
			121.017 6				(M1)		1.7 ⁺				328.291 5	(2) ⁻		328.291 5	(2) ⁻	
			188.059 3				M1	1.248	10 ⁺				261.253 3	2 ⁻		261.253 3	2 ⁻	
			201.878 5				E2, M1		1.5 ⁺				247.430 3	1 ⁻ , 2 ⁻		247.430 3	1 ⁻ , 2 ⁻	
			234.467 5				(M1)		7 ⁺				214.842 3	4 ⁻		214.842 3	4 ⁻	
			449.327 11				M1(E2)		9 ⁺				0	2 ⁻		0	2.696d 2	
			144.521 4				(M1, E2)		0.9 ⁺				405.775 4	1 ⁻ , 2 ⁻		405.775 4	1 ⁻ , 2 ⁻	
			158.347 3				M1(E2)		10 ⁺				261.253 3	2 ⁻		261.253 3	2 ⁻	
			169.860 4				(M1, E2)		1 ⁺				247.430 3	1 ⁻ , 2 ⁻		247.430 3	1 ⁻ , 2 ⁻	
			212.937 4				(M1, E2)		0.5 ⁺				235.914 3	(2) ⁻		235.914 3	(2) ⁻	
			350.630 7				(M1, E2)		6 ⁺				192.833 2	1 ⁻		192.833 2	1 ⁻	
			405.76 2				(M1, E2)		0.2 ⁺				55.151 1	1 ⁻		55.151 1	1 ⁻	
			145.061 3				M1, E2		1.1 ⁺				0	2 ⁻		0	2.696d 2	
			164.130 3				(M1, E2)		1 ⁺				380.978 4	3 ⁻ , 4 ⁻		380.978 4	3 ⁻ , 4 ⁻	
			380.991 8				E2	0.0524	10 ⁺				214.842 3	4 ⁻		214.842 3	4 ⁻	
			113.448 7				(E2)		0.5 ⁺				0	2 ⁻		0	2.696d 2	
273.143 7						0.2 ⁺				55.151 1	1 ⁻		55.151 1	1 ⁻				
328.291 6				M1	0.270	10 ⁺				0	2 ⁻		0	2.696d 2				
204.104 4				(M1)	0.969	2.8				53.151 1	1 ⁻		53.151 1	1 ⁻				
261.253 4				M1	0.503	63				261.253 3	2 ⁻		261.253 3	2 ⁻				
46.354 3				(M1)		0.8 ⁺				259.194 3	1 ⁻		259.194 3	1 ⁻				
168.236 3				M1	1.710	10 ⁺				0	2 ⁻		0	2.696d 2				
204.039 4				(M1)		1.2 ⁺				55.151 1	1 ⁻		55.151 1	1 ⁻				
259.196 9				(M1)		0.06 ⁺				0	2 ⁻		0	2.696d 2				
156.474 4				(M1, E2)		0.2 ⁺				247.430 3	1 ⁻ , 2 ⁻		247.430 3	1 ⁻ , 2 ⁻				
192.279 3				M1(E2)		6.4 ⁺				55.151 1	1 ⁻		55.151 1	1 ⁻				
247.430 4				M1(E2)		0.48 8				0	2 ⁻		0	2.696d 2				
180.759 3				E2	0.540	9				235.914 3	(2) ⁻		235.914 3	(2) ⁻				
235.916 4				M1(E2)	0.44 11	59				0	2 ⁻		0	2.696d 2				
214.841 3				E2	0.297	77				214.842 3	4 ⁻		214.842 3	4 ⁻				
101.8717 3										192.833 2	1 ⁻		192.833 2	1 ⁻				
137.680 2				(M1)	3.02	12				90.953 2	0 ⁻		90.953 2	0 ⁻				
192.835 3				(E2)	0.430	36				55.151 1	1 ⁻		55.151 1	1 ⁻				
35.799 3				M1	27.6	2.7				0	2 ⁻		0	2.696d 2				
90.952 2				E2	7.90	2.4				55.151 1	1 ⁻		55.151 1	1 ⁻				
55.1506 14				M1(E2)	12.5 7	7.4				0	2 ⁻		0	2.696d 2				

*Relative photon intensity

TABLE OF SELECTED LOW ENERGY NUCLEAR TRANSITIONS - page 13

TABLE OF SELECTED LOW ENERGY NUCLEAR TRANSITIONS - page 13															
ISOMER		PUMPING RAD.			DE-EXCITING TRANSITIONS					UPPER LEVEL			LOWER LEVEL		
A Z	T _{1/2}	E(keV)	L ^π	E(keV)	I _r (%)	Mult.	ICC	I _{ex} (%)	E(keV)	J ^π	T _{1/2}	E(keV)	J ^π	T _{1/2}	
197 _m Mg	23.8h 1	8.9 2	(4) ⁻	173.78 10	30	M1	1.71	11	307.8 2	(5/2) ⁻		133.98 5	5/2 ⁻	8.1ns 2	
				307.8 2	70	(E2)		0.100	64			0	1/2 ⁻	44.14h 5	
		9.6 2	(5) ⁻	156.41 12	22	(M1+E2)	1.7	8	308.5 2	(3/2) ⁻		152.16 8	3/2 ⁻	64.14h 5	
				308.6 2	78	(M1)	0.35	58				0	1/2 ⁻	64.14h 5	
				Cascading Gamma-rays											
				18.18	7	(M1)	2.24	0.03	152.16 8	3/2 ⁻		133.98 5	5/2 ⁻	8.1ns 2	
				152.22 7	93	M1	2.48	27			8.1ns 2	0	1/2 ⁻	44.14h 5	
				133.99 7	100	E2	1.73	37	133.98 5	5/2 ⁻		0	1/2 ⁻	64.14h 5	
196 _m Tl	1.41h 2	-28.1	(6 ⁻ , 5 ⁻)	113				2 ⁻	366.6 10	(1,2) ⁻		253.2 4	(1 ⁻)		
				128				2 ⁻				240.3 4	(2 ⁻)		
				175				4 ⁻	191.8 4			0	(0 ⁻)		
				366.6 10		(M1)	0.24	100 ⁻				0	2 ⁻	1.84h 3	
				Cascading Gamma-rays											
				253.2	41	M1	0.65	61	253.2 4	(1 ⁻)		0	2 ⁻	1.84h 3	
				240.3 4	100	M1+E2	0.65	10 41	240.3 4	(2 ⁻)		0	2 ⁻	1.84h 3	
				191.8 4	100	E2	0.48	48	191.8 4	(0 ⁻)		0	2 ⁻	1.84h 3	
202 _m Pb	3.62h 3	38.66 15	(2) ⁻	168.11 4	98	E2	0.809	54	2208.45 8	(7) ⁻	42ns 4	2040.34 7	5 ⁻	1.97ns 2	
				823.4 3	2	(E3)	0.0247	2				1382.85 6	4 ⁻		
				Cascading Gamma-rays											
				124.75 9	(97)	(E1)	0.255	77	2040.34 7	5 ⁻		1915.13 7	4 ⁻		
				417.3 2	(1)	(E1)	0.014	1				1623.07 7	4 ⁻		
				637.49 6	(2)	E1	0.0055	2				1382.85 6	4 ⁻	1.97ns 2	
				Only gammas with E>200 keV follow.											
234 _m Pa	1.17m 3	29.5	(2 ⁻)	29.49 2	100	E2	4.48E+3	0.02	103.41+K	(2 ⁻)	<0.5ns	73.92+K	(0 ⁻)	1.17m 3	
235 _m U	~25m	12.963 2	1 ⁻	12.963 2	100	(M1+E2)	~1E+3	0.1	13.040 2	3/2 ⁻	0.50ns 3	0.0768 5	1/2 ⁻	~25m	
		46.127 3	4 ⁻	46.204 6	100	M1+E2	60 20	1.6	46.204 3	9/2 ⁻	~14ps	0	7/2 ⁻	703.8E+6y 5	
240 _m Np	7.22m 2	44.1	1(1 ⁻)	44.10 7	100	M1	60.5	1.6	44.1+K	1(1 ⁻)		0.0+K	1(1 ⁻)	7.22m 2	
242 _m Am	141y 2	4.3	(2 ⁻)	52.9377	1007	(E2)	362	0.37	52.9	(3 ⁻)		0	1 ⁻	16.02h 2	
		27.2	(3 ⁻)	73.818	1007	(M1)	15.10	6.27	73.8	(2 ⁻)		0	1 ⁻	16.02h 2	
		-4.57	(5 ⁻)	44.092	100				44.17	(0 ⁻)		0	1 ⁻	16.02h 2	
244 _m Am	~26m	12 3	(1) ⁻	Decay unknown					100.3092 11	(2) ⁻					
		35 3	(2) ⁻	22.975 10	98	M1	126	0.8	123.2811 11	(3) ⁻		100.3092 11	(2) ⁻	~26m	
				35.31 3	2	E2	2.56E+3	8E-4				88 3	1 ⁻		
246 _m Am	25.0m 2	16.23 3	(1) ⁻	(16.23) ⁻	100				16.23 3	(1 ⁻)	4.3ns 2	20	2 ⁻	25.0m 2	
		43.81 2		27.58 2	24	(E1)	3.97	5	43.81 2	(1 ⁻)		16.23 3	2 ⁻	25.0m 2	
				43.81 2	76	(E1)	1.194	35				20	2 ⁻	25.0m 2	

-Gamma-ray not observed

-Relative photon intensity

-Gamma-ray not observed
-Relative photon intensity

II. SYMMETRY APPROACH TO ENHANCED SPONTANEOUS DECAY OF NUCLEI

A. INTRODUCTION

The requirements for nuclear superradiance have now been discussed by Baldwin and Feld (Ref. 8). The requirements are based on the approach of coupled Maxwell-Schrodinger equations in a semiclassical model developed by Feld (Ref. 9) and references therein.

Concurrent with the developments by Baldwin and Feld, we have considered the question of what all of this means for a gamma-ray laser. The questions of actual candidate nuclei have, in part, been answered; the data for many "useful" levels is missing for states in the vicinity of long-lived isomers (Re^{186} , Am^{242} and Ho^{162} for example); yet, still no known scheme allows for the successful production of a lasing transition from a long-lived state. Nonetheless, Re^{186} looks quite interesting, as does Am^{242} , for the possible production of isotropic x-ray energy sources in plasmas. The possibility of lasing by excitation from a ground state of a nucleus is certainly an interesting one; for this reason we will consider some aspects of the theory of superradiance.

The theory of superradiance is not necessarily well known to nuclear chemists and nuclear physicists, but the underlying symmetry as first presented by Dicke (Ref. 10) generally is. Consequently, we set out to see if a simple treatment of the effect could be summarized using the group theoretical approach.

In proceeding, we note that there are still some differences between the original approach of Dicke and the semiclassical approach. These distinctions, outlined in Ref. 11, are (1) the effect arises from an assumed symmetry, (2) other than photon bosonic fields can be considered (Ref. 12), and (3) other than totally symmetric states (i.e., subradiant states) can enter [as recently seen in single-photon experiments (Ref. 13)].

Here we address item 1 in sufficient detail to show that the conditions for "superradiance" in the group-theoretical approach are in general agreement with those derived in the semiclassical approach. Specific problems in the gamma-ray regime are then

addressed. We are also ultimately interested in more than two-level systems. The symmetry approach can be extended to N-level systems through the extension of the SU(2) Dicke symmetry to SU(N) and treating the many two-level systems as SU(2) subgroups (which now, in general, do not commute with each other.) The dynamics is certainly expected to be rich and important for nuclear problems since many-level schemes are more complicated than simple, two-level systems.

Item 2 refers to the coherent pion emission problem, discussed in Ref. 11. Since the extension of Dicke's approach to such problems has thus far been straightforward, no further allusions to the "pion laser" are made here.

Item 3, the mixed symmetry states, may play a physical role. They all have reduced radiation rates and must be considered in treatments of off-axis emission or dephasing.

A brief summary of group theory jargon is included in Appendix A, and textbook descriptions of Dicke's model and the semiclassical approach are presented in Appendices B and C.

Finally, we emphasize the symmetry aspects of Dicke's theory. We refer to the results of his theory as "enhanced spontaneous decay" to avoid the experimental observations called "superradiance" or "superfluorescence". Dicke's theory must still be applied to particular models. For example, one can add to Dicke's theory stimulated emission or absorption terms to take account of the radiating material being in some electric field (e.g., self-generated). This can alter the pulse characteristics and lead, for example, to ringing effects. These approaches (for example, mean field theories, Ref. 14) are still not necessarily the causes of observed ringing. Ultimately, the semiclassical approach has best treated the propagation effects; and most-particularly, the transverse field effect accounts for the observed ringing in the two-level Cs system (Ref. 15). Thus, as far as nomenclature is concerned, we use Dicke's original term of "enhanced spontaneous decay" for the physical essence of the problem, "stimulation terms" for the effects of including photon occupancy number in simple extensions of Dicke's approach (in one-dimensional models), "superradiance" and "superfluorescence" for the actual effects which include more detailed three-dimensional propagation, as originally intended.

Since, the photon absorption cross sections by nuclei in the gamma-ray regime are so small, due to the short wavelength, the linear (whisker) geometry naturally arises, as discussed in the final sections of the text. The linear geometry is also historically preferred,

since practical problems, such as limiting heating effects in pumping, may also be lessened in a linear geometry.

B. GROUP APPROACH TO DICKE SUPERRADIANCE

1. Objectives

In Ref. 10, R.H. Dicke presents an extensive study of enhanced spontaneous decay (some states of which he calls "superradiant"). The basic premise in the work is that all emitters (in the actual paper he treats molecules) interact with a common radiation field and hence cannot be treated as independent entities. The key mathematical aspects of the theory proposed by Dicke are summarized in Appendix B. The model can be used to simulate some actual conditions to gain insight into "superradiant" models.

The advantages in constructing a simple model to examine aspects of all of the possible states of the system as originally described by Dicke are summarized below:

1. It is useful to program Dicke's model and simulate the superradiant pulse formation by observing decay from highest energy ("weight") states. This is done to gain an understanding of the relationship of the group versus semiclassical approaches.
2. It is useful to simulate pumping of the low-energy states to higher energy states from some initial distribution and calculate the follow-on emitted pulse to understand effects of incomplete inversion.
3. It is useful to derive analytical expressions in Dicke's approach to compare to analytical formulae, where known.
4. The theory is inherently based on the symmetries P_N (permutation group of N objects) and $U(2)$ (internal dynamical symmetry of the quantum mechanical two-level system). Successive symmetry labels or "quantum numbers" are τ from P_N and r from $SU(2)$ (these are described in Appendix A). By introducing operators affecting $\Delta\tau$ and Δr transitions, one can introduce "dephasing" or loss terms into the previous exercises (Nos. 1, 2, and 3), and reexplore the superradiant pulse formation process.

Of the items discussed in the original part of the proposal, items 1 and 3 are examined. Items 2 and 4 are qualitatively discussed.

2. Summary of the Theory and Aspects of Mixed-Symmetry States

Consider an atom, A, having two internal states--excited and unexcited--denoted by an index k ($k = \alpha$ or β , respectively). Then all states of N -such atoms; completely and simultaneously classified according to the permutation group P_N of atoms with indices i and the unitary group $U(2)$ of internal states are denoted $|\tau r m\rangle$. This nomenclature is discussed in greater detail in Appendix A. Here, τ is a Young tableau label of P_N while r and m are $U(2)$ group eigenvalues. Physically, τ is descriptive of the relative phasings between the individual wave functions of cooperating emitters, r is descriptive of the number of cooperating emitters, and m is a measure of the population inversion. The $U(2)$ group operators are R_+ , R_- , R_0 , and N . Hence $r(r+1)$ is the eigenvalue of R^2 and m is the eigenvalue of R_0 . The square of the matrix element, $M(r,m)$, is proportional to the transition rates between states of the system and is also significant:

$$M(r,m) = [(r+m)(r-m+1)] = |\langle \tau r m-1 | R_- | \tau r m \rangle|^2. \quad (1)$$

Then the lattice diagram (weight diagram) Fig. 1 is set up (illustrated for the case of three emitters, see Appendix A for details on nomenclature):

The matrix element $M(r,m)$ of the shifting generator does not allow for transitions between the multiplets (depicted as columns) in Fig. 1. Physically, the matrix element is proportional to the interaction with the electromagnetic field. Thus, τ and r remain good quantum numbers as long as the permutation symmetries and $SU(2)$ symmetries are unbroken. Only transitions depicted in Fig. 2 occur. Assume a spontaneous decay rate for the transition of λ_0 , then $\lambda(r,m) = \lambda_0(r,m)M(r,m)$, where $\lambda(r,m)$ is the spontaneous decay rate which is now dependent on r and m . We can calculate the rates as illustrated in Fig. 2, assuming for convenience that $\lambda_0 = 1$:

Figure 2 illustrates the totally symmetric irreducible representation (irrep) has enhanced decays of $3X$, $4X$, and $3X$ faster than the other two two-level multiplets. For small N this simple model is easy to program, and this is done in the next section. First, though, it is clear even beforehand that the totally symmetric irrep is, from an engineering standpoint, most favorable to laser developers. Note also that even N systems have a non-decaying multiplet; all odd N systems decay, regardless of multiplet.

τ	<table><tr><td>1</td><td>2</td><td>3</td></tr></table>	1	2	3	<table><tr><td>1</td><td>2</td></tr><tr><td>3</td><td></td></tr></table>	1	2	3		<table><tr><td>1</td><td>3</td></tr><tr><td>2</td><td></td></tr></table>	1	3	2		<table><tr><td>1</td></tr><tr><td>2</td></tr><tr><td>3</td></tr></table>	1	2	3
1	2	3																
1	2																	
3																		
1	3																	
2																		
1																		
2																		
3																		
	$r = 3/2$	$r = 1/2$	$r = 1/2$	No multiplet allowed in SU(2)														
$m = +3/2$	_____																	
$m = +1/2$	_____	_____	_____															
$m = -1/2$	_____	_____	_____															
$m = -3/2$	_____																	

Figure 1. The eight states of the three-particle system illustrate the classification of states according to the permutation group tableaux, the cooperation number (r), and the inversion (m). The symmetric multiplet is associated with Dicke superradiance. Mixed symmetry states would have subradiant or reduced decay rates corresponding to a Bloch vector of diminished length.







	$r = 3/2$	$r = 1/2$	$r = 1/2$
$m = +3/2$			
$m = +1/2$			
$m = -1/2$			
$m = -3/2$			

Figure 2. Decay rates for the multiplets illustrated in Fig. 1 according to Dicke's theory. The rates are listed as multiples of the spontaneous decay rate (e.g., 3X means three-times faster, etc.)

Later, we examine the pulse characteristics of the totally symmetric multiplet in greater detail, using simple differential equations. These equations apply for cases having larger numbers of cooperating emitters, where it is inconvenient to exploit the almost continuous behavior of m . For large N systems we can substitute $m = r \cos \theta$ where θ is the angle between a vector of length $\sqrt{r(r+1)}$ and a z -component of length m . Then:

$$\begin{aligned} M(r,m) &= | \mathbf{r} \cdot \mathbf{r} | - m(m-1) \\ &= r^2 \sin^2 \theta + r \cos \theta + r \\ &\equiv r^2 \sin^2 \theta \end{aligned} \quad (2)$$

Here $| \mathbf{r} \cdot \mathbf{r} |$ refers to the length of the vector which, of course, is $r(r+1)$ in the quantum case. For large r , the quadratic term overrides the linear term; but for small θ the linear term characteristic of the quantum approach (as well as the non-zero value for the angle) insures that the pulse is initiated.

The intensity of emitted light (I):

$$I = M(r,m) I_0 \quad (3)$$

is equal to the rate of energy loss. (Here E is the energy spacing $E_a - E_b$):

$$\begin{aligned} -d(mE)/dt &= M(r,m) I_0 \\ -d(r E \cos \theta)/dt &= M(r,m) I_0 \\ -(dr/dt) E \cos \theta + E r \sin \theta d\theta/dt &= r^2 \sin^2 \theta I_0 \end{aligned} \quad (4)$$

At this point we can assume that *without* symmetry breaking effects, r always remains a good quantum number, and $dr/dt = 0$. We then get:

$$d\theta/dt = (r I_0/E) \sin \theta \quad (5)$$

By solving this equation, the basic characteristics of the pulse emitted from decay of the highest weight state of the totally symmetric irrep are easily determined. (In general, a model could start from a distributed set of initial states and pump up and relax. The problem is then only slightly more complicated, but easily examined for small N and perhaps analytic expressions exist for large N .)

Further details of enhanced spontaneous decay are discussed in later sections. Now it is convenient to discuss the mechanisms by which non-ideal effects can be treated in the Dicke picture. Detrimental effects can arise by considering transitions which change r , transitions which change the tableaux symmetry, or the presence of other levels which

change all quantum numbers. In general, the system may start from a distributed ground state and be pumped up as illustrated in Fig. 3. This further complicates the pulse formation process since cross-multiplet transitions occur both in pumping and decay.

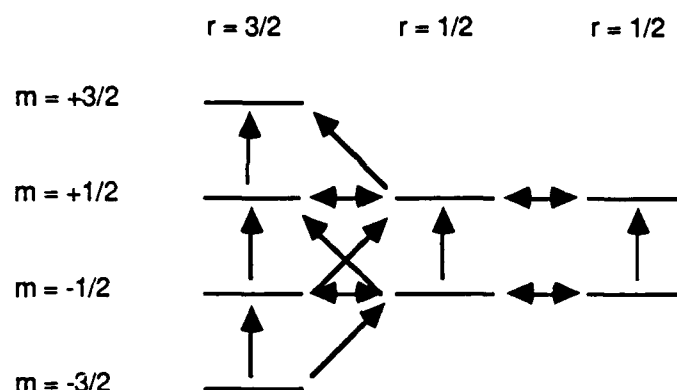


Figure 3. Detrimental effects in pumping. Realistic effects, as discussed in the text, can mix r -multiplets (ruining the ideal symmetry) and thus allow some transitions between multiplets. Some of those transitions are illustrated here where the system is being pumped up. The same intra-band transitions also occur in deexcitation.

Qualitatively, effects which alter the simple model based on the totally symmetric irrep in simple physically meaningful ways are as follows:

1. Restriction of the emission to a single specific direction, k . Then, for emission in direction k' different from k , the states of r are not good states of r' . After a single emission in direction k other than k' , in the ladder, $\Delta r = \pm 1, 0$ since some state of r is a mixture of states of r' . In reality, many ladders can be mixed and the more successful are probably the longest ones.
2. Deviations from the characteristics of pure two-level systems. Decay of state "a" or state "b" to some state "c" leads to competing superradiant multiplets and at the minimum, Δr processes. This is because, even in Dicke's approach, non-commuting $SU(2)$ subgroups of $SU(N)$ enter.
3. Dephasing. This appears as a $\Delta\tau$ process between multiplets of degenerate τ , assuming "special" phasings are associated with states of the mixed symmetry irreps (irreducible representations).
4. Photon losses. Here, Δm processes not contributing to the photons in the pulse must be included to account for photon absorption in the medium.

Lacking explicit treatment of these previous four realities, even in Dicke's picture, we examine the characteristics of pulses from the totally symmetric irrep in the following sections. The three-level system, approachable by using the algebra of the three SU(2) subgroups of SU(3) is addressable using the background information summarized in Appendix A. With these problems aside, the totally symmetric irrep is expected to give the most optimistic results.

C. DICKE SUPERRADIANCE FOR THE CASE OF THE TOTALLY SYMMETRIC MULTIPLY-STATISTICAL MODELS

1. Characteristics of Pulses

The totally symmetric multiplet in the Dicke model is the unique multiplet labelled by the cooperation number $r = N/2$ where N is the number of two-level atoms participating. This multiplet has the largest r for a given N . Other multiplets have N participating atoms but a cooperation number less than $N/2$. Thus, cooperation number and total participating numbers are distinguished for other than totally symmetric multiplets.

The lattice or weight diagram for the totally symmetric irreducible representation labelled by $r = N/2$ has $2r + 1$ steps labelled by m . As previously noted, the decay rate for each step on the lattice diagram is given by $\lambda = \lambda_0 (r + m)(r - m + 1)$ where m is the lattice step occupied previously in time and λ_0 will hence be set equal to one second (here we use λ to denote rates and the distinction from the wavelength is evident in context; these rates are equivalent to the widths used in the previous section). Assuming that a photon from each spontaneous decay appears at intervals $1/\lambda$, the number of photons in some time interval Δt can be counted, so that is what we first do. Here Δt is a suitable fractional multiple of the time duration of the complete pulse. For the moment, we assume that none of the photons created in the decay interact with the atoms to produce stimulated emission or absorption effects. Consequently, we are strictly treating Dicke superradiance or "pure superfluorescence". Typical pulses in this approach are depicted in Fig. 4.

Alternatively, the statistical nature of the spontaneous decay rate can be incorporated by introducing a normalized distribution function $\rho(\lambda, t)$ for each λ ; recalling $\lambda = \lambda(m)$: $\rho[\lambda] = \lambda(m)e^{-\lambda(m)t}$. The resulting pulse is then an ensemble average of many pulses, each with counts collected in a set of common time bins. Results for a typical single statistical pulse and an average of many pulses is detailed in Fig. 4 for comparison with the

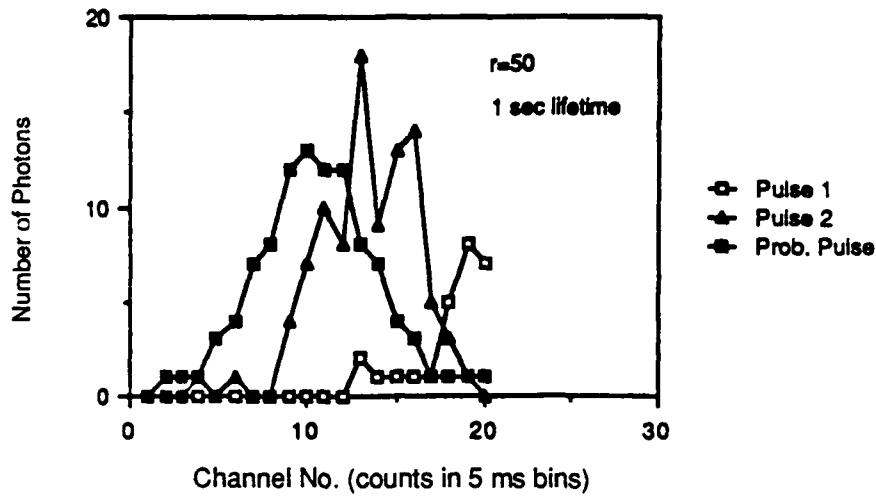


Figure 4. Three statistical pulses and one most probable pulse are based on a computer simulation for a small value of r .

previous result. Here, the cooperation number is unchanged, and the agreement with the "most probable" pulse shape is clear. By "most probable" pulse we are referring specifically to the case where the successive time sequences $\Delta t(m)$ for photon appearance from state m is given by $1/\lambda(m)$.

As the r quantum number increases, the pulse duration decreases, as indicated in Table 2.

Table 2. Cooperation Number and Pulse Duration

r	Pulse Duration (ms)
1	1000
2	830
4	600
8	400
16	250
32	150
64	84
128	47
256	27
512	15
1024	8.0
2048	4.3
4096	2.3

The pulse associated with $r = 8192$ is depicted in Fig. 5, and the strong r dependence of the pulse duration is depicted in Fig. 6. For the "8192" pulse we observe a symmetric distribution with delay times comparable to pulse width. The complete pulse duration is 1.3 ms.

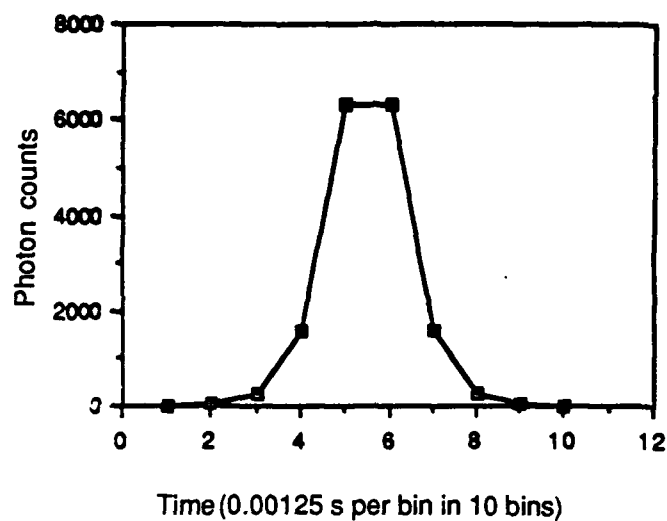


Figure 5. A typical pulse shape for $r = 8192$.

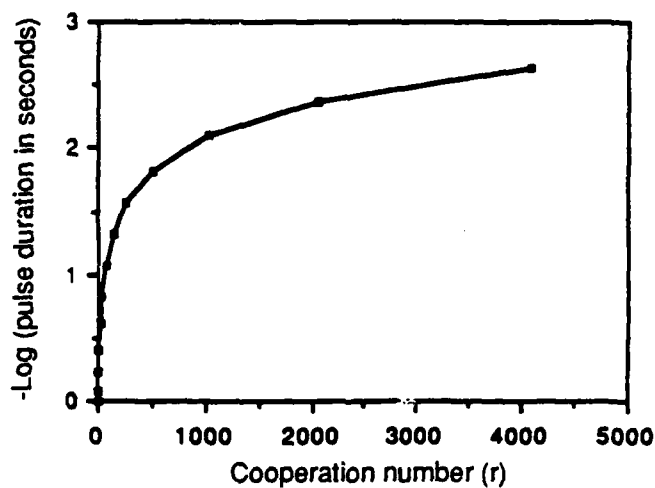


Figure 6. Pulse duration as function of r from the statistical simulations, assuming a spontaneous lifetime of 1 s.

The $1/r$ dependence of the pulse duration is seen in Figs. 7 and 8. As more easily seen in the second of the two figures, the $1/N$ dependence is seen as an approach towards a constant slope near the origin. Strong deviations in the points for $r = 1$ and $r = 2$ (and smaller r in general) are observed due to the quantum effects which arise when the r -dependent terms in the spontaneous decay rate are comparable to the r^2 terms.

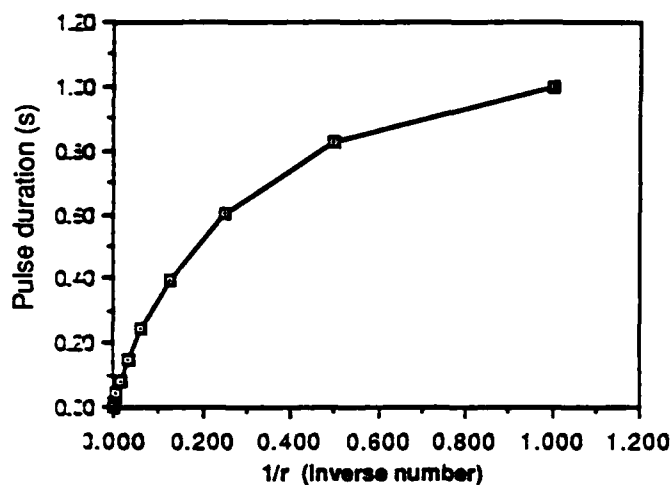


Figure 7. The $1/r$ dependence of the pulse duration (assuming a spontaneous lifetime of 1 s) shows the crude $1/N$ dependence inherent in superradiance.

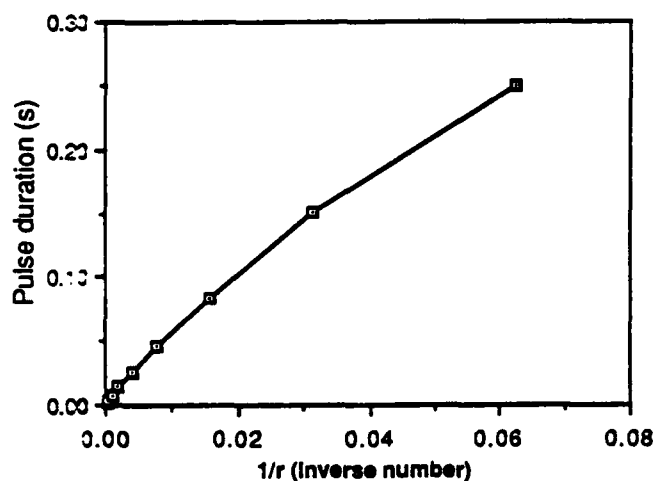


Figure 8. A blowup of the high r region on Fig. 7 depicting the near-linear behavior for larger values of the cooperation number.

2. Expressions for the Pulse Duration Time

A convenient empirical relation for the pulse duration time is $\Delta t = 3.2 (1/r)$ (specifically, for a fit to $a + b/r$; $a = 0.017$ and $b = 3.2$). This is based on fits to the previous curves.

For larger r it is much more convenient to exploit the almost continuous behavior of m . In the simplest approach, where terms linear in r are dropped and the substitution $m = r \cos \theta$ is made: $d\theta/dt = (r\lambda_0/E) \sin \theta$, $dr/dt = 0$, $r \gg 1$ (see previous section). The photon emission rate is simply $d\theta/dt = r \sin \theta$. The pulse duration (Δt_θ) associated with the time to evolve from θ_1 to θ_2 is:

$$\int_{\theta_1}^{\theta_2} \sin^{-1} \theta \, d\theta = \ln [\tan(\theta_2/2)/\tan(\theta_1/2)] = r \lambda_0 \Delta t_\theta = a(\theta) \quad (6)$$

Now we note that for $\theta_1 = 0$ a singularity is obtained corresponding to an infinite pulse width. This corresponds in the classical limit to an untipped Bloch vector in a metastable state--vertical and just waiting to fall. Once again, this is because we have neglected the linear term in r as well as the finite but non-zero value for the initial angle. The additional quantum term (sometimes referred to as the noise term) is sufficient to insure θ_1 is not zero. This naturally arises in Dicke's theory. Specifically, $\theta_1 = \cos^{-1} (1/r + 2) \approx (2/N)^{1/2}$.

We can test this expression using the characteristics of a typical statistical pulse. Let us assume for the moment that the pulse is emitted, for the most part, between $\theta_1 = 20^\circ$ ($\pi/9$ or bin 2) and $\theta_2 = 160^\circ$ ($8\pi/9$ or bin 8) as seen in the previously depicted "8192" pulse. Then for this case $a(\theta) = 3.5$ ($\Delta t = 3.5/r$) is in agreement with the empirical fit.

We now consider $a(\theta)$, which we refer to as an "angular scaling factor" in more detail. For pulses between θ_1 and $\pi - \theta_1$ for various θ_1 , we plot $a(\theta)$. The dependence is depicted in Fig. 9 for θ_1 near zero up to θ_1 near 0.5π . The dependence of $a(\theta)$ is not nearly as strong as the r dependence--graphically portraying the dominant $1/N$ characteristic time scale of superradiance.

For the moment we use a simple numerical fit for the pulse angle scale factor: $a(\theta) = 6.75 \exp(-1.7 m)$ where $m = \theta_1/\pi$, although the logarithm is more analytically correct. Since the significant pulse width is expected around $m > 0.4$ we can estimate m such that $\Delta t_{\text{delay}} \approx \Delta t_{\text{width}}$. This occurs when $\exp(-1.7 m) = 0.5$ or $m = 0.4$; consistent with the

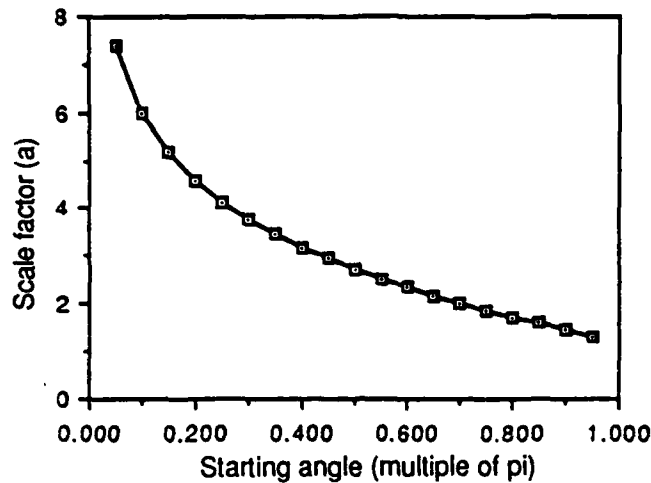


Figure 9. Behavior of the scaling factor from the statistical simulations.

physically expected value. In summary, $\Delta t_{\text{delay}} \approx \Delta t_{\text{width}} \approx 3.4/r$. For example, consider the $r = 8192$ pulse previously depicted. The pulse width is roughly 0.5 ms, corresponding to $m = -1/1.7 \ln(r\Delta t/6.75) \approx 0.3$, suggesting significant pulse formation at an angle of 54° . The empirical delay time is: $\Delta t_{\text{delay}} = (6.2 - 3.9)/8192 = 0.28$ ms. These delay and pulse width time periods are depicted in Fig. 10, along with the associated Bloch angles.

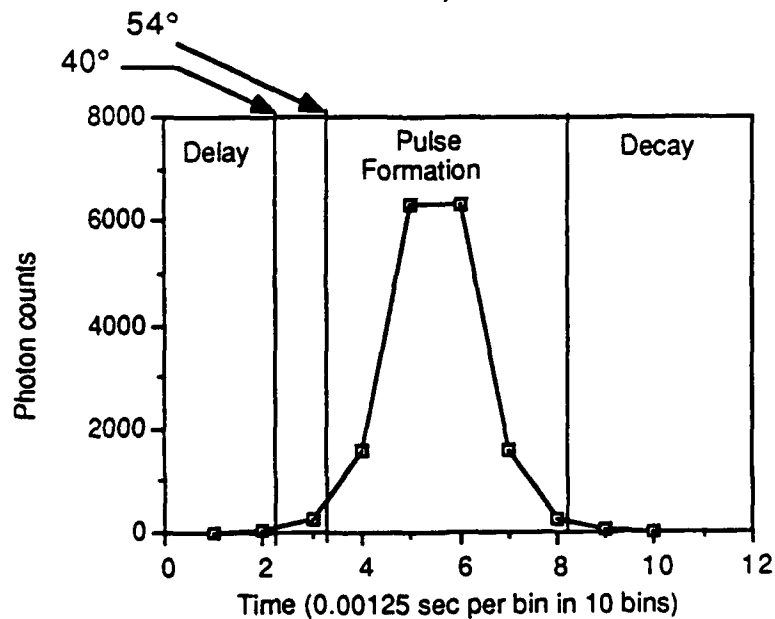


Figure 10. Basic pulse characteristics and associated Bloch vector angles for the statistically simulated $r = 8192$ pulse.

3. Empirical Estimates for Practical Values of the Cooperation Number

We can quickly get order-of-magnitude values for r using the empirical relations. For a pulse of time scale $\Delta t = 3.4/r\lambda_0$ s, the complete light cone distance in two directions is $6.8c/r\lambda_0 = 1$, ($1 = \text{length}$). Assuming Dicke superradiance occurs on length scales governed by c , the self-consistent value for maximum r solves:

$$(\pi\lambda^2) 1 n^* = 2r , \quad (7)$$

where n^* is the maximum excited state atom density, λ is the reduced photon wavelength, λ_0 is the spontaneous decay rate for one emitter and the term in parentheses is the cross-sectional area. This latter cross-sectional area multiplied by the cooperation length is usually called the cooperation volume. Numerically:

$$\begin{aligned} r &\approx \lambda (3.4\pi c n^* / \lambda_0)^{1/2} \\ &\approx 1 \times 10^{-5} (1/E) (n^* / \lambda_0)^{1/2} , \end{aligned} \quad (8)$$

where E is in MeV, λ_0 in s^{-1} and n^* in no./cm^3 .

In the x-ray region, $E = 0.040$ MeV and $n^* < 10^{23}$ no./cm^3 so $r \leq 10^8 \lambda_0^{-1/2}$. For short-lived states ($1 s^{-1}$) $r < 10^8$. For long-lived states, e.g., $\lambda_0 \approx 10^{-2} s^{-1}$, $r \approx 10^9$. For large r , a slight correction to this empirical result is obtained from well known analytical results discussed in Section G. For the case $\lambda_0 = 1 s^{-1}$; the cooperation time is 10^{-8} s and the cooperation length is roughly on the order of 10 m (refined later). Here we note that the atoms are, for the most part, in a perfectly straight line. If limited by sample size, r is correspondingly smaller by the geometric size of the sample.

D. ENHANCED SPONTANEOUS DECAY IN THE PRESENCE OF EXTERNAL OR SELF-CREATED RADIATION FIELDS

This section describes simple Dicke superradiator models calculated with the programming assistance of John Neuberger. These should help in the understanding of the features of Dicke superradiance. They include, for the most part, some aspects of many previous ideas. The basic tenet of Dicke remains intact--"all emitters emitting to a common electromagnetic field" form a collective state wave function with respect to the field. The pulses herein depict various features of the models and the chosen parameters are typical of those for γ -lasers. This work is not complete--other multiplets remain. The equations are well suited for the treatment of very large values of the cooperation number in contrast to the smaller values for the cooperation number treated in the previous section.

The following models are particularly useful in the regime of interest to the gamma-ray researchers.

1. Background for Dicke Superradiator Models

Consider the state $|r, m, p\rangle$ (where p is the photon number occupancy) and the Dicke operators are $a_p R_-$ and $a_p R_+$. As shown in Fig. 11, the "enhanced spontaneous decay" rate is given by $(r^2 + r - m^2 + m)$ and the net p -dependent decay rate is given by $2pm$. Physically, the p -dependent decay rate is equivalent to $2m$ systems, each having spontaneous decay rates dependent on p .

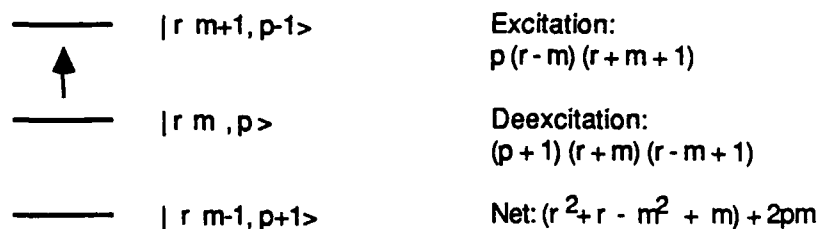


Figure 11. Net decay rate, including stimulated absorption and emission

2. The Simple Superradiance Limit

In this case:

$$dm/dt = -\lambda_0 (r^2 + r - m^2 + m), \quad (9)$$

where the p -field plays no role. This means that emitted photons leave the system without interacting with the emitters in the system. Such photons are called n -field photons in an arbitrary nomenclature simply to distinguish "cavity" photons from emitted photons. A pulse calculated using this equation is depicted in Fig. 12 for $r = 10^6$ and $\lambda_0 = 1$ s.

3. Simple Superradiator in a Cavity

For a simple superradiator in a closed cavity:

$$dm/dt = -\lambda_0 (r^2 + r - m^2 + m + 2pm) \quad dp/dt = -dm/dt \quad (10)$$

There is a simple expression for the maximum change of the Bloch vector angle. Since $p = N - m - r = 2r - m - r = r - m$ then $d\theta/dt = 0$ implies $\cos\theta \sim -1/3$ or $\theta \sim 109^\circ$ (closer in practice to 103°). A pulse is depicted in Fig. 13 for $r = 10^6$ and in Fig. 14 the population inversion is shown to hang up at about 110° . This provides a good check, at least on our understanding of what should happen in this trivial model for this limiting case.

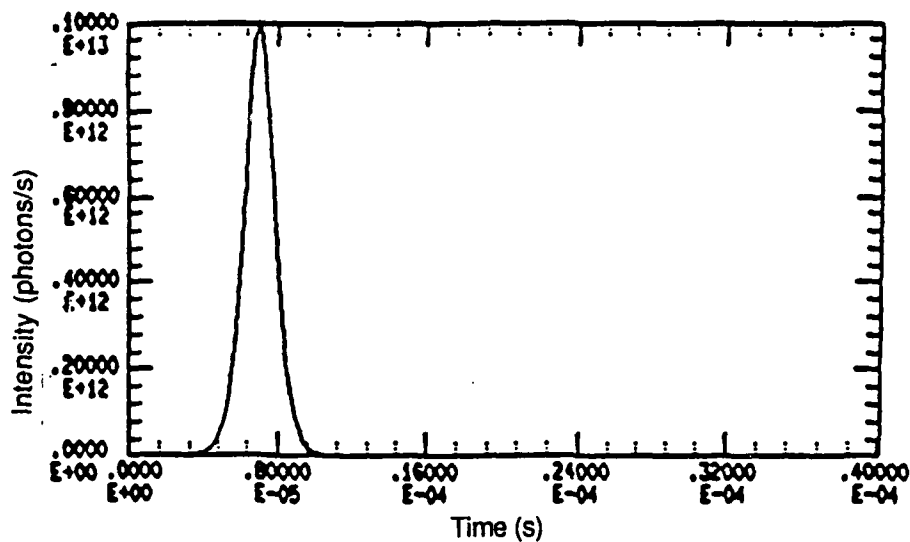


Figure 12. A simple superradiant pulse for the case of $r = 10^6$ calculated using the simple Dicke model. The pulse appears symmetrical, with the delay time comparable to the inverse of r as expected from the previous sections. Moreover, the area under the pulse is also comparable to r .

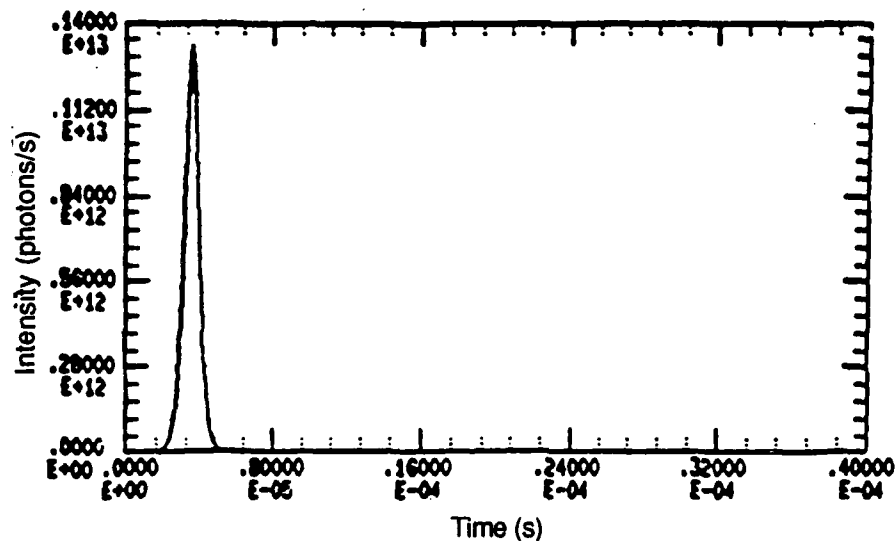


Figure 13. The Intensity of photon emission into an ideal closed box for the case of $r = 10^6$ reveals characteristics similar to that of the previous figure, except the pulse width is severely shortened. The Bloch vector has hung up at about 110° , just past superradiant emission (see next figure), since stimulated absorption is now overcoming the emission rate. This simple limit provides a check on the trivial dynamical equations.

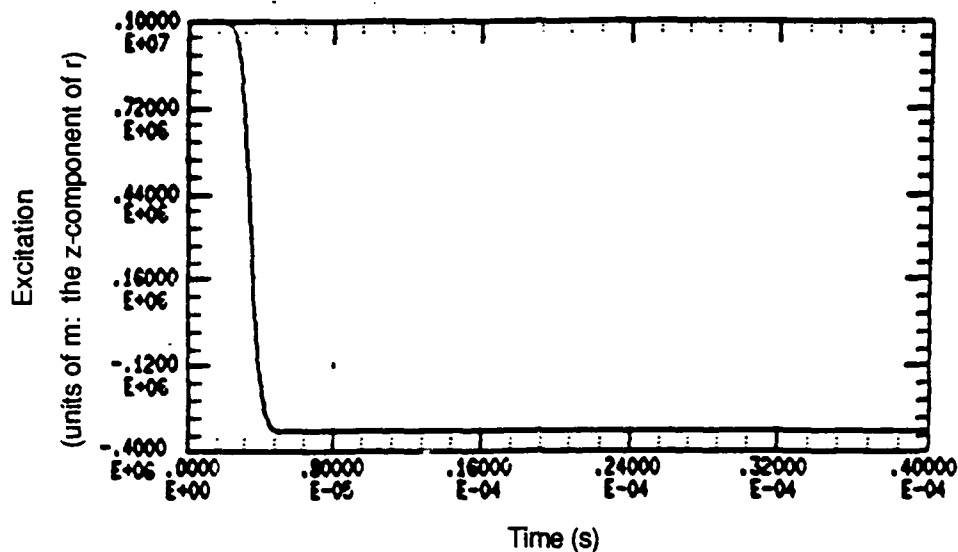


Figure 14. In the ideal cavity, the population of excited states decays quite rapidly, but then hangs up just past the $m = 0$ level. The m -component corresponds to an approximate Bloch vector angle near 110° , which is easily derived to be a rough constant angle, regardless of cooperation number. This provides a limiting case of the more complicated simple models.

4. Simple Superradiance in Fields Which Emit--Markovian Model

In considering two loss mechanisms for p -photons we can consider the following coupled equations:

$$-dm/dt = \lambda_0 (r+m) (r-m+1) + 2\lambda_0 mp, \quad (11)$$

where

$$dn/dt = cp/L \text{ and } dn/dt + dp/dt + dm/dt = 0. \quad (12)$$

The basic features of these equations are summarized :

1. Stimulated emission and absorption are included in Dicke-superradiance via the p -field number occupancy
2. The p -photon field appears adiabatically following the instantaneous evolution of dm/dt (the emission process) and p -photons are lost at constant rate c/L
3. This set of equations cannot lead to geometric ringing unless p is fed from some external source.

There are two limiting cases worth noting:

1. In the case of an infinite length L , $k = c/L = 0$, $dn/dt = 0$ and the lossless radiator in a cavity appears.
2. For c/L large dn/dt follows dm/dt and $p \rightarrow 0$, thus giving the coherently spontaneously decaying "simple" Dicke superradiator.

Typical pulses are depicted in Figs. 15(a) through 15(f). The figures portray pulses from samples of increasing length. Parameters are listed in Table 3. The parameters for pulses a through e are repeated in the next subsection for the case of a Markovian radiator. We find that as k decreases and λ_0 increases the trend is towards exponential decay, whereas for decreasing k and increasing λ_0 , the trend is towards "pure" Dicke superradiance. For the case of $r = 1.5 \times 10^6$ and $k = 1.0 \times 10^6$; dn/dt , $n(t)$, $m(t)$ and $p(t)$ are shown in Figs. 16(a) through 16(d).

In this approach, dm/dt follows the instantaneous p -field and not a p -field which is averaged over previous magnitudes of dm/dt by some weighting factor. Thus, we must consider a non-Markovian model which is the usual simple approach to dealing with this problem.

5. Simple Superradiance in Fields which Emit--non-Markovian Model

In this case, the system decays at a rate dependent on the previous (weighted) history of the system, thus physically reflecting, or modeling, effects due to the finite speed of light. We consider $\lambda(s) = \lambda_0(r^2 + r - m^2 + m + 2pm) = \lambda_0 \rho(s)$ where $m = m(s)$ and $p = p(s)$ where s is some unit of time. Then, weighting of previous decay rates according to past history is achieved by the same photon loss factor $k = c/L$ in the factor $e^{k(t-s)}$ to get:

$$-dm/dt = 10 k \int_0^t \exp[-k(t-s)] \rho(s) ds \quad (13)$$

Still keeping the previous equations:

$$p + n + r + m = N ; dp/dt + dn/dt + dm/dt = 0 \text{ and } dn/dt = kp \quad (14)$$

we examine superradiant pulses for the conditions studied in the previous section. Figures 17(a) through 17(e) depict various pulses for the parameters in Table 4. With increasing sample length, more pronounced ringing occurs. For the case of $r = 1.5 \times 10^6$ and $k = 1.0 \times 10^6$; dn/dt , $n(t)$, $m(t)$ and $p(t)$ are depicted in Figs. 18(a) through 18(d).

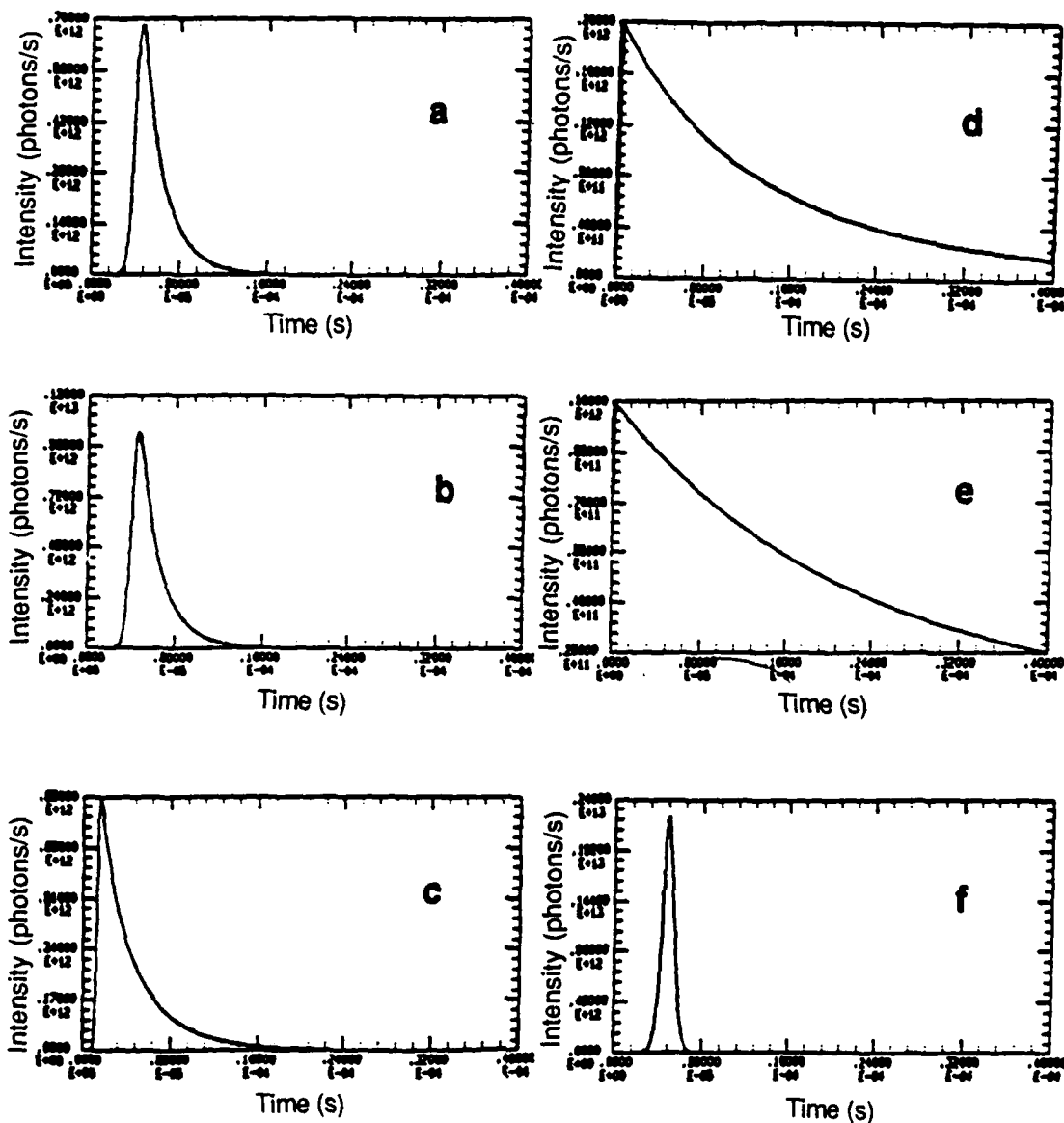


Figure 15. Views a through f depict pulses calculated according to a simple Markovian radiator for the case $r = 10^6$ and varying values of the length and spontaneous decay rates listed in Table 3. The sequence of pulses from a to e indicates a trend towards a long exponential-like decay roughly following the ringing in the non-Markovian model of the next subsection. Pulse f is from a radiator of length shorter than the radiator in a, thus depicting less of a tail and closer behavior to the simple Dicke superradiator.

Table 3. Parameters for Illustrated Pulses

Figure 15	$k (\times 10^{-6}) (s^{-1})$	$\lambda_0 (s^{-1})$
a	1	1
b	1.5	0.67
c	0.5	2
d	0.1	10
e	0.05	20
f	100	1

for a - e, the product $k\lambda_0$ is constant

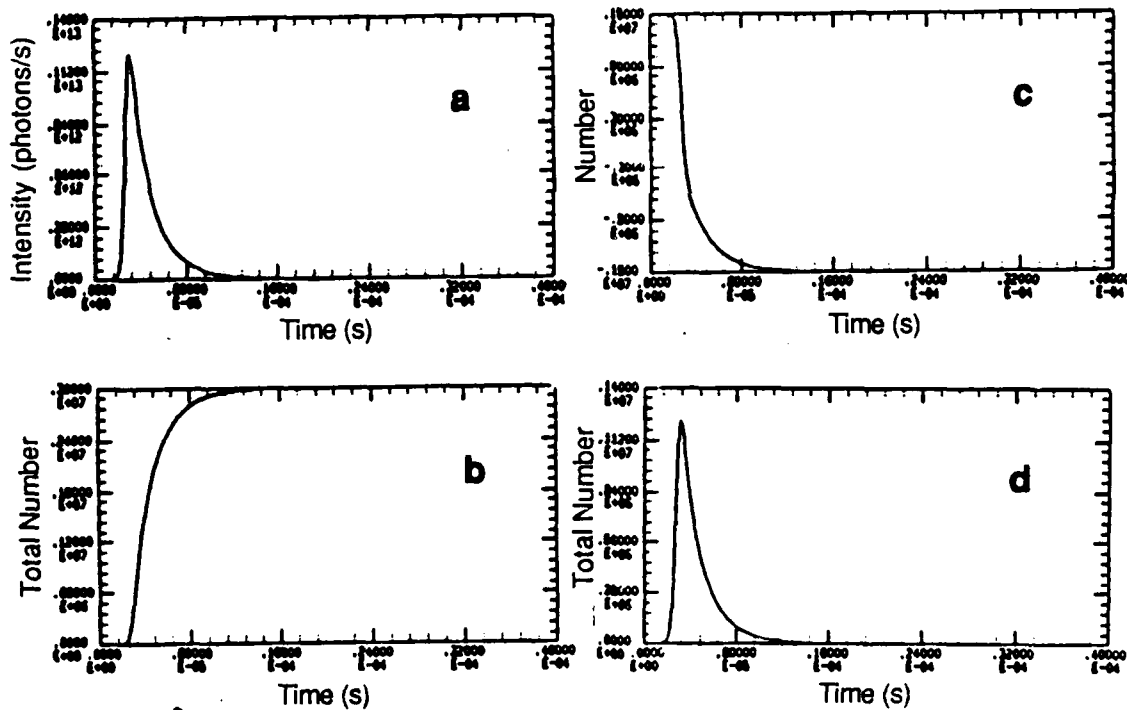


Figure 16. The (a) quantities dn/dt corresponding to the emitted intensity; (b) $n(t)$ corresponding to the running sum number of emitted photons; (c) $m(t)$ z-component of the cooperation number; and (d) $p(t)$ the photons in the "cavity" are depicted for the case of $r = 1.5 \times 10^6$ and $k = 1.0 \times 10^6$. The example shows the rise and fall of p-field intensity as the simple radiator dumps its photons from $m(t)$ to $n(t)$.

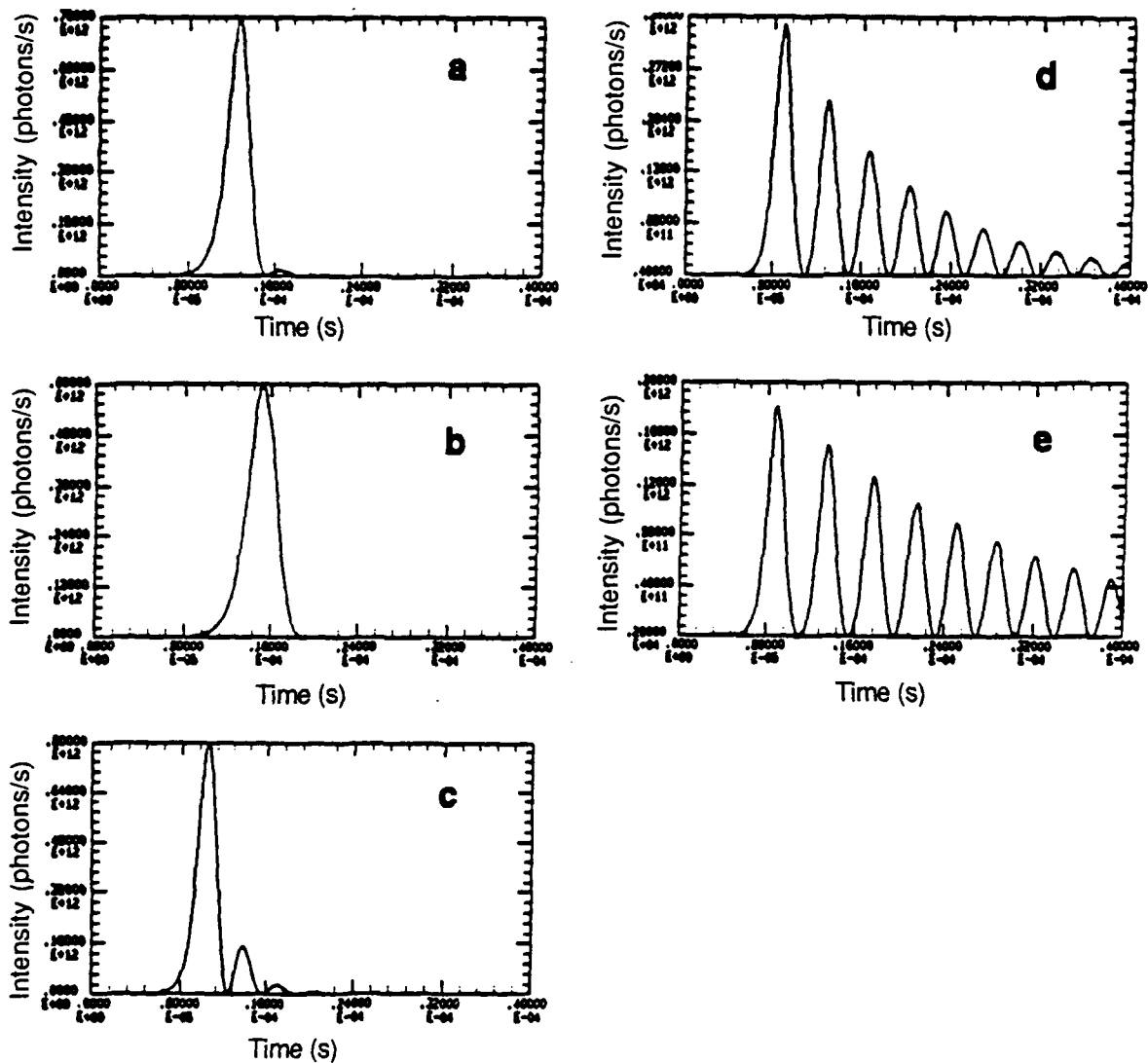


Figure 17. Views a through e depict pulses calculated according to a simple non-Markovian radiator for the case $r = 10^6$ and varying the length of the radiator and spontaneous decay rates as was done in Figs. 15(a) through 15(e). For conditions where the p-field plays an increasing role, ringing is observed to increase in scope.

Table 4. Parameters for Illustrated Pulses

Figure 17	$k (\times 10^{-6}) (s^{-1})$	$\lambda_0 (s^{-1})$
a	1	1
b	1.5	0.67
c	0.5	2
d	0.1	10
e	0.05	20
the product $k \lambda_0$ is constant		

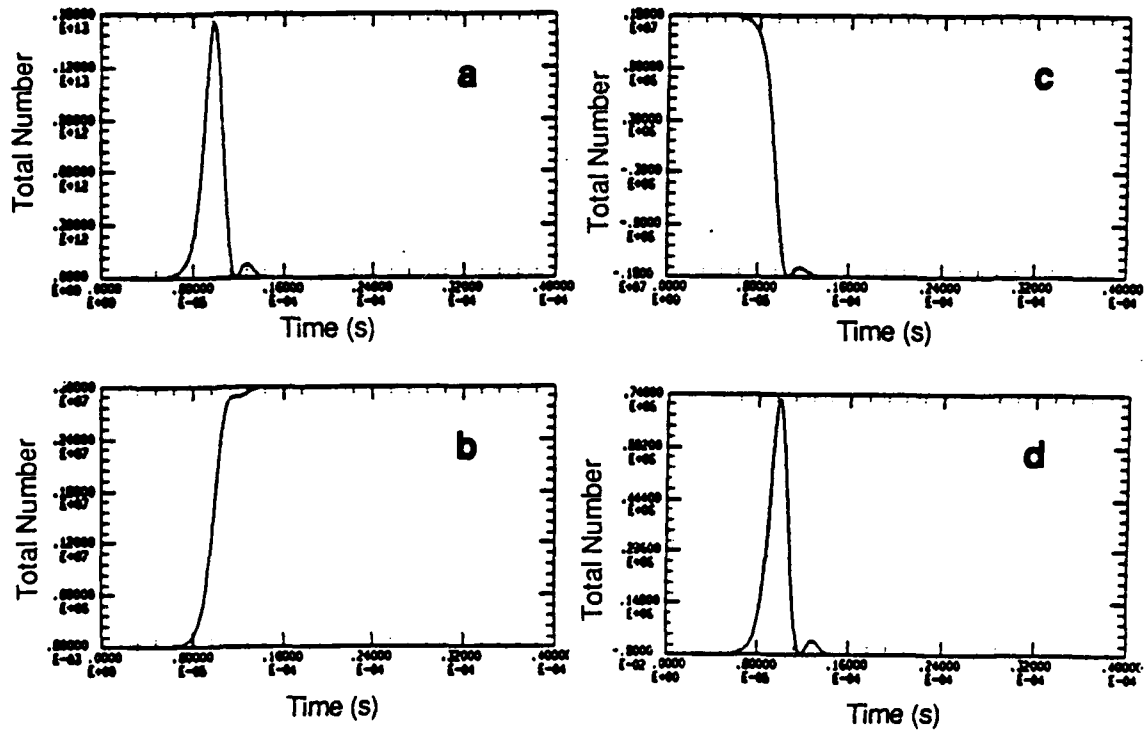


Figure 18. The (a) quantities dn/dt corresponding to the emitted intensity; (b) $n(t)$ corresponding to the running sum of emitted photons; (c) $m(t)$ z-component of the cooperation number; and (d) $p(t)$ the photons in the "cavity" are depicted for the case of $r=1.5 \times 10^6$ and $k=1.0 \times 10^6$. Ringing effects are indicated in oscillations of $p(t)$.

Five items are noted:

1. For s restricted to t rather than the interval $(0, t)$; the adiabatic limit (Markov) is retained.
2. From the integral expression for $-dm/dt$ it is easy to show that the differential equation has the following form:

$$d^2m/dt^2 + k dm/dt = -\lambda_0 k [r^2 + r - m^2 + m + 2mp(t)] \quad (15)$$

This equation is identical to the Markov form except for second derivatives and factors of k , which allow for the ringing. This is the "pendulum" equation.

3. For times $t \gg k^{-1}$ ($kt \gg 1$) then s near t contributes strongly;

$$\begin{aligned} k \int_0^t ds \exp[-k(t-s)] \rho(s) &\sim \rho(t) \exp(-kt) k \int_0^t ds \exp(ks) \\ &\sim \rho(t) [1 - \exp(-kt)] \end{aligned} \quad (16)$$

for $\rho(t)$ slowly varying. Then very large kt implies $-dm/dt = \lambda_0 \rho(t)$ or:

$$dm/dt = -\lambda_0 (r^2 + r - m^2 + m + 2mp) \quad (17)$$

This is the previous equation for the case where d^2m/dt^2 plays no role. Since d^2m/dt^2 leads to oscillations; this a "no ringing" limit, i.e., normal Dicke superradiant emission.

4. For comparable k^{-1} and t , significant "memory" is maintained, corresponding physically to a situation where p -field photons have a significant effect for some intervals of time.
5. Finally, we note that as d^2m/dt^2 goes to zero, k plays no role. Thus, the second derivative term and the memory (k) go hand in hand, as we should expect.

E. CONDITIONS FOR GAMMA-RAY ENHANCED DECAY RATES

The conditions for gamma-ray enhanced decay rates have been listed previously. They can be understood using the properties of the totally symmetric multiplet in Dicke's model. In fact Dicke points out many of the requirements, and they can be found in his paper or as summarized in Appendix B.

The conditions are easily seen. In the limit of large r , that is, for a large number of cooperating emitters, we first evaluate the pulse angle factor, $a(\theta)$. In order to do that we

need to estimate the initial angle and final angle. As noted previously, the initial angle is precluded from having the value zero. We denote as θ_D that particular angle between a vector of length of $r(r+1)$ and a z-projection of $m = r$. In a simple approximation, $\theta_D = (2/N)^{1/2}$, as discussed previously. The pulse angle scale factor $a(\theta)$ can now be evaluated for θ in the interval θ_D to $\pi - \theta_D$:

$$\begin{aligned} a(\theta) &= \ln [\tan (\theta_2/2) / \tan (\theta_1/2)] \\ \tan (\theta_1/2) &\cong \theta_1/2 \cong 1/2 (2/N)^{1/2} \\ \tan (\theta_2/2) &\cong 2/\theta_2 \cong 2 (2/N)^{-1/2} \end{aligned} \quad (18)$$

from which:

$$a(\theta) \cong \ln [2N] \quad (19)$$

Much of what is described here is easy to understand in terms of the simple model (model 1 in the previous section) the case of Dicke superradiance with no stimulated emission or absorption.

1. Effective Gain

There is an "effective gain" for an emitted superradiant pulse. To see this we can take equation (6) and substitute $\tau = 1/\lambda_0$ and the cooperation time $\tau_c = \Delta t_0$ to get the very simple expression:

$$r \tau_c = \tau a(\theta) \quad (20)$$

which now becomes:

$$\tau_c = (\tau/N) 2 \ln [2N] \quad (21)$$

Then, $\tau_c \ll \tau$, which for all practical purposes is the evidence for a superradiant pulse. This implies that $(1/N) 2 \ln [2N]$ is small or:

$$(\tau/\tau_c) = N/[2 \ln (2N)] \gg 1 \quad (22)$$

Since we can introduce a cooperation number $N_c = n^* \lambda^2 \pi l_c$ and for $L < l_c$ (which is expected to be the case in the gamma-ray regime) $N_c = n^* \lambda^2 (2\pi) L$. (For example we can estimate $l_c \approx 3.8$ m, as detailed later, whereas the current manufactured or experimental length would be much smaller). If we now associate σ_R , the resonant absorption cross section, with $\pi \lambda^2$, then:

$$(\tau/\tau_c) = (\alpha_{\text{eff}} L) / [2 \ln (2N)] \gg 1 \quad (23)$$

where α_{eff} is the effective gain per unit length, provided we associate $\alpha_{\text{eff}} = \sigma_{\text{Rn}}^* L$. Clearly a gain in enhanced spontaneous decay is an awkward concept; if, on the other hand, we try to think of a gain per unit length for an "equivalent laser", α , then:

$$\begin{aligned} \exp(\alpha L) &\approx (\alpha_{\text{eff}} L) / [2 \ln(2N)] \\ \alpha &\approx (1/L) \ln [N/2 \ln(2N)] \quad (\text{length limited}) \\ \alpha &\approx (1/\tau_c) [r/a(\theta)] \ln [r/a(\theta)] \quad (\text{cooperation length limited}) \\ (\alpha L) &> \ln \{N/[2 \ln(2N)]\} \end{aligned} \quad (24)$$

where, depending on how you care to approximate,

$$(\alpha L) > \ln(N) \quad (25)$$

[It is interesting to note in comparison to Ref. 8 that the gain defined in equation (24) is really a log of the ever-present log term $\ln(2N)$, the latter log term effectively dropping out to regive, for all practical purposes, the same log term.) Since N_c is expected to be $\approx 10^8$ in the gamma-ray regime (plus or minus a number of decades, depending on the spontaneous decay rate); αL is certainly greater than 10. We now examine the conditions for γ -ray enhanced spontaneous decay. (This is the equivalent $(1/2) \ln N$ factor or " ϕ " of other Ref. 8 working in the coupled Maxwell-Schrodinger approach.)]

2. Condition for Gamma-Ray Superradiance

From:

$$\tau_c = a(\theta)/\lambda_0 N_c \quad (26)$$

where:

τ_c = cooperation time

λ_0 = spontaneous decay rate

N_c = cooperation number = $2r$ where r = Dicke multiplet,

and:

$$\rho l_c \lambda^2 \pi = N_c = \rho c \tau_c \lambda^2 \pi \quad (27)$$

where:

$l_c = c\tau_c =$ cooperation length

$\rho =$ number density of emitters

$\lambda =$ radiation wavelength,

then:

$$N_c = \lambda [2\rho\pi c a(\theta) / \lambda_0]^{1/2} . \quad (28)$$

For p percentage of emitters participating, then a general equation for N_c is:

$$N_c = 2 \times 10^7 / E \text{ (MeV)} [p / \lambda_0]^{1/2} . \quad (29)$$

3. Size of a Gamma-Ray Superradiator

Let us use N_c from above for the cooperation number and l_c from above. Then, crudely:

$$l_c = 75000 E \text{ (in MeV)} (p\lambda_0)^{-1/2} . \quad (30)$$

for $E = 10 \text{ keV}$, $\lambda_0 = 1 \text{ s}^{-1}$ and $p = 0.25$ the cooperation length l_c becomes about 380 cm--consistent with a strictly straight line geometry. For shorter lifetimes the cooperation length is obviously less, for longer lifetimes the length is longer.

A quick summary of the characteristics of a superradiator in the gamma-ray regime is made here. The characteristics are based on a superradiator comprised of one cooperation length. The quantity E is the transition energy (in MeV), the quantity p is the percent of emitters participating (taken as the percentage of complete maximum inversion density, $5 \times 10^{22} \text{ emitters/cm}^3$) and λ_0 is the spontaneous decay rate (s^{-1}). The angular scale factor is assumed to be 25; it varies from 1 to 50.

Power (W) = $1.28 p/E$

independent of lifetime,
higher for lower E

Total Energy Out (J) = $(3 \times 10^{-6}) (p/\lambda_0)^{1/2}$

independent of E
higher for longer lifetime

Cooperation Length (cm) = $75000 E (p\lambda_0)^{-1/2}$

dependent on both E and lifetime
shorter for lower E
longer for longer lifetime

Number of Emitters (no.) = $(2 \times 10^7/E) (p/\lambda_0)^{1/2}$ dependent on both E and lifetime,
 increases with lower E,
 increases with longer lifetime.

Figure 19 presents the results.

F. COMMENT ON COOPERATION, CAUSALITY AND VIOLATION OF MICROSCOPIC CAUSALITY

Dicke says little about upper limits on the cooperation number as set by macroscopic causality. One could argue that cooperativity is governed by the deBroglie wavelength of the emitted boson. This would be a very bad situation for gamma-ray lasers. Thus, it is assumed by most, as was done here, that the volume of cooperating emitters is set by $c\tau$ for some time τ related to the lifetime of the emitter or collection of emitters. There are suggestions that microscopic causality is violated* and this shows up in the shapes of lines (particularly the Compton scattering terms). The time scale for this violation is on the order of the time required by light to travel the "size" of the elementary particle. This size is related to the spatial extent of the particle. That size, if estimated from the width of the free particle Newton-Wigner wavefunction (a spatial wavefunction in the Foldy-Wouthuysen representation for the position of a free mass), is roughly $\hbar/(2E)$ where E is the total (relativistic energy). (Here we also assume the particle behaves in accord with the Klein-Gordon equation, i.e., we do not consider here Dirac or Weyl particles.)

The quantity τ arises quite naturally in the pre-acceleration problem, as well as in the standard quantum limit for position measurements of massive particles. For the massless photon it is $\approx \hbar/2p$. For times roughly less than this, microscopic causality as well as the standard quantum limit may be violated; but these are very, very small distances. Consequently, we must assume that Dicke's effect are governed by *macroscopic causality*, since limiting it to distance scales where quantum effects (spatial extent of wavefunctions) play a role appears much too restrictive, given published experimental results.

* C.L. Bennett, private communication (results to be published in *Phys. Rev. A.*).

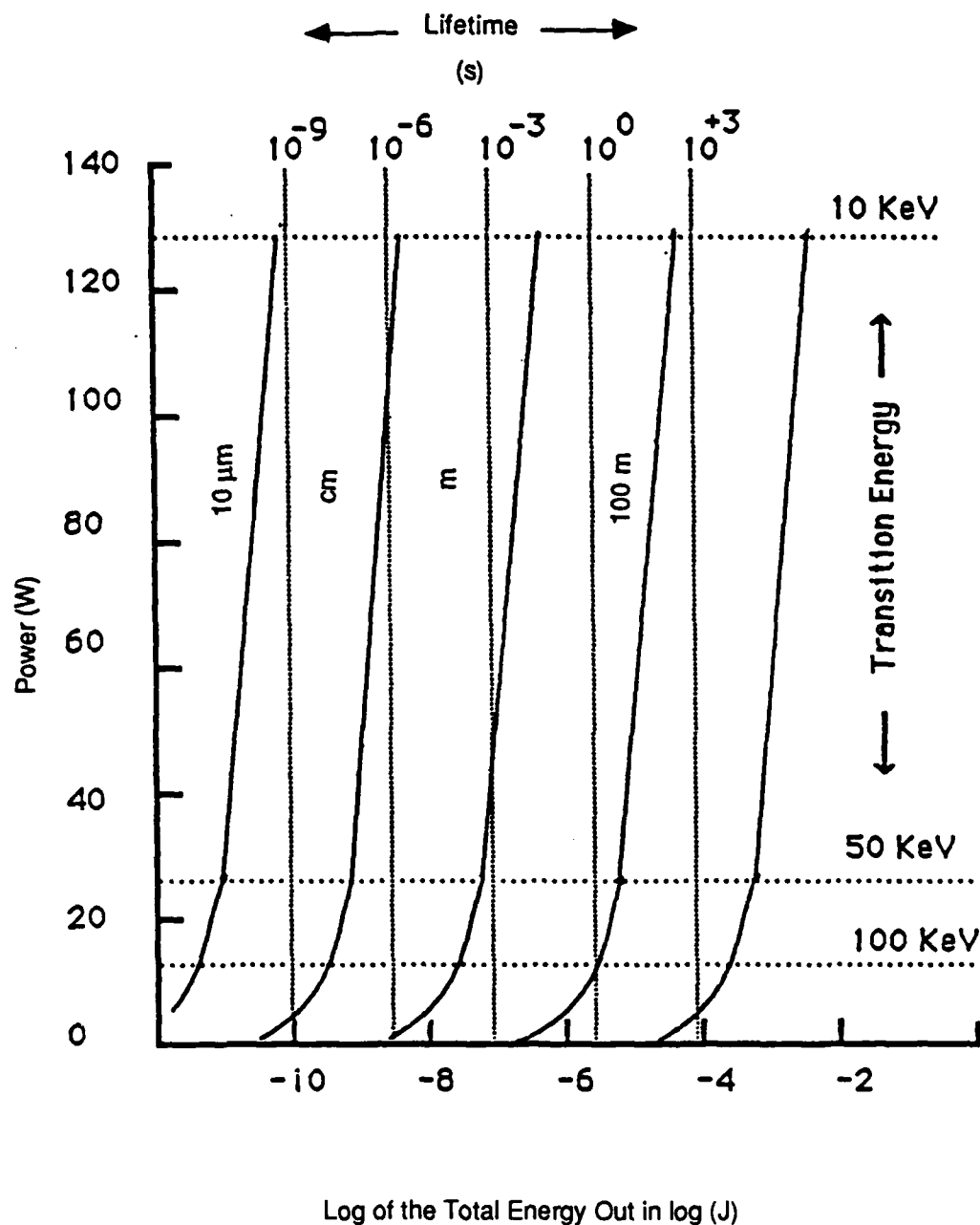


Figure 19. Superradiating Operating Region. The operating region is illustrated for the conditions and assumptions discussed in the text with $p = 1$. The power and total energy out are for the case of one cooperation length. The cooperation lengths are indicated on the curves for a given lifetime and transition energy.

G. CONCLUSIONS

Some distinctions remain with respect to the semiclassical electromagnetic field approach to superradiance and the somewhat more general approach of Dicke. In particular, the symmetric multiplet results agree with the semiclassical approach. More specific aspects of the pulse (such as ringing) are determined on geometrical features of the particular radiator. Although two types of ringing can appear (transverse effects or photon field "memory" effects in stimulation terms) it is generally accepted that transverse effects lead to observed ringing. Regardless, the conditions for gamma-ray superradiance remain, and they are not easy conditions to achieve.

III. EVALUATION AND COMPARISON OF SUPERRADIANT MODELS

A. INTRODUCTION

It is generally expected that if a gamma-ray laser is developed it will probably emit in a superradiant mode instead of a stimulated emission mode (Ref. 1). Trammell and Hannon (Ref. 16) investigated the emission characteristic of inverted nuclear populations and described two extreme types of possible emitted pulses (1) a pulse obtained from a high gain nuclear amplifier due to stimulated emission (SE) of nuclear transition and (2) a superradiant (SR) pulse emitted in a cooperative fashion by the inverted nuclear population.* It has been pointed out on several occasions (Refs. 17, 18, and 19) that SE and SR are closely related, they are, in fact, two distinct limiting cases of the same phenomena. SR is the transient limit of cooperative emission and SE is the steady state limit. Under appropriate conditions these two processes can interfere and produce a ringing phenomena (a sequence of sharp pulses decaying in time). "Pure" superradiance, on the other hand, produces a single pulse and a single-pass laser also produces a single pulse.

Superradiance has been observed in atomic and molecular systems and the phenomena have been explained theoretically (Ref. 20). An excellent discussion of the experimental results is presented by Q.H.F. Vreken and H.M. Gibbs (Ref. 21) and of the present state of theoretical understanding by M. Gross and S. Haroche (Ref. 22) and M.F.H. Schuurmans, Q.H.F. Vreken and D. Polder (Ref. 23). A cooperative phenomenon with nuclear transitions, but not superradiance or superfluorescence, has also been observed through the shortening of the lifetime of a nuclear state (Ref. 24). Just as

* Whereas most authors use superradiance to refer to all phenomena where radiation is emitted cooperatively and the intensity is proportional to N^2 , where N is the number of atoms or nuclei in the cooperative volume, Bonifacio and Lugiato (Ref. 17) distinguish between radiation emitted by coherently prepared systems and with a macroscopic dipole moment initially, which they call superradiant, and incoherently prepared systems which do not have a macroscopic dipole moment initially but interact through normal fluorescent decay to evolve a macroscopic dipole which then radiates coherently in a cooperative mode.

the observation of resonance in nuclear systems requires special conditions which are more stringent than in atomic systems, the realization of superradiance on the nuclear level must overcome restrictions that are often not important in atomic and molecular systems. Some special consideration has to be made to crystalline structure and its effect on SR, the Mössbauer and Borrmann effects, attenuation of the beam due to inelastic scattering, destruction of resonance due to inhomogeneous broadening, and relaxation effects.

Our purpose in these investigations was to determine the state of the theoretical understanding of superradiance in general and to what extent the phenomena that are expected to affect nuclear superradiance have been incorporated into the theory. In order to develop a theoretical structure to study these effects, we worked in the framework of the quantum mechanical Bonifacio-Lugiato (B-L) model (Refs. 17 and 25), which seemed most appropriate because it was derived from general quantum, mechanical principles and thus could accommodate nuclear conditions even though it was clearly restricted to a few modes. This study checks the region of applicability of the (B-L) model, compares the (B-L) model with the more restrictive but mathematically more tractable diffusion equations of Narducci, et al. (Ref. 26), investigates the extent of quantum fluctuations under different initial conditions and during the time development of the superradiant pulses. The simplest superradiant models are based on the semiclassical pendulum equations. These were also compared with the quantum mechanical calculations.

This chapter provides a thorough analysis of some of the assumptions of B-L theory, shows real instabilities in the dynamics and identifies the source of the instabilities. Besides the well-known weak points of the B-L theory such as the assumptions of few modes and the independence of modes, the theory also does not easily allow for the calculation of effects due to competing transitions (internal inversion, emission with recoil, etc.) and transport effects (photoelectric absorption). Other theories have been developed which are based on the Bloch-Maxwell equations and allow for the inclusion of quantum initiation statistics and modeling of the fluctuation statistics. This is not of particular importance or interest to the γ -ray laser problem at the present state of sophistication and development. What is of interest is that these theories can deal in a straightforward way with the phenomena of competing transitions and photon transport in the medium; two problems of great insignificance to the γ -ray laser feasibility study. Further work should be devoted to the exploitation of these theories in the γ -ray laser problem.

B. THE BONIFACIO-LUGIATO MODEL FOR SUPERRADIANCE

1. General Characteristics of the Model

The extensive literature on superradiance offers a fairly detailed physical understanding of the phenomenon, which is due to the cooperative behavior of identical atoms in a configuration satisfying certain well-defined conditions. However, it is not yet clear whether any of the proposed mathematical models of superradiance is accurate enough to give reliable quantitative predictions of effects in nuclear rather than atomic emission levels.

The model that appears to be the most complete, with the fewest *ad hoc* assumptions, is the one presented by R. Bonifacio and L.A. Lugiato in Ref. 17. It includes (non-relativistic) quantum effects, line-broadening, and (non-Markovian*) stimulation of the atomic system by the spontaneously emitted photons.

The only significant *ad hoc* assumption in the model appears to be its restriction of the electromagnetic field to a pair of independent resonant modes. The authors justify this assumption by limiting the geometrical configuration to a needle-shaped cavity which, if thin enough, will support just two identical endfire waves propagating in opposite directions.

However, self-consistency is the only justification offered for treating the modes as independent. Doing so has the advantage of reducing the analysis to considering just a single mode for which the equivalent inverted atomic population is equal to $N/2$, where N is the actual population, and the equivalent interaction coupling constant is equal to $g_0\sqrt{2}$, where g_0 is the actual resonant mode coupling constant.

On the other hand, before invoking the assumption that the two modes can be treated separately, B-L show that their model implies two basic conservation laws. One preserves the balance between emitted radiation and stored energy, and the other preserves the Dicke cooperation eigenvalue defined in terms of the time-varying atomic dipole polarization and population inversion states.

* B-L use the term "Markovian" in reference to a system that has no memory of prior interactions. The term implies that differential equations rather than differentio-integral equations, which the non-Markovian case would require, govern the operator expectation values.

The first equation has the form

$$\begin{aligned} \frac{d}{dt} \left\{ \sum_{\alpha = k_0, -k_0} \left[\langle A^\dagger(\alpha) A(\alpha) \rangle(t) \right] + \langle R_3 \rangle(t) \right\} \\ = -2K \sum_{\alpha = k_0, -k_0} \left[\langle A^\dagger(\alpha) A(\alpha) \rangle(t) \right], \end{aligned} \quad (31)$$

where $A(k_0)$ is the resonant mode of the internal field, k_0 is the vector wave number at resonance, R_3 is the population inversion, and K (given by $c/2L$, where L is the axial length of the active volume and c is the velocity of light) is the reciprocal maximum transit time of photons in the active volume. The brackets $\langle \rangle$ refer, as usual, to the expectation value of the operator that they enclose; and parentheses $()$, to a functional dependence on the independent variable that they enclose. The second equation, in which R^+ and R^- are collective dipole moment operators, has the form

$$\frac{d}{dt} \left\{ \sum_{\alpha = k_0, -k_0} \left[\langle R^+(\alpha) R^-(\alpha) \rangle(t) \right] + \langle R_3^2 \rangle(t) - \langle R_3 \rangle(t) \right\} = 0 \quad (32)$$

Any Hamiltonian system would imply the first law. The second is analogous to and formally identical with the standard conservation of angular momentum (resulting in this case from a collection of pure spin states) when the total angular momentum is identified with the Dicke cooperation eigenvalue associated with a collective total angular momentum (spin) operator R , and the angular momentum vector components are identified with R_3 and the real and imaginary parts of R^+ .

The conservation laws are therefore physically reasonable in their own right. In fact, they appear to be quite general and could be regarded as essential requirements for any model based on the collective behavior of identical two-state atoms.

From their general master equation, specialized to the case of identical, independent, single-resonant modes, B-L also derive another equation involving the expectation values of the atomic and electromagnetic field operators:

$$\begin{aligned} \langle \dot{R}_3 \rangle (t) + \left(K + \frac{1}{2T_2^*} \right) \langle R_3 \rangle (t) = \\ - \frac{2g_0^2}{v} e^{-\frac{t}{T_2^*}} \left\{ \sum_{\alpha=k_0-k_0} \left[\langle R^+(\alpha) R^-(\alpha) \rangle (t) + 2 \langle A^\dagger(\alpha) A(\alpha) R_3 \rangle \right] \right\}. \end{aligned} \quad (33)$$

where v is the volume of the active region and T_2^* is a time constant due primarily to inhomogenous line broadening. The unknown quantities appearing in equation (33) and the two conservation laws (1) and (2) are the photon number expectation $\langle A^\dagger A \rangle$, the atomic inversion expectation $\langle R_3 \rangle$, the photon number/atomic inversion correlation $\langle A^\dagger A R_3 \rangle$, and the fluctuations $\langle R^+ R^- \rangle$, $\langle R_3^2 \rangle$ of the atomic dipole/inversion vector components.

Although equations (31), (32), and (33) derived from the B-L model do not form a complete set of relations for all of the explicitly involved quantities that must be taken as independent in a quantum mechanical treatment, in the semi-classical approximation they reduce to a differential equation, similar to that derived from classical mechanics for the motion of a pendulum, and a corresponding energy relation which, together, do form a closed system:

$$\begin{aligned} \sum_{\alpha=k_0, -k_0} \langle A^\dagger(\alpha) A(\alpha) \rangle (t) = \frac{v}{4g_0^2} \left[\dot{\phi}(t) \right]^2 e^{-\frac{t}{T_2^*}} \\ \phi(t) + \left(K + \frac{1}{T_2^*} \right) \phi(t) - \frac{g_0^2 N}{v} e^{-\frac{t}{T_2^*}} \sin \phi(t) = 0, \end{aligned} \quad (34)$$

where $\phi(t)$ is a modified Bloch angle defined by

$$\langle R_3 \rangle (t) = [1 + N \cos \phi(t)]/2. \quad (35)$$

With these two relations, calculating the population inversion and the emitted electromagnetic radiation, given by

$$I(t) = \frac{Kv}{2g_0^2} \left[\dot{\phi}(t) \right]^2 e^{-\frac{t}{T_2^*}} \quad (36)$$

as functions of time is comparatively simple.

Thus, where the semi-classical approximation is valid, the B-L model gives a firm footing to a numerically tractable differential equation, permitting straightforward calculations of the most important quantities associated with superradiance. The equation includes line-broadening and accounts fully for the effects of atomic stimulation by the local field which is due to spontaneous emission by the initially excited atoms.

2. Comparison with the Feld-McGillivray Model

Because the semi-classical approximation offers a practical avenue for numerical calculation, it leads to quantitative predictions that can be compared with experiment. For this reason, as well as the fact that it appears to be valid in very general circumstances, it has been the favored approach in such enterprises, in particular, those of M.S. Feld and J.C. McGillivray.

By invoking the semi-classical approximation from the start, Feld and McGillivray are able to include explicitly the spatial effects of a propagating electromagnetic field and atomic polarization in their calculations. This mechanism leads to the prediction (Refs. 18 and 28), already observed experimentally, that ringing will occur in the emitted field under appropriate conditions.

However, the B-L model, although it does not explicitly involve spatial considerations, also predicts ringing by virtue of a mechanism that is ultimately due to the propagation of photons in the polarized volume. In place of the spatial reference, the model includes the parameter K defined by the propagation time of a photon moving across the active volume. The value of K determines whether all emitted photons leave the volume, in which case ringing does not occur, or whether some are absorbed, reexciting a portion of the atoms that have dropped from the inverted to the ground state, in which case ringing does occur.

Equivalently, a critical relation

$$K\tau_c \gg 1 ,$$

involving K and another quantity τ_c , called the cooperation time, determines whether the time-dependent interaction between the atoms and the local field is Markovian (large $K\tau_c$) or non-Markovian in nature. In addition to cooperative spontaneous emission, which is the sole effect in the Markovian case, the non-Markovian interaction causes the local field to stimulate the atoms, thereby producing the observed ringing effect.

In its basic form, the Feld-McGillivray model assumes a single-mode electromagnetic field. Since this is the only *ad hoc* assumption in the B-L model, with the semi-classical approximation it should lead to the same results as the Feld-McGillivray model when equivalent physical parameters in the two models have the same values.

References 18 and 28 claim that agreement with experiment depends on not assuming a constant average photon propagation time but rather requires taking into account the transverse distribution of the electromagnetic field. Nevertheless, the B-L model of Ref. 25, which violates this precept, apparently does predict the gross experimentally observed behavior of superradiant emissions. It is hard to believe that the detailed spatial distribution of the transverse electromagnetic field could be known accurately enough to distinguish between the abilities of the Ref. 25 and Ref. 27 models to predict experimentally observed pulse shapes.

On the other hand, the single pulse experiments of Gibbs et al.(Ref. 28), the more recent two color experiments of Florian, et al.(Ref. 29) and the experiments studying the transition region between superfluorescence - amplified spontaneous emission of Malcuit et al.(Ref. 30) require "a more detailed theory" for this explanation., This is provided by the Haake et al. model (Refs. 31, 32) which will be investigated in future work.

3. Validity of the Semi-Classical Approximation

Section C will present some numerical results obtained from the B-L model with the aid of approximations from Ref. 25 and 17 that, unlike the semiclassical, preserve first-order quantum mechanical effects. Those results indicate the presence of large quantum fluctuations during the time period when most of the radiant pulse energy is emitted. This is somewhat disturbing because the validity of the semiclassical approximation over any time interval appears to depend on quantum fluctuations being small enough to be neglected during the interval.

In Ref. 33 Bonifacio et al. report a similar finding derived from an earlier (Ref. 34), more primitive version of the B-L model: one that does not include stimulation effects. Physically, the earlier model (which is Markovian and is a limiting form of the more sophisticated version as the ratio of the cooperation time to the photon propagation time becomes large) differs from that of Ref. 27 by virtue of the fact that the radiated photons leave the active volume before they can interact with the atoms. As a result, they follow the atomic state changes adiabatically and do not produce a ringing effect in the emitted pulse.

With the earlier model, the authors are able to show (Ref. 33) by direct calculation that quantum fluctuations are large when initially the atomic system is totally inverted. But when the active population is sufficiently large and initially less than totally inverted, their calculations show that the fluctuations are small. They also demonstrate that, consistent with this result, the semi-classical approach is valid whenever the initial atomic system is less than totally inverted.

Although the results in Ref. 33 appear to validate the use of the semi-classical approximation to predict spontaneous cooperative radiation whenever the initial state of atomic inversion is not due to a π pulse (which would be necessary for total inversion of the atoms), the more sophisticated Ref. 25 model does not necessarily lead to the same conclusion when non-Markovian effects are important. This puts the validity of the semi-classical approach in doubt during the time period when most of the radiation takes place.

Unfortunately, the region of validity of the Ref. 25 approximations, which take into account quantum mechanical effects, is, itself, uncertain, at least for the case in which the process is non-Markovian. Thus, calculations based on those approximations cannot be used directly to assess the accuracy of the semi-classical approach over the questionable time period.

To take into account quantum fluctuations in the non-Markovian case, B-L make two approximations. One is the Born approximation which, without some additional step, such as invoking the semiclassical, does not lead directly to a closed system of equations for expectation values of photon and atomic operators.

In the Dicke state representation, the Born approximation leads at first to a finite system of integro-differential equations for the occupation probabilities $p(m,t)$ of the Dicke state basis vectors $|r,m\rangle$:

$$\begin{aligned} \dot{p}(m,t) = & -\frac{2g_0^2}{v} \int_0^t ds e^{-(t+s)/2T_2^* - K(t-s)} \\ & \{ g(m) p(m,s) - g(m+1) p(m+1,s) + [g(m) + g(m+1)] N(m,s) \\ & - g(m+1) N(m+1,s) - g(m) N(m-1,s) + g^{1/2}(m) g^{1/2}(m-1) L(m,s) \\ & - 2g^{1/2}(m) g^{1/2}(m+1) L(m+1,s) + g^{1/2}(m+1) g^{1/2}(m+2) L(m+2,s) \} , \quad (37) \end{aligned}$$

where

$$g(m) = \begin{cases} (\frac{1}{2} N + m) (\frac{1}{2} N - m + 1) & \text{for } -\frac{1}{2} N \leq m \leq \frac{1}{2} N , \\ 0 & \text{otherwise ,} \end{cases}$$

$N(m,t)$ is the photon number expectation for the inversion state m , and $L(m,t)$ is the expectation value of an operator derived from the interaction of the electromagnetic field with the atomic dipole operators R^+ , R^- . Unfortunately, the number of unknown quantities to be determined from equation (37) is larger than the number of equations in the system.

When the authors enlarge the system to include time derivatives of the unknowns other than the Dicke state occupation probabilities, the resulting set of equations is still not closed because it contains new unknowns, consisting of higher order moments of the photon and atomic operators. Obviously, repeating the process indefinitely will result in an infinite hierarchy of (finite) systems of equations, involving moments of ever increasing order.

The authors observe that a simple way of getting a closed system is to drop the photon expectation values and all second-order moments from the first set of equations in this hierarchy, involving time derivatives of just the Dicke state occupation probabilities and the photon number expectations. However, that procedure should be valid only under conditions that would justify substituting the earlier Markovian model. It would therefore add nothing new, serving only to verify that their earlier model is a limiting case of the more general non-Markovian model.

Their next step is to retain the equations involving time derivatives of both the Dicke state occupation probabilities and the photon expectation values, but to drop all second-order and higher moments. The result is a larger, but closed, system:

$$\begin{aligned}
\dot{p}(m,t) = & -\frac{2g_0^2}{V} \int_0^t ds \, e^{-K(t-s) - (t+s)/2T_2^*} \\
& \{ g(m) p(m,s) - g(m+1) p(m+1,s) + [g(m) + g(m+1)]N(m,s) \\
& - g(m+1)N(m+1,s) - g(m)N(m-1,s) \} , \\
\dot{N}(m,t) = & \left(-2KN(m,t) + \frac{2g_0^2}{V} \int_0^t ds \, e^{-K(t-s) - (t+s)/2T_2^*} \right) \\
& \{ g(m+1) [p(m+1,s) + N(m+1,s) - N(m,s)] \} . \quad (38)
\end{aligned}$$

Significantly, the equations resulting from this approximation imply a relationship between atomic and photon operator expectation values that is also implied by the exact (i.e., with no approximations) operator equations of the model. Therefore, the three previously discussed equations, (31), (32), and (33), follow from (38). In addition, (38) guarantees conservation of probability: the sum of the Dicke state occupation probabilities satisfying (38) must remain constant over time.

Because the approximate equations yield the basic conservation laws, it might be expected that their solutions would be physically well-behaved. However, numerical calculations indicate otherwise.

After a certain time interval, before the emitted pulse reaches its maximum amplitude, quantities derived from the approximate solution become non-physical in at least two respects. First, although conservation of total probability is still satisfied, individual Dicke state occupation probabilities become negative. Second, although conservation of energy is still satisfied, individual Dicke state photon number expectation values also become negative.

The case in which the number of atoms in the active volume is limited to two is simple enough to be treated in detail analytically if inhomogeneous line-broadening is neglected. An investigation of it using the Laplace transform reveals that all states below the maximum Dicke occupation number (which is two in the case considered) exhibit a resonance phenomenon; i.e., some of the transformed solution functions have double poles. In the inverse transform domain such a function must have a factor proportional to the time variable.

In the absence of double poles, when parameters are such that ringing does not occur, the solution functions decay exponentially with time. When the converse is true, i.e., parameters are such that ringing does occur, the solution functions have factors that are linear combinations of trigonometric functions of time. At least in the second case, the additional time variable factor imposed by a double pole guarantees increasingly larger oscillations with linearly increasing amplitudes that must eventually produce negative expectation values.

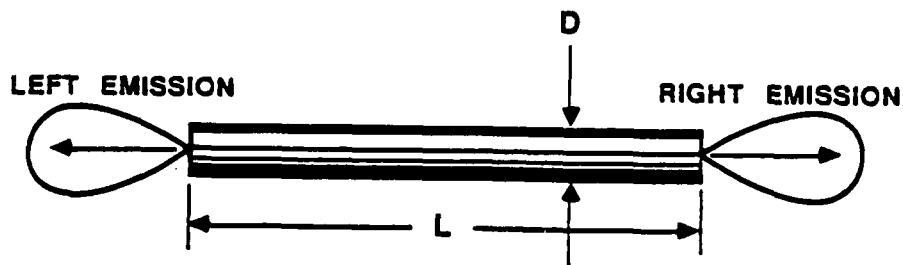
In principle, a similar analysis for an arbitrary number of atoms could be carried out in the same way, using the Laplace transform, since the equations can be treated recursively in pairs, no matter what the total number of atoms may be. Because of the symmetry of the inversion operator eigenvalues about zero, the coefficients due to the lower Dicke states will always produce double poles for the transformed solution functions, just as in the case of two atoms.

In fact, in Ref. 33 the authors make the same observation in connection with the earlier Markovian model, i.e., that due to this coefficient symmetry, double poles must always occur in the transformed solution functions. However, in Ref. 33 the remark is made in passing, without noting the consequence that, in approximate solutions for a more general model, such resonances may lead to physically impossible negative expectation values.

C. CALCULATED RESULTS

In the previous section we discussed some of the problems involved with the various treatments of superradiance, emphasizing the B-L model. In this section we describe the calculations performed to check some of these interesting points, in particular (1) the relationship of quantum fluctuation to the pulse shape, (2) the justification of the semiclassical approximation, and (3) the limitations of and differences between pulses calculated by means of different approximations.

In all cases, the geometrical model assumed is of a long acicular shape, with the diameter $D \ll L$, the length, as shown in Fig. 20.



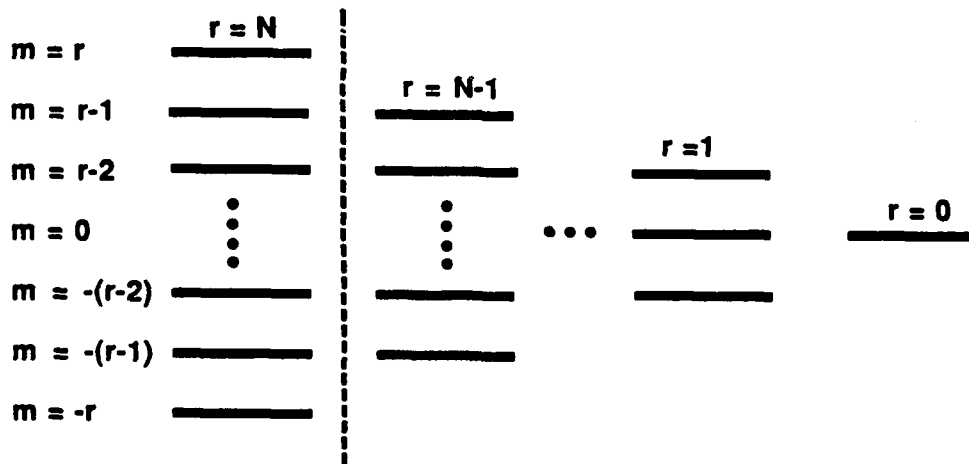
1-16-87-4M

Figure 20. Geometry of the Superradiator Showing the Two Possible Modes of Emission

The calculations are actually done for one of the possible emission modes, right emission, as shown in Fig. 20. The nuclear model consists of an energy level structure as depicted in Fig. 21, with the Dicke quantum states $|r, m\rangle$ satisfying the eigenvalue equations

$$R^2 |r, m\rangle = r(r+1) |r, m\rangle$$

$$R_3 |r, m\rangle = m |r, m\rangle ,$$



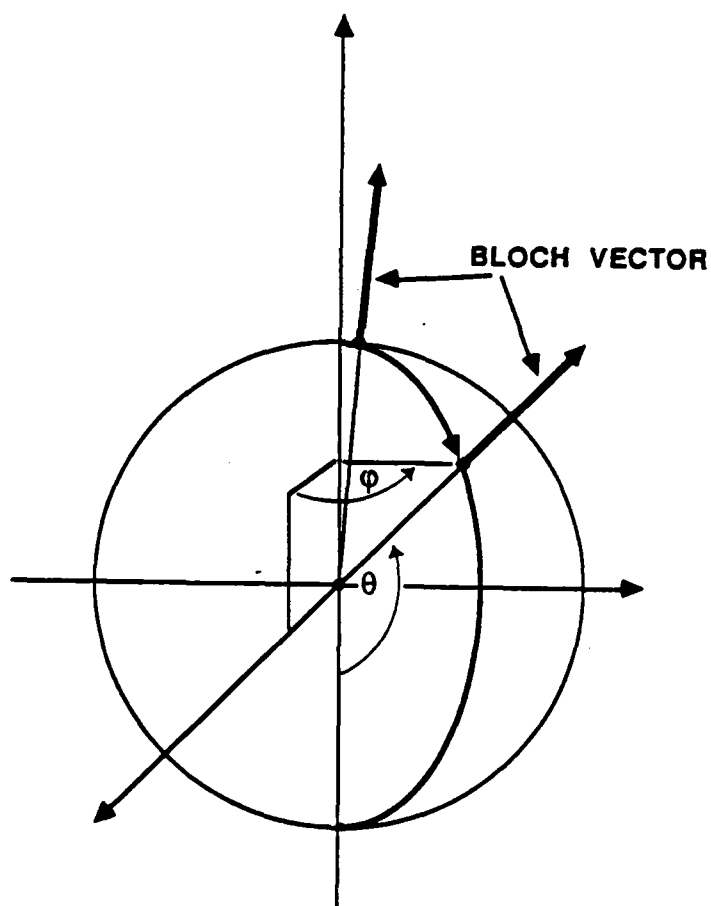
1-16-87-3M

Figure 21. Dicke Superradiant Model Showing the Various Multiplets of $2N$ two-level Resonators

where r is the cooperation number ranging from 0 or $1/2$ to $1/2 N$, and m is the energy eigenvalue restricted to the range $(-r, +r)$. The Bloch states which are fully symmetrized states if the two-level nuclei are defined in the subspace of cooperation number r as

$$\begin{aligned}
 |\theta, \phi\rangle &= \sum_{m=-r}^r |r, m\rangle \langle r, m | \theta, \phi\rangle \\
 &= \sum_{m=-r}^r |r, m\rangle \left(\frac{2r}{m+r}\right)^{1/2} \left(\sin \frac{1}{2}\theta\right)^{r+m} \left(\cos \frac{1}{2}\theta\right)^{r-m} e^{-i(r+m)\phi} \quad , \quad (39)
 \end{aligned}$$

where θ and ϕ define points in the spherical coordinate system with $\theta = 0$ corresponding to the south pole as shown in Fig. 22.



1-16-87-2M

Figure 22. The Bloch Sphere

For convenient reference, the parameters useful in the description of superradiant phenomena, together with their definitions, are listed in Table 5. The conditions for superradiance are

$$K^{-1} \leq \tau_R \leq T_2^* .$$

A phenomena sometimes referred to as pure superradiance, which produces a single pulse, is observed when

$$K\tau_c \gg 1 .$$

This occurs because the photons escape so fast from the volume that they do not stimulate emission. Multiple pulses are obtained when

$$K\tau_c \approx 1 .$$

In this case, $\tau_R \approx \tau_c$, the radiation field can interact with the atoms or nuclei and the character of the resulting emitted pulse is due to both cooperative emission and stimulated emission and absorption.

We first describe the superradiant pulse shape obtained from the diffusion equation derived by Narducci et al., as mentioned earlier. The diffusion equation is derived from the B-L theory in the limit $K \rightarrow \infty$ and $T_2^* \rightarrow \infty$ so that there is no interaction of the cooperation emission process and stimulated emission. We assumed the initial distribution to be normal with variance σ^2 so that the probability of occupation of a Bloch state is given by

$$P(\theta) \approx e^{-(\theta - \pi)^2 / \sigma^2} . \quad (40)$$

Our calculations were performed with a computer program SR1 described in Appendix E. Figure 23 shows some calculated results of this superradiant pulse obtained from the diffusion equation for $N = 1$ to 10^6 . Note the change in the shape of the pulse as N decreases. For $N = 10^2$ to 10^6 , the pulse is well-developed and is characterized by a delay time τ_D and a pulse width τ_R , both proportional to $N^{1/2}$. On the other hand, for low N and in particular for $N = 1$ and σ large, the pulse is exponential and does not exhibit cooperative effects and, in fact, reflects independent single-particle emission.

Table 5. Table of Parameters Describing Superradiance

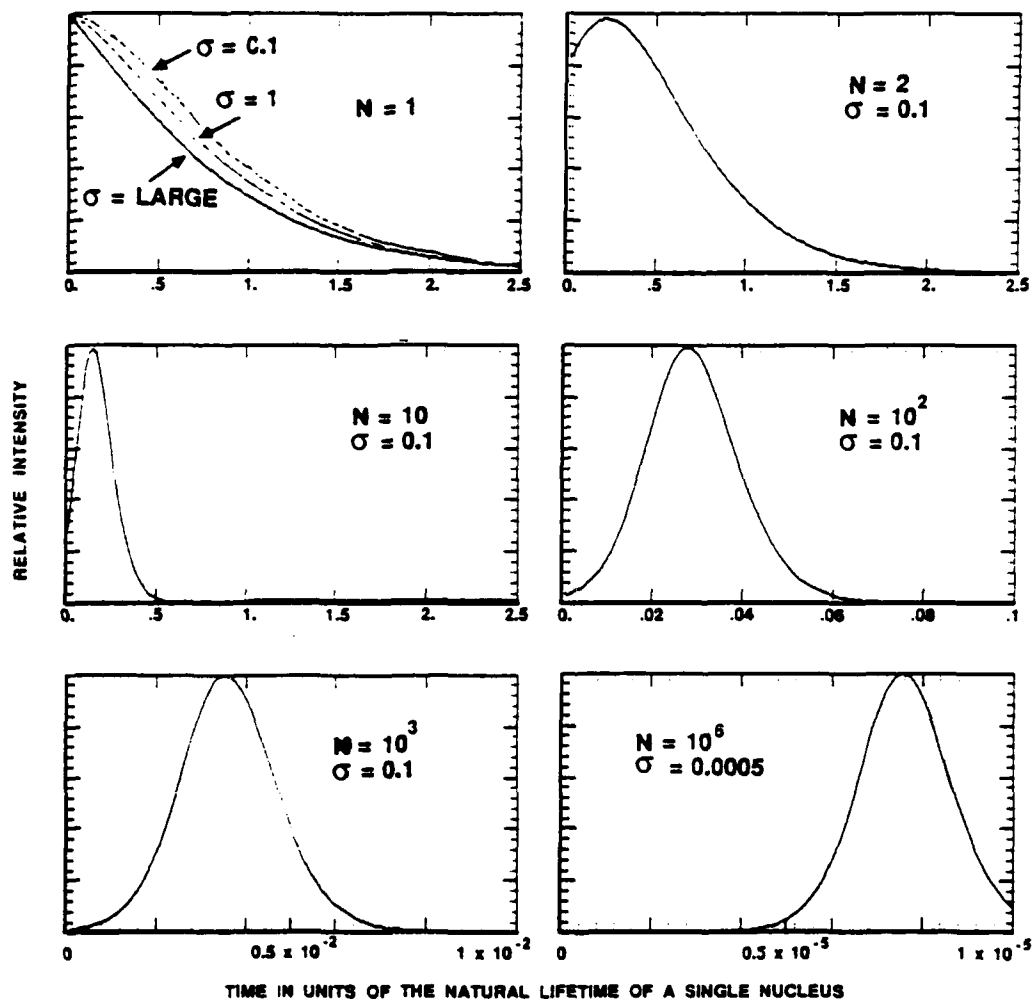
Parameter	Definition	Description	Reference
γ_c	$\frac{1}{\tau_c} = \frac{1}{2} (c \rho \gamma \lambda^2)^{1/2}$	maximum superradiant rate	A-C*
N_c	$(c/\gamma_c) A \rho$	maximum cooperation number	A-C**
γ_D	$\frac{1}{4} N_c \gamma_c \lambda^2 A$	enhanced emission rate of N_c resonators	A-C
g_k	$(c k \mu^2 / 2 \hbar)^{1/2}$	coupling constant	B-L
τ_c	$\frac{1}{g_0} \left(\frac{v}{N} \right)^{1/2}$	cooperation time	B-L
τ_R	$\frac{8 \pi \tau_0}{\rho \lambda_0^2 L}$	duration time of pure superradiance	B-L
τ_D	$\frac{1}{2} t_R' N$	delay time, or reduced time during which pure superradiance reaches its maximum	B-L
τ_0	$\frac{c \lambda_0^2}{16 \pi g_0^2}$	lifetime of isolated resonator	B-L
K	$\frac{c}{2L}$	photon escape rate	B-L
k_1	$\frac{c}{2L} \tau_c$	photon escape rate (in units of τ_c)	B-L
k_2	$\frac{1}{T_2^*} \tau_c$	inhomogeneous line broadening equivalent rate	B-L
T_2^*		inhomogeneous linewidth dephasing time	B-L

LIST OF PRIMARY PARAMETERS

N = number of resonators (nuclei or atoms) in volume v	μ = electric dipole moment
ρ = density of resonators = N/v	c = speed of light
λ = wavelength of emitted radiation	γ = emission rate of isolated resonator
λ_0 = wavelength at resonance	A = cross section of window of length L
k = $2\pi/\lambda$ wavenumber	τ_0 = lifetime of isolated resonator
	v = volume occupied by radiators.

* F.T. Arrecchi and E. Courtens, *Phys. Rev. A*, 2 (5), 1730, 1970.

** R. Bonifacio and L.A. Lugiato, "Cooperative Radiation Processes in Two-Level Systems: Superfluorescence II," *Phys. Rev.* 12 (2), 587-598, August 1975.



2-2-47-12

Figure 23. Characteristics of a pure superradiant pulse calculated from the diffusion equation of Narducci et al. (program SR1 in Appendix E) for different values of the cooperation number and variance σ of the initial distribution of states on the Bloch sphere.

To study superradiance in the more complex regime, where emission by cooperative phenomena and stimulated emission interfere, we solved equations (8) numerically. The program (SR 2, Appendix F) calculates the probability of the occupation of the Bloch states $P(m')$ and the electromagnetic field states $N(m)$ or $Q(m')$ as a function of time.* The calculation is done for arbitrary initial distributions $P(m)$ and $N(m)$ and arbitrary K and T_2^* . The cooperation number N is a constant of motion; thus the dynamics are restricted to the first ladder of the Dicke states as shown in Fig. 21.

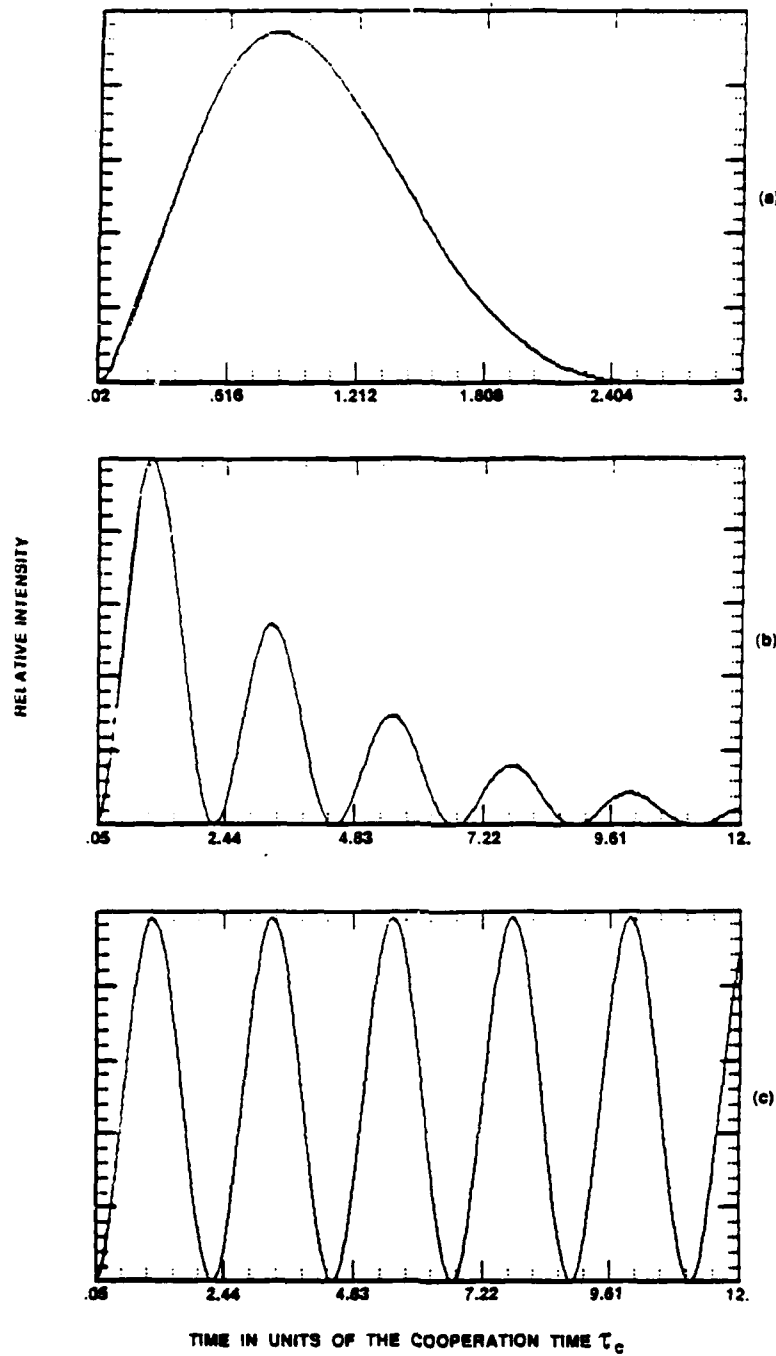
Figure 24 shows some characteristic pulses obtained with the Master's equation treatment of Bonifacio and Lugiato in the region of $k_1 > k_0$, $k_1 \approx k_0$ and $k_1 < k_0$, where $k_0 = 2\sqrt{2}$ and corresponds to the K value in units of τ_c at which ringing first occurs (see Appendix E). Note the appearance of a single pulse in Fig. 24a, corresponding to the pure superradiant region and ringing, or multiple pulses, when stimulated emission interferes with superradiance, Figs. 24b and 24c.

The effect of the coupling constant $g_0' = \sqrt{2} g_0$ on the superradiant pulses is shown in Fig. 25 where g_0' is varied from 0.051 to 0.817, effectively changing the cooperation time since

$$\tau_c = \frac{1}{g_0} \left(\frac{\nu}{N} \right)^{1/2}. \quad (41)$$

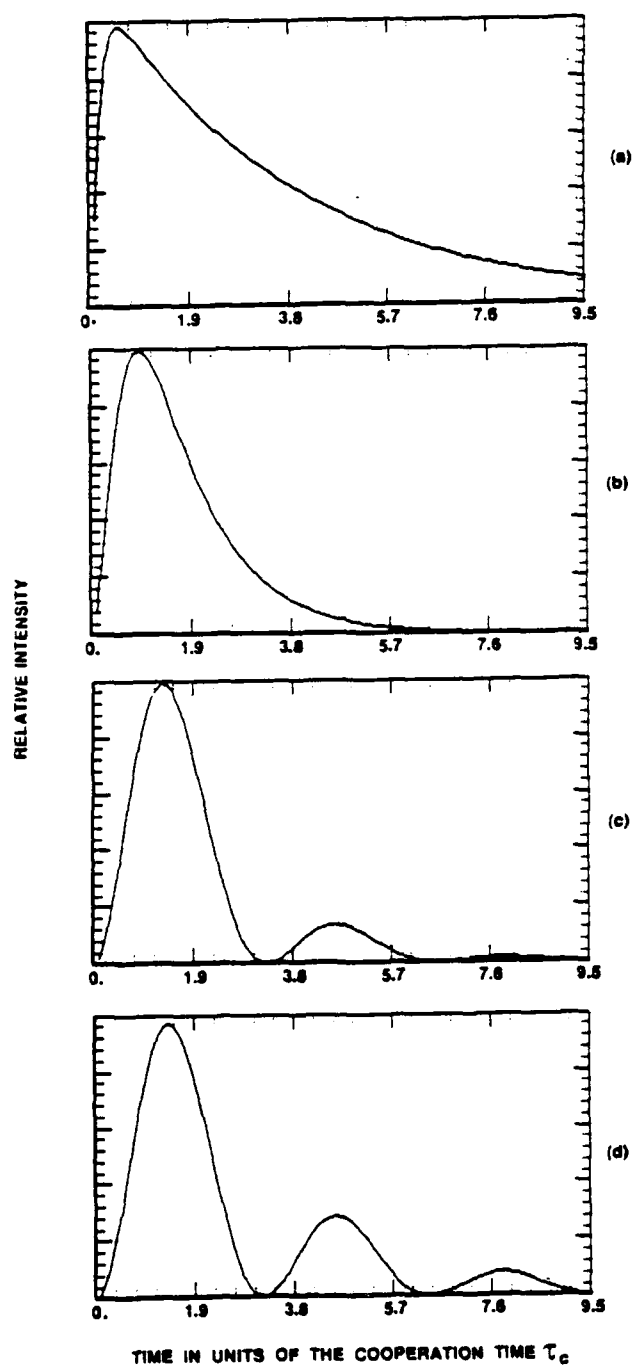
The master equation formalism allows one to investigate the interaction between the photon field and the master system through equations (8). The results shown up to now assumed that $N(m) = 0$ initially, thus the photon field was not activated. Figures 7a through 7f show the superradiant emission when $N(m) \approx 0$ initially. Notice that as the initial value $N(m)$ increases the emission which is obtained from $\sum N(m)$ starts at low values (Figs. 26a and 26b) and reverses to full ringing pulses which start at high values initially. There is a phase change in the ringing phenomena with the transition characterized by a decaying, slightly wavy pulse (Figs. 26c and 26f).

* A note on notation. In this chapter we use $p(m)$ and $N(m)$ for Dicke state occupation probability and the photon number expectation value when the basis system varies from $m = -r$ to $+r$. When the basis system is $m' = 1$ to $N + 1$ we use $P(m')$ and $Q(m')$ for these quantities. Also, $K = c/2L$ is used for the photon escape rate in c.g.s. units but $k_1 = K\tau_c$ is used when it is given in terms of the cooperation time.



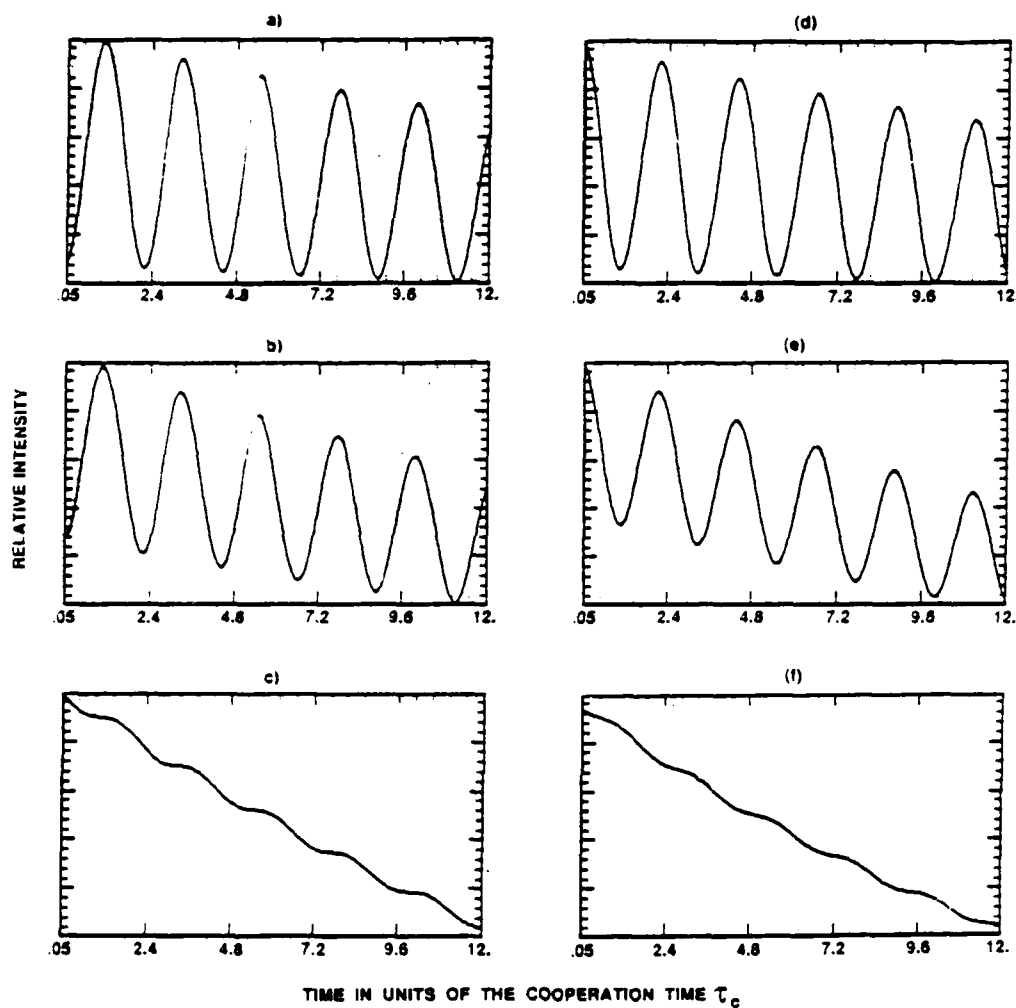
2-2-87-6

Figure 24. Variation in the superradiant pulse shape as a function of $k_1 = (c/2L) \tau_c$ for $N = 100$ and $k_2 = 10^{-7}$. The initial conditions are $P(m) = 0$ for $m = 5$, $P(5) = 1$ and with $k_1 = 1.5, 0.26, 10^{-20}$ for (a), (b), and (c), respectively.



2-2-87-7

Figure 25. Variation in the superradiant pulse as a function of the coupling constant g_0' , with $n = 4.4 \times 10^{-24} \text{ cm}^3$, $N = 2$ and initial conditions $P(1) = P(3) = 0$, $P(2) = 1$.



2-2-47-8

- | | | |
|-----|------------------------------|----------------------------|
| (a) | $Q(1) = 10^{-4},$ | $Q(m') = 10^{-6}$ |
| (b) | $Q(1) = 5 \times 10^{-4},$ | $Q(m') = 10^{-6}$ |
| (c) | $Q(1) = 10^{-3},$ | $Q(m') = 10^{-6}$ |
| (d) | $Q(1) = 5 \times 10^{-3},$ | $Q(m') = 10^{-6}$ |
| (e) | $Q(1) = 7.5 \times 10^{-3},$ | $Q(m') = 10^{-6}$ |
| (f) | $Q(1) = 5 \times 10^{-4},$ | $Q(m') = 5 \times 10^{-5}$ |

Figure 26. A study of the effect on the superradiant lineshape of the initial photon field distribution or $Q(m')$ for the case $N = 100$, $P(m') = 0$, $m' = 5$, $P(5) = 1$, $k_1 = 0.0269$, $k_2 = 2 \times 10^{-20}$ in.

We have observed during our investigation of the B-L model that under some conditions the calculated results would oscillate violently and even blow up. We suspected that this could be caused by numerical error (a truncation made by B-L) as discussed in Chapter II. In order to examine this problem, we solved equations (8), analytically for the case $N = 2$ and showed that the negative probabilities and blow up were also obtained from that solution. This is discussed in detail in Appendix D.

The numerical solution and the analytical solution gave identical results. Three emission pulses calculated for $N = 2$ are shown in Fig. 27. For the initial conditions $P(1) = P(2) = 0, P(3) = 1$ as shown in Fig. 27a and for $P(1) = 0, P(2) = P(3) = 1$ as shown in Fig. 27b the probability goes negative, whereas for $P(1) = P(3) = 0$ and $P(2) = 1$, a physically meaningful solution is obtained.

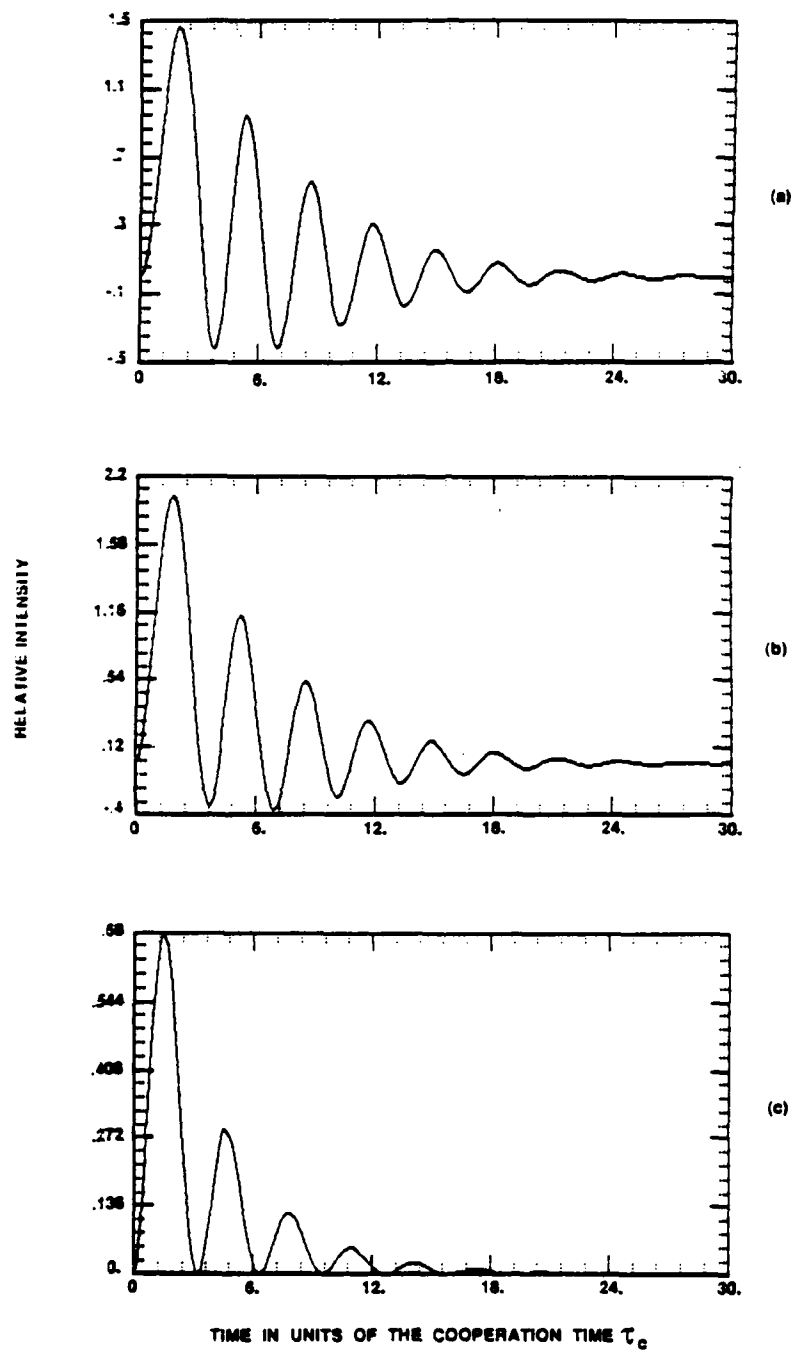
Quantum mechanical fluctuations are responsible for the triggering of the superradiant pulse from the inverted population. It has been argued that when these fluctuations are small, semiclassical solutions give good approximations to the superradiant pulse emission and that these fluctuations are small at the maximum emission rate (Refs. 18, 34, and 35). The following sequence of figures was generated to check this assumption. Figures 28a through 28d show in the top figures the emitted pulse which is calculated from equations (8) and is given by

$$\sum_m N(m) \quad (42)$$

The lower figure gives the variance

$$\begin{aligned} \langle\langle R_3 \rangle\rangle &= \langle R_3^2 \rangle - \langle R_3 \rangle^2 \\ &= \sum_m m^2 p(m) - \left(\sum_m m p(m) \right)^2 \end{aligned} \quad (43)$$

Our results indicate that the quantum fluctuations are not necessarily negligible during the course of the emission process. Figure 29 shows similar results for the initial distribution $P(5) = 1$ and $P(m) = 0, m \neq 5$ and $k_1 = 0.0269$. Here the variance is zero initially, goes positive for a good part of the first pulse and then oscillates around zero. The unphysical oscillations are due to the truncation error discussed earlier. However, during the major part of the first pulse in the ringing emission process the variance is positive. In the pure superradiant region (Fig. 30) the variance is positive and not negligible during the major part of the pulse.



2-2-87-5

Figure 27. Calculated superradiant pulses for $N = 2$ and different initial conditions, (a) $P(1) = P(2) = 0$, $P(3) = 1$, (b) $P(1) = 0$, $P(2) = P(3) = 1$, and (c) $P(1) = P(3) = 0$, $P(2) = 1$

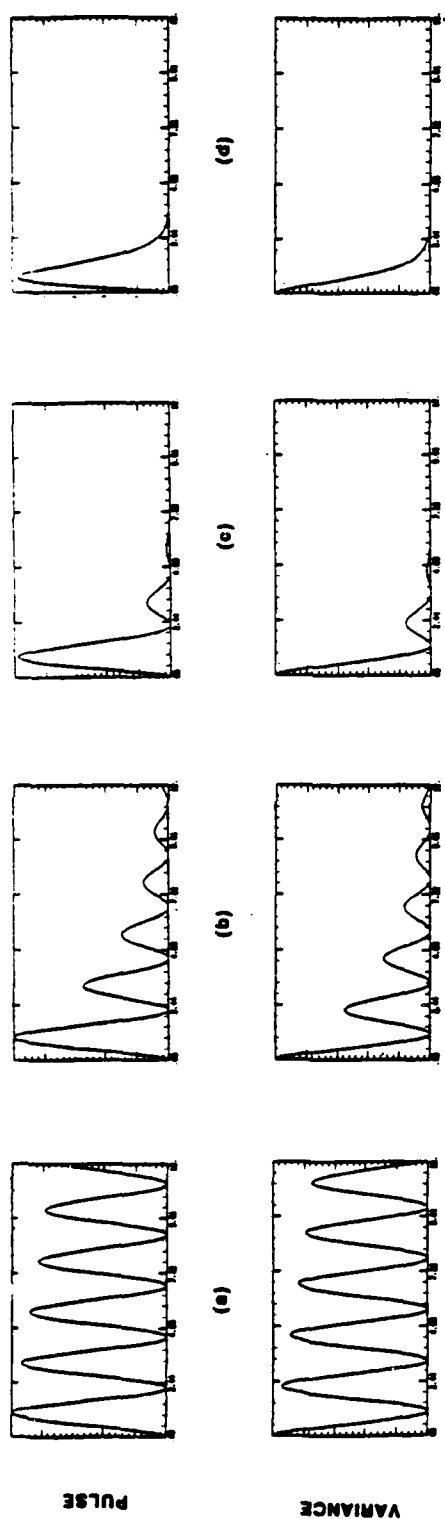
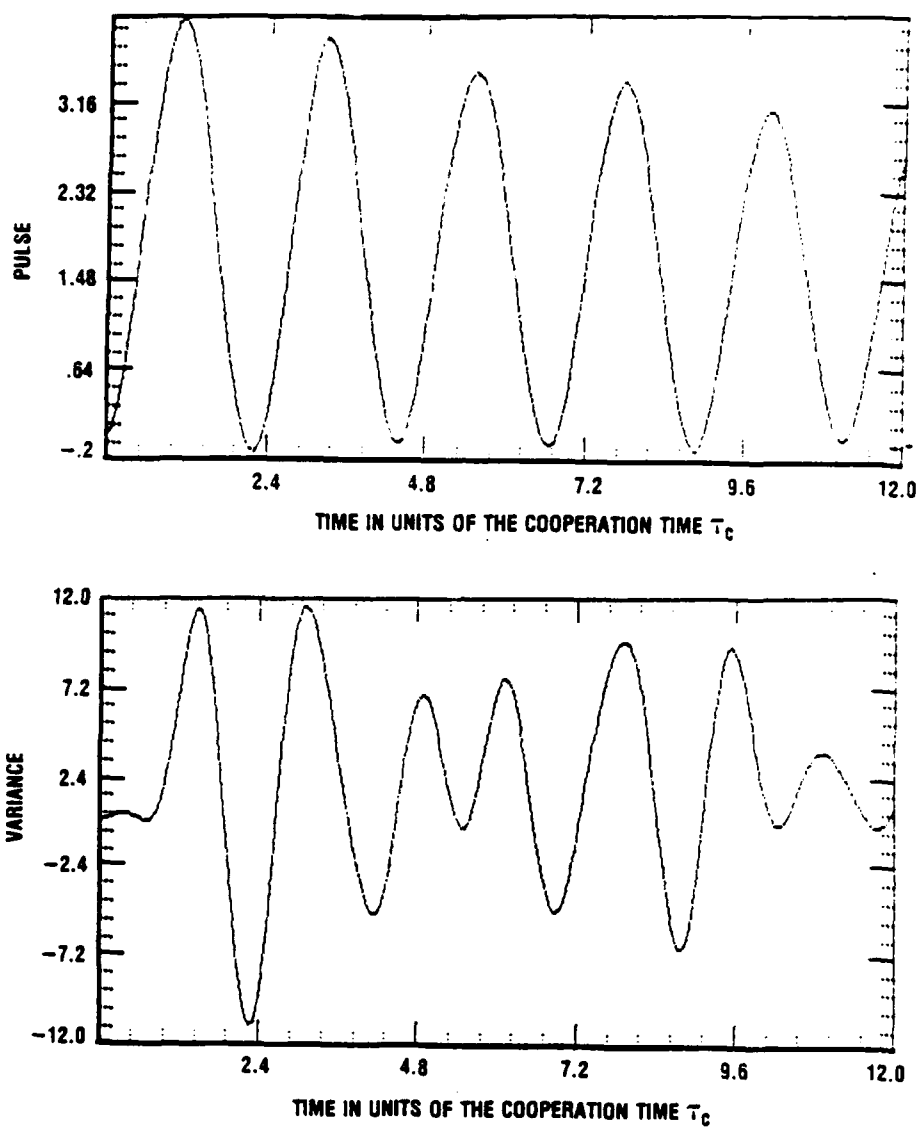
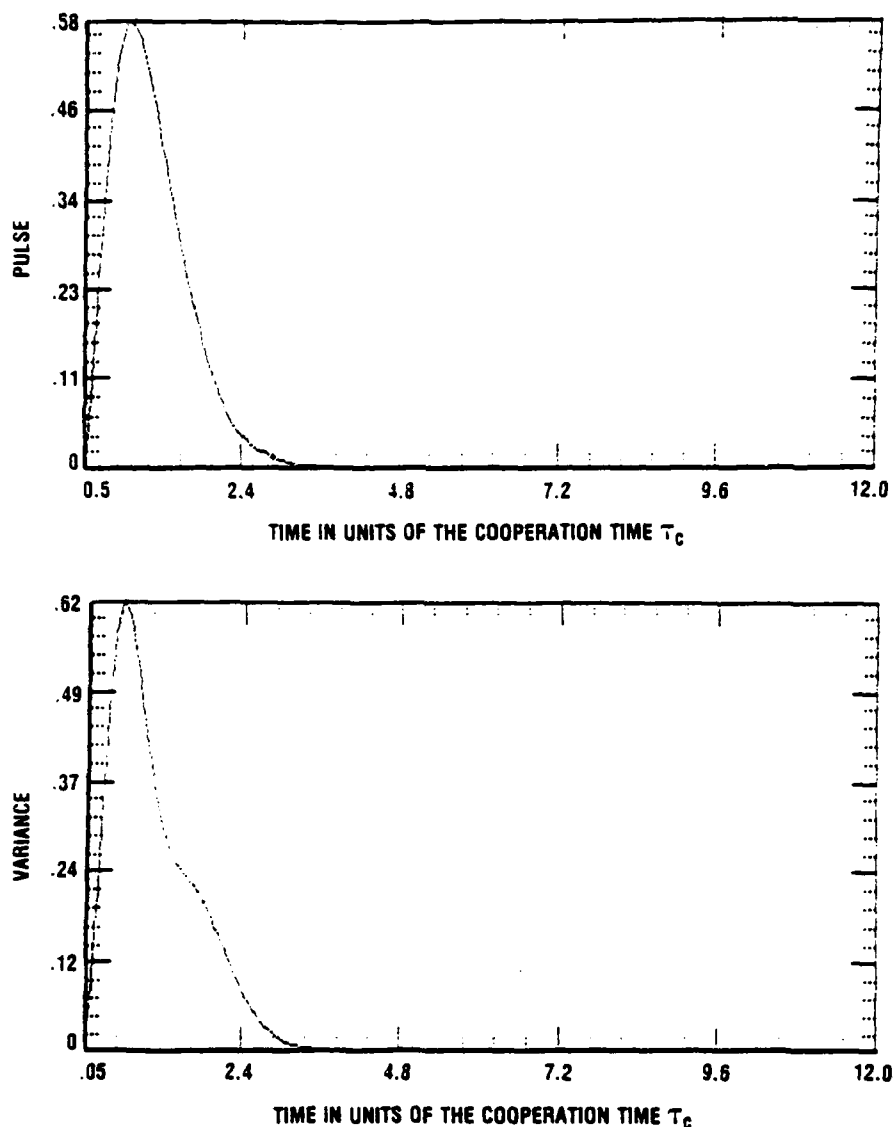


Figure 28. Radiative pulse and quantum fluctuations (variance) for different initial conditions. The initial distribution for $P(m')$ is Poisson with $P_c = 10^{-5}$ and $N(m) = 0$. The k values are 0.0269 in (a), 0.269 in (b), 0.8 in (c), and 2.69 in (d).



11-10-88-1

Figure 29. Pulse and variance for the initial conditions $P(5) = 1$, $P(m') = 0$, $m' = 5$, $N = 100$ and $k_1 = 0.0269$.



11-10-88-2

Figure 30. Pulse and variance for the initial conditions $P(5) = 1$, $P(m') = 0$, $m' = 5$, $N = 100$ and $k_1 = 2.69$.

In our final discussion we compare the results of quantum mechanical calculations using the B-L model with semiclassical calculations using the pendulum equations (programs SR 3 and SR 4, Appendix G). Figures 31a and 32a show quantum mechanical results, and Figs. 31 and 32 the corresponding semiclassical results. In both cases, the same parameters were used, but in 32 the Dicke state was initially specified as $m = 2$. Such a precise specification is not possible in the semiclassical treatment.

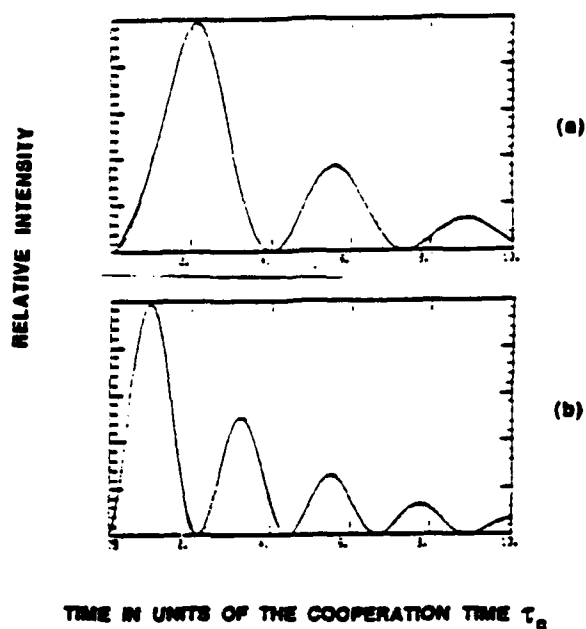


Figure 31. Quantum mechanical calculation (a) and semiclassical calculation (b) for the case $N = 2$, $k_1 = 0.03$. In Fig. (b) it was assumed $P(m') = 0$, $m' = 2$, $P(2) = 1$.

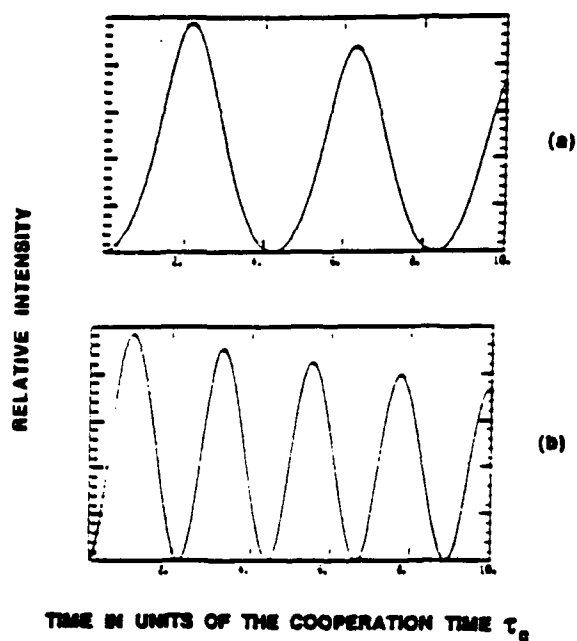


Figure 32. Quantum mechanical calculation (a) and semiclassical calculation (b) for the case $N = 2$, $k_1 = 0.3$. In Fig. (b) it was assumed $P(m') = 0$, $m' = 2$, $P(2) = 1$.

D. CONCLUSIONS

The general equations of B-L describe the phenomena of superradiance in the regime where stimulated emission interferes with cooperative emission as well as in the pure superradiant regime. The theory has the capability of explaining certain features of the experimental results with or without the occurrence of ringing. To explain correctly the experimentally observed pulse fluctuations, quantum initiation statistics have to be included correctly and this is done in other theories. Also, the truncation introduced by B-L to make the equations tractable produces unphysical results for some initial conditions. This can appear as negative variance, negative pulses, or complete blow up of the solution. This problem has to be dealt with to make the theory more generally useful. It would be important to do this because the general theory includes inhomogeneous broadening effects which are important in nuclear considerations. Also, calculations with the B-L theory showed that quantum fluctuations are large and important over the complete pulse when stimulated emission is important. Thus, the usual justifications for the validity of semiclassical theories breaks down.

In conclusion, we feel that for the study of certain features of nuclear superradiance the B-L theory can be used to advantage, especially if the truncation error can be removed. Effects of coherent excitation, relaxation, inhomogeneous and homogeneous broadening in nuclear superradiance could be studied with the B-L theory. For taking into account incoherent excitation, competing transitions, and transport effects, other theories based on the Maxwell Bloch equations (Haake-Haus group effort and the Eindhoven group effort) (Refs. 31, 32, and 36) should be considered.

ACKNOWLEDGMENTS

The authors would like to express their appreciation to Professor Joseph Eberly for enlightning discussions on this work and helpful comments on the manuscript.

IV. MULTIPHOTON DEEXCITATION OF ISOMERIC LEVELS

A. INTRODUCTION

Among the many concepts introduced over the years for developing a γ -ray laser (Refs. 1, 2, and 37) the upconversion or pumping of a nuclear level from an isomeric level to achieve inversion is the one most vigorously pursued by researchers at present. The idea is to pump the isomeric level by a short burst of electromagnetic radiation from a powerful optical laser or x-ray source to a nearby short-lived level. This would provide the inverted population if the decay rate of the upper lasing level is not too short. The lifetime of the upper lasing level should be short enough to provide a large cross section for the stimulated emission but not so short that it would introduce pumping problems with large power requirements. In general, the upper lasing level may be populated through a cascade process, thus reducing the requirements on the lifetime of the lasing level.

For the purpose of analysis, the operation of a γ -ray laser can be conveniently divided into three steps as discussed in Ref. 2. The first step is the initial pumping or inversion stage, which involves the preparation of the isomer. The second step is the triggering of the lasing action. In the case of interest, this is the pumping or the upconversion to the upper lasing level by a low-energy photon. The third step is the emission of the radiation in a lasing or superradiant mode. All three stages present their special problems as discussed in Ref. 2. In particular, the emission stage requires the operation of the Mössbauer Effect (ME). This effect could be destroyed by heating or the destruction of the isomeric crystal during the triggering stage by inefficient upconversion mechanisms. In general, threshold conditions, depending on solid state and nuclear properties, have to be satisfied (Refs. 38, 39, and 40).

In this paper, we are only concerned with the triggering stage in the upconversion concepts as shown in Fig. 33. During this stage, the population of the upper level with high fluxes of low-energy photons has to be accomplished.

The processes referred to as "coherent and incoherent upconversions" have been discussed by Collins (Ref. 41). We are interested in the requirements imposed by nuclear

properties on the realization of those processes. Furthermore, one of the critical proofs of concept experiments on the way to the development of a γ -ray laser, based on upconversion techniques would be the demonstration that the energy stored in an isomeric level can be "pumped out," or the decay rate of the level increased. A Raman scattering experiment (Ref. 42) has already been proposed to do just that. The feasibility of this would have to be shown before lasing on the nuclear level with upconversion techniques (a much more difficult problem) is seriously considered.

We have divided this Chapter into two parts. First, we examine the single-photon Raman scattering experiment and compare requirements set by atomic and nuclear systems. Second, we discuss multiphoton processes and examine the requirements for pumping out isomeric levels and preparing an inverted population for lasing.

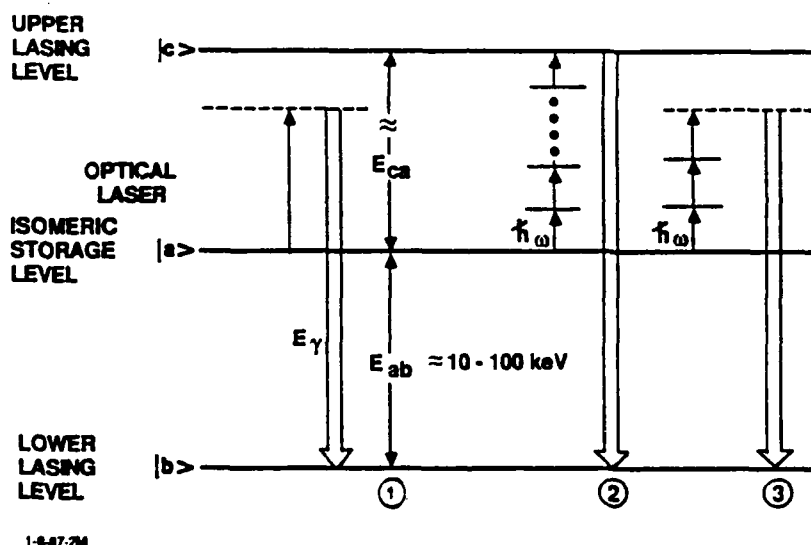


Figure 33. A three-state system showing the isomeric level, or initial state $|a\rangle$, the upper lasing level $|c\rangle$ and the ground state $|b\rangle$. In the subsequent analysis we keep E_{ba} and γ_a constant and vary E_{ca} , ω , $n\omega$, I , and γ_c . Process 1 in the figure shows a single photon off-resonance excitation, process 2 a multiphoton on-resonance excitation, and process 3 a multiphoton off-resonance excitation.

B. COMPARISON OF ATOMIC AND NUCLEAR ELECTROMAGNETIC TRANSITIONS

At this point, a brief discussion of general trends in atomic and nuclear transitions would be appropriate. Particular optical lasing and potential gamma-ray lasing transitions are best contrasted against such a background discussion. Features of atomic and nuclear transitions are very different, with major differences arising both from kinematics and structure. Three of the four aspects to be considered (multipolarity, frequency, lifetime, and single-particle structure) involve primarily kinematics. A dimensionless figure of merit with which to relate these features, and contrast the atomic with the nuclear case, is kr , the photon wave number ($k = 2\pi/\lambda$) multiplied by the system radius.

Atomic transitions are almost exclusively electric dipole transitions with frequencies in or near the visible range, and lifetimes longer than a nanosecond. They arise from single electron level jumps. For a 1-eV transition $\lambda = 12,000 \text{ \AA}$, and kr is about 3×10^{-4} . The radiative decay width for electric decays is given by an atomic matrix element, multiplied by $(kr)^{2l+1}$. If the interaction potential is e^2/r evaluated at an effective distance of about an angstrom, this leads to a width of $5 \times 10^{-10} \text{ eV}$, or a lifetime of about a microsecond (see Table 6). Electric quadrupole radiation would be inhibited by an additional factor of $(kr)^2$, or about 10^{-7} . Magnetic dipole radiation would be inhibited by a factor of $(hc/m_e c^2 a_0)$, or about 5×10^{-5} (a_0 is the Bohr radius of the Hydrogen atom).

Table 6. Atomic and Nuclear Decay Rates

Name of Parameter	Atomic			Nuclear		
	1	2	4			
E-Gamma (eV)				100,000	300,000	1,000,000
k-Gamma (1/Å)	0.000507	0.001014	0.002027	50.67653	152.0296	506.7653
$\lambda(\text{Å})$	12398.61	6199.305	3099.652	0.123986	0.041329	0.012399
(ka_0)	0.000268	0.000536	0.001072	0.002681	0.008042	0.026808
Width (eV)	5.25E-10	4.2E-09	3.36E-08	0.005246	0.141634	5.245713
E1 Rate (s) ⁻¹	797503.7	6380029	51040234	7.89E+12	2.15E+14	7.98E+15
M1 Rate (s) ⁻¹	42.49773	339.9819	2719.855	1.26E+10	3.41E+10	1.26E+13
E2 Rate(s) ⁻¹	0.057314	1.834036	58.68914	57313614	1.39E+10	5.73E+12
E2 Rate*Z*Z(s) ⁻¹	0.057314	1.834036	58.68914	1.43E+11	3.48E+13	1.43E+16

The dominance of electric dipole, or E1 radiation, and the approximate lifetime are set by the available energy of an electronic transition together with the radius of an atom. Electric quadrupole radiation is much weaker because (kr) is so small. Since major shells in atoms contain a series of adjacent l -values, many electric dipole transitions exist.

For a nuclear transition, with a characteristic energy of 1 MeV and a characteristic radius of 5.29 fm ($= 10^{-4} a_0$), we have (kr) two orders of magnitude larger than in the atomic case. Using the same, somewhat naive, procedure to estimate a nuclear E1 lifetime gives a width of 5 eV, or a lifetime of about 10^{-16} s. Electric quadrupole radiation would be only three orders of magnitude slower, and have lifetimes much shorter than those of the fastest atomic electric dipole transitions. From energy and size considerations alone we expect that nuclear transitions will be faster than atomic, and will have higher multipolarities which are more competitive with dipole radiation. (See Table 6.) It is important to recall that candidate gamma-ray lasing transitions must compete with all available channels. The 10 to 100 keV energy range for the lasing transition does not set the energy scale if other decays with higher energy gamma rays are allowed, as is the case for most candidates. The lower energy desired for the lasing transition only imposes further kinematic difficulties.

Further differences arise from the dissimilarities in structure of atoms and nuclei. In atoms, charge separation involves moving a light electron relative to the center of mass of the atom and is fairly simple. In nuclei, charge separation involves moving the much heavier protons relative to the neutrons to which they are bound by the strong interaction. As a result, most E1 strength corresponds to an unobservable motion of the center of mass of the system, and cannot contribute to decay rates. The exception to this is in isospin changing excitations, which involve spatial separation of neutrons and protons, and hence tend to occur at high excitation energy. This results in E1 rates which are orders of magnitude slower than single-particle estimates.

In contrast, E2 transitions are enhanced by collective participation of many nucleons in a single transition. Frequently, an E2 (or M1) branch will dominate decay of a nuclear level even though it has an allowed E1 transition to another final state. Furthermore, since the major shells in nuclei are frequently comprised of single-particle states of the same parity, many states have no angular momentum allowed E1 decay. The distinction between E1 (allowed) and other (forbidden) transitions, so useful in atomic physics, completely breaks down in nuclei. The assumption that there could be a nearby state connected to an isomer by an E1 operator which itself decayed rapidly is almost surely incorrect.

These differences have implications for the nature of multiphoton excitation in the atomic and nuclear cases. In the atomic case, it is easy to find a state which has a large E1 matrix element with a given isomeric state. Pumping can proceed by Rabi oscillations between the two states. In the nuclear case this is very unlikely--most states do not have any nearby state to which they are connected with an appreciable E1 matrix element. Furthermore, because of the high (\hbar) values associated with nuclear transitions, isomeric transitions tend to require much higher multipolarity than E2, and hence have very large total angular momentum. States with rapid decay would have much smaller values, and could not be reached via a single E1 transition.

However, multiphoton upconversion need not proceed only by Rabi flopping between two states; since the process is to proceed by many photons, the angular momentum could be changed by one unit on each of many steps. Furthermore, it might be possible to engineer a mixed process, whereby initially the isomeric state would undergo Rabi oscillations with a more distant resonance with which it is connected. This would be followed by a few steps in which the angular momentum was lowered appreciably, to the final lasing state which could also oscillate with another distant resonance state for a few steps. This would lead both to larger matrix elements and larger energy denominators, and it is an open question at this point whether this would help or hurt; however, the large matrix elements would help at every step, whereas the large energy denominators would only hurt at every other step. This possibility should be examined critically and in detail.

In summary, the following things seem to be clear:

1. Nuclear structure is such that a state with a direct dipole connection to an isomeric level is very unlikely to be a suitable lasing or feeder state.
2. Many nuclear states have no identifiable nearby state with which they connect via a dipole operator. This will eliminate many of the isomeric transitions under consideration.
3. Use of distant resonances for upconversion should be considered.

We turn now to a discussion of off-resonance photon excitation of nuclei.

One of the proposals for making a gamma-ray laser involves pumping a metastable excited state up to a higher, short-lived lasing state which would then decay to the ground state or some other lower energy state. Because of the relatively low level densities in nuclei, compared with the energies of available intense sources, it is necessary to

understand the off-resonance or virtual excitation of these lasing states. This off-resonance excitation in the nuclear context was first proposed by Arad, Eliezer and Paiss (Ref. 30).

They estimated the cross section using the Breit-Wigner formula:

$$\sigma = \frac{\lambda^2}{2\pi} \frac{\Gamma_e \Gamma_i}{[(E-E_0)^2 + (\Gamma_t/2)^2]},$$

where λ is the particle wavelength, the Γ 's are the elastic, inelastic, and total widths, and E and E_0 are the energies of the particle and the resonance.

This expression is derived for particles with energy near the excitation energy, $(E-E_0)/E_0 \ll 1$. Usually, when one refers to far off-resonance processes, one means $\Gamma_t \ll (E-E_0)$, and for these off-resonance processes the Breit-Wigner formula is accurate, again provided that $(E-E_0)/E_0 \ll 1$. However, for very-low-energy particles, in the limit $E/E_0 \ll 1$, it is necessary to include the energy dependence of the width Γ_e . This results in a finite elastic scattering cross section and an inelastic cross section with a singularity which is only linear in the wavelength λ .

For low-energy photon scattering, a similar situation arises. Following the treatment in Sakurai (Ref. 43), but neglecting a small contribution due to emission preceding absorption leads to a multiplication of the naive Breit-Wigner result by the ratio of the on-resonance wavelength, λ_0 , to the real photon wavelength, λ :

$$\sigma = \frac{\lambda^2}{2\pi} \frac{\Gamma_e \Gamma_i}{[(E-E_0)^2 + (\Gamma_t/2)^2]} \left(\frac{E_{ab} + E}{E_{ab}} \right).$$

Before presenting detailed results, some comments on these infinite cross sections are in order. First, there is nothing necessarily unphysical in an infinite cross section--it is the count rate that must be finite. In the particle case, the count rate remains finite because it is the cross section multiplied by the velocity. In the case of photon-induced E1 excitations, the long wavelength singularity is eliminated by the polarizability of the atom, which decreases the field strength at the nucleus by the ratio of the nuclear size to the wavelength squared. (See the discussion by Brueckner, elsewhere in this report.)

For photons driving transitions of other than electric dipole character, a more careful treatment of the count rate is necessary, since for fixed number density, the flux does not decrease with the energy of the photons. The count rate, I , is given by

$$I = N_s \sigma n_\gamma c / V,$$

where N_s is the number of scatterers, σ is the cross section, n_γ is the number of photons, c is the speed of light, and V is the volume. Once the wavelength of the light is as long as a characteristic dimension of the target, the volume must increase as the wavelength cubed. The total power required therefore increases as the wavelength squared, and the ratio of count rate to input power actually tends to zero as one over the wavelength. Despite the infinite cross section, the result is physically reasonable.

These corrections having to do with the size of the target are only of interest by virtue of showing that the infinite cross sections are not a problem *per se*. Numerically, getting the correct behavior is crucial. Incorrect treatment of the frequency dependence at the threshold has led to published estimates that are off by several orders of magnitude.

We shall now compare relative cross sections with and without the threshold factors for three cases of interest. These are the original isomeric case proposed by Arad, Eliezer and Paiss, a pair of "generic" nuclear cases, and finally, a case from atomic physics in which the upconversion was observed. In all cases, the cross sections are normalized to 1 at the resonance.

In Fig. 34, the naive Breit-Wigner and correct low-energy cross sections are compared for the transition studied by Arad, Eliezer, and Paiss. Only the energy regime around 1 eV, the energy they proposed, is shown. For these energies, neglecting the frequency dependence introduces an error of about 6 orders of magnitude.

In Fig. 35, relative cross sections are presented for photons in the energy range 0.1 to 10,000 eV, exciting resonances at 1000 and 10,000 eV. Again, we find that neglecting the threshold factor leads to severe errors. From these calculations it would appear that far off resonance triggering of a gamma-ray laser will be impossible.

Despite these difficulties, "upconversion" or "lifetime shortening" has been observed in atomic physics. Cooper and Ringler (Ref. 44) have observed decays from a forbidden two-quantum transition in He, by applying microwave radiation to virtually excite a nearby state with an allowed two-quantum decay to the ground state. In their case however, the photon energy was about one third the transition energy. This leads to a substantial threshold effect, but not so drastic as to make the induced decay unobservable. Our calculated relative cross sections are shown in Fig. 36. The microwave energy for their experiment is indicated with an arrow. Since their experiment relied on relative cross sections, their results do not directly test the details of the threshold dependence.

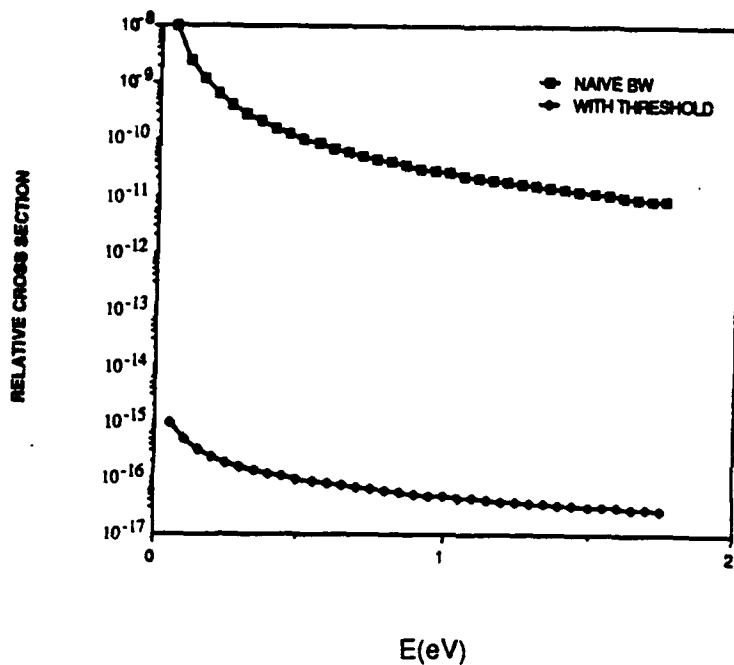


Figure 34. Relative cross section as a function of photon energy is shown for the nuclear case proposed by Arad, Eliezer, and Paiss, for the naive Breit-Wigner case, and for a case with the correct threshold behavior.

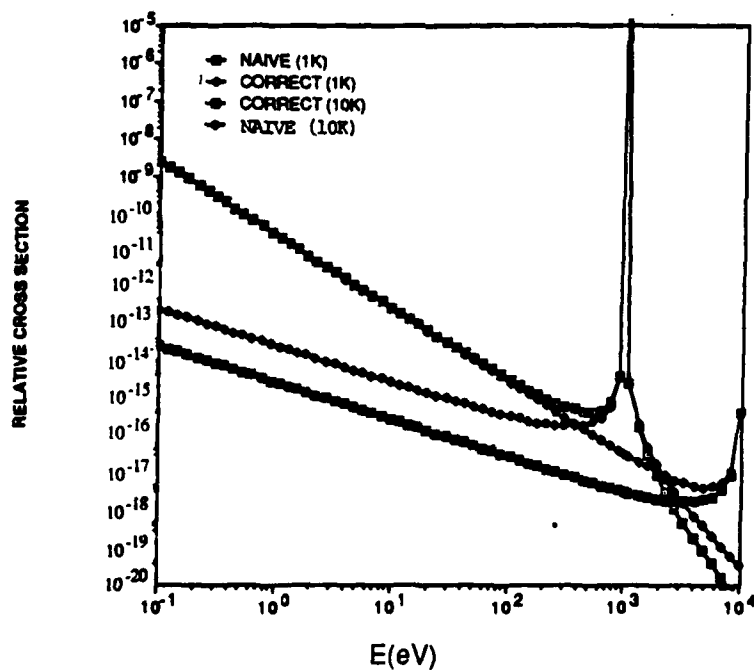


Figure 35. Comparison of naive and correct Breit-Wigner expressions for typical nuclear cases of interest.

In addition to the absorption-emission process, their experiment observed the stimulated-emission process. Theoretically, if one were many widths from resonance, $(E_0 - E) \gg \Gamma$, but still close to the resonance in the sense that $(E_0 - E) / (E_0) \ll 1$, these processes would be of comparable magnitude. This in fact was the case. Since these are the conditions under which single photon upconversion of a gamma-ray laser occurs, these processes should be included in future investigations.

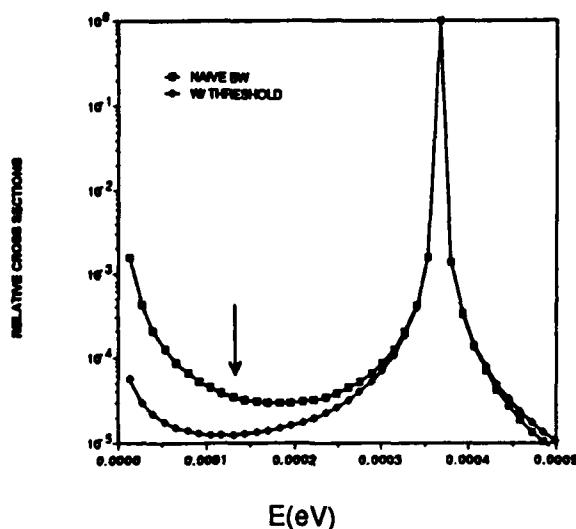


Figure 36. The effect of the correct threshold behavior on the atomic physics experiment of Cooper and Ringler, with their photon energy indicated by the arrow. Because their photon energy was an appreciable fraction of the resonance energy, the threshold effect was not fatal to their experiment.

In summary, we conclude:

1. It is essential to use the correct threshold behavior when using the Breit-Wigner formula to estimate upconversion cross sections.
2. This factor greatly reduces the probabilities for single-photon upconversion.
3. Given a material with an excitation energy from a metastable state to a lasing state, only a few times the energy of available light sources, single-photon upconversion might be possible. In that case, absorption-emission and stimulated-emission-emission would be of comparable strength, leading to two gamma-ray lines with energies differing by twice the incident photon energy. The existence of this second line has been overlooked in previous discussions of the gamma-ray laser.

C. MULTIPHOTON EFFECTS ON ATOMIC AND NUCLEAR SYSTEMS

Most work in experimental atomic and nuclear physics has been done under conditions where single-photon processes are predominant. Thus, for purposes of theoretical evaluation one calculates a cross section, assuming the interaction between a nuclear or atomic system and a single photon of the electromagnetic field. Such a cross section would be independent of the field intensity and the only effect of the interaction would be to induce a transition between well-established nuclear or atomic states. In stronger fields, the electromagnetic interaction modifies the nuclear level structure so that the dynamics is best described by a combined nuclear photon field Hamiltonian (Ref. 45). Under such conditions the transition matrix element between states or the absorption cross section would be a function of the intensity of the field. One effect of this nonlinear interaction is the A.C. Stark shift observed in atomic systems (Ref. 46). The electromagnetic field of the photons modifies the level structure so that frequency changes in the resonance of the cross sections as a function of the field intensity can be observed. As far as we know, no effects have been observed on nuclear structure; however, there is great interest in observing such effects both for their intrinsic worth and for possible application to the development of gamma-ray lasers (Ref. 1).

In this section we describe our parametric study of the possibilities for the observation of multiphoton processes on the nuclear level and their application to the development of a gamma-ray laser.

For the investigation of multiphoton processes we have selected a three-level system was shown in Fig. 33. States $|a\rangle$ and $|c\rangle$ are excited states with decay rates $\gamma_c \gg \gamma_a$ and $|b\rangle$ is the ground state. It is assumed that initially state $|a\rangle$ is populated. The purpose of the photon field, with $\hbar\omega \leq E_c - E_a$ is to excite the higher and faster decaying level $|c\rangle$ so that an inversion is produced between b and c and at the same time a high stimulation cross section is obtained for the transition c to b . An experimental depopulation of state $|a\rangle$ with an electromagnetic field would be considered a major proof-of-concept achievement on the way to the development for gamma-ray laser.* We have therefore looked at length at the conditions under which such an experiment could be successful. Our calculations were performed for atomic and nuclear systems in parallel because multiphoton processes have already been observed in atomic systems and for this reason it

* Rapid pumping out of an isomer would also be intrinsically interesting, and would likely have practical applications even if genuine lasing of the decay were unattainable.

is often assumed that they can be observed in nuclei. However, nuclear radii are five orders of magnitude smaller than atomic radii. Thus, for photons with similar wavelengths the interaction would be drastically reduced. Furthermore, nuclear dipole transitions are often inhibited by nuclear structure effects, as discussed in detail in Section B. Constraints imposed by nuclear structure continue to be important at every step of a multiphoton process.

Our investigation of multiphoton interactions with atoms or nuclei was based on the semiclassical formalism described in Appendices H and I. Since calculations using dressed state (Ref. 44) theory have been reported in the literature (Refs. 47 and 48) we show the equivalence of semiclassical and dressed state approaches to the treatment of the interaction of electromagnetic radiation with atomic and nuclear systems in Appendix H. In Appendix I the actual dynamic equations for the density matrix in the rotating wave approximation are derived from

$$\hbar \frac{d\rho}{dt} = -i [H_0 + V, \rho] + \Gamma \rho \quad , \quad (44)$$

where H_0 is the noninteractive part of the Hamiltonian, V is the interaction Hamiltonian and Γ is the decay matrix which is a function of γ_a and γ_c . (There are two simplifying assumptions made in these calculations. First, the near-resonance response was assumed. The corrections analogous to those presented above for single-photon processes have not been incorporated. Second, the rotating wave approximation is used. Both these approximations are valid near resonance. We believe that the trends revealed in this parametric study will hold up after these approximations are removed.) The three-state system shown in Fig. 33 is used to model the nuclear or atomic system. Application of equation 1 to this model gives 10 complex (or 16 independent real) equations for the diagonal and off-diagonal matrix elements of the density matrix ρ . Of special interest are ρ_{bb} and ρ_{cc} which give the population of the ground state $|b\rangle$ and the excited state or upper lasing level $|c\rangle$.

The transition matrix elements have to be calculated according to the multipolarity of the allowed transition (E1, E2, M1, etc.) and the number of photons participating in the process. For E1 single-photon transitions, the interaction Hamiltonian is

$$V = -\mu \sqrt{\frac{2\pi\hbar\omega}{V_n}} (a + a^\dagger) - \mu' \sqrt{\frac{2\pi\hbar\omega'}{V_n}} (a' + a'^\dagger) \quad , \quad (45)$$

where μ is the dipole moment, ω the frequency of the incoming photon, ω' the frequency of the outgoing photon and V_n the normalization volume. The matrix element is calculated from

$$V_{if} = \langle i | V | f \rangle . \quad (46)$$

For the transition from level a to level c, where a photon of energy $\hbar\omega$ is absorbed by level c,

$$\begin{aligned} V_{ac_2} &= \langle a ; n, 0 | V | c ; n - 1, 0 \rangle \\ &= -\mu_{ac} \sqrt{\frac{2\pi\hbar\omega'}{V_n}} = V_{c_2} a \\ &= r_{ac} \sqrt{\frac{2\pi\alpha I}{\hbar}} \end{aligned} \quad (47)$$

where μ_{ac} is the dipole moment matrix element, r_{ac} is the effective atomic or nuclear radius between states a and c, α_0 is the fine structure constant and I is the photon beam intensity in units of W/cm^2 . States $|a\rangle = |a; n, 0\rangle$ and $|c_2\rangle = |c; n - 1, 0\rangle$ are defined in Appendix I.

In terms of single photon matrix elements, the matrix element in question can be calculated according to perturbation theory from:

$$V_{ac_2}^{(m)} = \sum_{1,2,m-1} \frac{\langle a | V | 1 \rangle \langle 1 | V | 2 \rangle \cdots \langle m-1 | V | c_2 \rangle}{\hbar(\omega_a - \omega_1 + \omega) \hbar(\omega_a + 2\omega - \omega_2) \cdots \hbar(\omega_a + (m-1)\omega - \omega_{m-1})} \quad (48)$$

States $|1\rangle$, $|2\rangle$ through $|m-1\rangle$ are the intermediate states obtained by excitation of real states of resonance. In our case, in the three-level system they would involve $|a\rangle$ and $|c\rangle$ only. This is a simplifying assumption which we expect to have no effect on the observed trends of the calculations. For the interpretation of an experiment at high intensities the contribution to the time variation of the populations P_a , P_b , and P_c for the initial intermediate and ground states of all the single and multiphoton processes have to be

considered. The tails of many levels far from the isomers could make important contributions to the MP multiphoton transitions matrix elements.

We were interested in a parametric investigation to determine the effect on the populations of levels a, b, and c of various parameters such as the intensity I , the parameter $\Delta = E_a - E_c - \omega$ or the off-resonance effect, the photon number m , the strength of the interaction r_{ac} (the effective nuclear or electronic dipole radius) and the pulse length of the photon beam Δt .

In the next section we give some results for the three-state system shown in Fig. 33 for:

- (a) $r_{ac} = 0.5 \cdot 10^{-8}$ cm (typical atomic radius)
- (b) $r_{ac} = 5 \cdot 10^{-13}$ cm $\times 0.1$ (typical nuclear radius times a minimal hindrance factor)

Finally, for a realistic case we considered the time dependence of the population of level $|c\rangle$, since a large population inversion, in addition to depumping, will be required for a genuine laser.

Before presenting the detailed calculations we want to stress a major qualitative result; atomic dipole moments are five orders of magnitude larger than their nuclear counterparts. For fixed count rate, a 10^5 decrease in matrix element will require a 10^{10} increase in beam intensity. While attending to the detailed results of the parametric study, one should not lose sight of the enormously increased difficulty in working with a nuclear system.

The discussion of single-photon excitation focused on the Breit-Wigner expression for resonant cross sections. In the multiphoton case we will frequently present plots of the population of the ground state $|b\rangle$, P_b . For all the cases under discussion, intensities, I , are quoted, assuming a characteristic atomic system with a dipole moment of about 1A; the given values of P_b for a nuclear system would be obtained with intensities some 10 orders of magnitude larger. Unless otherwise noted, the population probabilities are given for the end of a 5 ns burst. The lifetime of state $|c\rangle$ was 1 ns, so the pumping out should be completed. The lifetime of state $|a\rangle$ was taken to be 10^7 s.

In Fig. 37, multiphoton population of the ground state, P_b , for $n_\omega = 9$ is plotted as a function of the detuning, or the distance off resonance for several photon intensities. For the lowest intensity plotted, 5×10^{13} W/cm², we find the peak population to be around 30 percent, and to fall two orders of magnitude as the energy moves 10 widths off

resonance, in keeping with the single-photon results. Increasing the intensity by a factor of two leads to a maximum final population, P_b , of 1.0, and a very slow decrease compared with the single-photon prediction--the width has been effectively broadened by around a factor of 10. Further increases in the intensity lead to a further increase in the effective width. If in the nuclear depopulation case, one is intensity limited, it will be very important to have minimal detuning.

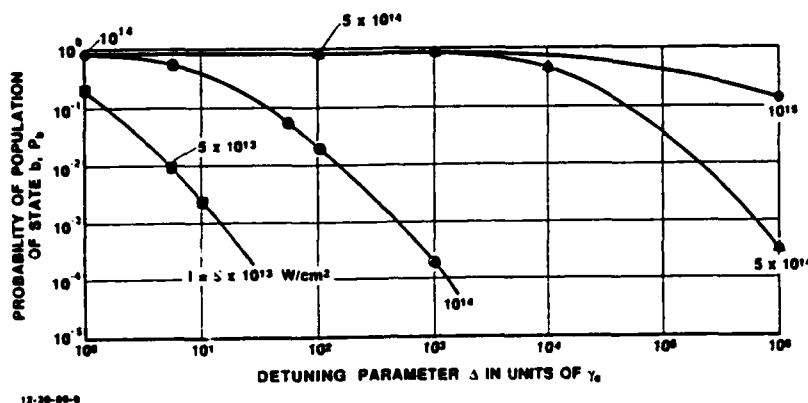
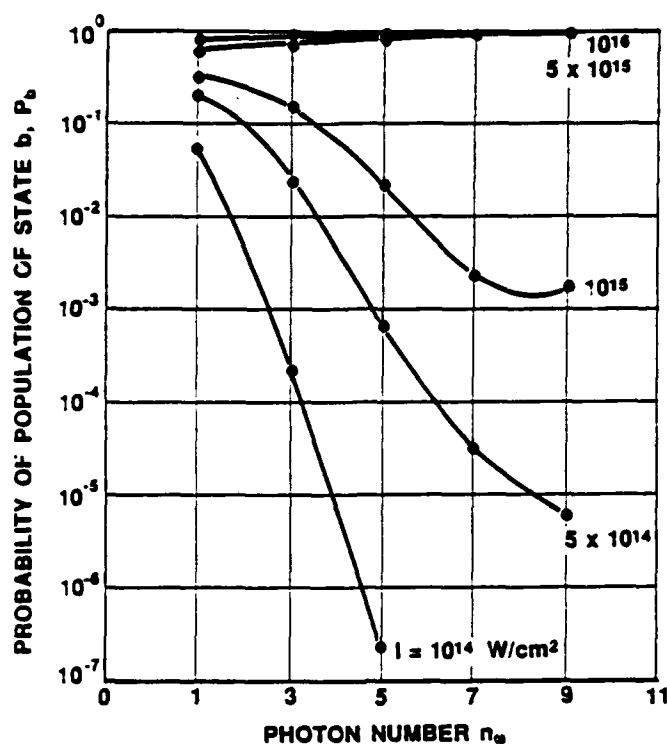


Figure 37. Multiphoton pumping of the isomeric level as a function of the detuning parameter in units of γ_c . The ordinate is the population of the ground level b . These results are for typical atomic transitions. For typical nuclear transitions the power requirements would have to be increased by a factor of 10^{10} .

The population probability is presented as a function of photon number for both off-resonance and on-resonance energies, again for several intensities. In the off-resonance case (Fig. 38), $\omega_{ca} = 100$ eV, and $\omega = 10$ eV. For electric dipole transitions, parity requires an odd number of photons to be absorbed, hence there is no photon number which is on-resonance. We find that for high enough intensities the ground state is nearly fully populated with a single photon, and the multiphoton process would fully populate the ground state. As the intensity decreases, the single-photon population begins to fall first, but the multiphoton ultimately falls much faster, as expected.

In Fig. 39, the same calculations are repeated, except the excited state energy, ω_{ca} , has been changed to 90 eV, allowing on-resonance excitation of level $|c\rangle$ with a 9-photon process. The results are quite similar to $\omega_{ca} = 100$ eV, except for the 9-photon, on-resonance case (Fig. 39) when the population of state $|b\rangle$ saturates even for the lowest intensities.

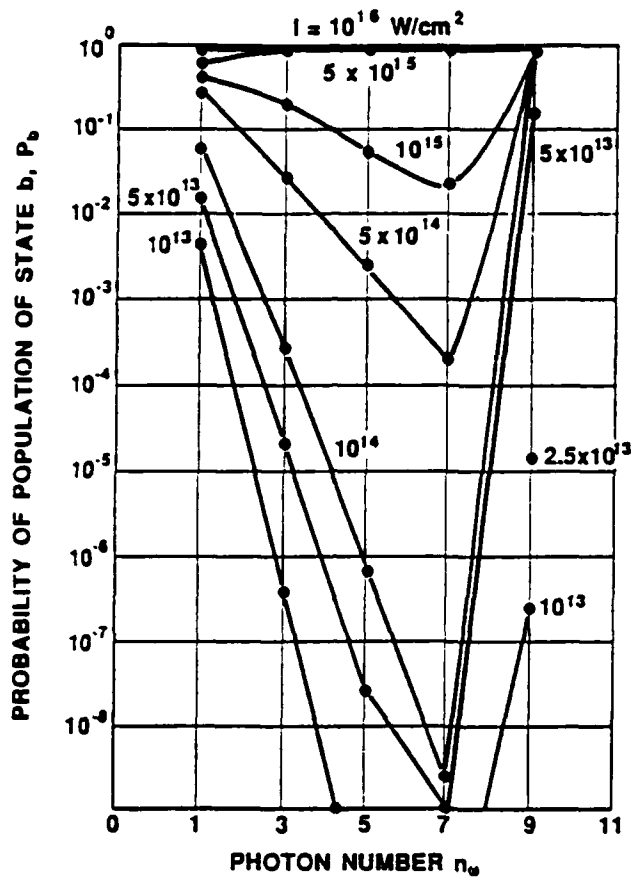


12-30-66-18

Figure 38. Multiphoton pumping of the isomeric level $|a\rangle$. The abscissa gives the number of photons used in the process and the ordinate the population of the ground level $|b\rangle$ when $\omega_{ca} = 100$ eV and $\omega = 10$ eV. Since an odd number of photons is required for excitation, this process cannot be on-resonance.

Figures 40 and 41 illustrate ground state population as a function of field intensity. In Fig. 40 this is shown for off-resonance, 9-photon excitation of a 100-eV state with 10 eV photons. The probability increases like the intensity to the 9th power until it reaches about 10 percent at about 2×10^{15} W/cm², at which point the saturation effects level out the curve. For the single-photon, on-resonance excitation in Fig 41, there are two significant differences. First, the saturation occurs at a much lower intensity; only about 100 W/cm². Second, the fall-off with intensity is only linear, and hence is much more gradual.

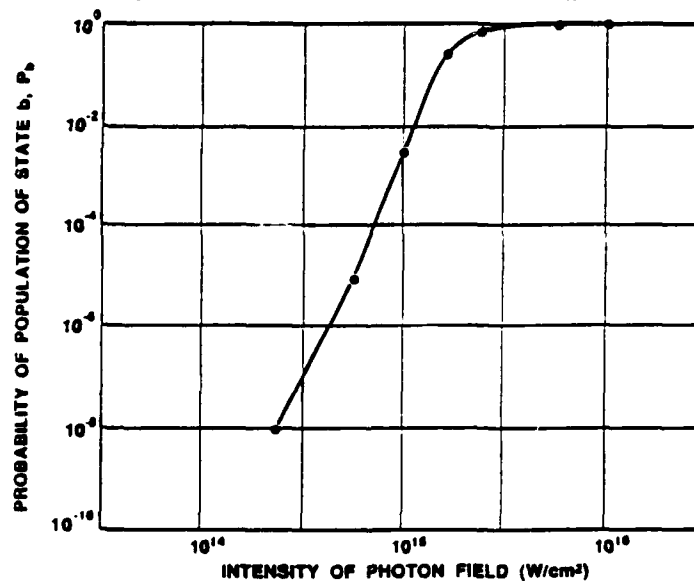
Single-photon, off-resonance depopulation of the isomeric level as a function of photon energy and field intensity is shown in Figs. 42 and 43. For low intensities, population of $|b\rangle$ is proportional to the intensity for all photon energies. For high field strengths, or energies close to the resonance, saturation is again clearly visible.



12-36-86-17

Figure 39. Multiphoton pumping of the isomeric level $|a\rangle$. The abscissa gives the number of photons used in the process and the ordinate the population of the ground level $|b\rangle$ when $\hbar\omega_{ca} = 90 \text{ eV}$ and $\hbar\omega = 10 \text{ eV}$.

This process is on resonance for $n_\omega = 9$.



12-36-86-12

Figure 40. The effect of photon field intensity on pumping of the isomeric level a . The nine photon transitions are used in the calculation with $\hbar\omega_{ca} = 100 \text{ eV}$ and $\hbar\omega = 10 \text{ eV}$.

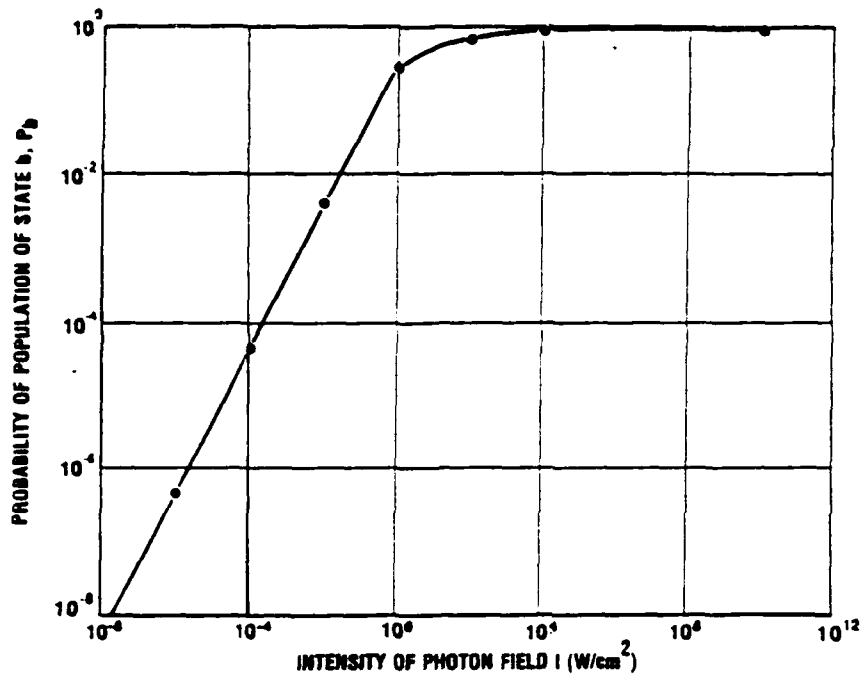
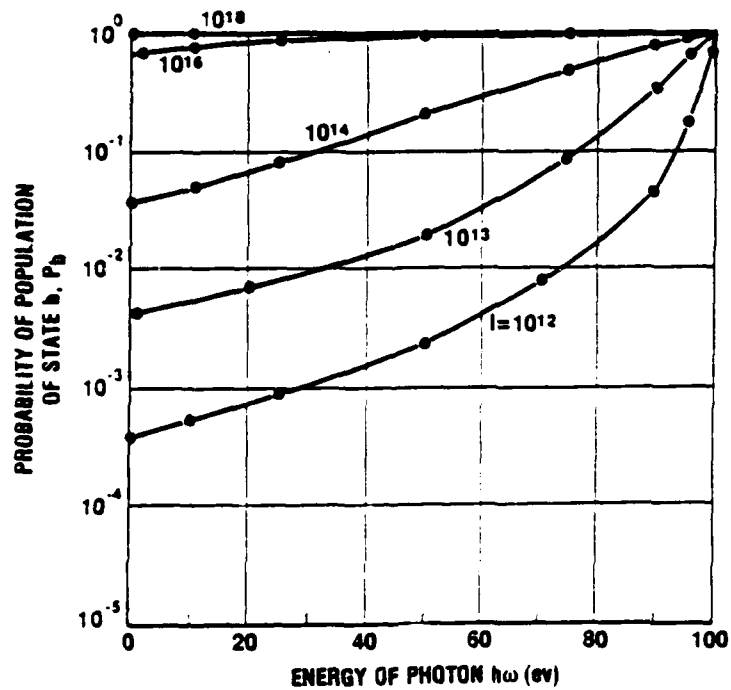
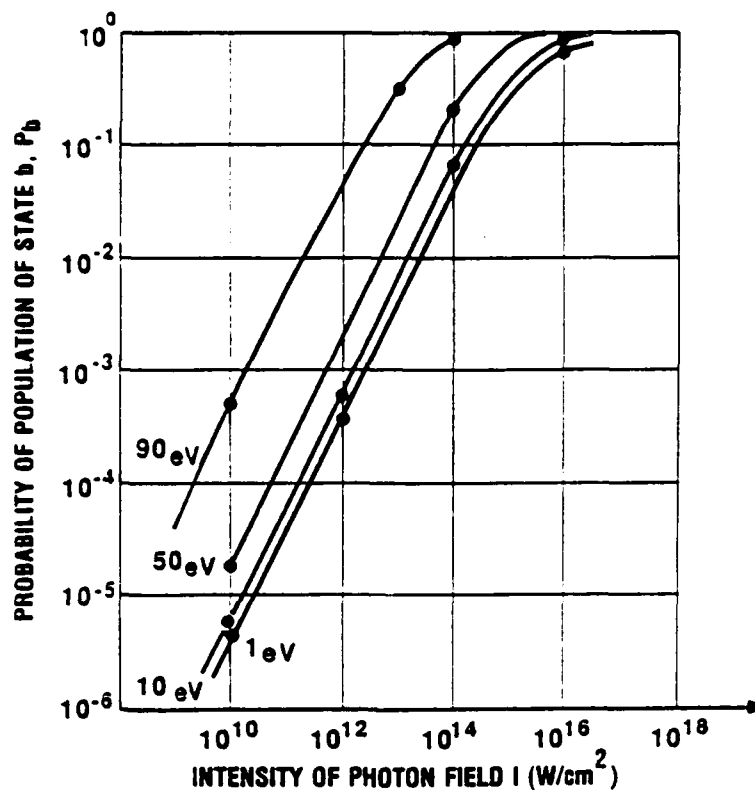


Figure 41. On-resonance, single-photon depopulation of isomeric level $|a\rangle$, as a function of photon field intensity, I



12-36-86-14

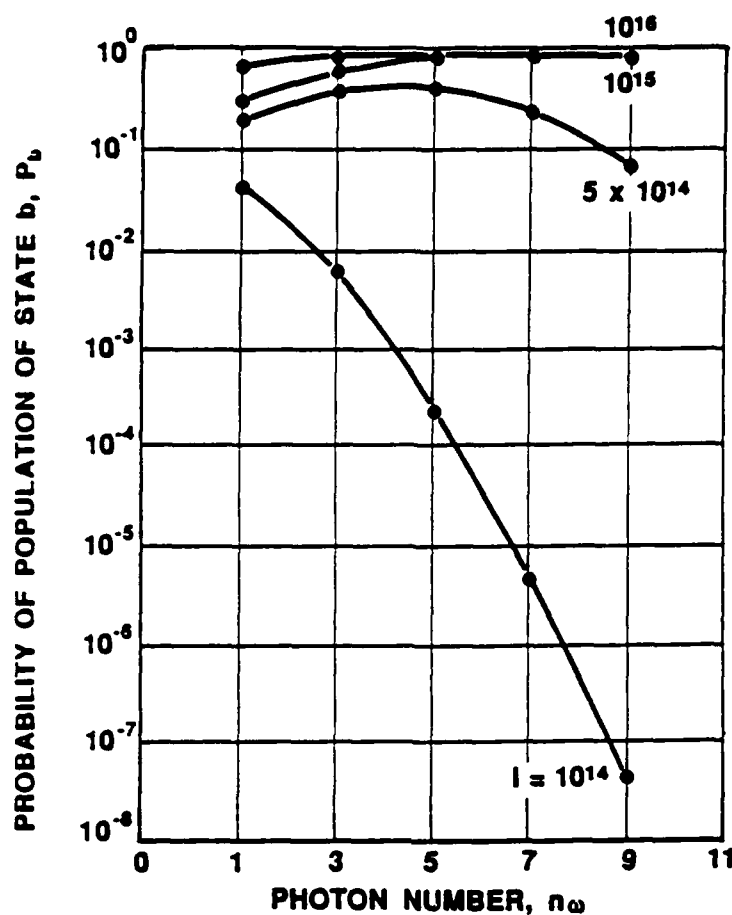
Figure 42. Single-photon depopulation of the isomeric level $|a\rangle$ as a function of photon energy for various photon field intensities with $h\omega_{ca} = 100 \text{ eV}$.



12-30-86-15

Figure 43. Single-photon depopulation of isomeric level $|a\rangle$ as a function of photon field intensity, I , for various photon energies with $\hbar\omega_{ca} = 100$ eV.

While it will probably be important to use on-resonance excitation to get a workable gamma-ray laser, there are certain subtleties worth noting about the off-resonance region. These have to do with the fact that for fixed intensity there is a higher density of low-energy photons than there would be for high-energy photons. Furthermore, once you are very far from resonance it is possible to benefit from the factor of $1/\omega$ from density of states. Figure 44 shows the probability of populating the ground state as a function of number of photons for several values of the intensity, when exciting a 100-eV resonance with 1-eV photons. Compared to the similar curve for 10-eV photons in Fig. 38, we find the 1-eV case much more favorable. For intensities of $5 \times 10^{15} \text{ W/cm}^2$ or higher, the population is saturated. For the single-photon case, the results are essentially the same, since the energy denominators are nearly equal. For all other cases, the lower energy and concomitant higher photon density are an advantage, especially for the cases with large photon numbers.



12-30-88-16

Figure 44. Off-resonance depopulation of the isomeric level $|a\rangle$ as a function of photon number n_ω for 1 eV photons.

Figure 45 presents a parametric study of the effects of both detuning and photon number on final ground state population. The more rapid fall of population with intensity when more photons are involved is clearly seen in this figure. The effects of detuning are smaller for the multi-photon cases. Since increased intensity both broadens the resonance and favors multi-photon processes, the penalty for either decreases.

The ground state population responds very differently to changes in decay rate, depending on whether the process is on- or off-resonance. This can be deduced from the Breit-Wigner line shape, which on resonance varies as the reciprocal of Γ_i , but off-resonance increases linearly in Γ_i . The off-resonance case is studied in Fig. 46, where the increase in population with increasing decay rate is clearly illustrated.

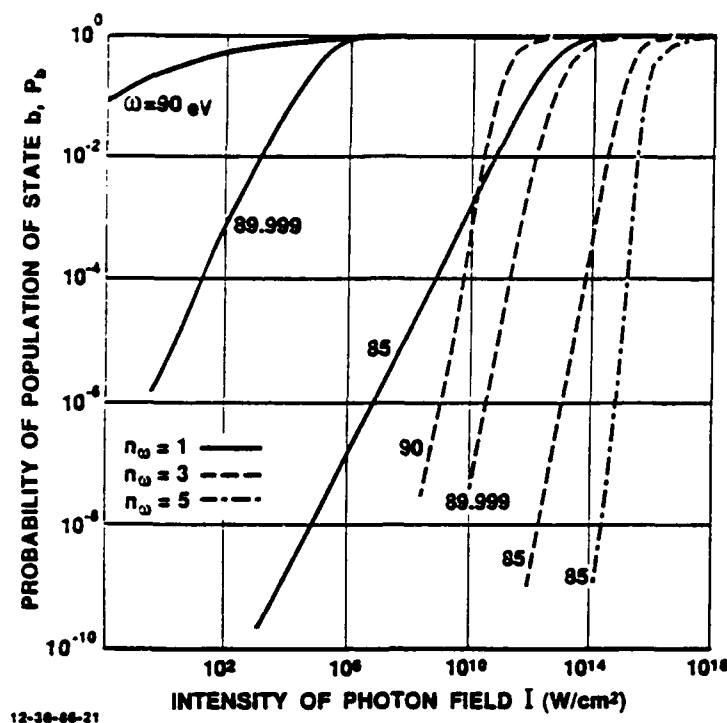
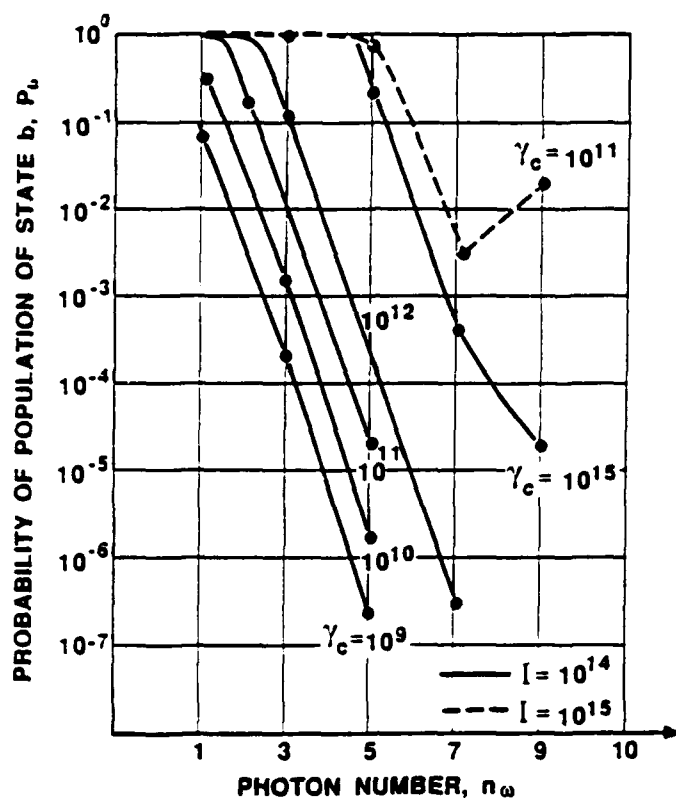


Figure 45. Off-resonance depopulation of isomeric level $|a\rangle$, as a function of photon field intensity for different detuning parameters and number of photons participating in the process

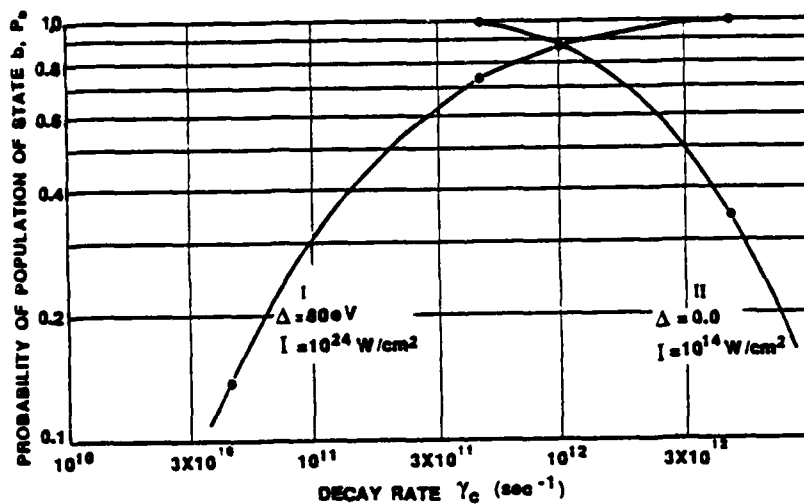
The final two figures are specifically oriented to triggering nuclear gamma rays. At present there are no overwhelmingly attractive candidates, so as an illustration we have taken parameters from Hf 179 , and modified some of the structure to make it a better case. There is a $25/2^-$ isomer in Hf 179 with a $7/2^+$ excited state only 200 eV above it. We have assumed they can be connected by dipole radiation with a matrix element as large as is found in that region of the periodic chart. In other words this "mock-hafnium" calculation is a drastic overestimate for that nucleus, but it is not inconceivable that such a favorable case would be found somewhere. We estimated the decay rate of state $|c\rangle$ from the Weisskopf formula for an M1 transition with a factor of 100 inhibition, giving a rate of $\gamma_c = 4.3 \times 10^{11}/s$.

For single-photon, off-resonance processes to populate this state appreciably would require an intensity of 10^{24} W/cm 2 (see Fig. 47). For a faster decay rate, complete depopulation of the isomer could be achieved. For on-resonance excitation using 200 eV photons, intensities of 10^{14} W/cm 2 would suffice for depopulation, unless the rate were too fast. As mentioned above and illustrated in the figure for the on-resonance case, too fast a decay rate, γ_c , diminishes the out pumping.



12-30-66-22M

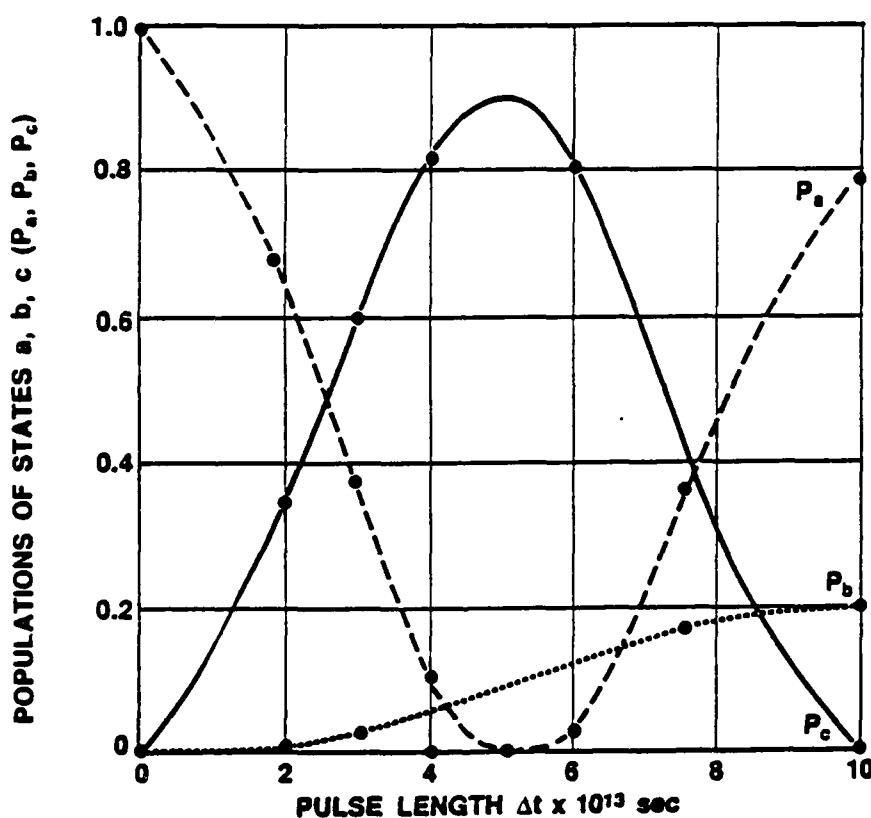
Figure 46. Effect of upper level decay rate γ_c (or linewidth) on off-resonance depopulation of the isomeric level $|a\rangle$, as a function of photon number n_ω .



12-30-66-22M

Figure 47. Effect of upper level decay rate γ_c on the off-resonance and on-resonance depopulation of the isomeric level $|a\rangle$.

Finally, we would like to remind the reader that the ability to pump out the isomer is not sufficient for the development of a gamma-ray laser. What is actually desired is a population inversion. To achieve this with the rapidly decaying nuclear states will require very short, intense bursts. A sample of what one might expect in terms of population as a function of time for the three states in our mock-hafnium case is shown in Fig. 48. One desires not merely to increase P_b , but rather to achieve at some known time a population inversion where most of the nuclei are in state $|c\rangle$, as shown at $t = 0.5$ ps. Identifying the genuine candidates, collecting the data necessary for more realistic calculations, and performing those calculations are the next tasks to be performed.



12-30-86-19

Figure 48. Level populations for the three-state system as a function of the pulse length of the exciting photon beam

D. CONCLUSIONS

Most plans for a gamma-ray laser can be divided into three stages: (1) preparation of an isomer or storage state; (2) upconversion to a lasing or intermediate state; and (3) extraction of the energy. This paper has focused exclusively on the upconversion process.

So much experience and expertise derives from lasing in atomic physics that it is important to note the differences in nuclear and atomic systems. The essential difference is the much smaller nuclear size, leading to matrix elements five orders of magnitude smaller than their atomic counterparts. This results in cross sections ten orders of magnitude smaller. An essential step in the development of the gamma-ray laser will be to find materials and procedures to overcome this disadvantage.

There are a number of specific results obtained in our investigations. First, we have derived the correct expressions for the off-resonance cross sections and power requirements for single photon excitations. Previously used expressions have overestimated the cross sections and underestimated power requirements by as much as six orders of magnitude.

A parametric study of multiphoton upconversion was completed, relying on some simplifying assumptions for the calculations far from resonance. These calculations were carried out for both atomic and "mock-nuclear" systems. The results underscore the difficulty of working with nuclear systems due to the 10 orders of magnitude greater power requirements, and point to the need for detailed evaluation of candidate isomers revealed by computer searches.

We are now positioned for calculation of on- and off- resonance, single- and multiphoton upconversion using the most realistic nuclear structure information available. We hope to begin the code development and isomer evaluation in the coming year.

V. AN INVESTIGATION INTO SOME PROBLEMS IN THE DEVELOPMENT OF GAMMA-RAY LASERS: ATOMIC SHIELDING OF NUCLEI AND UPCONVERSION BY MASSIVE PARTICLES

A. INTRODUCTION

In this paper several basic physics questions associated with making a gamma-ray laser are discussed. These include constraints on proximity of other states, pumping requirements and shielding, and the use of particles with mass to drive upconversion.

B. ISOMER DECAY

Consider an isomer with lifetime of 10^7 s (115 days) which decays by an E5 transition. The transition rates for electric and magnetic multipoles for a nuclear dimension of 10^{-12} cm (Refs. 49 and 50) are given in Fig. 49. The excitation energy for a decay rate of 10^{-7} /s and an E5 transition is 390 keV. This state could decay by other transitions if lower-lying levels were accessible. The distance below the isomer level at which a level could lie, without appreciably affecting the isomer lifetime (50 percent branching) is at most:

Transition	$\Delta\epsilon$
E1	3×10^{-2} eV
M1	0.2 eV
E2	0.2 keV
M2	0.5 keV
E3	9 keV
M3	20 keV
E4	90 keV
M4	170 keV

The existence of the isomer therefore is a severe constraint on the lower-lying levels.

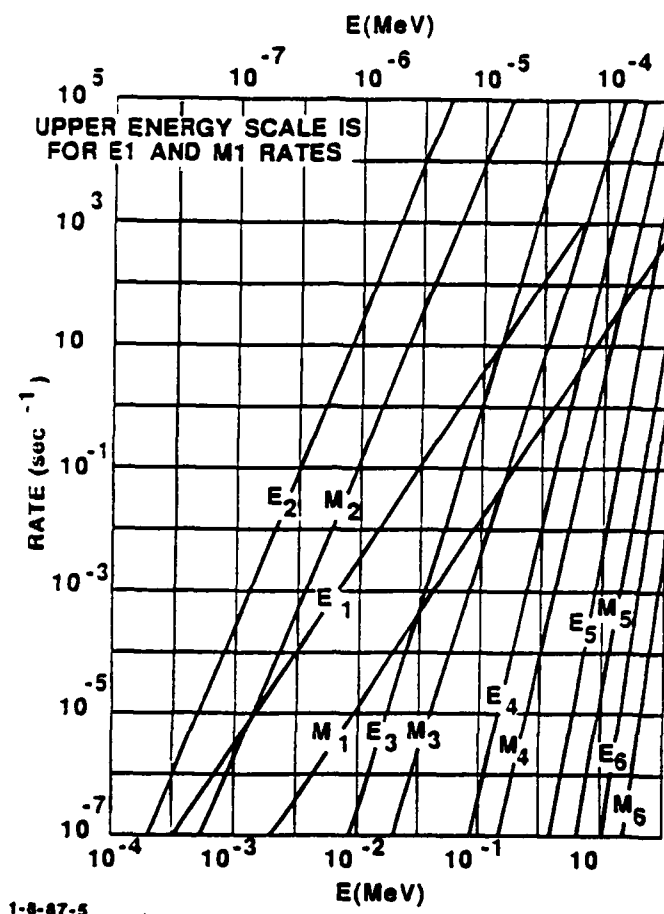


Figure 49. Transition rates for electric and magnetic multipoles for a nuclear dimension of 10^{-12} cm

C. PUMPING TRANSITION

Many gamma-ray laser proposals consider the excitation of a level of a few electron volts above the isomer level, which is the upper level of a lasing transition or which decays to an upper lasing level. For the example in Section B, an E1 transition could be produced by radiation absorption. If this level decayed directly to the ground state by an E4 transition, the lifetime would be several seconds. If the decay were by an E1 transition to an upper lasing level, this level would be reached by an E2 transition from the isomer and therefore would lie less than 0.2 keV below the isomer. For a spacing of 0.2 keV, the pump level would decay by E1 transition with a lifetime of about 10 μ s. The lasing level would decay by an E3 transition, with an energy of nearly 390 keV, with a lifetime of 50 μ s. This possible level sequence therefore is suitable for a gamma-ray laser.

If the upper pump level were reached by an M1 transition and decayed to an upper lasing level by an E1 transition, the lasing level could be reached by an M2 transition from the isomer and would lie less than 0.5 keV below the isomer level. The decay time from the pump level to the upper laser level, for a spacing of 0.5 keV, would be about a microsecond and the M3 decay of the lasing level a lifetime of about 30 μ s; again, possible for a gamma-ray laser.

D. PUMPING REQUIREMENTS

The field at the nucleus required to excite the upper pump level can be estimated from the requirement that the excitation rate R (pump) exceed the decay rate R (laser) of the upper lasing level. This condition for an E1 transition is

$$R \text{ (pump)} \equiv \frac{2\pi}{\hbar} \langle eEr \rangle^2 \frac{1}{\Gamma_{\text{pump}}} > R \text{ (laser)} . \quad (48)$$

The pump width is $\Gamma_{\text{pump}} \equiv \hbar R \text{ (decay)}$ giving the necessary pumping flux (at the nucleus)*

$$c \frac{E^2}{4\pi} \equiv \frac{1}{8\pi^2} \frac{\hbar^2 c}{e^2 \langle r^2 \rangle} R \text{ (laser)} R \text{ (decay)} . \quad (49)$$

For a lifetime of the lasing level of 50 μ s and of the pump level of 10 μ s, the required flux at the nucleus is 0.33 W/cm². The electric field at the nucleus is 0.10 esu or 30 V/cm.

To produce this field at the nucleus, a much larger external field must be applied. An external electric field is screened by the polarization of the atomic electrons.** A theorem due to L.I. Schiff (Ref. 51) proves that a uniform electric field is exactly cancelled at the nucleus by an atomic electron polarization. A similar effect in the electronic excitation of heavy atoms is analyzed by Wendin et al. (Ref. 52). This is easily seen to be required by the absence of acceleration of a neutral atom by a uniform electric field. A spatially varying field at the nucleus therefore is reduced relative to the external field by a factor of the order of (atomic dimensions/wavelength) as discussed in Ref. 50. For a Fermi-Thomas atom this factor is of the order of $10^{-7} \Delta E(\text{eV})^2 Z^{-2/3}$. This is a major correction to the laser

* This is the energy flux required by excitation of a *single* nucleus, in an on-resonance absorption of visible light. Excitation of an appreciable percentage of the nuclei in a solid sample would be many orders of magnitude higher.

** The screening effect of electrons was pointed out to the author by C.K. Rhodes.

flux requirement and must be carefully evaluated. The effect is probably small only if the radiation wavelength is smaller than atomic dimensions.

The screening effect is much less important for an M1 transition, the polarization of atomic electron spins having little effect on an external magnetic field. The flux required is the order of

$$c \frac{E^2}{4\pi} \cong \frac{1}{8\pi^2} \frac{\hbar^2 c^2}{e^2 g_N^2} \frac{R(\text{laser}) R(\text{decay})}{\lambda_c^2}, \quad (50)$$

where

g_N = nucleon gyromagnetic ratio

λ_c = nucleon Compton wavelength.

This is increased relative to the example of the E1 transition by a factor of

$$\left(\frac{R_N}{g_N \lambda_c} \right)^2 \cong 625, \quad (51)$$

giving an incident flux of the order of 20 W/cm².

E. SEARCH FOR CANDIDATE ISOMERS

An isomer with a level only a few electronvolts above the isomer level could have decay excited by interaction of the level with the atomic electrons, by internal crystalline fields, by close collisions in a high-temperature gas, or by bombardment with ions at energies too low to cause direct excitation by nuclear collisions. For example, isomers in a thin foil bombarded by a relatively low-energy ion or electron beam might show an increase in decay rate. This could be the easiest procedure for a search for isomers possibly suitable for a gamma-ray laser.

1. Isomer Excitation in Collisions

An isomer bombarded by ions with energy too low to produce a nuclear collision can be excited by the coulomb field of the ions. The perturbing potential due to the transverse component of the field is

$$\begin{aligned}
 V &= e \vec{r}_N \vec{E} \\
 &= ze^2 \frac{\vec{r}_N \vec{\rho}}{(\rho^2 + v^2 t^2)^{3/2}} e^{-r/r_s}, \quad (52)
 \end{aligned}$$

with r_s the screening radius of the bound electron and $\vec{\rho}$ the impact parameter (closest approach). The excitation probability for the isomer level with $\Delta E = \hbar\omega$ is

$$P(\text{excite}) = \left| \frac{V_\omega}{\hbar} \right|^2, \quad (53)$$

with

$$\begin{aligned}
 V_\omega &= \int_{-\infty}^{\infty} ze^2 \frac{\vec{r}_N \vec{\rho} e^{-r/r_s} e^{i\omega t}}{(\rho^2 + v^2 t^2)^{3/2}} dt \\
 &\equiv 2ze^2 \frac{\vec{r}_N \vec{\rho}}{\rho^2 v} \exp\left(-\frac{\omega\rho}{v}\right) e^{-\rho/r_s}. \quad (54)
 \end{aligned}$$

This gives an excitation cross section of the order of

$$\begin{aligned}
 \sigma_{\text{ex}} &= 2\pi \int_0^\infty \rho d\rho \left| \frac{V_\omega}{\hbar} \right|^2 \\
 &\equiv \left(\frac{ze^2}{\hbar v} \right)^2 \frac{8\pi r_N^2}{3} \int_0^\infty \frac{d\rho}{\rho} \exp\left(-2\frac{\omega\rho}{v}\right) e^{-2\rho/r_s} \\
 &\equiv \frac{8\pi}{3} \left(\frac{ze^2}{\hbar v} \right)^2 r_N^2 \log_e \frac{\rho_{\text{max}}}{\rho_{\text{min}}}. \quad (55)
 \end{aligned}$$

This result can also be derived from time-independent perturbation theory, treating the interaction with the ion by perturbation theory. The result, ignoring screening, is

$$d\sigma = \frac{2\pi}{\hbar} |V_{if}|^2 \frac{k M^2 d\Omega'}{(2\pi\hbar)^3 k} \quad (56)$$

with

$$V_{if} = \int e^{-i\vec{k}\cdot\vec{r}} \psi_{\text{ex}}^*(r) \frac{ze^2}{|\vec{r} - \vec{r}'|} \psi_{\text{iso}}^{(r)} e^{i\vec{k}\cdot\vec{r}'} d\vec{r} d\vec{r}'$$

$$\begin{aligned}
&= \frac{4\pi e^2 z}{q^2} \int \psi_{ex}^* (r') \psi_{iso}^{(r')} e^{i \vec{q} \cdot \vec{r}'} d\vec{r}' , \\
&= \frac{4\pi e^2 z}{q^2} i \vec{q} \cdot \vec{r}_N
\end{aligned} \tag{57}$$

with

$$\begin{aligned}
\vec{q} &= \vec{k} - \vec{k}' \\
\vec{r}_N &= \int \psi_{ex}^* (r') \vec{r}' \psi_{iso} (r') d\vec{r}' .
\end{aligned} \tag{58}$$

This gives, averaging over the orientation of r_N ,

$$\sigma \equiv \frac{8\pi}{3} \left(\frac{ze^2}{\hbar v} \right)^2 r_N^2 \log_e \left| \frac{k + k'}{k - k'} \right| . \tag{59}$$

This is the same as equation 55 if the logarithmic factor is interpreted to be the ratio of the interaction ranges.

In equations (54) and (57), the cutoff ranges are of the order of

$$\begin{aligned}
\rho_{\max} &= \left. \begin{aligned} &\frac{v}{\omega} \\ &= r_s \end{aligned} \right\} \text{lesser of} \\
\rho_{\min} &\equiv \frac{z z_{\text{isomer}} e^2}{\epsilon_{\text{ion}}} .
\end{aligned} \tag{60}$$

These estimates of ρ_{\max} and ρ_{\min} are valid only if ρ_{\min} is greater than the nuclear radius. For bombarding protons and a screening length equal to the Fermi-Thomas length $a_0 z_{\text{iso}}^{-1/3}$, proton energy above which $\rho_{\max} = r_s$ is

$$\epsilon_{\text{proton}}^{(\text{eV})} = 36.6 \frac{\Delta \epsilon^2 (\text{eV})}{z_{\text{iso}}^{4/3}} . \tag{61}$$

The electron screening therefore is usually dominant. The minimum distance ζ_{\min} is

$$\begin{aligned}\rho_{\min} &= \frac{z_{\text{isomer}} e^2}{\epsilon} \\ &= \frac{z_{\text{isomer}}}{\epsilon_{\text{eV}}} 1.14 \times 10^{-7} \quad .\end{aligned}\quad (62)$$

This is greater than the nuclear radius for $z_{\text{isomer}} = 64$, for proton energy less than 12 MeV. Thus, for protons with energy of a few mega electronvolts, a screening length r_s of 10^{-9} cm, a nuclear radius of 5×10^{-13} cm, the cross section for excitation is roughly 4×10^{-27} cm². This depends only weakly on the excitation energy $\hbar\omega$, as long as ω is less than v/r_s .

As an example, we consider isomers embedded in a foil with thickness much less than the proton range. The excitation rate for a proton flux ϕ is

$$\text{rate (ex)} = \sigma_{\text{ex}} \phi n_{\text{isomer}} , \quad (63)$$

which will exceed the spontaneous decay rate if

$$\sigma_{\text{ex}} \phi > \text{rate (decay)} , \quad (64)$$

giving a particle current of 5 MeV protons of

$$j > 4 \times 10^7 \text{ rate (decay)} \text{ A s/cm}^2 . \quad (65)$$

Thus, for a lifetime of 10^7 s, a current of 4 A/cm² will roughly double the net decay rate. A current of 1 mA/cm² would give an increase of the order of a percent in the decay rate, which is easily detectable. The excitation probability depends, however, only weakly on the excitation energy $\hbar\omega$, making it difficult to determine the energy from measurement of the γ -rays.

2. Isomer Decay Induced by Atomic Electrons

An isomer can decay by coupling to the internal conversion resulting from atomic electrons, with the transition energy carried off by the electron. The internal conversion is often large, showing the strong perturbation of the electromagnetic transition by the electrons. A related process can also occur if a nuclear level lies just above the isomer, from which a transition to an intermediate state can be produced by the electron coupling. We assume,

Ψ_0 = isomer level; high angular momentum relative to ground state;

Ψ_2 = final nuclear ground state;

Ψ_n = intermediate nuclear state, angular momentum one relative to isomer;

ϕ_0 = initial electronic state

ϕ_1 = final electron state with $\Delta L = 1$ from initial state

The matrix element for the decay is

$$\sum_n \left(\phi_1 \Psi_n \frac{e^2}{|\vec{r} - \vec{r}_N|} \Psi_0 \phi_0 \right) \frac{1}{E_0 + \epsilon_0 - E_n - \epsilon_1} \times \left[\Psi_2, e \vec{E} \cdot \vec{r}_N \frac{(\vec{k} \cdot \vec{r}_N)^{L-2}}{(L-2)!} \Psi_n \right] \quad (66)$$

The matrix element for the direct decay is

$$\left[\Psi_2, e \vec{E} \cdot \vec{r}_N \frac{(\vec{k} \cdot \vec{r}_N)^{L-1}}{(L-1)!} \Psi_0 \right] \quad (67)$$

The sum over n in equation (66) can be approximately by closure, replacing the excitation energy by an average ΔE . The ratio of the matrix elements then is of the order of

$$\frac{M(\text{electronic})}{M(\text{direct})} \approx e^2 \left\langle \frac{\vec{r}}{r^3} \right\rangle < \frac{N (\vec{k} \cdot \vec{r}_N)^{L-2}}{\Delta E < (\vec{k} \cdot \vec{r}_N)^{L-1}} > (L-1) \approx (L-1) \frac{\tilde{\lambda}_e^2}{\Delta E r_a^2} \quad (68)$$

with $\tilde{\lambda}$ the γ -ray wavelength and r_a an atomic dimension. As an example, we take r_a to be the Fermi-Thomas $a_0/z^{1/3}$, $L = 5$, and $z = 64$. The ratio of the matrix elements then is

$$\frac{M(\text{electronic})}{M(\text{direct})} \approx \frac{128}{\Delta E (\text{Rydbergs})} \frac{\lambda}{a_0} \quad (69)$$

For a 100 keV γ -ray, $\lambda/a_0 = 0.04$, giving a ratio of $5/\Delta E$ Rydbergs). For typical nuclear level spacings of many keV, this effect is small. For an excitation energy of a fraction of a Rydberg, however, the ratio is large and the isomer decay would nearly always be accompanied by atomic electron ejection.

The presence of the electron enhances the decay because the bound electron can provide a unit of angular momentum for the decay without the severe kinematic inhibition which comes with low energy free electrons or photons. Provided bound electrons with a

given higher L are present, this enhancement need not be restricted to $\Delta L = 1$ processes for the isomer and the electron.

Consider a nucleus with isomer level "0" and an excited state "1" which is the possible state to be reached by external excitation. If the level is reached by an electric multipole transition, the matrix element is of the order of

$$M_{10} \int \psi_1^*(r_N) e \vec{E} \vec{r} \frac{(\vec{q} \cdot \vec{r}_N)^{L-1}}{L!} \psi_0(r_N) d\vec{r}_N .$$

with r_N the nuclear coordinate. This transition can also be produced by the electrostatic interaction with an atomic electron excited by the external source. We let the initial electron level be "a," the intermediate level "n," and the final level "b." The matrix element is

$$M_{1b,0a} = \sum_n \int d\vec{r} \int \psi_1^*(r_N) e^2 \frac{r_N^L}{r^{L+1}} P(\hat{r}_N \hat{r}) \psi_0(r_N) d\vec{r}_N \phi_b^*(r) \phi_n(r) \\ \times \frac{1}{\Delta E} \int \phi_n^*(r') (e \vec{E} \vec{r}') \phi_a(r') d\vec{r}' ,$$

with

$$\Delta E = E_0 + \epsilon a + \hbar \omega - E_1 - \epsilon_n .$$

This can be estimated, using closure on the n sum, which gives

$$M_{1b,0a} = \frac{e^2}{\Delta E} \int d\vec{r} \int \psi_1^*(r_N) r^L P(\hat{r}_N \hat{r}) \psi_0(r_N) d\vec{r} \phi_b(r) e \vec{E} \vec{r}_a(r) .$$

This matrix element is finite only if the electronic state ϕ_b differs from the state ϕ_a by $L + 1$ units of angular momentum.

The matrix element for the transition $a \rightarrow b$ is, however, not necessarily small since the integral over r has the factor $(r_N r)/r^2$. The ratio of the matrix elements is the order of

$$\frac{M_{1b,0a}}{M_{1,0}} = \frac{L! e^2}{\Delta E_a^L q^{L-1}} .$$

This ratio can be very large if the system is near resonance and the radiation wavelength g^{-1} is large compared with the electronic scale a , which is possible if the excited nuclear state is only a few electronvolts above the isomer level.

VI. INVESTIGATION OF ENERGY TRANSFER TO NUCLEI THROUGH ELECTRON NUCLEAR COUPLING

A. INTRODUCTION

In the other chapters of this report pumping schemes have been examined which it is hoped would excite nuclear levels that could lead to grasing transitions. These schemes involve the direct transfer of energy from an external electromagnetic field to the nucleus while totally ignoring the intervening electronic cloud of the atom (Ref. 53). Brueckner* has pointed out that under some conditions the electron cloud can be very efficient in shielding the nucleus. On the other hand, the electron cloud can also serve to enhance the coupling of the electromagnetic field to the nucleus. This chapter describes a technique utilizing semi-classical calculations to study the effect of electron-nuclear coupling in mediating that transfer. The technique has already proved to be successful in atomic and molecular applications.** In the case of an atom, two or more valence electrons interact with the atomic nucleus and with each other through the coulomb field. In the electron-nuclear case, one or more valence nucleons and one or more extranuclear electrons interact with each other and with the nuclear core. In the process, both nuclear and coulomb potentials are active. In the application of the technique, a Hamiltonian is set up as in any quantum mechanical problem; however, the trajectories of the valence particles are treated classically. The use of the technique in the present case is driven by previous successes. In atomic and molecular applications, calculated eigenvalues match their quantum mechanical counterparts in precision (Ref. 54). It is the purpose of this work to investigate the utility of using this semi-classical technique for nuclear-electronic interaction problems.

* See Chapter V of this report.

** The semi-classical approach, if valid, is very useful because it is amenable to computation. It has been applied in at least two cases, one atomic and one nuclear. In the atomic case, the senior author, D. Noid, used the approach to calculate eigenvalues in atomic helium. The results agreed with the more precise quantum calculations to a high degree of precision. The semi-classical approach was used successfully by L. Biedenharn in the studies of nuclear coulomb excitation to study and explain experimental results in low-energy nuclear structure.

In the realm of experimental physics, the excitation of nuclear isomers in laser-produced plasmas has been reported (Ref. 55). The possibility of nuclear excitation by laser-driven coherent outer electron oscillations has also been discussed (Ref 56). The existence of electron-nuclear coupling has long been known in such phenomena as internal conversion and electron capture. In the first, a nucleus deexcites by transferring energy to an extranuclear electron. In the second, the nucleus transmutes by capturing a nearby electron.

B. THE SEMI-CLASSICAL METHOD

The Hamiltonians for the problems to be posed are nonseparable in terms of nuclear and electronic coordinates. The Semi-Classical Method (SC) was selected because the quantum mechanical methods, e.g., variational and perturbation techniques, led to difficulties in the selection of good basis sets. Very large numbers of terms would have to be used, and to carry out the diagonalization of the matrices involved would put severe burdens on the capacity and running times of the computer. Several problems were examined:

1. Doubly magic nucleus with one valence proton and one electron
2. Two protons and one neutron (He-3)
3. Two protons and two neutrons (He-4).

The first problem, Nuclear Electronic Coupling (NEC), was modeled by the Hamiltonian

$$H = \frac{P_{X_n}^2 + P_{Y_n}^2}{2M_n} + \frac{P_{X_e}^2 + P_{Y_e}^2}{2m_e} + V_o \left\{ 1 + \exp \left[\frac{(R_n - R_o)}{a} \right] \right\}^{-1} \\ + \eta \frac{(Z - K) e^2}{r_e} + \eta K \frac{e^2}{r_e - R_n} , \quad (70)$$

where the first two terms represent the kinetic energies of the proton and electron, respectively. The next term is the Saxon-Woods Potential (Ref. 57) describing the interaction between the proton and the nuclear core. The last two terms are the coulombic interactions of the electron with the nucleus and proton, respectively. The parameters are:

R_n = the nucleon position = (X_n, Y_n, Z_n)

R_o = the nuclear radius = $1.25 A^{1/3}$ fm

a = the nuclear diffusivity = 0.65 fm

r_e = the electron position = (x_e, y_e, z_e)

K = 1, 0 for the coupled/uncoupled case

η = the screening parameter.

In the NEC Code, the particles are confined to a plane, and motions are described by Cartesian coordinates. The trajectories of both the coupled and uncoupled systems are generated using Hamilton's equations of motion:

$$\begin{aligned} \dot{X}_n &= \frac{\partial H}{\partial P_{X_n}} & \dot{x}_e &= \frac{\partial H}{\partial P_{x_e}} \\ \dot{Y}_n &= \frac{\partial H}{\partial P_{Y_n}} & \dot{y}_e &= \frac{\partial H}{\partial P_{y_e}} \\ \dot{P}_{X_n} &= -\frac{\partial H}{\partial X_n} & \dot{P}_{x_e} &= -\frac{\partial H}{\partial x_e} \\ \dot{P}_{Y_n} &= -\frac{\partial H}{\partial Y_n} & \dot{P}_{y_e} &= -\frac{\partial H}{\partial y_e} \end{aligned} \quad (71)$$

Initial conditions for the nucleon and electron trajectories are obtained by fixing the positions and momenta at the classical outer turning points. For the proton, these coordinates are found by applying a WKB approximation to the Saxon-Woods potential well. Initial conditions for the electron are similarly obtained for the coulombic well as described in Ref. 58. In obtaining the trajectories for both particles, integrations are performed over short time intervals to obtain the coordinates for each point. The basic time unit is the transit time of light through a distance of 1 fm (a basic nuclear dimension). Typical trajectories with and without coupling are shown in Fig. 50. In this example, the proton is situated on the surface of a nucleus having a radius of about 7.5 fm. Its trajectory points involve integration steps of two basic time units (during which the proton moves a distance of about 0.5 fm). For the electron's orbit, steps of 25 basic time units were used. Then, from these orbital calculations, the time-dependent dipole moment

$$\mu_x = eX_n - eX_e = eX_n - ex_e$$

$$\mu_y = eY_n - eY_e = eY_n - ey_e$$

is obtained. One then obtains the autocorrelation function of the dipole moment

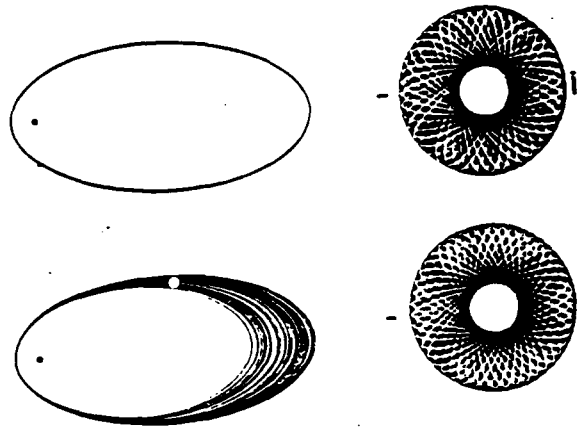


Figure 50. Uncoupled electron and nuclear trajectories (upper left). Magnified nuclear trajectory (upper right). Coupled trajectories (lower half). In the uncoupled case the maximum electron $r = 1188$ fm and the maximum nucleon $r = 8.66$ fm.

$$C(\tau) = \langle \mu_X(\tau) \mu_X(t+\tau) \rangle = \lim_{T \rightarrow \infty} \frac{1}{2T} \int_{-T}^{+T} \mu_X(\tau) \mu_X(t+\tau) dt \quad (72)$$

and, taking its Fourier transform, obtains the unpolarized power spectrum. The result is:

$$I(\omega) = \left| \frac{1}{\pi} \int_{-\infty}^{+\infty} C_X(\tau) e^{-i\omega\tau} d\tau \right|^2 + \left| \frac{1}{\pi} \int_{-\infty}^{+\infty} C_Y(\tau) e^{-i\omega\tau} d\tau \right|^2. \quad (73)$$

This procedure is carried out for both the coupled and uncoupled cases. The differences in the two spectra yield transition energies at which nuclear excitation may result.

Similar procedures were applied in the He-3 and He-4 cases, but the Hamiltonians are different. For He-3

$$H = \frac{1}{2M_n} \left[P_{X_1}^2 + P_{X_2}^2 + P_{X_3}^2 + P_{Y_1}^2 + P_{Y_2}^2 + P_{Y_3}^2 \right] + V(R_{12}) + V(R_{13}) + V(R_{23}), \quad (74)$$

where

$$\begin{aligned} V(R_{12}) &= -A*B*(1/R_{12}) * \exp(-BR_{12}) \\ V(R_{13}) &= -A*BC*(1/R_{13}) * \exp(-BR_{13}) \end{aligned} \quad (75)$$

$$V(R_{23}) = -A*BC*(1/R_{23}) * \exp(-BR_{23}) + 1.44/R_{23} \quad , \quad (76)$$

and for He-4

$$H = \frac{1}{2M_n} \sum_{i=1}^4 (P_{xi}^2 + P_{yi}^2) + V(R_{12}) + V(R_{13}) + V(R_{14}) \\ + V(R_{23}) + V(R_{24}) + V(R_{15}) \quad .$$

The two cases are similar. In He-3, there are two p-n and one p-p interactions; whereas, in He-4 there is one additional neutron and, therefore, 6 two-body interactions. In the latter case, there are, then, three more potential terms in the Hamiltonian, and these have the same form as $V(R_{12})$. Here,

A = depth of well in MeV

BC = scaling parameter for potential

B = scaling parameter for R in femtometers

R_{ij} = distance between particles i and j .

In the above expressions, there are two types of potential terms. One has the Yukawa (see, for example, Ref. 49) potential to describe the short-range two-body nuclear force which is the same for charged and uncharged nucleons. The other is the coulomb potential acting between the pair of charged nucleons (protons) only. As before, the particles are restricted to motions in a plane. The PNP computer code was used for He-3; code NP2 is used for the four-body system. These codes, as well as NEC are listed as Appendices K, L, M. The two problems were done for bare nuclei as a step in the investigation of the validity of this classical approach in studying the dynamics of simple nuclei. No electrons were involved. Only trajectories, not spectra were calculated.

C. RESULTS

First, let us consider the HE-3 and HE-4 calculations. The heart of the codes used to solve the Hamiltonian equations is the well documented ordinary differential equation solver (ODE) of Shampine and Gordon (Ref. 59). For a discussion of the algorithm, see Ref. 60. Small time steps (Δt) are selected to keep the error estimate less than the preselected value. Calculations of trajectories show that some interparticle distances grow rapidly with time so that, even though the total energy and angular momentum are conserved, the PNP complex behaves unstably in a manner indicating fragmentation into a

diproton and a neutron. It must be pointed out that the nuclear potential failed to include both spin and exchange. Since in chemical analogs, e.g., in H_2^+ , exchange forces are known to be responsible for binding, one may logically attribute the fragmentation to that omission.

As stated above, the He-3 and He-4 problems were exercises in studying the application of semi-classical calculations to nuclear dynamics. The application of the spectral analysis method to coupled electro-nuclear classical trajectories is more relevant to the actual gamma-ray laser problem than were the two previous exercises. A good approach is to select heavy nuclei so that excitations in the few keV to 1 MeV regime would be realistically attainable. In addition, narrowing the candidates to nuclei consisting of one proton outside a singly or doubly closed shell would more closely model the desired situation. We would then have an inner electron interacting only with one loosely bound valence nucleon and a spin zero tightly bound nuclear core. The possibility of selecting a nucleus with a valence neutron was dismissed. That choice would require using a magnetic dipole interaction; and that, in turn, would complicate the Hamiltonian by making it spin-dependent. Magic numbers for closed shells of protons include $Z = 2, 8, 20, 28, 50,$ and 82 ; for neutrons, in addition to the same numbers, 126 is also a magic number. Therefore, *the nuclei initially studied include those for which $Z = 29, 51,$ and 83 .*

We have already seen a comparison of the trajectories of uncoupled and coupled systems. In Fig. 51, we again see orbitals for the three cases cited, but only for the coupled motion. In Fig. 52, we see a sample of a time-dependent dipole moment derived from such a trajectory. The higher frequency nuclear contribution is clearly seen superposed on the electron motion. There is a visible change in amplitude and frequency when the coupling is turned on. Finally, Fig. 53 shows the spectral intensities derived from the autocorrelation functions of the dipole moments for the three cases. As Z (or A) is increased, the effect of coupling greatly increases. For $Z = 29$, the coupled spectrum is essentially identical to the uncoupled. But as Z is increased, the difference is quite marked; and, for $Z = 83$ ($^{209}\text{Bi} = ^{208}\text{Pb}$ plus ^1H), the electron's orbit is chaotic. From the trajectories, one can see that the nucleus is at one of the foci of the electron's elliptic orbit. The major electron-nucleon energy transfer occurs during the short time of closest approach, but the effect of the change is best revealed when the electron is furthest from the nucleus.

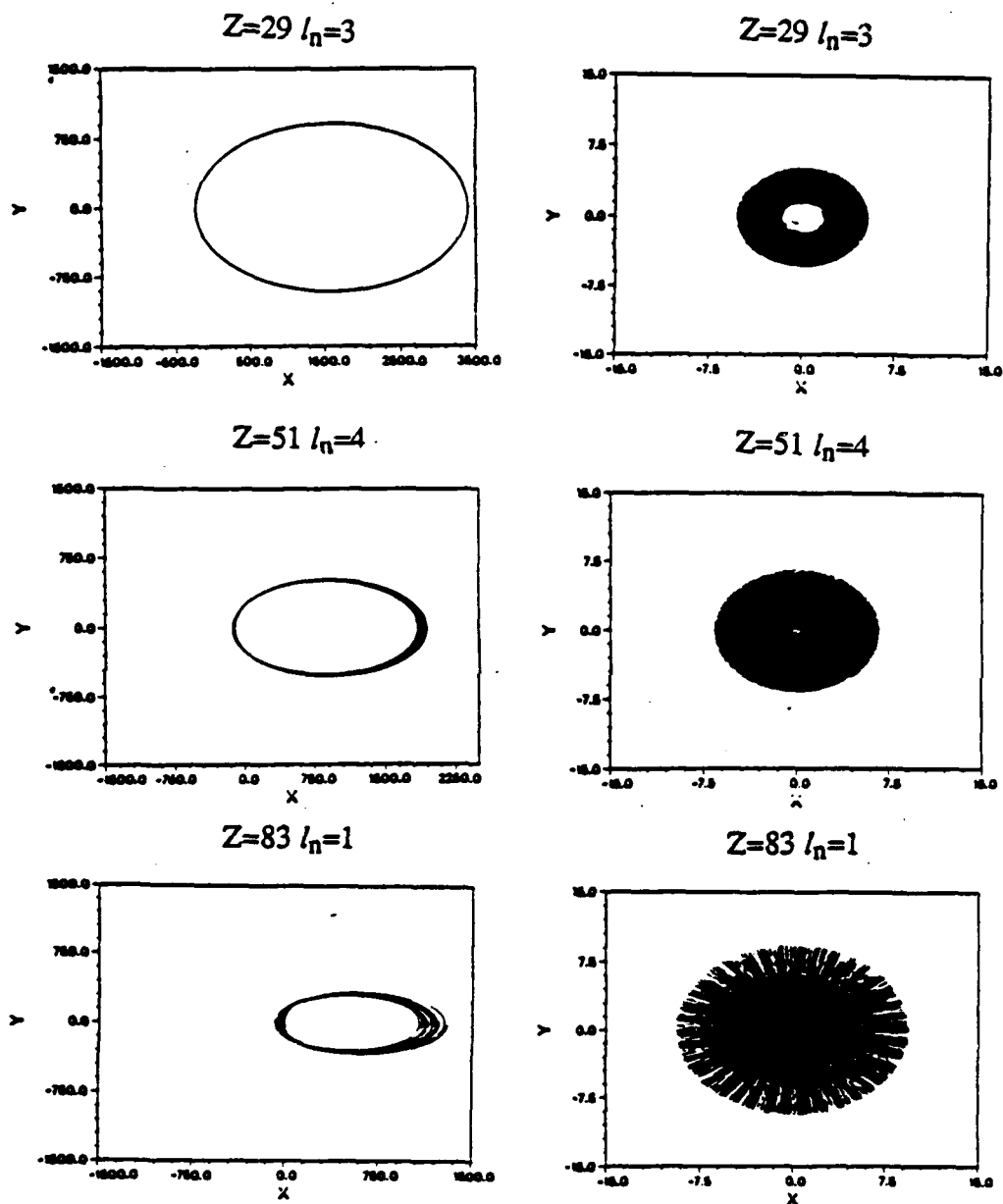


Figure 51. Coupled electron and nuclear orbits for three nuclei consisting of a closed shell plus one proton. Nuclear core, one proton, and one electron are interacting. In the figure, Z is the atomic number and l_n the nucleon orbital angular momentum. The distances X, Y are given in femtometers.

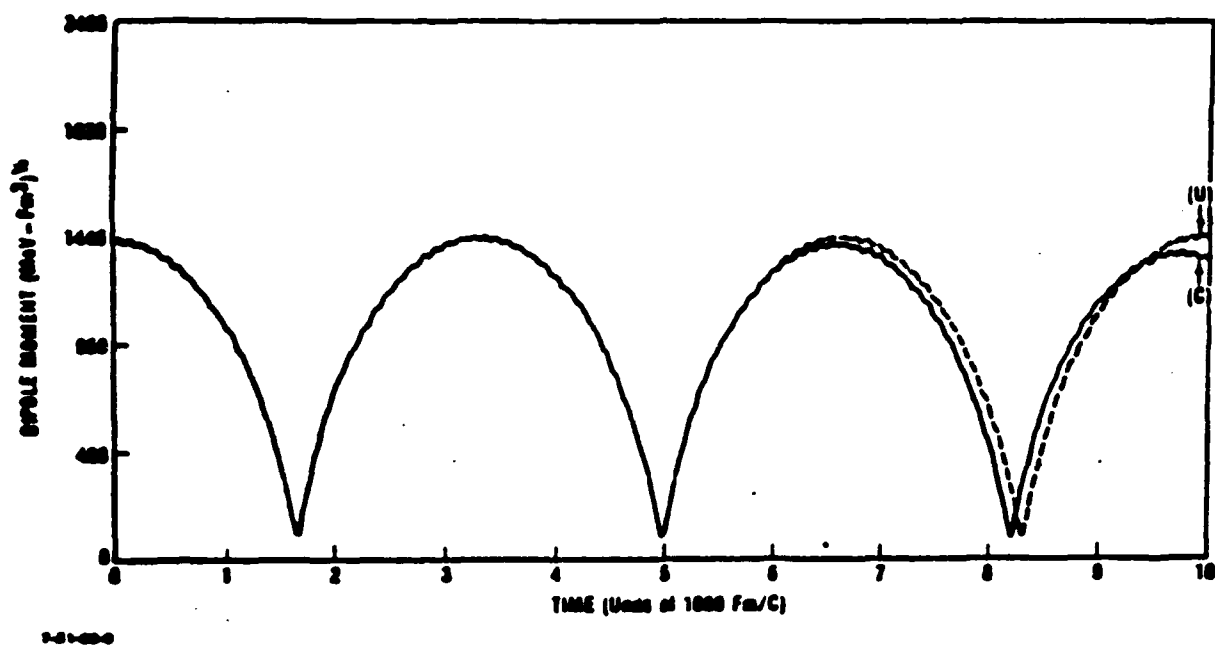


Figure 52. The dipole moment as a function of time for both coupled (C) and uncoupled (U) cases.

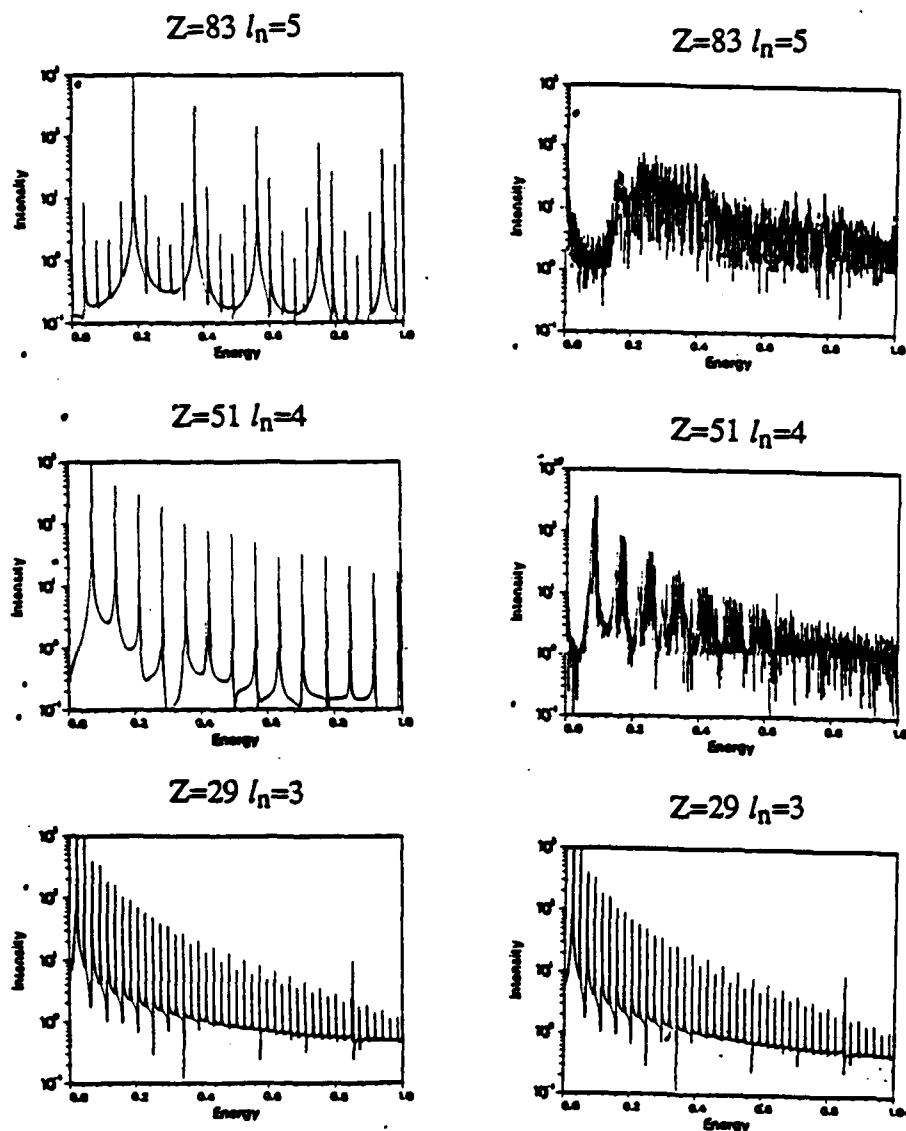


Figure 53. Spectral intensities derived from magnetic moment autocorrelation functions for atoms near closed nuclear shells. The uncoupled case is on the left; the coupled on the right. In the figure, Z is the atomic number and l_n the nucleon angular momentum. The energies are given in MeV.

D. CONCLUSIONS

Preliminary studies with simple potentials indicate that the semi-classical model does yield information on transition amplitudes for electron-nuclear excitation. More realistic potentials, including spin dependence and exchange terms should be used in future calculations. These studies indicate that nuclear excitation by electron-nuclear interactions is a possible approach to achieving graser pumping.

VII. A NUCLEAR LIFETIME MEASUREMENT-- AN UNCERTAINTY PRINCIPLE

Among the ideas that have been proposed for making a gamma-ray laser is the scheme which requires the rapid narrowing of an inhomogeneously broadened long-lived isomeric level by a series of specially structured RF pulses (Refs. 61 through 64). When this scheme was recently resurrected, modified, and examined in depth (Ref. 65), the criticisms that resulted included a dual statement ostensibly related to the time-energy or time-frequency uncertainty principle. The linewidth (or lifetime)* of a level can be determined only by an operation that lasts at least as long as the reciprocal of that linewidth (i.e., the lifetime)* (p. 39, Ref. 1); a broadened level can only be narrowed in a time of the order of the lifetime (Ref. 66). These ideas were debated during the workshop described in Ref. 1.

To better understand this problem, we shall examine one method for measuring the lifetime of an isomeric level. We shall assume, for simplicity, that the transition is not at all internally converted, i.e., each transition leads to a detectable gamma-ray. Assume that, at the time $t = 0$, we have a point source of precisely N_0 nuclei in an isomeric state of lifetime τ . A reasonable assumption for a laboratory setup is that, nearby, we have a well-shielded NaI(Tl) detector with an overall detection efficiency of 0.1 and a relatively negligible cosmic ray or manmade background. The number N of isomeric nuclei remaining at time t (Ref. 67) is given by

$$N(t) = N_0 e^{-t/\tau} , \quad (78)$$

and the number of gamma-rays emitted per second by the point-source is

$$-\dot{N}(t) = \frac{N_0}{\tau} e^{-t/\tau} . \quad (79)$$

The counting rate registered by the detection system is then given by

$$-0.1 \times \dot{N}(t) = \frac{0.1 N_0}{\tau} e^{-t/\tau} . \quad (80)$$

* The words in parentheses are the author's.

Let us assume that, at time t_0 we register C counts in the detection system in a time interval $\Delta t \ll \tau$. The reason for this assumption is that N be essentially constant during the detection time. Since detection is a Poisson statistical process which is approximated by a Gaussian description for $C > 10$, the fluctuation, ΔC , in the signal C , is given by \sqrt{C} which can be considered a source of noise large compared to all other background noise in our "clean" laboratory. Thus,

$$\frac{S}{N} = \sqrt{C} \quad . \quad (81)$$

We now have

$$C = 0.1 \times \dot{N}(0) \times \Delta t = 0.1 \frac{N_0}{\tau} \Delta t \quad . \quad (82)$$

We assume that, in comparison to counting statistics, N_0 and Δt are known or measured with precision. The lifetime, as determined by experiment using equation (82) is given by

$$\tau_{\text{expt.}} = \tau \pm \tau \left(\frac{\Delta \tau}{\tau} \% \right) = \tau \pm \Delta \tau \quad (83)$$

$$= 0.1 \frac{N_0}{C} \Delta \tau \pm \tau \frac{\Delta C}{C}$$

$$\Delta \tau = \frac{\Delta C}{C} = \frac{\tau}{\sqrt{C}} \quad , \quad (84)$$

or

$$\frac{\Delta \tau}{\tau} = \frac{1}{\sqrt{C}} \quad . \quad (85)$$

This merely tells us that in order to measure the lifetime to, say, a 1 percent precision

$$\frac{\Delta \tau}{\tau} = 0.01 = \frac{1}{\sqrt{C}} \quad , \quad (86)$$

or

$$C = 10^4 \quad . \quad (87)$$

That is, we must detect 10^4 gamma rays in a time Δt short compared to τ . Is this reasonable? Consider that we have a radioactive source with a mean lifetime of, say, one

week, and a strength of 1.0 μCi . Note, at the Naval Research Laboratory there is a radiation facility of ^{60}Co with a strength greater than 1000 Ci (lifetime $\tau = 7.56$ yr). A 1.0 μCi source (a typical strength for a laboratory calibration source) emits 3.7×10^4 gamma rays per s. The detector will produce a counting rate of $3.7 \times 10^3/\text{s}$. Thus, to achieve the requisite total number of counts, $C = 10^4$, will require a $\Delta t < 3$ s. In other words, with our idealized assumptions, the mean lifetime of one week was determined to a one percent precision in a time of 3 s. In a general laboratory situation, N_0 is not well known--but the possibility of obtaining a pure macroscopic sample of the isomeric material violates no known principle. Thus, to determine a lifetime τ in a time much less than τ merely requires a source of sufficient but not excessive strength.

The relationship between the mean lifetime, τ , of an exponentially decaying eigenstate and Γ , the full width at half maximum of the Lorentz-shaped energy spectrum (Ref. 68) is given by

$$\tau \Gamma = \hbar \quad . \quad (88)$$

Note, from equation (82), we have

$$\frac{\Delta\tau}{\tau} = \frac{1}{\sqrt{C}} = \frac{1}{S/N} \quad . \quad (89)$$

With equation (88), this yields

$$\Delta\tau \Gamma = \frac{\hbar}{S/N} \quad . \quad (90)$$

We must emphasize that, in the "uncertainty" relationship, $\Delta\tau$ is the uncertainty or standard deviation in the measurement of τ . It is interesting to note that when $C = 1$, $\Delta\tau = \tau$. Using the relationship

$$\Gamma = \hbar\Delta\omega \quad , \quad (91)$$

we obtain

$$\Delta\tau \Delta\omega = \frac{1}{S/N} \quad , \quad (92)$$

which resembles the uncertainty relationship well known in electrical engineering (Ref. 69), namely,

$$\Delta\tau \Delta\omega \geq \frac{1}{S/N} \quad . \quad (93)$$

In this expression, Δt and $\Delta\omega$ are the uncertainties in the simultaneous measurements, respectively, of the round trip time and frequency of the radar signal. Here, S and N are the signal energy and the noise power per cycle.

One point remains. Equation (88) merely tells us that a determination of τ with a given percentage error is automatically a measurement of the width of the level with the same precision; and equation (89) states that if the lifetime is measured in a time interval short compared to that lifetime, the precision of that measurement depends only on the strength of the source. None of this mandates a limitation on the time required to narrow an inhomogeneously broadened level.

REFERENCES

1. *Proceedings of the IST/IDA Gamma-Ray Laser Workshop*, edited by Bohdan Balko, Leslie Cohen, and Francis X. Hartmann, IDA Memorandum Report M-162, January 1986.
2. *IDA Gamma-ray Laser Annual Summary Report (1985): Investigation of the Feasibility of Developing a Laser Using Nuclear Transitions*, edited by Bohdan Balko, Leslie Cohen, and Francis X. Hartmann, IDA Paper P-2021, June 1986.
3. *Nuclear Wallet Cards*, edited by J.K. Tuli, National Nuclear Data Center, Brookhaven National Laboratory.
4. *Nuclear Data Sheets*, Vol. 10-48, (1973-1986), edited by Nuclear Data Project, Academic Press, Inc., New York (1973-1986).
5. *Table of Isotopes*, Seventh Edition, edited by C.M. Lederer and V.S. Shirley, Lawrence Berkeley Laboratory, UCLA, John Wiley & Sons, Inc., New York, 1978.
6. R.S. Hager and E.C. Seltzer, *Nucl. Data A*, **4**, 1, 1968.
7. I.M. Band, M.B. Trszhaskovskaya, and M.A. Listengarten, *Atomic Data and Nuclear Data Tables*, **18**, 433, 1976.
8. G.C. Baldwin and M.S. Feld, *J. Appl. Phys.* **59**, 3665, 1986.
9. M.S. Feld and J.C. MacGillivray in *Coherent Nonlinear Optics*, edited by M.S. Feld and V.S. Letokhov, Springer-Verlag, Berlin, 1980.
10. R.H. Dicke, *Phys. Rev.* **93**, 68, 1954.
11. F.X. Hartmann, "Distinctions in Superradiant Theories--Coherent Particle Emission" in *Gamma-Ray Laser Annual Summary Report (1985): Investigation of the Feasibility of Developing a Laser Using Nuclear Transitions*, IDA Paper P-2021, June 1986.
12. G.N. Fowler and R.M. Weiner, *Phys. Rev. Lett.* **55**, 1373, 1985.
13. G. Kruizki and A. Ben-Reuven, *Phys. Rev. A Rapid Commun.* **4**, 1560, 1985.
14. R. Bonifacio, J.D. Farina, and L.M. Narducci, *Opt. Commun.* **31**, 377, 1979.
15. F.P. Mattar, H.M. Gibbs, S.L. McCall, and M.S. Feld, *Phys. Rev. Lett.* **46**, 1123, 1981.
16. G.T. Trammell and J.P. Hannon, *Opt. Commun.* **15**, 3, 325-329, 1975.

17. R. Bonifacio and L.A. Lugiato, *Phys. Rev. A*, **11**, 5, 1507-1521, May 1975.
18. M. Feld, "Superradiance and Laser-controlled Gamma Emission," *Proceedings of the IST/IDA Gamma-ray Laser Workshop*, edited by Bohdan Balko, Leslie Cohen and Francis X. Hartmann, IDA Memorandum Report M-162, January 1986.
19. F.T. Arrecchi and E. Courtens, *Phys. Rev. A*, **2**, 5, 1730, 1970.
20. N. Skribononitz, I.P. Herman, J.C. MacGillivray, and M.S. Feld, *Phys. Rev. Lett.* **30**, 8, 308, 1973.
21. Q.H.F. Vrehen and H.M. Gibbs in *Dissipative Systems in Quantum Optics*, ed. R. Bonifacio, Springer-Verlag, New York, 1982.
22. M. Gross and S. Haroche, *Phys. Rep.* **93**, 5, 301-396, 1982.
23. M.F. H. Schuurmans, Q.H.F. Vrehen, and D. Polder, in *Adv. At. Mol. Phys.* **17**, 167, 1981.
24. E. Gerdau, R. Ruffer, R. Hollatz, and J.P. Hannon, *Phys. Rev. Lett.* **57**, 9, 1986.
25. R. Bonifacio and L.A. Lugiato, *Phys. Rev.* **12**, 2, 587-598, August 1975.
26. L.M. Narducci, C.A. Coulter, and C.M. Bowden, *Phys. Rev. A*, **9**, 2, 1974.
27. F.P. Mattar and H.M. Gibbs, "Transverse Effects in Burnham-Chiao Ringing and Superfluorescence," *Proceedings of the International Conference on Lasers '80*, New Orleans, Louisiana, December 15-19, 1980, edited by C.B. Collins, 777-782.
28. H.M. Gibbs, Q.H.F. Vrehen, and H.M.J. Hikspoors, *Phys. Rev. Lett.* **39**, 547, 1977.
29. R. Florian, L.O. Schwan, and D. Schmid, *Phys. Rev. A*, **29**, 2709, 1984.
30. M.S. Malcuit, J.T. Maki, D.J. Simkin, and R.W. Boyd, *Phys. Rev. Lett.* **59**, 11, 1189, 1987.
31. F. Haake and R. Reibolt, *Phys. Rev. A*, **29**, 6, 3208, 1984.
32. R. Glauber and F. Haake, *Phys. Lett.* **68A**, 1, 29, 1978.
33. R. Bonifacio, P. Schwendimann, and F. Haake, *Phys. Rev.* **4**, 2, 854-864, September 1971.
34. R. Bonifacio, P. Schwendimann, and F. Haake, *Phys. Rev.*, **4**, 1, 302-313, July 1971.
35. L. Allen and J.H. Eberly, *Optical Resonance and Two-level Atoms*, Wiley-Interscience Pub. 1, New York, 1975.
36. M.F.H. Schuurmans and D. Polder, *Phys. Lett.* **72A**, 4.5, 306, 1979.

37. C.B. Collins, F.W. Lee, D.M. Shemwell, and B.D. DePaola, *J. Appl. Phys.* **53**, 7, 4645-4651, 1982.
38. F.X. Hartmann, A. Artna-Cohen, B. Balko, L. Cohen, and C. Hayes, "Study of the Photon Gain Condition for Long-Lived Nuclear Isomeric Transitions," *IDA Gamma-ray Laser Annual Summary Report (1985): Investigation of the Feasibility of Developing a Laser Using Nuclear Transitions*, edited by Bohdan Balko, Leslie Cohen, and Francis X. Hartmann, IDA Paper P-2021, June 1986.
39. J.P. Hannon and G.T. Trammel, *Opt. Commun.* **15**, 3, 330-334, 1975.
40. G. Baldwin, Johndale Solem, and V.I. Gol'danskii, *Rev. Mod. Phys.* **53**, 4, 687-744, 1981.
41. C.B. Collins, "Coherent and Incoherent Upconversion Techniques for the Pumping of a Gamma-ray Laser," *Proceedings of the IST/IDA Gamma-ray Laser Workshop*, edited by Bohdan Balko, Leslie Cohen, and Francis X. Hartmann, IDA Memorandum Report M-162, January 1986.
42. B. Arad, S. Eliezer, and Y. Paiss, *Phys. Lett. A*, **74**, 395, 1979.
43. J.J. Sakurai, *Advanced Quantum Mechanics*, Addison Wesley, 1967.
44. W.S. Cooper and H. Ringler, *Phys. Rev.* **179**, 226, 1969.
45. Y.R. Shen, *Principles of Non-Linear Optics*, John Wiley & Sons, New York, 1984.
46. L.A. Rahn, R.L. Farrow, M.L. Koszykowski, and P.L. Mattern, *Phys. Rev. Lett.* **45**, 620, 1980.
47. C.B. Collins, S. Olarin, M. Petrascu, and Iovitzu Popesur, *Phys. Rev. C*, **20**, 5, 1942, 1979.
48. C.B. Collins, S. Olarin, M. Petrascu, and Iovitzu Popesur, *Phys. Rev. Lett.* **42**, 21, 1397, 1979.
49. Blatt and Weisskopf, *Theoretical Nuclear Physics*, John Wiley & Sons, New York, 1952.
50. A. de-Shalit and I. Talmi, *Nuclear Shell Theory*, Academic Press, New York, 1963.
51. L.I. Schiff, *Phys. Rev.* **132**, 2194, 1963.
52. Wendin et al., *Phys. Rev. Lett.* **56**, 1241, 1986.
53. L.C. Biedenharn, G.C. Baldwin, and K. Boyer, *Phys. Rev. Lett.* **51**, 1986.
54. D.W. Noid, M.L. Koszykowski, and R.A. Marcus, *J. Chem. Phys.* **67**, 7, 1977 and *Annu. Rev. Phys. Chem.* **32**, 267, 1981.
55. Y. Izawa and C. Yasmanaka, *Phys. Lett. B*, **59**, 88, 1979.

56. L.C. Biedenharn, K. Boyer, and J.C. Solem, "Advances in Laser Science I," Editors W.C. Stwalley and M. Lapp, *A.I.P. Conference Proceedings*, **146**, 50, 1986.
57. R.D. Woods and D.S. Saxon, *Phys. Rev.* **95**, 577, 1954.
58. R. Langer, *Phys. Rev.* **51**, 669, 1937.
59. M.K. Gordon, Sandia Laboratories Report, AND 75-0211.
60. L.F. Shampine and M.K. Gordon, *Computer Solution of Ordinary Differential Equations*, Freeman, San Francisco, 1975.
61. V.A. Namiot, *Zh. Eksp. Teor. Fiz. Pis'ma Red.* **18** (JETP Lett.), 6, 369, 1973.
62. Yu. Kagan, *Zh. Eksp. Teor. Fiz. Pis'ma Red.* **19** (JETP Lett.), 722, 1974.
63. V.I. Gol'danskii, S.V. Karyagain, and V.A. Namiot, *Fiz. Tverd. Tela.* **16** (Sov. Phys. Solid State), 2517, 1974.
64. A.V. Andreev et al. *Zh. Eksp. Teor. Fiz.* **67** (Sov. Phys.-JETP), 1647, 1974.
65. B. Balko and Wasyl Wasylkiwskyj, "The Gamma-ray Laser Concept Using Long-lived Nuclear Isomers: Critical Issues and Their Resolutions," *Proceedings of the IST/IDA Gamma-ray Laser Workshop*, IDA Memorandum Report M-162, January 1986.
66. G.C. Baldwin et al., *Rev Mod. Phys.* **53**, 4, Part 1, October 1981.
67. E. Rutherford, J. Chadwick, and E.C. Ellis, *Radiations from Radioactive Sources*, Cambridge University Press, p. 8, 1951.
68. A. Messiah, *Quant. Mech.*, **1**, John Wiley & Sons, Inc., New York, 403, 1961.
69. M.I. Skolnik, *Introduction to Radar Systems*, McGraw Hill Book Co., New York, 1962.

APPENDIX A

SYMMETRY IN SPONTANEOUS DECAY-- BACKGROUND INFORMATION

APPENDIX A

SYMMETRY IN SPONTANEOUS DECAY-- BACKGROUND INFORMATION

A.1 BASIC SYMMETRY

A number of algebraic results of the theory of groups is applicable in models of physical systems in which symmetry plays a role. Examples of such systems are the structure of molecules, atoms, and nuclei as well as the original classification scheme of elementary particles. These same aspects of symmetry arise in the enhanced spontaneous decay theory as presented by Dicke. The notes in this Appendix summarize common ideas and nomenclature used in group models (Ref. A.1), and are particularly useful in understanding Dicke's model.

Symmetry arises when something "looks the same". The Pentagon, if rotated by an angle of 72° will look the same when viewed by an observer on the outside. Of course, following the rotation some workers on the inside will also be moved. Let us refer to the inside workers as degrees of freedom in an internal reference frame. As far as they are concerned, we could move their assignment to offices 72° in the opposite direction to compensate for the change.

In general, the movement of rooms, labeled by numbers, and the movement of people, labeled by letters requires the use of two types of symmetry operations; operations on the numbers in the number space and operations on the letters in the letter space. We can denote the letter operator $G(\alpha\beta)$ where $G(\alpha\beta)$ replaces the letter β by the letter α . In general, the letters are $\alpha, \beta, \gamma, \dots$ although we need only consider α and β for our purposes. We can further denote the number operator $P(ab)$ where a and b actually take on integer values. For our purposes there are ultimately many such integer values; say up to 10^{20} .

For illustration we consider the operation on a configuration:

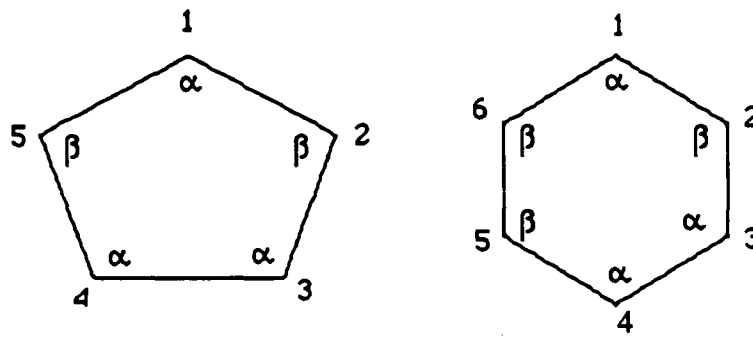


Figure A-1. Configurations of Letters and Numbers

The configuration for the Pentagon can be labeled " $\alpha_1\beta_2\alpha_3\alpha_4\beta_5$ " but it is clear that as long as we list the letters in their "bins" in numerical order; we can drop the integral subscripts. Thus, the previous Pentagon configuration is now labeled $\alpha\beta\alpha\alpha\alpha$. The hexagon has configuration $\alpha\beta\alpha\alpha\beta\beta$.

A.2. OPERATING IN THE NUMBER SPACE--THE PERMUTATION GROUP

All permutations of the integral numbers can be written as interchanges of the two numbers, or cycles. Thus, $P(12)$ means interchange the contents of bin one with the contents of bin two. For the hexagon configuration:

$$P(12) \alpha\beta\alpha\alpha\beta\beta = \beta\alpha\alpha\alpha\beta\beta$$

The new configuration is distinguishable from the old configuration.

In general, the collection of all permutation operators for n objects forms the permutation group denoted S_k . Even though all permutations can be written as bi-cycles some can also be written in longer sequences; such as replace one by two, two by five and five by one, $P(125)$.

$$P(125) \alpha\beta\alpha\alpha\beta\beta = \beta\beta\alpha\alpha\alpha\beta$$

In fact, the lengths of the maximum cycles of the permutations in S_k are $k, k-1, k-2, \dots, 1$. The permutations are then put into classes labeled by the cycle lengths. For $n = 3$, there are classes labeled by $[3]$, $[2,1]$ and $[1,1,1]$ indicating cycles of the form (123) ; $(12)(3)$ and $(1)(2)(3)$. The cycles can be arranged in graphs of boxes:

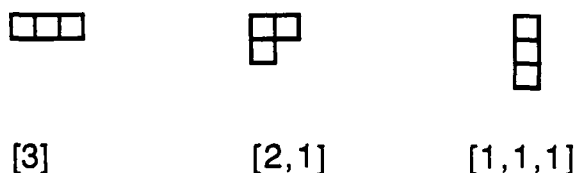


Figure A-2. Box Diagrams of the Classes

The number of classes in a group (here the example treats the group S_3) is equal to the number of irreducible representations, which are now explained.

A configuration, say $\alpha\beta\beta$, is an example of a basis function, f_i . All of the basis states (limited to those with one α and two β 's) are $\alpha\beta\beta$, $\beta\alpha\beta$ and $\beta\beta\alpha$, denoted f_i ; $i = 1, 2, 3$. The space spanned by these basis states (linear combinations of the basis states) is invariant when the group operators map the space to itself and not outside the space. The representation of the group gives the result of the operation on a state in the space and is often written as a matrix, thus:

$$P(12)(3) \alpha\beta\beta = \beta\alpha\beta ,$$

implies that a column vector $[100]$ (where the basis is in the order $\alpha\beta\beta$, $\beta\alpha\beta$ and $\beta\beta\alpha$) maps to the vector $[010]$. Furthermore, it is easy to see:

$$P(12)f_1 = f_2$$

$$P(12)f_2 = f_1$$

$$P(12)f_3 = f_3$$

can be written in matrix form

$$P(12) = \begin{bmatrix} 0 & 1 & 0 \\ 1 & 0 & 0 \\ 0 & 0 & 1 \end{bmatrix}$$

Figure A-3. Matrix Representation of the Permutation Operator

which is how one might obtain a matrix representation. The invariant space sometimes can be subdivided into smaller invariant spaces. Such spaces are reducible and so are their representations. Irreducible spaces and their associated irreducible representations cannot be further reduced.

The basis states of the irreducible representations can be found from the box diagram or Young graph by a set of rules. Since the number of classes is equal to the number of irreducible representations, the rules can be well-defined. This marvelous result, worked out by Young, is accomplished in three steps; construction of the Young tableau, identification of a starting function, and construction of the state. This is depicted in Fig. A-4.

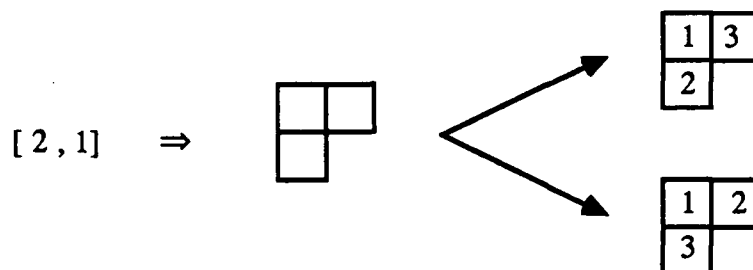


Figure A-4. Young Tableaux for the Case of $[2,1]$ in S_3

Step One. Fill the Young graph with the integers 1, 2, ... K such that the numbers increase across a row and increase down the column.

This irreducible representation will be two-dimensional since there are two Young tableaux.

Step Two. Construct the starting function by placing the letters $\alpha, \beta, \gamma \dots$ in the Young graph such that the letters "increase" or "stay the same" across the row and increase down a column. This is shown in Fig. A-5 for the α, β space [to later be called $SU(2)$], in the case of the Young graph of the previous example. There are only two allowed starting functions; now read off as $\alpha\alpha\beta$ and $\alpha\beta\beta$.

Step Three. Operate with the Young operator on the starting function. This requires getting a Young operator from a Young tableau. This is done by symmetrizing across a row followed by anti-symmetrizing down a column. This means writing the complete operator as the sum of the identity operator and all possible permutation operations involving the integers in the row with plus signs. Anti-symmetrizing is accomplished by writing all possible permutation operations looking down a column with the sign $(-)^c$ where c is the number of bi-cycles that the permutation operation can be decomposed into. Example operators are shown in Fig. A-6.

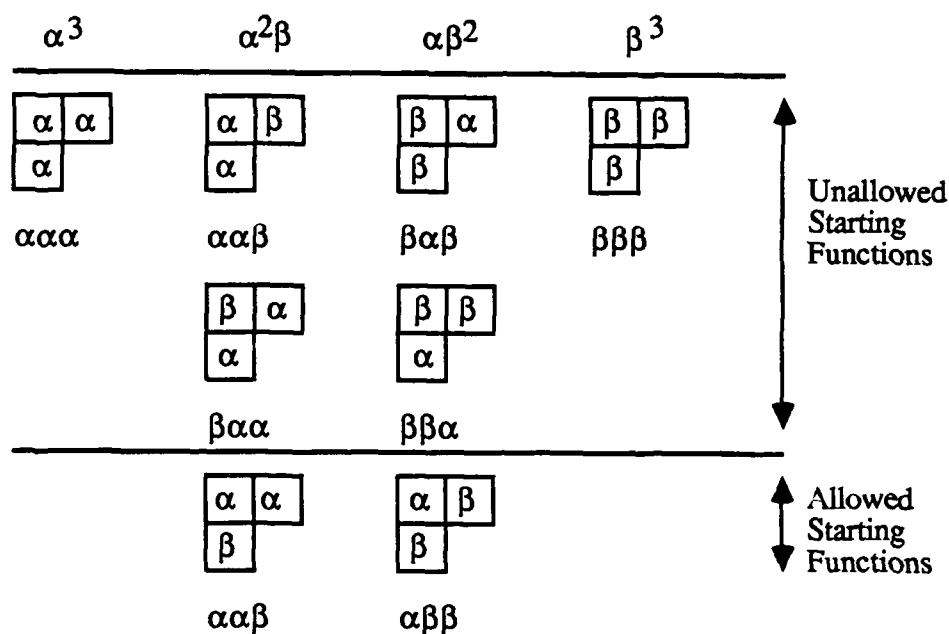


Figure A-5. Unallowed and allowed starting functions for the example of [2,1]

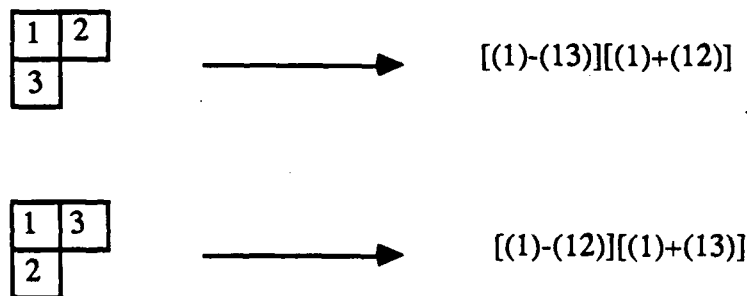


Figure A-6. Associations of Tableaux and Permutation Operators (Ignoring Normalization)

Now one operates with the Young operator (obtained from the tableau) on the starting function ($\alpha\beta\beta$):

$$[(1) - (13)] [(1) + (12)] \alpha\beta\beta = \alpha\beta\beta + \alpha\beta\beta - \beta\beta\alpha$$

$$[(1) - (12)] - [(1) + (13)] \alpha\beta\beta = \alpha\beta\beta + \alpha\beta\beta - \beta\alpha\beta$$

whereas from the completely symmetric tableau one obtains

$$\alpha\beta\beta + \beta\beta\alpha + \beta\alpha\beta.$$

For the configuration $\alpha\beta^2$ and the completely antisymmetric tableau, there is no function. The orthonormal irreducible basis states for $\alpha\beta^2$ are summarized in Table A-1.

Table A-1. Classification of Orthonormal States of $\alpha\beta^2$

Symmetric	Mixed-symmetric	Anti-symmetric
$\frac{1}{\sqrt{3}} [\alpha\beta\beta + \beta\alpha\beta + \beta\beta\alpha]$	$\frac{1}{\sqrt{2}} [\alpha\beta\beta - \beta\beta\alpha]$ $\frac{1}{2\sqrt{3}} [\alpha\beta\beta - 2\beta\alpha\beta + \beta\beta\alpha]$	No State

Thus, we now can fully understand the origin of mixed-symmetry states. The classification of states having internal degrees of freedom (in the examples α and β) according to the permutation group is important in understanding Dicke's theory of enhanced spontaneous decay. This section has explained the role of permutation number symmetry. The internal degrees of freedom α and β are further explained in the next section.

A.3 UNITARY SYMMETRY

The nature of the unitary groups is important to our understanding of certain physical quantities of interest--spin, isospin, angular momentum, etc. Now it is of interest in understanding collective interactions in a field.

A brief "history" helps. The general (complex) linear group in N dimension denoted $GL(N)$ consists of all non-singular homogeneous linear transformations of the points in an N -dimensional complex space or, more simply, $N \times N$ dimensional matrices with complex coefficients a_{ij} , $i, j = 1, 2, \dots, N$, and a non-vanishing determinant (so an inverse exists). The group $U(N)$ is a subgroup of $GL(N)$ where the complex conjugate transpose of the matrix $[u_{ij}]$ is its inverse. The group $SU(N)$ is the subgroup of $U(N)$ consisting of all matrices having determinant-of-magnitude unity. The group $O(N)$ is an important subgroup of $GL(N)$, consisting of all real orthogonal transformations in an N -dimensional real space. $O(N)$ is a direct product of the three-dimensional rotation group $R(3)$ or $SO(3)$ and the two-element group containing the identity element and the inversion operator. Each particular group has a number of degrees of freedom $\alpha_1, \alpha_2, \dots, \alpha_h$ in h

parameter space. These parameters lie in a range over closed intervals for SU(N), U(N) and O(N); thus, these latter groups are "compact". For a particular point in the parameter space; say $\alpha_1, \alpha_2, \dots, \alpha_h = \alpha$ there is a group element A. For another parameter set, α' , there is an element B. Since AB is in the group, there is some mapping f which gives the parameter set α'' of AB in terms of the parameter sets α and α' .

$$\alpha'' = f(\alpha, \alpha') \quad . \quad (A-1)$$

The parameter set of the identity is α^0 . The existence of an inverse set of parameters, say α^{-1} , requires

$$\alpha^0 = f(\alpha, \alpha^{-1}) \quad . \quad (A-2)$$

Likewise, one may have a function g, such that

$$\alpha^{-1} = g(\alpha, \alpha^0) \quad (A-3)$$

when the functions f and g are well-behaved and possess derivatives to all orders, the group is said to be a Lie group. This essentially means group elements can be found from a "Taylor" expansion from some specific element; such as the identity and the group can be understood "from the infinitesimal" through the use of infinitesimal group generators. The group generators physically act as quantum mechanical operators.

If a group element A(α) is near the identity element E(α^0) (in this notation we refer to the group element with its parameters in parentheses) then " $\alpha = \alpha^0 + d\alpha$ " and we can say,

$$A(\alpha_1^0 + d\alpha_1, \dots, \alpha_h^0 + d\alpha_h) = E + G_1 d\alpha_1 + \dots + G_h d\alpha_h \quad . \quad (A-4)$$

The G's are the generators:

$$\begin{aligned} G_i &= \lim_{d\alpha_i \rightarrow 0} \frac{[A(\alpha_1^0, \dots, \alpha_i^0 + d\alpha_i, \dots, \alpha_h^0) - E]}{d\alpha_i} \\ &= \frac{\partial A}{\partial \alpha_i} \quad . \end{aligned} \quad (A-5)$$

In matrix form:

$$\begin{bmatrix} a_{11} & a_{12} \\ a_{21} & a_{22} \end{bmatrix} = \begin{bmatrix} 1 & 0 \\ 0 & 1 \end{bmatrix} + \begin{bmatrix} da_{11} & da_{12} \\ da_{21} & da_{22} \end{bmatrix} \quad (A-6)$$

and the generators are:

$$\begin{bmatrix} 1 & 0 \\ 0 & 0 \end{bmatrix} \quad \begin{bmatrix} 0 & 1 \\ 0 & 0 \end{bmatrix} \quad \begin{bmatrix} 0 & 0 \\ 0 & 1 \end{bmatrix} \quad \begin{bmatrix} 0 & 0 \\ 1 & 0 \end{bmatrix} \quad (\text{A-7})$$

We can now consider the effects of symmetry. If we rotate the Pentagon by 72° clockwise, a specific office now overlooking the Potomac was previously 72° counter-clockwise and facing more northerly. Mathematically, we can state that the rotation of the building is related to the inverse rotation of the office assignments:

$$Af(P) = f(A^{-1}P) . \quad (\text{A-8})$$

For a matrix A near the identity, the inverse A^{-1} has components: $\alpha_{ij}^{-1} = \gamma_{ij} - d\alpha_{ij}$. Hence, in the two-dimensional case:

$$\begin{aligned} A([a_{ij}]) f(x_1, x_2) &= f(x_1 - x_1 da_{11} - x_2 da_{12}, x_2 - x_1 da_{21} - x_2 da_{22}) \\ &= f(x_1, x_2) - (x_1 da_{11} + x_2 da_{12}) \frac{\partial f}{\partial x_1} - \dots \\ &= \sum_{ij} (E + G_{ij} da_{ij}) f . \end{aligned} \quad (\text{A-9})$$

where the generators have the forms:

$$G_{ij} = -x_j \frac{\partial}{\partial x_i} . \quad (\text{A-10})$$

the generators G_{ij} equation (A-7) and G_{ij} equation (A-10) have the same group properties.

The set of h generators satisfy:

$$G_i G_j - G_j G_i = \sum_{l=1}^h c_{ij}^l G_l , \quad (\text{A-11})$$

where $i, j = 1, 2, \dots, h$, and where c_{ij}^l are structure constants. Thus, we understand the role of commutation relations.

For $SU(N)$ groups there are $n^2 - 1$ parameters and consequently, $n^2 - 1$ generators. Of these, $n^2 - 1$ generators $n - 1$ are diagonal and can be used to fix eigenvalues. There are also $n - 1$ additional diagonal Casimir operators which are quadratic, cubic, etc., in powers of the generators. The generators are then important for our purposes. They govern the rates of decay of the Dicke states constructed previously.

When the generators of a group commute with the Hamiltonian of a system, then all of the operations of a group commute with the Hamiltonian and the group is a symmetry group. The diagonal generators are then operators corresponding to conserved physical quantities. Invariant operators will also commute with the Hamiltonian of a system; and the states of the system have well-defined eigenvalues of these operators. Moreover, the states of the system are then states of the irreducible representations.

The eigenvalues of the diagonal generators for the states of the defining representation can be used to construct a vector m in space whose coordinates are the eigenvalues of the diagonal generators. This vector is the "weight vector." The "root vectors" are the differences in the weight vectors. The diagram of states of irreducible representation is referred to as a weight diagram; and generators pictorially shift from point to point on the weight diagram. These pictorial concepts are useful in visualizing the group structure and symmetry of physical systems. We use them in the main section of this paper.

The group $SU(2)$ has three generators which we call j_x , j_y , and j_z . Their matrix form is well known (Pauli matrices) and the Casimir invariant is $J^2 = J_x^2 + J_y^2 + J_z^2$. The eigenvalue of J_z is called m , and the eigenvalue of J^2 is $J(J+1)$. The fundamental weight diagram is one dimensional since there is only one diagonal generator, J_z . The fundamental basis states are usually labeled α and β , having J_z eigenvalues of $+1/2$ and $-1/2$, respectively.

From the matrix representation for the $SU(2)$ group the $SU(2)$ algebra is (well known to pedestrians):

$$\begin{aligned} J^+ &= J_x + iJ_y, \quad J^- = J_x - iJ_y \\ [J_z, J^+] &= +J^+ \\ [J_z, J^-] &= -J^- \end{aligned} \quad (A-12)$$

The most significant aspect of the background group theory in this Appendix pertinent to understanding Dicke's theory of enhanced spontaneous decay is the classification of many-particle states simultaneously according to the permutation group of k objects and according to the unitary group in n -dimensions. This is most conveniently accomplished for our purposes here through the use of the Young techniques. The $SU(N)$ symmetry is indicated by the upper-left superscript in the Young box, as shown below:

$$\begin{array}{ccc}
 2 & \square & \text{for SU(2)} \\
 3 & \square & \text{for SU(3)} \\
 & \dots & \dots \dots \dots \\
 N & \square & \text{for SU(N)}
 \end{array} \tag{A-13}$$

A single box represents a "single particle" and, as used previously, it is convenient to introduce Greek labels. Thus, for SU(2) we use α, β . In Dicke's theory α and β refer to excitation states in a single two-level particle system. The wave functions of the many-particle states are found by the direct (outer) product:

$$\begin{array}{ccccccc}
 2 & & 2 & & 2 & & \text{etc.} \\
 \square & \otimes & \square & \otimes & \square & &
 \end{array} \tag{A-14}$$

For k particles, the resultant tableaux would extend to k boxes in height, except for the fact that no more than N internal states can be anti-symmetrized in a vertical column. Because of this constraint, the tableaux are always restricted to N rows for $U(N)$. For classification according to $SU(N)$, where the total number of boxes is unimportant, "closed" columns are conveniently dropped.

The simultaneous classification of $k = 5$ objects according to S_5 and two-level α and β excitations according to $SU(2)$ is depicted in the following example. The group S_5 has 7 classes, of which only three are allowed in $SU(2)$. They are $[5]$, $[4,1]$, and $[3,2]$. The four classes not allowed have more than two columns. The class $[5]$ has only one tableau, but it has six starting functions. They are $\alpha\alpha\alpha\alpha\alpha$, $\alpha\alpha\alpha\alpha\beta$, $\alpha\alpha\alpha\beta\beta$, $\alpha\alpha\beta\beta\beta$, $\alpha\beta\beta\beta\beta$, and $\beta\beta\beta\beta\beta$. Continuing in this manner, the classification scheme depicted in Fig. A-7 emerges.

The expressions for degeneracies are discussed in the main text; and here we show the degeneracies as found using the numbering of the Young graph. The mixed symmetry states depicted here are associated with higher dimensional, irreducible representations.

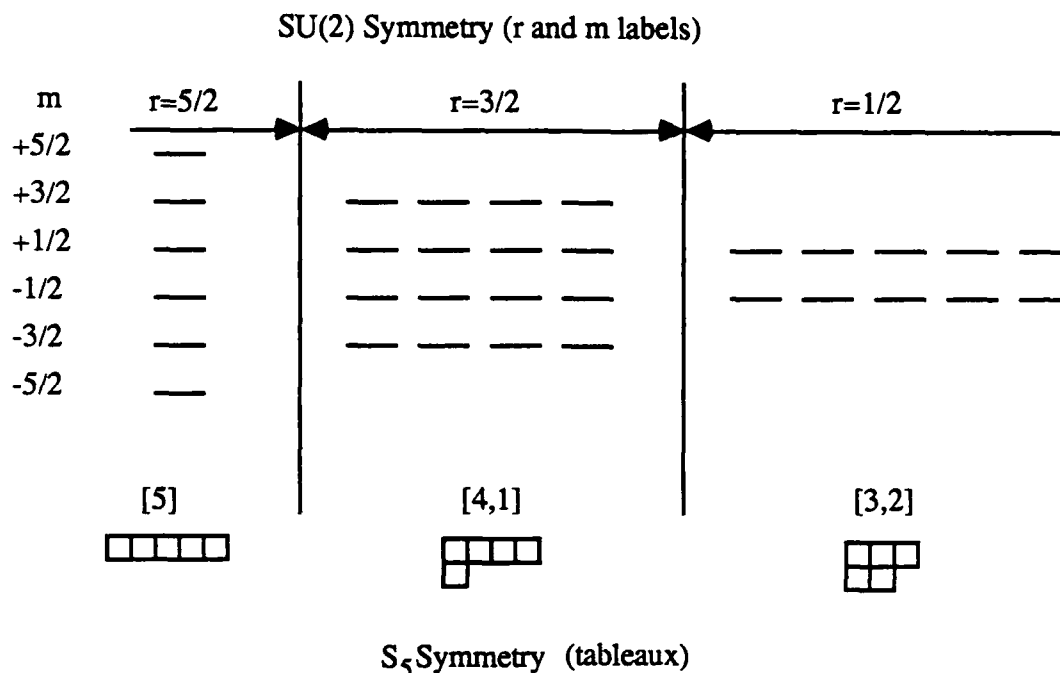


Figure A-7. The Simultaneous Classification of States of S₅ XSU(2) and Associated Quantum Numbers are Depicted Here for Five Particles.

Although the wave functions are rather tedious to express, they can be found using the Young operator on the starting function. We emphasize the Young technique since it is easy to visualize for higher N, in preference to the Clebsch-Gordon approach. As long as the quantum numbers remain "good quantum numbers" there is no need to know the states explicitly. For more than two-level systems, in SU(N), the coupling coefficients are needed and one way is to know the states according to the differing group chains. The four functions thus found for the [4,1] symmetry will be found to be linearly independent, which is sufficient to span the entire invariant space, but they will not, in general, be orthogonal. Thus, it is assumed that normalization is achieved at will, and the equivalent Gramm-Schmidt orthogonalization may be needed in practice.

REFERENCE, APPENDIX A

A.1 F.X. Hartmann, Ph.D. Thesis, Princeton University, 1985.

APPENDIX B

INTRODUCTION TO ENHANCED SPONTANEOUS DECAY THEORY

APPENDIX B

INTRODUCTION TO ENHANCED SPONTANEOUS DECAY THEORY

B.1 INTRODUCTION TO THE DICKE SUPERRADIANT THEORY

This appendix provides a brief introduction to aspects of Dicke superradiance used in modeling pulse characteristics. The original symmetry approach of Dicke is then pursued.

B.2 COHERENCE IN SPONTANEOUS RADIATION PROCESSES

Dicke's theory of superradiant emission is a theory of coherence in spontaneous radiation processes. The underlying assumption or "observation" of the theory is that all molecules (emitters) are interacting with a common radiation field and hence, cannot be treated as independent quantum mechanical processes. For non-overlapping spatial wavefunctions, particle symmetry plays a role with respect to the common radiation field.

The example of two two-level particles illustrates the main point. A proton in a uniform magnetic field has two states: one with spin component $m_s = + 1/2$ denoted $|\alpha\rangle$ and one with spin component $m_s = - 1/2$ denoted $|\beta\rangle$:

$$\begin{array}{lll} |\alpha\rangle & m_s = + 1/2 & \text{Spin-1/2 Multiplet} \\ |\beta\rangle & m_s = - 1/2 & \end{array} \quad (B-1)$$

For two such protons (labeled #1 and #2), there are four states:

$$\begin{array}{lll} \alpha_1\alpha_2 & & \\ 2^{-1/2}(\alpha_1\beta_2 + \beta_1\alpha_2) & 2^{-1/2}(\alpha_1\beta_2 - \beta_1\alpha_2) & \\ \beta_1\beta_2 & & \\ \text{Triplet (superradiant)} & \text{Singlet (subradiant)} & \end{array} \quad (B-2)$$

The state $\alpha_1\beta_2$ has a 50 percent probability of decaying to $\beta_1\beta_2$ since it is a linear superposition of the $m_s = 0$ singlet and triplet states. As far as emission is concerned, the triplet state is "superradiant" and the singlet state is "subradiant".

Some assumptions pertain to particles physically treated as "gaseous." The gaseous system as a whole is considered to be treated as one quantum mechanical system, and Dicke makes five assumptions concerning the radiating "molecules."

- (1) The gas dimensions are assumed to be small with respect to a radiation wavelength
- (2) The walls of the container are transparent to the radiation field
- (3) Collisions do not affect internal states of molecules
- (4) Transitions take place between two non-degenerate states of the molecule
- (5) There is insufficient overlap in wavefunctions of separate particles, requiring that wavefunctions be symmetrized.

The Hamiltonian for the two-level system is obtained as follows. First some definitions:

$E = \hbar\omega$ = excitation energy

H_0 = Hamiltonian; acts on center of mass coordinates

n = number of particles

j, i = particular particles

R_{j3} = an operator with eigenvalue $+ 1/2$ if the particle is excited, $- 1/2$ if not excited

Then the Hamiltonian is given by:

$$H = H_0 + E \sum_{j=1,n} R_{j3} , \quad (B-3)$$

where

$$[R_{j3}, H_0] = [R_{j3}, R_{i3}] = 0 .$$

A typical total system wavefunction for an energy eigenstate is

$$\Psi_{gm} = U_g (r_1 \dots r_n) [+ + + \dots] , \quad (B-4)$$

where the first factor U is a function of center of mass coordinates and the second factor gives the signs of the internal energies of the emitters. For n_+ particles in the excited state, and n_- in the unexcited state,

$$\begin{aligned} n &= n_+ + n_- \\ m &= 1/2 (n_+ - n_-) \end{aligned} \quad (\text{B-5})$$

and

$$E_{gm} = E_g + mE$$

The degeneracy of the states having energy E_{gm} is

$$n! / [(n/2 + m)! (n/2 - m)!] \quad (\text{B-6})$$

This is an important factor that warrants further study since it will predict diminishing superradiance if less than complete inversion is achieved.

Two other operators are of importance in addition to R_{j3} and H_0 . They are R_{j1} and R_{j2} . The three R_j operators are the three infinitesimal generators of a group with SU(2) algebraic structure:

$$\begin{aligned} R_{j1} [\dots \pm \dots] &= 1/2 [\dots -/+ \dots] \\ R_{j2} [\dots \pm \dots] &= \pm 1/2 i [\dots -/+ \dots] \\ R_{j3} [\dots \pm \dots] &= \pm 1/2 [\dots \pm \dots] \end{aligned} \quad (\text{B-7})$$

For all n particles:

$$R_k = \sum_{j=1,n} R_{jk} \quad k = 1,2,3 \quad (\text{B-8})$$

and the well known quadratic Casimir invariant of SU(2) is

$$R^2 = R_1^2 + R_2^2 + R_3^2 \quad (\text{B-9})$$

Finally,

$$H = H_0 + ER_3 \quad (\text{B-10})$$

$$R_3 \Psi_{gm} = m \Psi_{gm} \quad (\text{B-11})$$

B.3 INTERACTIONS WITH THE ELECTROMAGNETIC FIELD

That the interaction term of the particles with the electromagnetic field can be written in terms of the SU(2) generators is important in Dicke's theory. The interaction term is written as:

$$H_1 = - A(\vec{r}_j) \cdot \sum_{k=1, N-1} e_k \mathbf{p}_k / m_k c \quad , \quad (B-12)$$

where

\mathbf{r}_j = center of mass position of the j^{th} particle

e_k, m_k = charge and mass of the k^{th} particle

\mathbf{p}_k is an odd operator with off-diagonal elements

The general form of the interaction terms is

$$- A(\mathbf{r}_j) \cdot (e_1 R_{j1} + e_2 R_{j2}) \quad , \quad (B-13)$$

where e_1 and e_2 are constant real vectors; the same for all particles. Then the general form of H_1 is

$$H_1 = - \sum_j A(\mathbf{r}_j) \cdot (e_1 R_{j1} + e_2 R_{j2}) \quad . \quad (B-14)$$

In a small gas sample,

$$H_1 = - \sum_j A(0) \cdot (e_1 R_1 + e_2 R_2) \quad , \quad (B-15)$$

where $A(0)$ is evaluated at the center of mass. The small sample size eliminates effects of the center of mass coordinates. Assuming $\Delta g = 0$ (g could be a motion quantum number, for example) eliminates Doppler broadening of the transition frequency.

The operator H_1 has selection rules $\Delta m = \pm 1$. R_1 and R_2 account for transitions having $\Delta m = \pm 1$. R_3 is a diagonal operator. Since H and R^2 commute, and since the Casimir operator R^2 has eigenvalue $r(r+1)$ it is convenient to introduce r as the "cooperation number". Thus, $|m| \leq r \leq n/2$.

Ψ_{gmr} denotes the new eigenstates of r ,

$$H \Psi_{gmr} = (E_g + mE) \Psi_{gmr} \quad (B-16)$$

$$R^2 \Psi_{gmr} = r(r+1) \Psi_{gmr} \quad . \quad (B-17)$$

The operators of SU(2) are related to the permutation group S_2 of symmetry operations of the one-dimensional simplex. Thus, all weight diagrams will be lengths of one-dimensional lattice points. The highest weight state is denoted $\Psi_{g, n/2, n/2}$ and used to get the lower states

$$\begin{aligned}\Psi_{grr} &= \Psi_{g, n/2, n/2} = U_g [++ \dots +] \\ \Psi_{gmr} &= [(R^2 - R_3^2 - R_3)^{-1/2} (R_1 - iR_2)]^{r-m} \Psi_{grr} ,\end{aligned}\quad (B-18)$$

where the multiplicative factor obtained in "lowering" is described in most presentations on angular momentum theory. The matrix element:

$$\begin{aligned}(g, r, m | e_1 R_1 + e_2 R_2 | g, r, m -/+ 1) = \\ 1/2 (e_1 \pm ie_2) [(r \pm m)(r -/+ m + 1)]^{1/2} .\end{aligned}\quad (B-19)$$

Thus, spontaneous radiation probabilities are given by

$$I = I_0 (r+m) (r-m+1) . \quad (B-20)$$

For example, the decay rate for one excited particle is

$$m = r = 1/2 \quad I = I_0 (1/2 + 1/2) (0 + 1) = I_0 . \quad (B-21)$$

For n initially excited particles

$$I = nI_0 . \quad (B-22)$$

For n particles, where r is large $|m|$ is small; $r \approx n/2$, $m = 0$ (zero population inversion) and

$$I = I_0 (n/2) (n/2 + 1) . \quad (B-23)$$

This is the largest rate at which a gas with an even number of particles can radiate *spontaneously*. In summary, the characteristics of the enhanced spontaneous decay are

- (1) $I \propto N^2$
- (2) Δn (population inversion) is zero
- (3) with large values of r radiate more strongly than multiplets with smaller values of r

Note that n particles, where $r = m = 0$, never radiate.

A gas which is radiating strongly because of coherence is called "superradiant." Some ways to make a superradiant state are the following:

- (1) Excite all molecules to $r = m = n/2$ and wait for decay to the "superradiant region" given by $m \sim 0$.
- (2) Start in the ground state: $r = -m = n/2$ and irradiate with a sufficiently intense pulse to the state where $m \sim 0$.

Effects of thermal equilibrium provide for randomness in the initial state, which can be calculated using standard statistical mechanics techniques. At high temperature, it is found that $r = m = -nE/4kT$. Following an irradiating pulse to excited states with $m \sim 0$ the radiation rate is

$$I \sim I_0 r(r+1) \sim I_0 n^2 (E/4kT)^2 . \quad (\text{B-24})$$

Finally, for any temperature, Dicke shows

$$I = (1/4) I_0 n(n-1) \tanh^2(E/2kT) + nI_0 / 2 . \quad (\text{B-25})$$

B.4 CLASSICAL MODELS

For large r we can consider classical models of Dicke superradiance. This approach appears to provide convenient analytical solutions. Figure B-1 summarizes the coordinates.

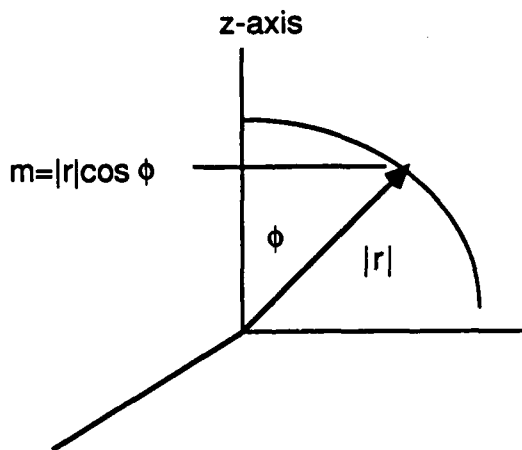


Figure B-1. Polar coordinate system used in the classical model.

The component m is approximately $m = r \cos \phi$. With this substitution, the radiation rate becomes $I = I_0 r^2 \sin^2 \phi$ (ignoring linear terms in r). The internal energy of the gas is

$$mE = rE \cos \phi = E_T . \quad (\text{B-26})$$

Then

$$dE_T/dt = -rE \sin\phi (d\phi/dt) . \quad (B-27)$$

Using $|I_0| = |dE/dt|$,

$$I_0 r^2 \sin^2\phi = r E \sin\phi (d\phi/dt) \quad (B-28)$$

or

$$(d\phi/dt) = (I_0 r / E) \sin\phi = \alpha \sin\phi . \quad (B-29)$$

For $\phi = 90^\circ$, $m = 0$ and $\sin\phi = \text{sech}(\alpha t)$. The form of the radiated wave is

$$A(t) = e^{i\omega t} \sin\phi , t > 0 . \quad (B-30)$$

The Fourier transform is

$$F(\beta) = (\pi/2)^{1/2} (\alpha^{-1}) \text{sech} [\pi (\beta - \omega)/2\alpha] , \quad (B-31)$$

which is a non-Lorentzian pulse shape. The width at half-intensity is

$$\Delta\omega = 1.12 \gamma r . \quad (B-32)$$

Here, γ is the linewidth for isolated single particles. For the case of maximum r ,

$$\Delta\omega = 1.12 \gamma n/2 . \quad (B-33)$$

B.5 A GAS OF LARGE EXTENT

This case considers:

- (1) A gas which occupies a region having dimensions larger than the radiation wavelength (for 50 keV, $l = 6 \times 10^{-10}$ cm or 0.06 Å)
- (2) A gas region small with respect to the reciprocal of the natural linewidth. (For $\tau = 1$ s. Γ is approximately 10^{-17} eV; thus, $1/\Delta k$ is approximately 10^{-11} cm.)

For this case, coherence is considered for a fixed direction \mathbf{k} , and now the R operators of the SU(2) symmetry are labeled by \mathbf{k} . Thus, correlated states of the gas for which radiation propagated in the \mathbf{k} direction is coherent are described by $\Psi_{\mathbf{m}\mathbf{r}}$ for direction \mathbf{k} . A photon of momentum \mathbf{k} arises from transitions having $\Delta r = 0$, $\Delta m = \pm 1$:

$$I(\mathbf{k}) = I_0(\mathbf{k}) (r+m) (r-m+1)$$

$$\Gamma = \frac{h}{2\tau} \quad . \quad (B-34)$$

On the other hand, where $\mathbf{k} \neq \mathbf{k}'$, the selection rules are

$$\Delta r = \pm 1, 0; \Delta m = \pm 1 \quad . \quad (B-35)$$

In summary:

- (1) Incident radiation is assumed to be plane with a propagation vector \mathbf{k}
- (2) The gas radiates in the \mathbf{k} direction
- (3) Radiations in directions other than \mathbf{k} tend to destroy the coherence with respect to the direction \mathbf{k} by causing transitions to states of lower r .

B.6 DOPPLER EFFECTS

Since H_0 and R_k^2 do not commute, the eigenstates are not stationary. Physically, there is relative motion between the oscillators, as depicted in Fig. B-2:

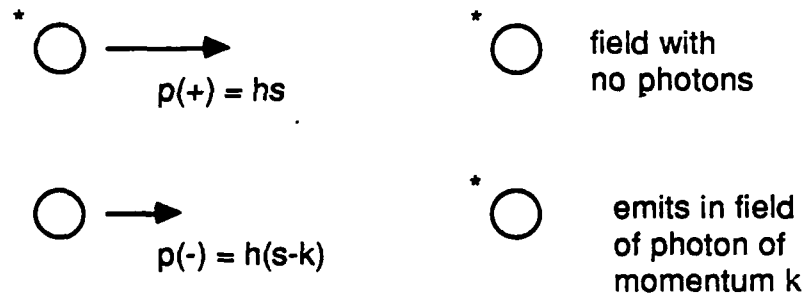


Figure B-2. When Recoil Effects Must be Included, the Emitters Emit Photons of Momentum \mathbf{k} with Momentum Changes Reflected by a Change in the Deexcited Emitter's Velocity (in the Simplest Form of Dicke's Theory).

Now the appropriate states are written as:

$$\Psi_{srr} = \exp(i s \sum_j r_j) [+++ \dots +], \quad (B-36)$$

$$\Psi_{smr} = [(R_k^2 - R_{k3}^2 - R_{k3})^{-1/2} (R_{k1} - iR_{k2})]^{r-m} \Psi_{srr} \quad . \quad (B-37)$$

These latter coherent states are superpositions of states such that the excited particles have one momentum and the unexcited have another (recoil then preserves the coherence).

B.7 PULSE-INDUCED COHERENT RADIATION

In this case the radiation field is turned on for a short period of time. The system evolves in a complicated manner as discussed in Chapter II. The emitted pulse is highly anisotropic and dependent on the duration of the pumping.

Further routes of investigation include the study of correlation of successive photons. For an inter-particle spacing large compared with a radiation wavelength, the radiation rate averaged over all directions is the incoherent rate.

B.8 SEMICLASSICAL SUPERRADIANCE

The Feynman, Vernon, and Hellwarth (FVH) representation provides a convenient pictorial framework for understanding superradiant emission in a standard semiclassical approach. Further details of the treatment of transitions in two-level systems in the FVH approach are discussed in Appendix C.

APPENDIX C

BRIEF OVERVIEW OF SEMICLASSICAL APPROXIMATIONS TO THE GROUP THEORETICAL APPROACH TO SUPERRADIANCE

APPENDIX C

BRIEF OVERVIEW OF SEMICLASSICAL APPROXIMATIONS TO THE GROUP THEORETICAL APPROACH TO SUPERRADIANCE

C.1 THE FEYNMAN, VERNON, HELLWARTH REPRESENTATION OF TRANSITIONS IN TWO-LEVEL SYSTEMS

The Feynman, Vernon, Hellwarth (FVH) representation provides for an alternate description of superradiance employing a semiclassical description of the radiation field. The theory of vectorial precession in three-dimensional space according to the group $O(3)$ is, not surprisingly, equivalent to a quantum approach based on $SU(2)$ since $SU(2)$ is homomorphic onto $O(3)$. The level scheme is the same two-level system discussed throughout the text, and the vector \mathbf{r} , its z component m , and the angle ϕ are depicted in Fig. B-1 of the previous Appendix.

Quite simply, in the FVH approach,

$$H\Psi = i\hbar\partial\Psi/\partial t \quad , \quad (C-1)$$

where

$$H = H_0 + V(t) \quad . \quad (C-2)$$

Let

$$\Psi(t) = a(t) u_a + b(t) u_b \quad , \quad (C-3)$$

where u_a and u_b denote excited and deexcited basis states.

Here, $a(t)$ and $b(t)$ have real and imaginary parts. One component (of the four) is the absolute phase of $\psi(t)$. The three-component Bloch vector is:

$$\mathbf{r} = (r_1, r_2, r_3) \quad , \quad (C-4)$$

where

$$r_1 = ab^* + ba^* ,$$

$$r_2 = i(ab^* - ba^*) ,$$

and

$$r_3 = aa^* - bb^* . \quad (C-5)$$

The following definitions apply:

$$\omega_1 = (V_{ab} + V_{ba}) / \hbar$$

$$\omega_2 = i(V_{ab} - V_{ba}) / \hbar$$

$$\omega_3 = \omega . \quad (C-6)$$

Here V_{ab} and V_{ba} are matrix elements of the potential V describing the electromagnetic transition:

$$V = -1/2 (\mu^+ E^- + \mu^- E^+) . \quad (C-7)$$

Using all of the previous equations, it is easy to show that the equation of motion is

$$d\mathbf{r}/dt = \boldsymbol{\omega} \times \mathbf{r} , \quad (C-8)$$

Its solution is well known.

C.2 SUPERRADIANCE IN THE VECTOR MODEL

Superradiance in the vector model is described in many elementary texts. The superradiant state arises from a $\pi/2$ pulse, as briefly summarized here. The transition energy is assumed to be $\hbar\omega$ where ω is the resonant frequency. Initially, all of the emitters in the system are in the state u_b ; thus, $\mathbf{r}_R(0) = -1 a_{III}$ where a_{III} is the z direction in an internal rotating reference frame (rotating at frequency ω). For a time t_0 , the field is turned on such that $|\omega_I| t_0 = \pi/2$. Here, the frequency $\omega_I = -2\mu E/\hbar$ corresponds to the interaction of the transition dipole μ with the field E and in the usual picture the vector $\boldsymbol{\omega} = \omega_I \mathbf{a}_I$. According to the dynamics of the vector \mathbf{r} discussed in section C.1, the vector is brought to the position depicted in Fig. C-1. When the field is turned off at $|\omega_I| t_0 = \pi/2$, the system is "midway" between the upper and lower states--this is the largest transition dipole moment; $|a|^2 = |b|^2$ and the projection on a_{III} is zero.

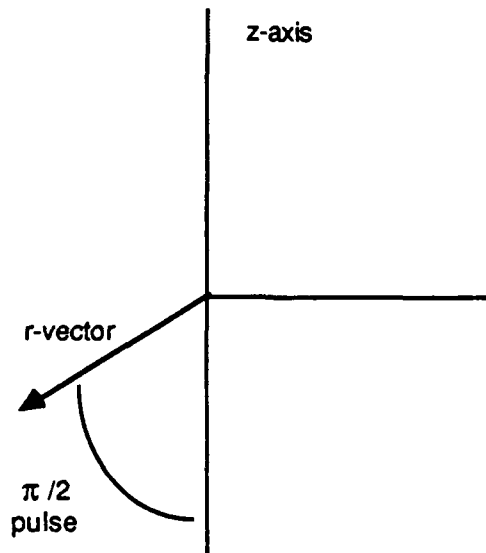


Figure C-1. The superradiant state is achieved from the ground state by a 90-degree exciting pulse leading to 50 percent population inversion. This state of maximum dipole moment radiates at the maximum rate described by the dynamical equation summarized in Section C.1. The FVH approach is thus an "O(3)" vector model achieving similiar dynamics as Dicke's original "SU(2)" theory.

In this particular superradiant state the particles are contributing coherently to a single giant dipole moment. The decay of this state is characterized from the increased radiation rate that characterizes the spontaneous decay of the giant dipole, that is the rate of fall of the r vector. There is no explicit reliance on the r "cooperation" quantum number other than its association with the length of the r vector. Also, no more than one state having $N_a = N_b$ is distinguished, in contrast to N such states in Dicke's quantum formulation. Specific applications of the semiclassical model are discussed in the main text in more detail, where various pulse characteristics are discussed.

APPENDIX D

RESONANCES IN THE APPROXIMATE BONIFACIO-LUGIATO MODEL

APPENDIX D

RESONANCES IN THE APPROXIMATE BONIFACIO-LUGIATO MODEL

This appendix outlines an analytical approach to the solution of the approximate equations for the general, non-Markovian, B-L model for superradiance when inhomogeneous line broadening is neglected. The method is that used in Ref. D.1 to calculate the atomic inversion and emitted radiation according to the earlier Markovian model introduced in Ref. D.2.

In Ref. D-3 B&L derived the approximate equations

$$\begin{aligned} \dot{p}(m,t) = & -\frac{4}{N} \int_0^t ds e^{-K(t-s)} \\ & \{g(m) p(m,s) - g(m+1) p(m+1,s) + [g(m) + g(m+1)]N(m,s) \\ & - g(m+1)N(m+1,s) - g(m)N(m-1,s)\} , \\ \dot{N}(m,t) = & -2KN(m,t) + \frac{4}{N} \int_0^t ds e^{-K(t-s)} \\ & \{g(m+1) [p(m+1,s) + N(m+1,s) - N(m,s)]\} , \end{aligned} \quad (D-1)$$

where

$$g(m) = \begin{cases} (\frac{N}{2} + m)(\frac{N}{2} - m + 1), & -\frac{N}{2} \leq m \leq \frac{N}{2} \\ 0, & \text{otherwise,} \end{cases} \quad (D-2)$$

for the occupation probabilities $p(m,t)$ of the atomic Dicke states $|r,m\rangle$ and the corresponding photon expectation values $N(m,t)$ of the radiating electromagnetic field, given a particular value $(N/2)(N/2 + 1)$ for the atomic cooperation eigenvalue. In equations D-1, in the form given here, the "inhomogeneous broadening" decay time T_2^* is assumed to be infinite, although in Ref. D.3 it is included as part of both integrands on the right hand side of the equations. Also in equation (D-1) time is measured in units of the cooperation

time τ_c and K is a corresponding dimensionless parameter equal to the product of τ_c with the reciprocal photon propagation time parameter originally designed as K in Ref. D.3. Thus, here

$$K = \tau_c K_{\text{original}} .$$

Along with equation (D-1) the standard initial conditions

$$N(m,0) = 0 ;$$

$$p\left(\frac{N}{2}, 0\right) = 1 ;$$

$$p(m,0) = 0, \quad m < \frac{N}{2} , \quad (D-3)$$

are assumed. These conditions imply that initially all N atoms are excited and the photon field is in the vacuum state. Together with equations (D-1) they imply that $N(N/2, t) \equiv 0$.

With neglect of T_2^* , the solution of equation D-1 can be found by means of the Laplace transform. Thus, setting $p(m,z)$ and $N(m,z)$ for the Laplace transforms of $p(m,t)$ and $N(m,t)$, equations (D-1) is equivalent to

$$\begin{aligned} (Z + 2K + \frac{4}{z+K}) \overline{N\left(\frac{N}{2} - 1, z\right)} - \frac{4}{z+K} \overline{p\left(\frac{N}{2}, z\right)} &= 0 , \\ -\frac{4}{z+K} \overline{N\left(\frac{N}{2} - 1, z\right)} + (z + \frac{4}{z+K}) \overline{p\left(\frac{N}{2}, z\right)} &= 1 , \end{aligned}$$

for the highest m values and

$$(z + 2K + \frac{\gamma_m}{z + K}) \overline{N(m-1, z)} - \frac{\gamma_m}{z + K} \overline{p(m, z)} = \frac{\gamma_m}{z + K} \overline{N(m, z)},$$

$$- \frac{\gamma_m}{z + K} \overline{N(m-1, z)} + (z + \frac{\gamma_m}{z + K}) \overline{p(m, z)} = - (\frac{\gamma_m + \gamma_{m+1}}{z + K}) \overline{N(m-1, z)}$$

$$- \frac{\gamma_{m+1}}{z + K} \overline{N(m+1, z)} - \frac{\gamma_{m+1}}{z + K} \overline{p(m+1, z)} \quad (D-4)$$

for the rest, where

$$\gamma_m = \frac{4g(m)}{N}. \quad (D-5)$$

The quantities $N(m-1, z)$ are naturally matched with the quantities $p(m, z)$ in equation (D-4) in recursive pairs, the quantity $N(N/2, t)$ already having been found to be zero identically. The determinant, $\text{Det}(z)$, of the matrix on the left side of equation (D-4) is given by

$$\text{Det}(z) = (z + 2K + \frac{\gamma_m}{z + K})(z + \frac{\gamma_m}{z + K}) - \frac{\gamma_m^2}{(z + K)^2} = z^2 + 2Kz + 2\gamma_m. \quad (D-6)$$

Accordingly, the inverse matrix, which can be used to solve the equation (D-4), is given by

$$A^{-1} = \begin{bmatrix} \frac{z^2 + Kz + \gamma_m}{\text{DET}(z)}, \frac{\gamma_m}{\text{DET}(z)} \\ \frac{\gamma_m}{\text{DET}(z)}, \frac{z^2 + 3Kz + 2K^2 \gamma_m}{\text{DET}(z)} \end{bmatrix}. \quad (D-7)$$

The zeroes of $\text{Det}(z)$ determine whether the solution pair $N(m, t)$ and $p(m, t)$ for a given value of m oscillate with a natural frequency that does not depend on the right side of equation (D-4). If the zeroes are both real, those quantities do not have a natural oscillation frequency; if the zeroes are complex (in which case they occur in conjugate pairs) they have a natural oscillation frequency ω given, except for sign which is conventionally positive, by the imaginary part of either zero.

The zeroes are given by

$$z = -K \pm \sqrt{K^2 - 2\gamma} = -K \pm \sqrt{K^2 - \frac{8g(m)}{N}}. \quad (D-8)$$

The condition for a natural oscillation frequency corresponding to a given m is therefore

$$K < 2 \sqrt{\frac{2g(m)}{N}} . \quad (D-9)$$

The definition of the $g(m)$, along with (D-8), together imply that ringing occurs in the system if and only if

$$K < 2\sqrt{2} .$$

This is a more precise condition for the existence of a non-Markovian stimulation effect than the Ref. D.3 condition, which in terms of the present notation would be $K \sim 1$.

If oscillation at a natural frequency ω occurs for some value m' of m , then, since the corresponding $N(m'-1, t)$ and $p(m', t)$ will contribute to the source in the equations for $N(m'-2, t)$ and $p(m'-1, t)$, those quantities will also oscillate with a component having the frequency ω . Thus, if there is a natural frequency again equal to ω for some $m < m'$, the corresponding $N(m-1, t)$, $p(m, t)$ will exhibit resonant vibrations.

It is evident from (D-8) that this can occur if and only if

$$g(m') = g(m) .$$

Since

$$g\left(\frac{N}{2} - \mu\right) = (\mu + 1)(N - \mu) ,$$

$$g\left(\frac{N}{2} - \mu\right) = g\left(\frac{N}{2} - \nu\right)$$

if and only if

$$N = \mu + \nu + 1 .$$

It follows that for any $N > 1$ and any ν such that $0 < \nu < N - 1$,

$$g\left(\frac{N}{2} - \nu\right) = g\left(\nu + 1 - \frac{N}{2}\right) . \quad (D-10)$$

It follows from equation (D-10) that, if a natural frequency occurs for some value of m given by $N/2 - \nu$ or $\nu + 1 - N/2$, resonance must occur for some lower value unless

$$\frac{N}{2} - \nu = \nu + 1 - \frac{N}{2} . \quad (D-11)$$

The condition (D-11) is equivalent to

$$N = 2v + 1, \quad (D-12)$$

so that to avoid resonance and still have oscillation, N must be odd.

Also, on comparing equation (D-10) with (D-12), it is found that this can only occur when $m = 1/2$, for which value

$$g(m) = g\left(\frac{1}{2}\right) = \left(\frac{N+1}{2}\right)^2.$$

Then, the natural frequency oscillation condition equation (D-9) becomes

$$K < (N+1) \sqrt{\frac{2}{N}} \sim \sqrt{2N}. \quad (D-13)$$

To avoid resonance due to the natural frequency for a larger value of m , the condition

$$K > 2 \sqrt{\frac{g\left(\frac{3}{2}\right)}{N}} = 2 \sqrt{\frac{(N+3)(N-1)}{2N}}. \quad (D-14)$$

In summary, the only case in which there is some oscillation of the system but no resonance occurs is when

$$\sqrt{\frac{2(N+3)(N-1)}{N}} < K < (N+1) \sqrt{\frac{2}{N}}. \quad (D-15)$$

The case of $N = 2$ provides an example for which the explicit analytical results are reasonably simple. On applying the matrix inverse equation (A-7) to equation (A-4) and inverting the Laplace transforms obtained thereby, the following solutions are obtained:

$$N(1,t) = 0, \quad p(1,t) = \frac{4}{8-K^2} e^{-Kt} \left[1 - \cos \left(\sqrt{8-K^2} t + \phi \right) \right],$$

where

$$\sin \phi = \frac{K \sqrt{8-K^2}}{4}, \quad \cos \phi = \frac{K^2-4}{4};$$

$$N(0,t) = \frac{4}{8-K^2} e^{-Kt} \left[1 - \cos \sqrt{8-K^2} t \right];$$

$$N(-1,t) = \frac{32}{(8-K^2)^2} e^{-Kt} \left[1 - \cos \sqrt{8-K^2} t - \sqrt{\frac{8-K^2}{2}} t \sin \sqrt{8-K^2} t \right];$$

$$p(0,t) = \frac{K^2}{8} N(-1,t) + \frac{4}{(8-K^2)^2} e^{-kt} \left[\sqrt{\frac{8-K^2}{2}} \sin \sqrt{8-K^2} t - \left(\frac{8-K^2}{2} \right) t \cos \sqrt{8-K^2} t + \frac{(8-K^2)^{3/2}}{2} t \sin \sqrt{8-K^2} t \right] ;$$

$$p(-1,t) = 1 - p(0,t) - p(1,t) . \quad (D-16)$$

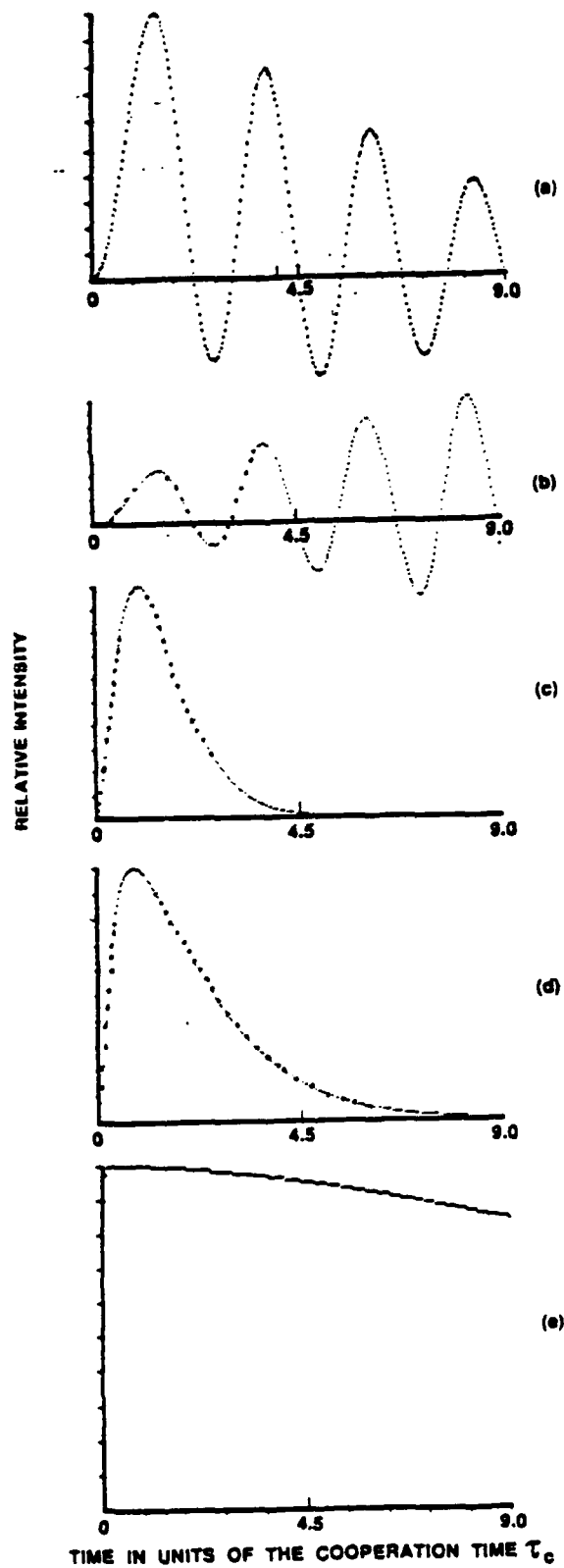
The last equation comes from the conservation of probability

$$\sum_m p(m,t) = 1 ,$$

which follows identically from the equation (D-1) and the assumed initial conditions.

Figures D-1(a) through (e) give some calculated results from equation (D-16). These results compare well with the calculations obtained using Code SR 2 for the same input parameters.*

* Ringing will occur because of at least one value of m , namely $m = 0$, when K is of the order of \sqrt{N} or less. To get ringing for all m values $K < 2\sqrt{2}$ is the necessary condition.



2-2-67-4

Figure D-1. Superradiant pulses for $M = 2$ calculated from equation (D-16).

REFERENCES, APPENDIX D

- D.1 M.S. Feld, "Superradiance and Laser-Controlled Gamma Emission," in *Proceedings of the IST/IDA Gamma-ray Laser Workshop*, Bohdan Balko, Leslie Cohen, and Francis X. Hartmann, editors. IDA Memorandum Report M-162, January 1986.
- D.2 G.T. Trammell and J.P. Hannon, *Opt. Commun.*, 15, 3, 325-329, 1975.
- D.3 R. Bonifacio and L.A. Lugiato, "Cooperative Radiation Processes in Two-Level Systems: Superfluorescence II," *Phys. Rev. V*, 12, 2, 587-598, August 1975.

APPENDIX E

THE CODE SR1.FOR

APPENDIX E

THE CODE SR1.FOR

The diffusion equation derived by Narducci et al. (Ref. E.1) for the atomic density operator is a differential equation for the so-called quasi-probability function that determines the density operator. The atomic density operator determines the time evolution of any statistical property of the ensemble of two-level atoms satisfying the conditions of superradiance as specified by Bonifacio and Lugiato (Refs. E.2 and E.3).

Specifically, this includes the expectation value of any operator that has a known representation in terms of the fundamental basis vectors used by the authors, namely, the Bloch states defined by Arrechi and Courtens and by Radcliffe (Refs. E.4 and E.5). It is also a straightforward matter to express the results in terms of the Dicke states.

Because the underlying model assumes that the atomic system emits photons "adiabatically", Bonifacio and Lugiato were able to derive a relation between the expectation of the electromagnetic photon number operator and the expectation of the atomic polarization operators. Thus, the atomic density operator will also give the time-dependent spontaneous radiation statistics of the atomic system.

The quantity of interest is a function $Q(\theta, t)$, which satisfies the differential equation

$$\begin{aligned} \frac{\partial}{\partial t} Q(\theta, t) = & - \frac{\partial}{\partial \theta} \left[\left(-r \sin \theta - \frac{\sin \theta}{2(1 + \cos \theta)} Q(\theta, t) \right) \right] \\ & + \frac{\partial^2}{\partial \theta^2} \left(\frac{1 - \cos \theta}{2} Q(\theta, t) \right). \end{aligned} \quad (E-1)$$

The density operator $W_A(t)$ is defined by

$$W_A(t) = \int_0^\pi d\theta Q(\theta, t) \Lambda(\theta), \quad (E-2)$$

where

$$\Lambda(\theta) = \sum_{m=0}^{2r} \binom{2r}{m} \left(\cos \frac{1}{2} \theta \right)^{2(2r-m)} \left(\sin \frac{1}{2} \theta \right)^{2m} |r, m\rangle \langle r, m|. \quad (E-3)$$

The vectors $|r, m\rangle$ are Dicke states with quantum numbers r, m representing the cooperation number and the internal energy of the atoms. The sum in the expression for Λ is finite for any given value of r ; therefore, the representation in terms of Dicke states is not significantly more complicated numerically than the original representation in terms of Bloch states.

We want to find an expression for

$$\text{tr} [R^+ R^- W_A(t)], \quad (E-4)$$

where the raising and lowering operators R^+ and R^- satisfy

$$R^+ |r, p\rangle = [(2r-p)(p+1)]^{1/2} |r, p+1\rangle \quad \text{and}$$

$$R^- |r, p\rangle = [(2r-p+1)p]^{1/2} |r, p-1\rangle \quad p = 0, 1, \dots, 2r.$$

Since

$$\text{tr} (|r, p\rangle \langle r, p|) = 1$$

and

$$R^+ R^- |r, p\rangle = (2r-p+1)p |r, p\rangle, \quad r = 0, 1, \dots, 2r,$$

it follows that

$$[\text{tr} R^+ R^- \Lambda(\theta)] = \sum_{p=0}^{2r} \binom{2r}{p} \{ [\cos^2(\theta/2)]^{2r-p} \} [(\sin^2(\theta/2))^p] (2r-p+1)p.$$

From formulas for the mean and variance, respectively of the binomial distribution one has that

$$\sum_{p=0}^{2r} \binom{2r}{p} (1-x)^{2r-p} x^p p = 2rx$$

and

$$\sum_{p=0}^{2r} \binom{2r}{p} (1-x)^{2r-p} x^p (2r-p)p = 2r(2r-1)x(1-x) .$$

Setting $x = \sin^2(\theta/2)$ and consequently $1-x = \cos^2(\theta/2)$ one has that

$$\text{tr} [R^+ R^- \Lambda(\theta)] = 2r(2r-1) \sin^2(\theta/2) [1 - \sin^2(\theta/2)] + 2r \sin^2(\theta/2)$$

using the fact that $(2r-p+1)p = (2r-p)p + p$.

This gives

$$\begin{aligned} \text{tr} [R^+ R^- W_A(t)] &= 2r(2r-1) \int_0^\pi d\theta Q(\theta, t) \sin^2(\theta/2) \cos^2(\theta/2) \\ &+ 2r \int_0^\pi d\theta Q(\theta, t) \sin^2(\theta/2) , \end{aligned}$$

with the definition $Q(\theta, t) = (\sin\theta) p(\theta, t)$. Using $2 \sin(\theta/2) \cos(\theta/2) = \sin\theta$,

$$\begin{aligned} \text{tr} [R^+ R^- W_A(t)] &= r(r-1/2) \int_0^\pi d\theta Q(\theta, t) \sin^2 \theta \\ &+ 2r \int_0^\pi d\theta Q(\theta, t) \sin^2(\theta/2) . \end{aligned} \quad (E-5)$$

This last expression is coded in SA1.FOR, which produces numerically the time evolution of $Q(\theta, t)$ for $0 \leq \theta \leq \pi$ and $t \geq 0$.

Narducci et al. (Ref. E.1) have given the general solution of the diffusion equation for $Q(\theta, t)$ in terms of an arbitrary initial condition. They have also given a simplified approximation for the case in which the initial value implies zero probability within some neighborhood about the state of total population inversion initially. The point of total population inversion on the Bloch sphere is a singular point of $Q(\theta, t)$; thus, if the initial condition does not exclude that point, the form of $Q(\theta, t)$ is more complicated than it would otherwise be.

The initial condition on $Q(\theta, 0)$, $0 \leq \theta \leq 2\pi$ in our calculations is given by

$$Q(\theta, 0) = e^{-(\theta - \pi)^2 / \sigma^2}, \quad 0 \leq \theta \leq \pi$$

for various choices of the standard deviation σ . For a given positive integer n , the unit circle is broken into n pieces by means of the points $\theta_1, \dots, \theta_n$ with

$$\theta_j = \frac{\pi}{n} + \frac{2\pi(j-1)}{n}, \quad j = 1, \dots, n.$$

This avoids having the singular point $\theta = \pi$ as a member of the grid.

Differential equation (1) is replaced by a finite difference scheme. In the following, t_a represents an "old" time at which values of Q are presumed known; and t_b represents a "new" time at which values of Q are to be calculated:

$$\begin{aligned} & \frac{Q(\theta_j, t_b) - Q(\theta_j, t_a)}{t_b - t_a} \\ &= \left[\left(r \sin \theta_{j+1} + \frac{\sin \theta_{j+1}}{2(1 + \cos \theta_{j+1})} \right) \left(\frac{Q(\theta_{j+1}, t_b) + Q(\theta_{j+1}, t_a)}{2} \right) \right. \\ & \quad \left. - \left(r \sin \theta_j + \frac{\sin \theta_j}{2(1 + \cos \theta_j)} \right) \left(\frac{Q(\theta_j, t_b) + Q(\theta_j, t_a)}{2} \right) \right] \\ & \quad + \left[\frac{1 - \cos \theta_{j+1}}{2} \frac{Q(\theta_{j+1}, t_b) + Q(\theta_{j+1}, t_a)}{2} \right. \\ & \quad - 2 \frac{1 - \cos \theta_j}{2} \frac{Q(\theta_j, t_b) + Q(\theta_j, t_a)}{2} \\ & \quad \left. + \frac{1 - \cos \theta_{j-1}}{2} \frac{Q(\theta_{j-1}, t_b) + Q(\theta_{j-1}, t_a)}{2} \right], \quad j = 1, \dots, n. \end{aligned}$$

Considering $Q(\theta_j, t_a)$, $j = 1, \dots, n$ as known, values of $Q(\theta_j, t_b)$ are calculated.

This process is repeated for

$$(t_a, t_b) = [(\Delta T) * (k - 1), (\Delta T) * (k)] \quad , k = 1, \dots, m \quad ,$$

where $M * \Delta T$ is the final time.

This procedure is essentially a Crank-Nicholson scheme adapted to this singular partial differential equation.

PARTIAL PARAMETER LIST FOR SR1.FOR

N = number of pieces into which the interval $[0, 2]$ is broken. Values from 2000 to 20,000 are appropriate. Multiple runs with different values of N should be made as a check on accuracy.

D = time-step length

T = final time

R = population size

SIGMA = standard deviation for initial distribution

I' = number of time steps skipped before data is retained for graphing

Generally, the larger the sample size R is, the smaller T and D must be. Roughly, a doubling of R implies that T and D should be cut in half.

SR1 SUPERRADIANCE CODE 1

```

C PROGRAM SR1.FOR - 19 AUGUST 1986 - J. NEUBERGER
  DOUBLE PRECISION P0(40000),R0(40000),S0(40000),Z(40000)
  DOUBLE PRECISION P(40000), R(40000),S(40000),U(40000)
  DOUBLE PRECISION WT(40000),WA(1000),Y(40000),W(40000)
  DIMENSION ABC(1000),SHA(1000)
  DOUBLE PRECISION P1,SIGMA,D,T,R1,X1,D2,D1,Q,Q0,T1,X,XX,F
  COMMON P1,SIGMA
  OPEN(1,FILE='SR1.PLT',STATUS='NEW')
  OPEN(2,FILE='SR1.DAT',STATUS='NEW')
C 'N' MAY BE CHANGED TO 1000, 20000 OR 40000 AS A CHECK
C 'N' IS THE NUMBER OF PIECES INTO WHICH THE CIRCLE IS BROKEN
  N=5000
C THE FOLLOWING ARE TO BE INPUT EACH TIME THE CODE IS RUN:
C D=TIME STEP SIZE (.00000100 IS A TYPICAL SIZE FOR N = 20000.00)
C TF = FINAL TIME (TF = .000100 IS TYPICAL FOR N = 20000.00)
C I1=NO. TIME STEPS SKIPPED BEFORE DATA IS RECORDED (I1 = 1 IS TYPICAL)
C N = NUMBER OF ATOMS IN MODEL (FROM 1. TO 10.**6 OR MORE)
C SIGMA IS THE STANDARD DEVIATION IN THE INITIAL GAUSSIAN DISTRIBUTION
  WRITE(*,*) 'INPUT D,TF,I1,N,SIGMA'
  READ(*,*) D,T,I1,R1,SIGMA
  WRITE(2,80) D,T,I1,R1,SIGMA
80  FORMAT(1X,' D=',D10.3,' TF=',D10.3,' I1=',I3,' N= ',
        ,D10.3,' SIGMA=',D10.3)
C TO COMPARE WITH OTHER CODES IN THE SERIES, 'K' AND 'T2-STAR' ARE
C HERE CONSIDERED INFINITE; TIME SCALE IS TC=(1/G0)*(V/N)**.5
  IS=ISK
  ISS=I1
  P1=3.1415926535900
  X1 = 2.00*P1
  M1=INT(T/D+.1)
  D2=D/2.00
  D1=2.00*P1/FLOAT(N)
  Q=D2/D1**2
  Q0=D2/(2.00*D1)
  NM1=N-1
  NM2=N-2
  DO 120 I=1,N
    T1=D1*FLOAT(I)-D1/2.00
    WT(I) = R1*((R1-.500)*DSIN(T1)**2 + 2.00*DSIN(T1/2.00)**2)
    S0(I)=Q*(1.00-DCOS(T1+D1))/2.00
      +Q0*DSIN(T1+D1)*(R1+.500/(1.00+DCOS(T1+D1)))
    R0(I)=-Q*(1.00-DCOS(T1))
120  P0(I)=Q*(1.00-DCOS(T1-D1))/2.00
      -Q0*DSIN(T1-D1)*(R1+.500/(1.00+DCOS(T1-D1)))
    DO 130 I=1,N
      S(I)=-S0(I)
      R(I)=1.00-R0(I)

```

```

130      P(I)=-P0(I)
        DO 140 I=1,N
          U(I)=0.D0
140      W(I)=0.D0
          U(1)=P(1)
          U(N-1)=S(N-1)
          U(N)=R(N)
          W(1)=S(N)
          W(N-1)=P(N)
          DO 210 I=2,NM2
            R(I)=R(I)-S(I-1)*P(I)/R(I-1)
            U(I)=U(I)-U(I-1)*P(I)/R(I-1)
            W(I)=W(I)-S(I-1)*W(I-1)/R(I-1)
210      U(N)=U(N)-U(I-1)*W(I-1)/R(I-1)
          U(N)=U(N)-W(N-1)*U(N-1)/R(N-1)
          DO 230 I=1,N
230      Z(I)=F(D1*FLOAT(I)-D1/2.D0)
          DO 1000 M=1,M1
            IF((M-1)/I1)*I1.LT.M-1) GOTO 330
            M9 = M/I1
            X=0.D0
            XX=0.D0
            DO 312 I=1,N
              IF (ABS(Z(I)).LT.0.1D-10) Z(I) = 0.D0
C          XX=XX+Z(I)
C          WRITE(6,*) I,Z(I),WT(I)
312      X=X+Z(I)*WT(I)
          WA(M9)=X*P1/FLOAT(N)
C          XX=XX/FLOAT(N)
C          WRITE(6,55) M9,XX,WA(M9)
55      FORMAT(1X,I4,2D16.6)
C          WRITE(6,*) (Z(I), I=1,N)
330      CONTINUE
          IF(M.EQ.M1) GOTO 1000
          Y(1)=Z(1)+S0(1)*Z(2)+R0(1)*Z(1)+P0(1)*Z(N)
          DO 350 I=2,NM1
350      Y(I)=Z(I)+S0(I)*Z(I+1)+R0(I)*Z(I)+P0(I)*Z(I-1)
          Y(N)=Z(N)+S0(N)*Z(1)+R0(N)*Z(N)+P0(N)*Z(N-1)
          DO 400 I=2,NM1
            Y(I)=Y(I)-Y(I-1)*P(I)/R(I-1)
400      Y(N)=Y(N)-Y(I-1)*W(I-1)/R(I-1)
          Y(N)=Y(N)-W(N-1)*Y(N-1)/R(N-1)
          Z(N)=Y(N)/U(N)
          Z(N-1)=(Y(N-1)-U(N-1)*Z(N))/R(N-1)
          DO 450 I=2,NM1
450      Z(N-I)=(Y(N-I)-S(N-I)*Z(N-I+1)-U(N-I)*Z(N))/R(N-I)
1000     CONTINUE
          M8 = M1/I1

```

```

DO 15 K=1,M8
ABC(K) = D*K*I1
15  SWA(K) = WA(K)
WRITE(1,14) M8
14  FORMAT(I5)
WRITE(1,12) (ABC(M),SWA(M), M=1,M8)
12  FORMAT(2E15.6)
STOP
END
FUNCTION F(X)
COMMON P1,SIGMA
DOUBLE PRECISION A,SIGMA,P1,X,F
A = 3.5D0*SIGMA
IF (P1-<.LT.X.AND.X.LT.P1+A) THEN
    F = DEXP(-(X-P1)**2/SIGMA**2)
ELSE
    F = 0.D0
ENDIF
RETURN
END

```

REFERENCES, APPENDIX E

- E.1 L.M. Narducci et al., *Phys. Rev. A*, 9, 2, February 1974.
- E.2 R.Bonifacio and L.A. Lugiato, *Phys. Rev. A*, 11, 5, 1507-1521, May 1975.
- E.3 R.Bonifacio and L.A. Lugiato, *Phys. Rev. A*, 12, 2, 587-598, August 1975.
- E.4 F.T. Arecchi and E. Courtens, *Phys. Rev. A*, 2, 1730, 1970.
- E.5 J.M. Radcliffe, *J. Phys. A*, 4, 1971.

APPENDIX F

THE CODE SR2.FOR

APPENDIX F

THE CODE SR2.FOR

This code deals with pair of integro-differential equations of Bonifacio and Lugiato (Ref. F.1):

$$\begin{aligned}
 \dot{p}(m,t) = & - \frac{2g_0^2}{v} \int_0^t ds e^{-K(t-s) - (t+s)/2T_2^*} \\
 & \{ g(m) p(m,s) - g(m+1) p(m+1,s) + [g(m) + g(m+1)] N(m,s) \\
 & - g(m+1) N(m+1,s) - g(m) N(m-1,s) \}, \\
 \dot{N}(m,t) = & -2K N(m,t) + \frac{2g_0^2}{v} \int_0^t ds e^{-K(t-s) - (t+s)/2T_2^*} \\
 & \{ g(m+1) [p(m+1,s) + N(m+1,s) - N(m,s)] \}.
 \end{aligned} \tag{F-1}$$

These equations are converted into a system of $4(2r + 1)$ equations by introducing two families of unknowns:

$$\begin{aligned}
 U(m, t) &= P(m, t) e^{Kt + t/(2T_2^*)} \\
 V(m, t) &= (\dot{N}(m, t) + 2K N(m, t)) e^{Kt + t/(2T_2^*)}, \\
 m &= 1, \dots, 2r + 1.
 \end{aligned} \tag{F-2}$$

The result is the system

$$\begin{aligned}
 \dot{P}(m, t) &= U(m, t) e^{-[Kt + t/(2T_2^*)]} \\
 \dot{Q}(m, t) &= -2K Q(m, t) - V(m, t) e^{-[Kt + t/(2T_2^*)]} \\
 \dot{U}(m, t) &= -e^{Kt} e^{-t/(2T_2^*)} [g(m) P(m, t) - g(m+1) P(m+1, t)] \\
 &\quad - g(m+1) Q(m+1, t) + [g(m+1) + g(m)] Q(m, t) \\
 &\quad - g(m) Q(m-1, t) \\
 \dot{V}(m, t) &= e^{-Kt} e^{-t/(2T_2^*)} g(m+1) \\
 &\quad [P(m+1, t) + Q(m+1, t) - Q(m, t)], \\
 m &= 1, \dots, 2r+1.
 \end{aligned} \tag{F-3}$$

This system is written compactly as

$$\dot{Y}(t) = A(t) Y(t), t \geq 0$$

where

$$Y(t) = \begin{pmatrix} P(1, t) \\ \vdots \\ P(2r+1, t) \\ N(1, t) \\ \vdots \\ N(2r+1, t) \\ U(1, t) \\ \vdots \\ U(2r+1, t) \\ V(1, t) \\ \vdots \\ V(2r+1, t) \end{pmatrix} \tag{F-4}$$

and $A(t)$ is the appropriate matrix to make equation (F-4) equivalent to equation (F-3).

A Runge-Kutta scheme is used for the calculation

$$Y(t_b) = Y(t_a) + \frac{\delta}{2} \left\{ A(t_a) Y(t_a) + A(t_b) [Y(t_a) + \delta A(t_a) Y(t_a)] \right\}, \quad (F-5)$$

where $Y(t_a)$, is the value of Y at an "old" time t_a and $Y(t_b)$ is the value of Y at the corresponding "new" time t_b .

Three different sets of initial values could be introduced into the calculation.

$$(1) P(m) = (1 - P_c)^{N-m+1} P_c^{m-1} \binom{N}{m-1}$$

$$Q(m) = e^{-\gamma} \gamma^{m-1} / (m-1)!$$

$$U(m) = 0$$

$$V(m) = 0 \quad m = 1, 2, \dots, N$$

$$(2) P(m) = g_o^2 / [g_o^2 + (m - m_o)^2]$$

$$Q(m) = 0 \quad m = 1, 2, \dots, N \text{ for same } m_o$$

$$U(m) = 0$$

$$V(m) = 0$$

$$(3) P(m) = 0 \quad \text{For } m = 1, \dots, 2r+1 \text{ except } P(m_1) = 1 \text{ for some } M_1$$

$$N(m) = 0$$

$$U(m) = 0 \quad m = 1, \dots, 2r+1$$

$$V(m) = 0$$

An annotated listing of SR2.FOR is given, together with some graphic output. What is plotted is $\sum_m Q(m,t)$ as a function of t . Repeated runs were made for various values of h (time-step size): $h = 10^{-17}$, 10^{-16} , 2×10^{-16} , 10^{-15} . Results for these runs show excellent agreement in that output is insensitive to the size of H in this range.

It should be noticed that although the main qualitative features of $\sum_m Q(m,t)$ are reasonable, the value of $\sum_m Q(m,t)$ turns slightly negative for certain values of t . This is physically wrong and is due to a truncation in Bonifacio's model. A closed form analytical solution was obtained for the case $N = 2$ and is described in Appendix D.

PARTIAL LIST OF PARAMETERS FOR SR2.FOR

N = sample size

XK1 = constant K

XK2 = $1/2T_2^*$

H = time step size

GOP = g_0

PC = (p), probability initial binomial distribution

GM = mean of corresponding Poisson distribution

IS = number of time steps computed before data is retained for purpose of graphing

V = physical volume

Generally, $\frac{(TF)}{(H) (IS)}$ should be in the range 200 to 500 for purposes of graphing. Data set

"1" contains data for graphing purposes.

SR2 SUPERRADIANCE CODE 2

```

C PROGRAM SR2.FJR - 19 AUGUST 1986 - J. NEUBERGER
  DOUBLE PRECISION P(201),Q(201),R(201),S(201),G(201)
  DOUBLE PRECISION PD(201),QD(201),RD(201),SD(201)
  DOUBLE PRECISION XK1,XK2,TF,T0,GOP,V,H,T,TPH,X,Y,PC,GM
  DOUBLE PRECISION P1(201),Q1(201),R1(201),S1(201)
  DOUBLE PRECISION P2(201),Q2(201),R2(201),S2(201)
  DOUBLE PRECISION X1,X2,X3,X4,X5,X6
  DIMENSION ABC(1000),SWA(1000)
  COMMON N,XK1,XK2,G
  OPEN(1,FILE='SR2.PLT',STATUS='NEW')
  OPEN(2,FILE='SR2.DAT',STATUS='NEW')
  OPEN(3,FILE='SR2A.DAT',STATUS='NEW')
  OPEN(4,FILE='SR2B.DAT',STATUS='NEW')
  WRITE(6,*) 'INPUT TF,H,IS,N,XK1,XK2,M1
C TF = FINAL TIME (TYPICAL VALUE 3.00)
C H = LENGTH OF TIME STEP (TYPICAL VALUE 2.0-4)
C IS = NO. OF TIME STEPS SKIPPED (TYPICAL VALUE 50)
C N = NUMBER OF ATOMS (TYPICAL VALUE 100 - IF>200, INCREASE DIM)
C XK1 = 'K' (TYPICAL VALUE 1.500)
C XK2 = 1/T2-STAR (TYPICAL VALUE 1.0-18)
C M1 = EXCEPTIONAL POINT FOR DELTA DISTRIBUTION
  READ(5,*) TF,H,IS,N,XK1,XK2,M1
  WRITE(2,80) TF,H,IS,N,XK1,XK2,M1
80  FORMAT(1X,'TF=',D10.3,' H=',D10.3,' IS=',I3,
  .    ' N=',I4,' XK1=',D10.3,' XK2=',D10.3,' M1=',I3)
C    GOP = 1.1700
C ABOVE IS A SAMPLE VALUE FOR GOP
C    V = 4.40-24
C ABOVE IS A SAMPLE VALUE FOR THE VOLUME V
  T0 = 0.00
C PC = PROBABILITY OF POISSON DISTRIBUTION
  PC = .10-4
C GM = CONSTANT 'GAMMA'
  GM = -DBLE(N)*DLOG(PC)
  NP1 = N+1
C MC = TOTAL NUMBER OF TIME STEPS
  MC = INT(SNGL(TF/H) + .1)
C M8 = NUMBER OF DATA POINTS
  M8 = MC/IS
  WRITE(1,94) M8
94  FORMAT(I5)
C INTRODUCTION OF G-CONSTANTS
  DO 1 M=1,NP1
1    G(M) = DBLE((M-1)*(N-M+2))*4.00/DBLE(N)
C THE FOLLOWING INITIALIZES P,Q,R,S FOR A POISSON DISTRIBUTION

```

```

      P(1) = (1.-PC)**N
      Q(1) = 0.3-4
C      Q(1) = CEXP(-GM)
      R(1) = 0.30
      S(1) = 0.30
      DO 2 M=2,NP1
      P(M) = P(M-1)*DBLE(N-M+2)*PC/(DBLE(M-1)*(1.-PC))
      Q(M) = 0.3-4
C      Q(M) = Q(M-1)*GM/DBLE(M-1)
      R(M) = 0.30
      S(M) = 0.30
2
C  END OF POISSON DISTRIBUTION INITIALIZATION
C  THE FOLLOWING INITIALIZES P,Q,R,S FOR A LORENZIAN DISTRIBUTION
C      G0 = G0/2.00
C      M0 = 1
C      DO 2 M=1,NP1
C      P(M) = G0**2/(G0**2+(FLOAT(M) - FLOAT(M0))**2)
C      Q(M) = 0.30
C      R(M) = 0.30
C2     S(M) = 0.30
C  END OF LORENZIAN DISTRIBUTION INITIALIZATION
C  THE FOLLOWING INITIALIZES P,Q,R,S FOR A DELTA DISTRIBUTION
C      DO 2 M=1,NP1
C      P(M) = 0.30
C      Q(M) = 0.30
C      R(M) = 0.30
C2     S(M) = 0.30
C      P(M1) = 1.00
C  END OF DELTA DISTRIBUTION INITIALIZATION
C  START OF MAIN LOOP
      DO 1000 J=1,MC
      T=DBLE(J-1)*H
      CALL AM(T,P,Q,R,S,PD,QD,RD,SD)
      TPH = T+H
      DO 3 M=1,NP1
      P1(M) = P(M) + H*PD(M)
      Q1(M) = Q(M) + H*QD(M)
      R1(M) = R(M) + H*RD(M)
3      S1(M) = S(M) + H*SD(M)
      CALL AM(TPH,P1,Q1,R1,S1,P2,Q2,R2,S2)
      DO 4 M=1,NP1
      P(M) = P(M) + (H/2.00)*(P2(M) + PD(M))
      Q(M) = Q(M) + (H/2.00)*(Q2(M) + QD(M))
      R(M) = R(M) + (H/2.00)*(R2(M) + RD(M))
4      S(M) = S(M) + (H/2.00)*(S2(M) + SD(M))
      IF((J/IS)*IS.EQ.J) THEN
      X1 = 0.00
      X2 = 0.00
      X3 = 0.00

```

```

X4 = 0.00
DO 5 M=1,N+1
X1 = X1 + DBLE(M)*P(M)
X2 = X2 + DBLE(M**2)*P(M)
X3 = X3 + DBLE(M)*Q(M)
X4 = X4 + Q(M)
5 CONTINUE
X5 = X1**2 - X2
X6 = X3 - X4*X1
WRITE(3,97) T+H,X1,X2,X5
WRITE(4,97) T+H,X3,X4,X6
97 FORMAT(1X,4D12.4)
TREAL = SNGL(T+H)
XREAL = SNGL(X4)
WRITE(1,95) TREAL,XREAL
95 FORMAT(2E15.6)
C WRITE(8,98) (P(M), M=1,NP1)
C WRITE(8,98) (Q(M), M=1,NP1)
C WRITE(8,98) (R(M), M=1,NP1)
C WRITE(8,98) (S(M), M=1,NP1)
ENDIF
C DO 11 M=1,NP1
C11 IF(P(M).LT.0.00) P(M)=0.00
C X=0.00
C DO 12 M=1,NP1
C12 X= X + P(M)
C DO 13 M = 1,NP1
C13 P(M) = P(M)/X
1000 CONTINUE
98 FORMAT(1X,10D13.4)
STOP
END
SUBROUTINE AM(T,P,Q,R,S,PD,QD,RD,SD)
DOUBLE PRECISION P(1),Q(1),R(1),S(1)
DOUBLE PRECISION G(1),PD(1),QD(1),RD(1),SD(1)
DOUBLE PRECISION T,C1,C2,XK1,XK2
COMMON N,XK1,XK2,G
C1 = DEXP(XK1*T)
C2 = DEXP(-XK2*T)
PD(1) = C2*R(1)/C1
QD(1) = -2.00*XK1*Q(1) + C2*S(1)/C1
RD(1)=-C1*C2*(G(1)*P(1)-G(2)*P(2)-G(2)*Q(2)+(G(2)+G(1))*Q(1))

SD(1) = C1*C2*G(2)*(P(2) + Q(2) - Q(1))
DO 1 M=2,N
PD(M) = C2*R(M)/C1
QD(M) = -2.00*XK1*Q(M) + C2*S(M)/C1
RD(M) = -C1*C2*(G(M)*P(M) - G(M+1)*P(M+1)
-G(M+1)*Q(M+1) + (G(M+1)+G(M))*Q(M) - G(M)*Q(M-1))

```

```

1      SD(M) = C1-C2*G(M+1)*(P(M+1) + Q(M+1) - Q(M))
      PD(N+1) = C2*R(N+1)/C1
      QD(N+1) = -2.D0*XK1*Q(N+1) + C2*S(N+1)/C1
      RD(N+1) = -C1*C2*(G(N+1)*P(N+1) + G(N+1)*Q(N+1) - G(N+1)*Q(N))
      SD(N+1) = J.D0
      RETURN
      END

```

REFERENCE, APPENDIX F

F.1 R. Bonifacio and L.A. Lugiato, *Phys. Rev. A*, *11*, 5, 1507-1521, May 1975.

APPENDIX G

CODES SR3.FOR AND SR4.FOR

APPENDIX G

CODES SR3.FOR AND SR4.FOR

Both codes SR3 and SR4 deal with the semiclassical calculation of the superradiant emission. The radiation intensity is obtained from Ref. G.1.

$$I(t) = \left(\frac{k\nu}{2g_0^2} \right) \dot{\phi}^2(t) e^{\nu T_2^*}. \quad (G-1)$$

Code SR3 calculates $\phi(t)$ from the damped pendulum equation

$$\frac{d^2\phi}{dt^2} + \left(k + \frac{1}{2T_2^*} \right) \frac{d\phi}{dt} - \frac{1}{\tau_c^2} e^{-\nu T_2^*} \sin \phi(t) = 0, \quad (G-2)$$
$$t \geq 0$$

which takes into account both cooperative emission and stimulated emission and thus produces ringing effects.

Code SR4 calculates $\phi(t)$ from the overdamped pendulum equation (12.2, Ref. G.2)

$$\frac{d\phi(t)}{dt} = \frac{1}{\tau_R} e^{-\nu T_2^*} \sin \phi(t) \quad (G-3)$$
$$t \geq 0$$

and calculates a pure superradiant emission.

Both codes incorporate the initial conditions

$$\phi(0) = \left(\frac{2}{N} \right)^{1/2}, \quad \frac{d\phi(0)}{dt} = 0 \quad (G-4)$$

to take into account the quantum noise polarization which initiates the pendulum motion.

A conventional second-order Runge-Kutta method was used in both codes. Annotated listings follow.

PARTIAL LIST OF PARAMETERS FOR SR3.FOR

TO = starting time

H = time-step length

TF = final time

F = population size

XK = constant 'K'

T2S = g_0

V = physical volume

IS = number of time-steps to be skipped before data is retained for graphing

Data set "1" contains data for graphing purposes

PARTIAL LIST OF PARAMETERS FOR SR4.FOR

T = final time

H = time-step length

R = sample size

Y = starting value [value of $\phi(0)$]

GO = g_0

V = physical volume

IS = number of time steps skipped before calculated data is printed out

SR3 SUPERRADIANCE CODE 3

```

C   PROGRAM SR3.FOR - 19 AUGUST 1986 - J. NEUBERGER
      DOUBLE PRECISION DM1,DM2,DN1,DN2,XM1,XN1,T,T0,R,H,TF,XM,XN
      DOUBLE PRECISION G0,V,T2S,XK1,TPH,XK2
      COMMON R,XK1,XK2,T2S,V,G0
      OPEN(1,FILE='SR3.PLT',STATUS='NEW')
      OPEN(2,FILE='SR3.DAT',STATUS='NEW')
C   H = LENGTH OF TIME INTERVAL (TYPICAL VALUE 1.0-15)
C   TF = FINAL TIME (TYPICAL VALUE 5.0-11)
C   IS = NO. TIME STEPS SKIPPED BEFORE OUTPUT (TYPICAL VALUE 100)
C   XK1 = CONSTANT 'K' (TYPICAL VALUE 1.5D11)
C   XK2 = 1/T2-STAR (TYPICAL VALUE 1.0-6)
C   N = NUMBER OF ATOMS (TYPICAL VALUE 100.00)
      WRITE(6,*) 'INPUT H,TF,IS,XK1,XK2,N'
      READ(5,*) H,TF,IS,XK1,XK2,R
      WRITE(2,80) H,TF,IS,XK1,XK2,R
80    FORMAT(1X,'H=',D10.3,' TF=',D10.3,' IS=',I3,
           ' XK1=',D10.3,' XK2=',D10.3,' N=',D10.3)
      T0 = 0.00
C   NEXT TWO LINES GIVE INITIAL VALUES OF DERIVATIVE AND UNKNOWN
      XN = 0.00
      XM = DSQRT(2.00/R)
C   CONSTANT
      G0 = 1.17D0/DSQRT(2.00)
      T2S = 1.00/XK2
C   V = VOLUME
      V = 4.4D-24
C   MC = TOTAL NUMBER OF TIME STEPS
      MC = INT(SNGL(TF/H) + .1)
C   M8 = NUMBER OF POINTS TO BE PLOTTED
      M8 = MC/IS
      WRITE(1,94) M8
94    FORMAT(I5)
C   START OF MAIN LOOP
      DO 1000 J=1,MC
        T=DBLE(J)*H
        CALL AM(T,XM,XN,DM1,DN1)
        XM1 = XM + H*DM1
        XN1 = XN + H*DN1
C       IF((J/IS)*IS.EQ.J) WRITE(6,97) T,XM1,XN1
        TPH = T + H
        CALL AM(TPH,XM1,XN1,DM2,DN2)
        XM = XM + (H/2.00)*(DM1 + DM2)
        XN = XN + (H/2.00)*(DN1 + DN2)
C       WRITE(6,*) XM,XN,DM1,DN1,DM2,DN2
        TREAL = SNGL(T)

```

```

C  REMOVE NEXT COMMENT IF OUTPUT PRINTOUT IS WANTED
C      IF((J/IS)*IS.EQ.J) WRITE(6,97) T,XM,XN
1000  CONTINUE
96    FORMAT(2E15.6)
97    FORMAT(1X,3D18.10)
      STOP
      END
      SUBROUTINE AM(T,XM,XN,DM,DN)
      DOUBLE PRECISION XM,XN,DM,DN,R,XK1,XK2,T2S,U,G0,T
      COMMON R,XK1,XK2,T2S,U,G0
      DM = XN
      DN = -(XK1 + 1.00/T2S)*XN + DEXP(-T/T2S)*DSIN(XM)
      RETURN
      END

```

SR4 SUPERRADIANCE CODE 4

```

C  PROGRAM SR4.FCR - 19 AUGUST 1986 - J. NEUBERGER
      DOUBLE PRECISION T,R,H,Y,G0,U,XK1,C,F,XK2
      COMMON C,XK2
      OPEN(1,FILE='SR4.PLT',STATUS='NEW')
      OPEN(2,FILE='SR4.DAT',STATUS='NEW')
C  T = FINAL TIME (TYPICAL VALUE 10.)
C  N = NUMBER OF ATOMS IS THE (TYPICAL VALUE 100.00)
C  H = LENGTH OF TIME STEP (TYPICAL VALUE 1.0-4)
C  IS = NO. TIME STEPS SKIPPED BEFORE OUTPUT (TYPICAL VALUE 500)
C  XK1 = CONSTANT 'K' (TYPICAL VALUE 10.)
C  XK2 = 1/T2-STAR (TYPICAL VALUE 5.0-7)
      WRITE(6,*) ' INPUT T,N,H,IS,XK1,XK2 '
      READ(5,*) T,R,H,IS,XK1,XK2
      WRITE(2,90) T,R,H,IS,XK1,XK2
80    FORMAT(1X,'T=',D10.3,' N=',D10.3,' H=',D10.3,
           ' IS=',I3,' XK1=',D10.3,' XK2=',D10.3)
C  Y = INITIAL VALUE OF SOLUTION - TIED TO 'N' BELOW
      Y = 1.00/DSQRT(R)
C  G0 = CONSTANT
      G0 = 1.1700/DSQRT(2.00)
      C = 1.00/XK1
C  MC = TOTAL NUMBER OF TIME STEPS
      MC = INT(T/H + .100) + 1
C  MB = NUMBER OF DATA POINTS SET TO PLOT ROUTINE
      MB = MC/IS
      WRITE(1,97) MB
97    FORMAT(I5)
      DO 1000 M=1,MC
      T = H*DBLE(M-1)
      Y = Y + .500*H*(F(Y,T) + F(Y + H*F(Y,T),T+H))
C  IF(((M-1)/IS)*IS.EQ.M-1) WRITE(6,99) T,Y
      TREAL = SNGL(T)
      YREAL = SNGL((R/4.00)*F(Y,T)**2*DEXP(T*XK2))
      IF(((M-1)/IS)*IS.EQ.M-1) WRITE(1,98) TREAL,YREAL
98    FORMAT(2E15.6)
1000  CONTINUE
99    FORMAT(1X,2D15.6)
      STOP
      END
      FUNCTION F(X,T)
      DOUBLE PRECISION X,C,F,T,XK2
      COMMON C,XK2
      F = C*DEXP(-T*XK2)*DSIN(X)
      RETURN
      END

```

REFERENCES, APPENDIX G

- G.1 R. Bonifacio and L.A. Lugiato, *Phys. Rev. A*, *11*, 5, 1507-1521, May 1975.
- G.2 R. Bonifacio and L.A. Lugiato, *Phys. Rev. A*, *12*, 2, 587-598, August 1975.

APPENDIX H

EQUIVALENCE OF THE SEMICLASSICAL AND THE DRESSED STATE APPROACHES TO THE TREATMENT AND INTERACTION OF ATOMIC AND NUCLEAR SYSTEMS

APPENDIX H

EQUIVALENCE OF THE SEMICLASSICAL AND THE DRESSED STATE APPROACHES TO THE TREATMENT AND INTERACTION OF ATOMIC AND NUCLEAR SYSTEMS

H.1 INTRODUCTION

In this appendix it is shown that for electromagnetic (EM) fields with a large number of photons, the treatment of the radiation either as a classical oscillating field or in the second quantized form ("dressed state") is completely equivalent. To simplify the algebra, we treat the interaction of EM radiation with a pure two-level system (TLS). We show that one obtains identical sets of dynamic equations in either of the two approaches. We shall use density matrix equations in both pictures. For concreteness and simplicity we shall consider the two-level system to be atomic and the interaction of the EM radiation with the electrons. The extension to the nuclear case is straightforward.

H.2 THE SEMICLASSICAL APPROACH

The electric field vector is written as

$$\vec{E}(t) = \vec{\epsilon} E_0 (e^{i\omega t} + e^{-i\omega t}) \quad , \quad (H-1)$$

where $\vec{\epsilon}$ denotes the polarization vector, E_0 the peak amplitude and ω the angular frequency (rad/s) of the radiation field. The interaction of an electron with this radiation field is represented by the Hamiltonian

$$V(t) = -\vec{\mu} \vec{E} = -\mu E_0 (e^{i\omega t} + e^{-i\omega t}) \quad (H-2)$$

in the electric dipole approximation (E1 transitions).

Let the two-level system be described by states $|1\rangle$ and $|2\rangle$ that have energies $\hbar\omega_1$ and $\hbar\omega_2$ and are connected by a dipole transition ($\mu_{12} = \mu_{21}$, and $\mu_{11} = \mu_{22} = 0$). If H_0 denotes the atomic Hamiltonian in the absence of the field, then we have

$$H_0 |1\rangle = \hbar \omega_1 |1\rangle$$

and

(H-3)

$$H_0 |2\rangle = \hbar \omega_2 |2\rangle$$

The density matrix operator ρ satisfies the differential equation

$$\frac{d\rho}{dt} = -\frac{i}{\hbar} [H_0 + V(t), \rho] \quad (H-4)$$

Taking matrix elements of equation H-4 between states $|1\rangle$ and $|2\rangle$ and, defining $\rho_{ij} = \langle i | \rho | j \rangle$, we obtain the following equation:

$$\frac{d\rho_{11}}{dt} = -\frac{i}{\hbar} V_{12} \rho_{21} + \frac{i}{\hbar} \rho_{12} V_{21} \quad (H-5a)$$

$$\frac{d\rho_{22}}{dt} = -\frac{i}{\hbar} V_{21} \rho_{12} + \frac{i}{\hbar} \rho_{21} V_{12} \quad (H-5b)$$

$$\frac{d\rho_{12}}{dt} = -i \omega_{12} \rho_{12} - \frac{i}{\hbar} (V_{12} \rho_{22} \rho_{11} V_{12}) \quad (H-5c)$$

$$\frac{d}{dt} \rho_{12} = -i \omega_{21} \rho_{21} - \frac{i}{\hbar} (V_{21} \rho_{11} \rho_{22} V_{21}) \quad (H-5d)$$

$$\omega_{12} = \omega_1 - \omega_2 = -\omega_{21} \quad (H-5e)$$

$$V_{12} = V_{21} = -\mu_{21} E_0 (e^{i\omega t} + e^{-i\omega t})$$

At this stage we make the rotating wave approximation (RWA). This amounts to pulling out the fast time variations in ρ_{ij} as shown below:

$$\rho_{11} \approx \sigma_{11}, \quad \rho_{22} \approx \sigma_{22}$$

$$\rho_{12} \approx e^{+i\omega t} \sigma_{12}(t) \quad \text{and} \quad \rho_{21} \approx e^{-i\omega t} \sigma_{12}(t) \quad (H-6)$$

This approximation is valid if

$$\omega + \omega_{21} \gg \omega - \omega_{21} \quad (\text{H-7})$$

$$(\text{or } \omega_2 \gg \omega_1) .$$

Substituting (H-6) into (H-5) we get

$$\begin{aligned} \frac{d\sigma_{11}}{dt} = & + \frac{i}{\hbar} \mu_{12} E_0 (e^{i\omega t} + e^{-i\omega t}) \sigma_{21} e^{-i\omega t} \\ & - \frac{i}{\hbar} \mu_{21} E_0 (e^{i\omega t} + e^{-i\omega t}) \sigma_{12} e^{+i\omega t} . \end{aligned} \quad (\text{H-8a})$$

$$\begin{aligned} \frac{d\sigma_{22}}{dt} = & + \frac{i}{\hbar} \mu_{21} E_0 (e^{i\omega t} + e^{-i\omega t}) \sigma_{12} e^{+i\omega t} \\ & - \frac{i}{\hbar} \mu_{12} E_0 (e^{i\omega t} + e^{-i\omega t}) \sigma_{21} e^{-i\omega t} . \end{aligned} \quad (\text{H-8b})$$

$$\begin{aligned} e^{+i\omega t} \left(\frac{d\sigma_{12}}{dt} + i\omega \sigma_{12} \right) = & -i\omega_{12} \sigma_{12} e^{+i\omega t} \\ & + \frac{i}{\hbar} \mu_{12} E_0 (e^{i\omega t} + e^{-i\omega t}) (\sigma_{22} - \sigma_{11}) . \end{aligned} \quad (\text{H-8c})$$

$$\begin{aligned} e^{-i\omega t} \left(\frac{d\sigma_{21}}{dt} - i\omega \sigma_{21} \right) = & -i\omega_{21} \sigma_{21} e^{-i\omega t} \\ & + \frac{i}{\hbar} \mu_{12} E_0 (e^{i\omega t} + e^{-i\omega t}) (\sigma_{11} - \sigma_{22}) . \end{aligned} \quad (\text{H-8d})$$

Finally, dropping antiresonant terms like $e^{\pm i2\omega t}$ in (H-8) we obtain the following semiclassical optical Bloch equations, where $\Omega = 2\mu_{12}E_0$ is defined as the Rabi frequency.

$$\frac{d\sigma_{11}}{dt} = \frac{1}{2} i \Omega \sigma_{21} - \frac{1}{2} i \Omega^* \sigma_{21} \quad (\text{H-9a})$$

$$\frac{d\sigma_{22}}{dt} = -\frac{1}{2} i \Omega \sigma_{21} - \frac{1}{2} i \Omega^* \sigma_{12} \quad (\text{H-9b})$$

$$\frac{d}{dt} \sigma_{12} - i \delta \sigma_{12} = \frac{1}{2} i \Omega (\sigma_{22} - \sigma_{11}) \quad (\text{H-9c})$$

$$\frac{d}{dt} \sigma_{21} + i \delta \sigma_{21} = -\frac{1}{2} i \Omega^* (\sigma_{22} - \sigma_{11}) \quad (\text{H-9d})$$

where

$$\delta = \omega_{21} - \omega \quad .$$

H.3 THE SECOND QUANTIZATION APPROACH "THE DRESSED-STATE METHOD"

Here the atom and the radiation field are treated together as a single system. The interaction between them is assumed to be absent for times $t \leq 0$. At time $t = 0$ an interaction is turned on. We would like to investigate the evolution of a two-level system for times $t > 0$.

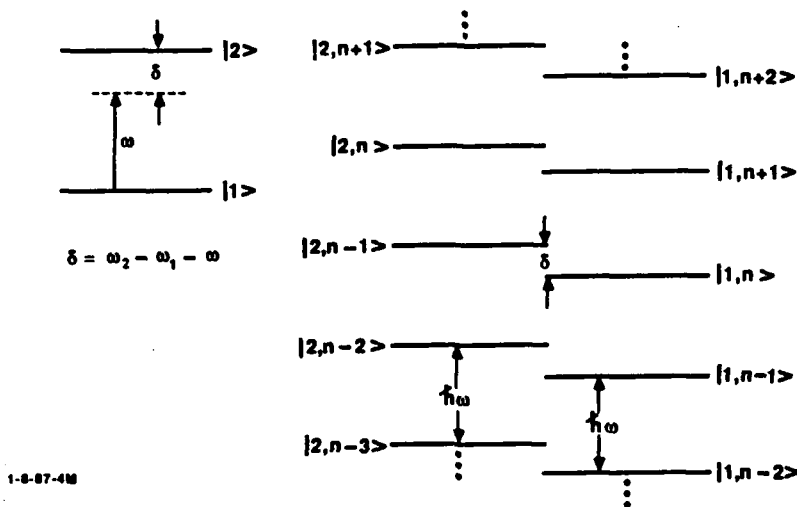
Let H_A and H_R denote the unperturbed atomic and the field Hamiltonians and V the interaction between them. Since atom + radiation is a closed system the total Hamiltonians

$$H = H_0 + V = H_A + H_R + V \quad (\text{H-10})$$

is time-independent. Let us assume a single mode field for simplicity. The eigenstates of H_0 are composite (dressed) states of atomic and field eigenstates. So, ignoring the $1/2 \hbar \omega$ term

$$H_0 |i, n\rangle = (H_A + H_R) |i, n\rangle = \hbar (\omega_i + n\omega) |i, n\rangle \quad (\text{H-11})$$

The manifold of dressed states formed by a two-level atom and the single-mode radiation field is shown below.



Note that on resonance, $\delta = 0$ and states $|1, n\rangle$ and $|2, n-1\rangle$ become degenerate. The interaction via the electric dipole transitions then splits these into two mixed states. In the electric dipole approximation, the interaction V can be written as

$$V = -\vec{\mu} \vec{E}$$

$$= -\mu \sqrt{\frac{\pi \hbar \omega}{V_n}} (a + a^\dagger) \quad \mu = \vec{\mu} \vec{E} \quad , \quad (\text{H-12})$$

where a and a^\dagger are, respectively, the annihilation and creation operators for the field mode and V_n is the normalization volume. Because of this interaction, the near-degenerate pairs $\{|1, n\rangle, |2, n-1\rangle\}$, $\{|1, n-1\rangle, |2, n-2\rangle\}$ become perturbed and evolve into two mixed states.

NOTE: $|1, n\rangle$ not only has allowed transitions to $|2, n-1\rangle$ but also to $|2, n+1\rangle$. However, as long as $|\omega_{12} + \omega| \ll \omega_{21} + \omega$ (Eq. H-7), such antiresonant transitions can be ignored.

The Hamiltonian matrix for the 2×2 pair is then written as follows:

$$H |1, n\rangle = \hbar(\omega_1 + n\omega) |1, n\rangle - \mu_{21} \sqrt{2\pi n \hbar \omega} |2, n-1\rangle \quad (\text{H-13a})$$

$$H |2, n-1\rangle = \hbar[\omega_2 + (n-1)\omega] |2, n-1\rangle - \mu_{21} \sqrt{2\pi n \hbar \omega} |1, n\rangle \quad . \quad (\text{H-13b})$$

Diagonalization of the above Hamiltonian gives rise to two mixed eigenstates $|\alpha_n\rangle$ and $|\beta_n\rangle$. These are expressed as

$$E_{\alpha} = \frac{1}{2} \left[\hbar\omega_1 + \hbar\omega_2 + (2n-1)\hbar\omega \right] + \frac{1}{2} \sqrt{\delta^2 + 4\mu_{21}^2 2\pi\hbar\omega}$$

$$= E_0 + \frac{1}{2} \Delta \quad (\text{H-14a})$$

$$E_{\beta} = \frac{1}{2} \left[\hbar\omega_1 + \hbar\omega_2 + (2n+1)\hbar\omega \right] - \frac{1}{2} \sqrt{\delta^2 + 4\mu_{21}^2 2\pi\hbar\omega}$$

$$= E_0 - \frac{1}{2} \Delta \quad (\text{H-14b})$$

$$|\alpha, n\rangle = \frac{-2\mu_{12}\sqrt{2\pi\hbar\omega}}{[(\delta + \Delta)^2 + 4\mu_{12}^2 2\pi\hbar\omega]^{\frac{1}{2}}} |1, n\rangle$$

$$+ \frac{\delta + \Delta}{[(\delta + \Delta)^2 + 4\mu_{12}^2 2\pi\hbar\omega]^{\frac{1}{2}}} |2, n-1\rangle \quad (\text{H-15a})$$

$$|\alpha, n\rangle \rightarrow |2, n-1\rangle \quad \text{as} \quad \mu_{12} \rightarrow 0$$

$$|\beta, n\rangle = \frac{\delta + \Delta}{[(\delta + \Delta)^2 + 4\mu_{12}^2 2\pi\hbar\omega]^{\frac{1}{2}}} |1, n\rangle$$

$$+ \frac{2\mu_{21}\sqrt{2\pi\hbar\omega}}{[(\delta + \Delta)^2 + 4\mu_{12}^2 2\pi\hbar\omega]^{\frac{1}{2}}} |2, n-1\rangle \quad (\text{H-15b})$$

Note that if $4\mu_{12}^2 2\pi\hbar\omega \ll \delta + \Delta$ then,

$$|\alpha, n\rangle \rightarrow |2, n-1\rangle, \quad E_{\alpha} \rightarrow E_0 + \frac{1}{2} \delta$$

and

$$|\beta, n\rangle \rightarrow |1, n\rangle, \quad E_\beta \rightarrow E_0 - \frac{1}{2} \delta. \quad (\text{H-15c})$$

Such diagonalizations have to be performed for each pair $[|1, n\rangle, |2, n-1\rangle]$. However, for $n \gg 1$ all of the dressed state pairs behave the same way.

The time evolution of the system is then described by

$$|\psi(t)\rangle = a_\alpha(0) e^{-i E_\alpha t/\hbar} |\alpha, n\rangle + a_\beta(0) e^{-i E_\beta t/\hbar} |\beta, n\rangle. \quad (\text{H-15d})$$

If one uses this solution to calculate the time evolution of the probability of the population in the upper state, one obtains exactly the same behavior as given by the solutions of (H-9). This is shown in the next section.

H.4 COMPARISON OF SEMICLASSICAL AND "DRESSED STATE" SOLUTIONS

The Rabi solution of equations (H-9a) through (H-9d) for a two-level system coupled to a monochromatic field will be obtained with the initial conditions

$$\begin{aligned} \sigma_{11}(t=0) &= 1 & \sigma_{22}(t=0) &= 0 \\ \sigma_{12}(t=0) &= \sigma_{21}(t=0) = 0. \end{aligned}$$

It can be shown that the four equations (H-9a) through (H-9d) are completely equivalent to the following two "amplitude" equations:

$$\frac{d}{dt} \begin{bmatrix} C_1 \\ C_2 \end{bmatrix} = iA \begin{bmatrix} C_1 \\ C_2 \end{bmatrix},$$

where

$$A = \begin{bmatrix} 0 & \frac{1}{2} \Omega \\ \frac{1}{2} \Omega^* & -\delta \end{bmatrix} \quad (\text{H-16})$$

and the eigenvalues of A are given by

$$\lambda_{\pm} = -\frac{\rho}{2} \pm \frac{1}{2} \sqrt{\rho^2 + |\Omega|^2}.$$

The density matrix elements are related to the complex amplitudes C_1 and C_2

$$\sigma_{11} = C_1^* C_1 \quad , \quad \sigma_{22} = C_2^* C_2$$

$$\sigma_{12} = C_1 C_2^* \quad , \quad \sigma_{21} = C_2 C_1^* \quad .$$

With the initial conditions

$$C_1(t=0) = 1 \quad C_2(t=0) = 0$$

the solution of equations H-16 is given by

$$\begin{bmatrix} C_1(t) \\ C_2(t) \end{bmatrix} = \frac{1}{\frac{1}{2} \Omega (\lambda_- - \lambda_+)} \begin{bmatrix} \frac{1}{2} \Omega & \frac{1}{2} \Omega \\ \lambda_+ & \lambda_- \end{bmatrix} \begin{pmatrix} e^{i\lambda_+ t} & 0 \\ 0 & e^{i\lambda_- t} \end{pmatrix} \begin{bmatrix} \lambda_- & \frac{1}{2} \Omega \\ -\lambda_+ & \frac{1}{2} \Omega \end{bmatrix} \begin{pmatrix} 1 \\ 0 \end{pmatrix} ,$$

or

$$C_1(t) = \frac{\lambda_- e^{i\lambda_+ t} - \lambda_+ e^{i\lambda_- t}}{\lambda_- - \lambda_+}$$

$$C_2(t) = \frac{\sqrt{-\lambda_+ \lambda_-}}{\lambda_- - \lambda_+} (e^{i\lambda_- t} - e^{i\lambda_+ t}) \quad ,$$

so that

$$\begin{aligned} \rho_{11}(t) &= |C_1(t)|^2 = \frac{\lambda_+^2 + \lambda_-^2}{(\lambda_+ - \lambda_-)^2} - \frac{2\lambda_- \lambda_+}{(\lambda_- - \lambda_+)^2} \cos [(\lambda_+ - \lambda_-)t] \\ \rho_{22}(t) &= |C_2(t)|^2 = \frac{\frac{1}{2} |\Omega|^2}{(\lambda_- - \lambda_+)^2} - \frac{\frac{1}{2} |\Omega|^2}{(\lambda_- - \lambda_+)^2} \cos [(\lambda_+ - \lambda_-)t] \quad . \end{aligned} \quad (H-17)$$

Note that $\rho_{11}(t) + \rho_{22}(t) = 1$ for all times.

In the dressed state picture, the states $|1, n\rangle$ and $|2, n-1\rangle$ mix to give rise to two "dressed" states $|\alpha_n\rangle$ and $|\beta_n\rangle$ whose energies and wave functions are given by equations (H-14) and (H-15), respectively.

In cgs units, the intensity is given by $I = (c/2\pi) |E_0|^2$ while in second quantization picture $I = n\hbar\omega$. These two equations together imply that $E_0 = \sqrt{2\pi n\hbar\omega}$ and, therefore $\hbar\Omega = 2\mu_{21}E_0 = 2\mu_{21}\sqrt{2\pi n\hbar\omega}$.

Using the definition $\delta_0 = \omega_2 - \omega_1 - \omega$, we get

$$E_\alpha = \hbar\omega_1 + n\hbar\omega + \frac{1}{2}\hbar\delta_0 + \frac{1}{2}\hbar\sqrt{\delta_0^2 + \Omega^2} \quad (\text{H-18a})$$

$$= \hbar(\omega_1 + n\omega) - \hbar\lambda_-$$

$$E_\beta = \hbar(\omega_1 + n\omega) - \hbar\lambda_+ \quad (\text{H-18b})$$

Using the definition of Ω , $\Delta = \hbar\Delta_0$ and λ_\pm the eigenstate equations H-15a and H-15b can be rewritten as

$$|\alpha, n\rangle = -\sqrt{\frac{-\lambda_+}{\lambda_- - \lambda_+}} |1, n\rangle - \sqrt{\frac{\lambda_-}{\lambda_- - \lambda_+}} |2, n-1\rangle \quad (\text{H-19a})$$

$$|\beta, n\rangle = -\sqrt{\frac{\lambda_-}{\lambda_- - \lambda_+}} |1, n\rangle + \sqrt{\frac{-\lambda_+}{\lambda_- - \lambda_+}} |2, n-1\rangle \quad (\text{H-19b})$$

The time-dependent solution to the problem is then given by

$$\psi(t) = a_\alpha(0) e^{-iE_\alpha t/\hbar} |\alpha, n\rangle + a_\beta(0) e^{-iE_\beta t/\hbar} |\beta, n\rangle, \quad (\text{H-20})$$

where $a_\alpha(0)$ and $a_\beta(0)$ are determined by initial conditions or equation (H-15d).

At time $t = 0$, before the interaction is turned on, $\psi(0) = |1, n\rangle$. This implies,

$$a_{\alpha}(0) = -\sqrt{\frac{-\lambda_+}{(\lambda_- - \lambda_+)}} , \quad a_{\beta}(0) = \sqrt{\frac{\lambda_-}{(\lambda_- - \lambda_+)}} . \quad (\text{H-21})$$

Then, using equations (H-17) through (H-21), $\psi(t)$ can be written as

$$\begin{aligned} \psi(t) = & -\sqrt{\frac{-\lambda_+}{(\lambda_- - \lambda_+)}} e^{-iE_{\alpha}t/\hbar} |\alpha, n\rangle - \sqrt{\frac{\lambda_-}{(\lambda_- - \lambda_+)}} e^{-iE_{\beta}t/\hbar} |\beta, n\rangle \\ & e^{i(\omega_1 + n\omega)t} \left[-\sqrt{\frac{-\lambda_+}{(\lambda_- - \lambda_+)}} e^{i\lambda_+t} \left\{ -\sqrt{\frac{-\lambda_+}{(\lambda_- - \lambda_+)}} |1, n\rangle - \sqrt{\frac{\lambda_-}{\lambda_- - \lambda_+}} |2, n-1\rangle \right\} \right. \\ & \left. - \sqrt{\frac{\lambda_-}{(\lambda_- - \lambda_+)}} e^{i\lambda_-t} \left\{ -\sqrt{\frac{\lambda_-}{(\lambda_- - \lambda_+)}} |1, n\rangle + \sqrt{\frac{-\lambda_+}{(\lambda_- - \lambda_+)}} |2, n-1\rangle \right\} \right] . \end{aligned}$$

Rearranging,

$$\begin{aligned} \psi(t) = e^{i(\omega_1 + n\omega)t} & \left\{ \frac{\lambda_- e^{i\lambda_+t} - \lambda_+ e^{i\lambda_-t}}{(\lambda_- - \lambda_+)} |1, n\rangle \right. \\ & \left. + \frac{\sqrt{-\lambda_- \lambda_+}}{(\lambda_- - \lambda_+)} (e^{i\lambda_-t} - e^{i\lambda_+t}) |2, n-1\rangle \right\} . \quad (\text{H-22}) \end{aligned}$$

The phase factor $e^{i(\omega_1 + n\omega)t}$ can be ignored as it makes no contribution to any observable quantities. We immediately see, by writing

$$\psi(t) = C_1(t) |1, n\rangle + C_2(t) |2, n-1\rangle \quad (\text{H-23})$$

that the coefficients $C_1(t)$ and $C_2(t)$ are exactly the ones calculated before. So the two methods give identical solutions.

APPENDIX I

ENHANCEMENT OF γ -EMISSION USING LONG- WAVELENGTH RADIATION

APPENDIX I

ENHANCEMENT OF γ -EMISSION USING LONG-WAVELENGTH RADIATION

Consider a three-state system as shown schematically in Fig. I-1 with a ground state $|b\rangle$, an isomeric state $|a\rangle$ and an upper level $|c\rangle$. Initially the system is in state $|a\rangle$, an isomeric level with a lifetime on the order of 10^7 s ($\gamma_a \approx 10^{-7}$ s) 10^4 eV above the ground state $|b\rangle$. The level $|c\rangle$ can be excited with a single photon or multiple photons. The energy separation between the isomeric level and the ground level is $E_{ab} = 10^4$ keV and between the upper level and the isomeric level is E_{ca} . The decay rates of the upper and isomeric levels are γ_c and γ_a , respectively, with $\gamma_c \gg \gamma_a$.

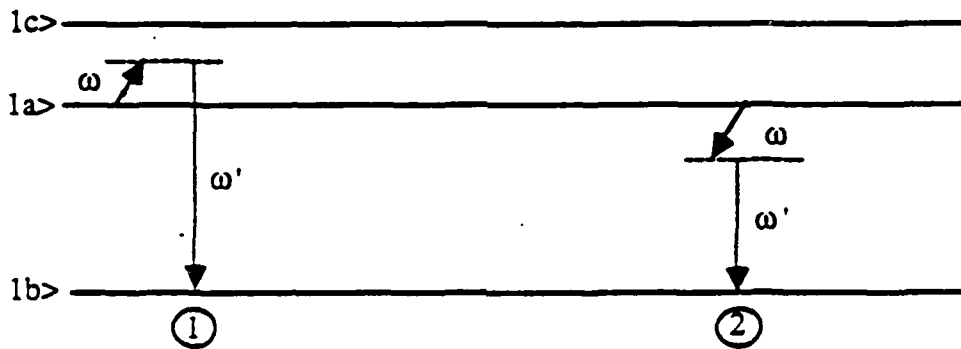


Figure I-1. Electromagnetic excitation of a three-level system showing photon absorption followed by emission (process 1) and emission followed by photon absorption (process 2)

We will assume that only the isomeric level is initially excited and calculate the probability as a function of the beam intensity I that a low-energy photon with energy $\hbar\omega > E_{ca}$ induces the transitions ($|a\rangle \rightarrow |c\rangle \rightarrow |b\rangle$), thus depopulating the isomeric level.

For convenience, we shall work within the second quantized formalism for treating the emission and absorption. The decay rates will be introduced phenomenologically. Both processes 1 and 2 depicted in Fig. I-1 will be considered. Process 2 is more prominent close to resonance.

The initial, final, and intermediate states for processes 1 and 2 are given by:

$$\begin{array}{ll}
 |a\rangle = |a; n, 0\rangle & \text{(initial state)} \\
 |b\rangle = |b; n-1, 1\rangle & \text{(final state)} \\
 |c_1\rangle = |c; n, 1\rangle & \left. \vphantom{\begin{array}{l} |c_1\rangle = |c; n, 1\rangle \\ |c_2\rangle = |c; n-1, 0\rangle \end{array}} \right\} \text{(intermediate states)} \\
 |c_2\rangle = |c; n-1, 0\rangle &
 \end{array}$$

where n is the number of photons in the beam and one photon is absorbed from the beam. The energies of these states divided by \hbar are:

$$\begin{aligned}
 \omega_a &= \omega_a' + n\omega \\
 \omega_b &= \omega_b' + (n-1)\omega + \omega' \\
 \omega_{c1} &= \omega_c' + n\omega + \omega' \\
 \omega_{c2} &= \omega_c' + (n-1)\omega
 \end{aligned} \tag{I-1}$$

with ω_a' , ω_b' , ω_c' the energies of the nuclear or atomic levels divided by \hbar , respectively, and $\hbar\omega$ and $\hbar\omega'$ the incoming and out-going photon energies, respectively.

The dynamics of the density matrix ρ is given by:

$$d\rho/dt = -i[H_0 + V, \rho] + \Gamma\rho, \tag{I-2}$$

where H_0 is the non-interactive part of the Hamiltonian, V is the interaction Hamiltonian and Γ is the decay matrix. In the above expression \hbar has been set equal to 1. We will focus on process 2 and assume the rotating wave approximation. The approximate error in this assumption

$$(\omega_c - \omega_a - \omega)/(\omega_c - \omega_a + \omega) \tag{I-2a}$$

is a function of the detuning.

The rate equations for the diagonal matrix elements from equation (I-2) are:

$$d/dt\rho_{aa} = -i V_{ac1} \rho_{cla} + i\rho_{ac1} V_{cla} - \gamma_a \rho_{aa} - i [V_{ac2} \rho_{c2a} - \rho_{ac2} V_{c2a}] \quad (I-3a)$$

$$d/dt\rho_{c1c1} = -i [V_{c1a} \rho_{ac1} - \rho_{c1a} V_{ac1}] - i [V_{c1b} \rho_{bc1} - \rho_{c1b} V_{bc1}] - \gamma_c \rho_{c1c1} \quad (I-3b)$$

$$d/dt\rho_{bb} = -i [V_{bc1} \rho_{c1b} - \rho_{bc1} V_{c1b}] - i [V_{bc2} \rho_{c2b} - \rho_{bc2} V_{c2b}] \quad (I-3c)$$

$$+ \gamma_a \rho_{aa} + \gamma_c (\rho_{c1c1} + \rho_{c2c2})$$

$$d/dt\rho_{c2c2} = -i [V_{c2a} \rho_{ac2} - \rho_{c2a} V_{ac2}] - i [V_{c2b} \rho_{bc2} - \rho_{c2b} V_{bc2}] - \gamma_c \rho_{c2c2} \quad (I-3d)$$

and for the off-diagonal matrix elements are:

$$d/dt\rho_{ac1} = - (1/2) (\gamma_a + \gamma_c) \rho_{ac1} - i\omega_{ac1} \rho_{ac1} - i (V_{ac1} \rho_{c1c1} + V_{ac2} \rho_{c2c1}) \quad (I-3e)$$

$$+ i (\rho_{aa} V_{ac1} + \rho_{ab} V_{bc1}) .$$

$$d/dt\rho_{ac2} = - (1/2) (\gamma_a + \gamma_c) \rho_{ac2} - i\omega_{ac2} \rho_{ac2} - i (V_{ac1} \rho_{c1c2} + V_{ac2} \rho_{c2c2}) \quad (I-3f)$$

$$+ i (\rho_{aa} V_{ac2} + \rho_{ab} V_{bc2})$$

$$d/dt\rho_{ab} = - (1/2) \gamma_a \rho_{ab} - i\omega_{ab} \rho_{ab} - i (V_{ac1} \rho_{c1b} + V_{ac2} \rho_{c2b}) \quad (I-3g)$$

$$+ i (\rho_{ac1} V_{c1b} + \rho_{ac2} V_{c2b})$$

$$d/dt\rho_{c1c2} = - \gamma_c \rho_{c1c2} - i\omega_{c1c2} \rho_{c1c2} - i (V_{c1a} \rho_{ac2} + V_{c1b} \rho_{bc2}) \quad (I-3h)$$

$$+ i (\rho_{c1a} V_{ac2} + \rho_{c1b} V_{bc2})$$

$$d/dt\rho_{c1b} = - (1/2) (\gamma_c) \rho_{c1b} - i\omega_{c1b} \rho_{c1b} - i (V_{c1a} \rho_{ab} + V_{c1b} \rho_{bb}) \quad (I-3i)$$

$$+ i (\rho_{c1c1} V_{c1b} + \rho_{c1c2} V_{c2b})$$

$$d/dt\rho_{c2b} = - (1/2) (\gamma_c) \rho_{c2b} - i\omega_{c2b} \rho_{c2b} - i (V_{c2a} \rho_{ab} + V_{c2b} \rho_{bb}) \quad (I-3j)$$

$$+ i (\rho_{c2c1} V_{c1b} + \rho_{c2c2} V_{c2b})$$

The solution of these 10 (complex) (or 16 real) equations will give ρ_{aa} , ρ_{bb} , ρ_{cc} for arbitrary intensities and detunings. This solution is equivalent to the dressed state result.

Near resonance, $\omega - \omega_c' - \omega_a'$ and the absorption + emission pathway is much stronger than the emission + emission pathway. Thus, matrix elements containing c_1 can

be neglected. The problem then reduces to a three-level system (a, c₂, b). Equations relevant to this case are:

$$d\rho_{aa}/dt = -\gamma_a \rho_{aa} - i [V_{ac2} \rho_{c2a} - \rho_{ac2} V_{c2a}], \quad (I-4a)$$

$$d\rho_{bb}/dt = \gamma_a \rho_{aa} + \gamma_c \rho_{c2c2} - i [V_{bc2} \rho_{c2b} - \rho_{bc2} V_{c2b}], \quad (I-4b)$$

$$d\rho_{c2c2}/dt = -\gamma_c \rho_{c2c2} - i [V_{c2a} \rho_{ac2} - \rho_{c2a} V_{ac2}] \\ - i [V_{c2b} \rho_{bc2} - \rho_{c2b} V_{bc2}], \quad (I-4c)$$

$$d\rho_{ac2}/dt = [-1/2 (\gamma_a + \gamma_c) - i\omega_{ac2}] \rho_{ac2} - i V_{ac2} (\rho_{c2c2} - \rho_{aa}) + i \rho_{ab} V_{bc2}, \quad (I-4d)$$

$$d\rho_{ab}/dt = [-1/2 \gamma_a - i\omega_{ab}] \rho_{ab} - i V_{ac2} \rho_{c2b} + i \rho_{ac2} V_{c2b}, \quad (I-4e)$$

$$d\rho_{c2b}/dt = [-1/2 \gamma_c - i\omega_{c2b}] \rho_{c2b} - i V_{c2b} (\rho_{bb} - \rho_{c2c2}) - i V_{c2a} \rho_{ab}. \quad (I-4f)$$

In the above equations the coherence between $a \rightarrow c_2$ and $c_2 \rightarrow b$ steps is retained. If we wish to neglect the $c_2 \rightarrow b$ coherence, set $\rho_{bc2} = \rho_{c2b} = 0 = \rho_{ab}$. These equations then reduce to two-level equations

$$d\rho_{aa}/dt = -\gamma_a \rho_{aa} - i [V_{ac2} \rho_{c2a} - \rho_{ac2} V_{c2a}], \quad (I-5a)$$

$$d\rho_{c2c2}/dt = -\gamma_c \rho_{c2c2} - i [V_{c2a} \rho_{ac2} - \rho_{c2a} V_{ac2}], \quad (I-5b)$$

$$d\rho_{ac2}/dt = [-1/2 (\gamma_a + \gamma_c) - i\omega_{ac2}] \rho_{ac2} - i V_{ac2} (\rho_{c2c2} - \rho_{aa}), \quad (I-5c)$$

$$d\rho_{bb}/dt = \gamma_a \rho_{aa} + \gamma_c \rho_{c2c2}. \quad (I-5d)$$

The matrix elements V_{if} used in equations (I-3) through (I-5) have to be calculated according to the multipolarity of the transition. We show how this is done for an electric dipole transition. The result has to be appropriately generalized for other transitions. The interaction Hamiltonian for an E1 transition is given by

$$V = -\mu \sqrt{\frac{2\pi\hbar\omega}{V_n}} (a + a^\dagger) - \mu' \sqrt{\frac{2\pi\hbar\omega'}{V_n}} (a' + a'^\dagger). \quad (I-6)$$

From this we calculate

$$V_{ac1} = \langle a; n, 0 | V | c; n, 1 \rangle = -\mu_{ac} \sqrt{\frac{2\pi\hbar\omega'}{V_n}} = V_{cla} \quad (I-7a)$$

$$V_{ac2} = \langle a; n, 0 | V | c; n-1, 0 \rangle = -\mu_{ac} \sqrt{\frac{2\pi\hbar\omega n}{V_n}} = V_{c2a} \quad (I-7b)$$

$$V_{bc1} = -\mu_{bc} \sqrt{\frac{2\pi\hbar\omega n}{V_n}} = V_{c1b} \quad (I-7c)$$

$$V_{bc2} = -\mu_{bc} \sqrt{\frac{2\pi\hbar\omega'}{V_n}} = V_{c2b} \quad (I-7d)$$

The above example was carried out for the case when a single photon participates in the upconversion process. To generalize to a multi-photon process, with m photons participating, the appropriate intermediate and ground states are

$$|c\rangle = |c, n-m, 0\rangle \quad (I-8)$$

$$|b\rangle = |b, n-m, 1\rangle$$

and the matrix element $V_{ac2}^{(m)}$ which is given by:

$$V_{ac2}^{(m)} = \sum_{1,2,m-1} \frac{\langle a | V | 1 \rangle \langle 1 | V | 2 \rangle \dots \langle m-1 | V | C \rangle}{\hbar(\omega_a - \omega_1 + \omega) \hbar(\omega_a + 2\omega - \omega_2) \dots \hbar[\omega_a + (m-1)\omega - \omega_{m-1}]} \quad (I-9)$$

should replace V_{ac2} in equations. Similarly, $V_{c2a}^{(m)}$ should be substituted for V_{c2a} . States $|1\rangle, |2\rangle$ through $|m-1\rangle$ are the intermediate levels obtained from excitations of real states off resonance as shown in Fig. I-2. In our case, in the three-level system they would involve $|a\rangle$ or $|b\rangle$ only.

The level energies for m photon processes, corresponding to equations (I-1) for single photon processes are:

$$\omega_a = \omega_a' + n\omega, \quad (I-10a)$$

$$\omega_b = \omega_b' + (n-m)\omega + \omega', \quad (I-10b)$$

$$\omega_{c1} = \omega_c' + n\omega + \omega', \quad (I-10c)$$

$$\omega_{c2} = \omega_c' + (n-m)\omega. \quad (I-10d)$$

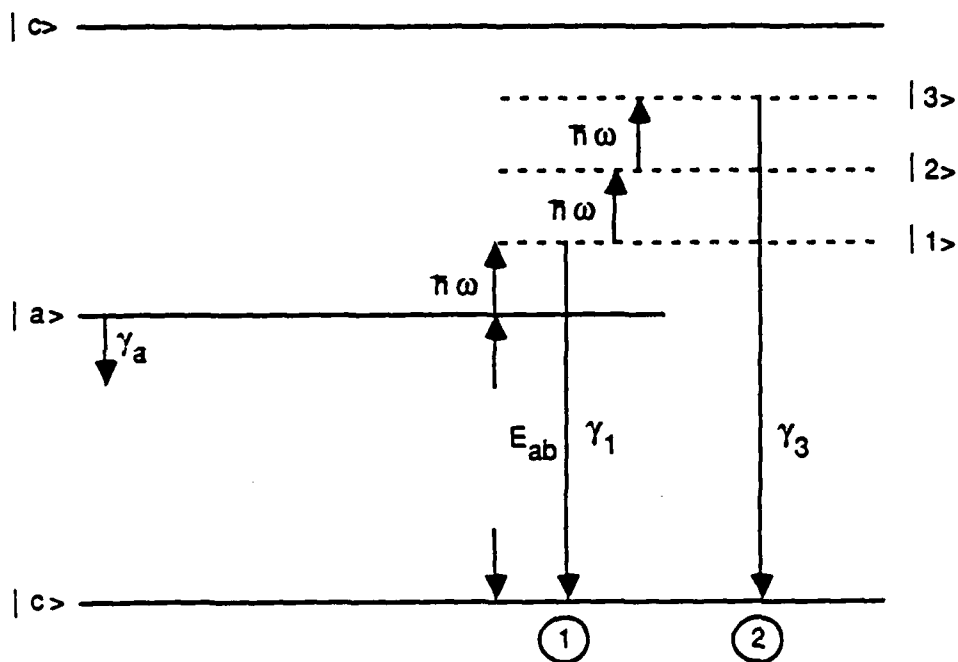


Figure I-2. Nuclear decay scheme for the two-level system showing a single photon with energy $h\omega$ absorbed from the beam and a higher energy photon with $h\omega' = h\omega + E_a - E_b$ emitted by the system as process 1. The spontaneous decay rates from $|a\rangle$ and $|c\rangle$ are γ_a and γ_c , respectively, with $\gamma_a \ll \gamma_c$. A multiphoton process with three photons of energy $h\omega$ absorbed by the system and a photon of energy $\pi\omega = 3h\omega' + E_a - E_b$ released by the system is shown as process 2.

APPENDIX J

**LISTING OF MULTIPHOTON UPCONVERSION CODE
GAMMAP**

GAMMAP MULTIPHOTON UPCONVERSION CODE

```

C
C DYNAMICS OF THE FOUR LEVEL SYSTEM
C S. N. DIXIT 5/6/86 (original version)
C B.BALKO 13/11/86 (MODIFIED)
C IMPLICIT REAL *8(A-H,O-Z)
C DIMENSION XI(100),RHOA(100),RHOC1(100),RHOC2(100),RHOB(100)
C DIMENSION AA(16,16),X0(16),X(16,10),VXC2(20),VXC2T(20),WTERM(20)
C COMPLEX *16 ZR(16,16),ZR0(16,16),ZRINV(16,16),ZW(16)
CKG Input answer variable.
C CHARACTER*1 ANS
C
C NEQ=16
C NPTS=10
C
C INPUT PARAMETERS
C GAMMA, GAMAC,VAC1,VAC2,VBC1,VBC2
C WAB,WAC1,WAC2,WBC1,WBC2,WC1C2
C
C IFLG = 0
C DO WHILE(IFLG.EQ.0)
C GAMAA=4.6D-7
C GAMAC=4.3D11
C T = -5.0-9
C VAC1=0.00
C VAC20=2.085D15
C VBC1=0.00
C VBC2=DSQRT(GAMAC)
C WAB=0.00
C WAC1=-2.42167D18
C WAC2=-1.20902D15
C WBC1=WAC1
C WBC2=WAC2
C WC1C2=WBC2-WBC1
C
C XW = 10.0
C XINT = 1.010
C XWCA = 100.
C XWAB = 1.06
C XWAC = - XWCA
C XWBC = XWAC - XWAB
C XGR = 0.0
C INPUT CONSTANTS
C XPI = 3.1428
C XPLAK = 1.0545887D-34
C PLANK = DSQRT(1./XPLAK)
C XALPA = 1.0/137.03604
C YALPA = XALPA/XPLAK

```

```

C      CONVERSION FROM EV TO HZ
      EV = 2.41304D14
C      ATOMIC RADIUS IN CM
      XRAC = 1.0D-8
C
C      NUCLEAR RADIUS IN CM
      XRAC = 1.0D-13
      XRAC = XRAC*5.07D-1
C
C      NEW INPUT
      MNFJT = 10
      W = XW*EV
      XWP = XW + XWAB
      WP = XWP*EV
CKG    Save the values.
      SGAMAA = GAMAA
      SGAMAC = GAMAC
      SVAC20 = VAC20
      SWAC1 = WAC1
      SWAC2 = WAC2
10     FORMAT(A1)
      WRITE(6,*) 'Input XW value? <RETURN>=NO, Y=YES'
      READ(5,10)ANS
      IF((ANS.EQ.'Y').OR.(ANS.EQ.'y'))THEN
        READ(5,*)XW
      END IF
      WRITE(6,*) 'Input XINT value? <RETURN>=NO, Y=YES'
      READ(5,10)ANS
      IF((ANS.EQ.'Y').OR.(ANS.EQ.'y'))THEN
        READ(5,*)XINT
      END IF

      WRITE(6,*) 'Input XWCA value? <RETURN>=NO, Y=YES'
      READ(5,10)ANS
      IF((ANS.EQ.'Y').OR.(ANS.EQ.'y'))THEN
        READ(5,*)XWCA
      END IF

      WRITE(6,*) 'Input XGR value? <RETURN>=NO, Y=YES'
      READ(5,10)ANS
      IF((ANS.EQ.'Y').OR.(ANS.EQ.'y'))THEN
        READ(5,*)XGR
      END IF

      WRITE(6,*) 'Input T value? <RETURN>=NO, Y=YES'
      READ(5,10)ANS
      IF((ANS.EQ.'Y').OR.(ANS.EQ.'y'))THEN
        READ(5,*)T
      END IF

```

```

C      XWAC = -XWCA
C
C      WRITE(6,30) XW,XINT,XWAC,XWAB,MNFOT
30  FORMAT(' INPUT PARAMETERS:XW,XINT,XWAC,XWAB,MNFOT//
1  1P4D12.4,I5)
C
C      N = MNFOT
C      M = N/2 + 1
C      W = XW*EV - (XGR/MNFOT)*GAMAC
C      XW = W/EV
C      WAC = XWAC*EV
C
C      VAC20 = XPAC*DSQRT(2.0*XPI*XALPA*XINT)*PLANK
C      WCI02=WBC2-WBC1
C      CALCULATION OF VAC2
C
C
C      WRITE(6,45)
45  FORMAT(1X, VAC20 CALCULATED AS A FUNCTION OF PHOTON NUMBER')
C
C      WTERM(1) = 1.0
C
C      DO 50 J=1,M
C      WTERM(2*J) = (WAC + (2*J-1)*W) + GAMAC
50  WTERM(2*J+1) = (2.*J)*W
C      VXC2(1) = VAC20
C      VXC2T(1) = VXC2(1)
C      DO 60 I=2,N-1
C      VXC2(I) = VXC2(I-1)*VAC20/WTERM(I)
60  VXC2T(I) = VXC2T(I-1) + VXC2(I)
C      VXC2(N) = VXC2(N-1)*VAC20/(WTERM(N) + GAMAC)
C      VXC2T(N) = VXC2T(N-1) + VXC2(N)
C
C      DO 62 I=1,N
62  WRITE(6,65) I,WTERM(I),VXC2(I),VXC2T(I)
65  FORMAT(1X,I5,1P3D15.6)
C
C      WRITE(6,*) 'ENTER 1 FOR VAC2, 2 FOR VAC2T '
C      READ(5,*) ICHOICE
C      WRITE(6,*) ' WHICH ONE? '
C      READ (5,*) IONE
C      IF (ICHOICE.EQ.1) THEN
C      VAC20 = VXC2(IONE)
C      ELSE
C      VAC20 = VXC2T(IONE)
C      END IF
20  FORMAT(/,A*)

```

```

C
MP = IONE
XWP = XWAB + MP*W/EV
WP = XWP*EV
WAB = 0.0
XWAC1 = XWAC - XWP
WAC1 = XWAC1*EV
XWAC2 = XWAC + MP*XW
WAC2 = XWAC2*EV
XWBC1 = XWBC - MP*XW
WBC1 = XWBC1*EV
XWBC2 = XWBC + XWP
WBC2 = XWBC2*EV
WC1C2 = WBC2 - WBC1

C
CKG
C
C
T=5.00-9
TINCA=0.00

C
PI=3.141592700
C=2.997925010
HBAR=1.05459190-27
H=6.62619630-27
TOPIC=2.00*PI*C

C
TA=T*TOPIC
C
TINCA=TINC*TOPIC
C
C
WRITE(6,1)
C
1 FORMAT('1')
WRITE(6,105)
105 FORMAT(1X,'DYNAMICS OF THE FOUR LEVEL SYSTEM',
1 // ' INTENSITY VARIATION'//)
WRITE(6,107) GAMAA,GAMAC,VAC1,VAC2,VBC1,VBC2
107 FORMAT(' INPUT PARAMETERS: GAMAA,GAMAC,VAC1,VAC2,VBC1,VBC2'//
1 1P6D12.4)
WRITE(6,111) XWAB,XWAC,XWBC,XGR,XWP,IONE
111 FORMAT(' INPUT PARAMETERS: XWAB,XWAC,XWBC,XGR,XWP,IONE'//
1 1P5D12.4,14)
WRITE(6,108) WAB,WAC1,WAC2,WBC1,WBC2,WC1C2
108 FORMAT(' INPUT PARAMETERS: WAB,WAC1,WAC2,WBC1,WBC2,WC1C2'//
1 1P6D12.4)
WRITE(6,109)T,TINCA
109 FORMAT(1X,'T,TINCA', 1P2D16.4)

C
GAMAA=GAMAA/TOPIC
GAMAC=GAMAC/TOPIC
VAC1=VAC1/TOPIC

```

```

VAC20=VAC20/TOPIC
VBC1=VBC1/TOPIC
VBC2=VBC2/TOPIC
WAB=WAB/TOPIC
WAC1=WAC1/TOPIC
WAC2=WAC2/TOPIC
WBC1=WBC1/TOPIC
WBC2=WBC2/TOPIC
WC1C2=WC1C2/TOPIC

C
C INCREMENT VAC2
C
E0=0.1
AINT=0.1
DO 5000 IDEL=1,NPTS
E2=E0+(IDEL-1)*AINT
VAC2=VAC20*E2
C IF(E2.GE.0.01D0) AINT=0.01D0
C
C DEFINE THE INTENSITY DEPENDENT QUANTITIES (VAC2,VBC1)
C
C SET UP AA AND X0
C
DO 303 IL=1,NEQ
X0(IL)=0.00
DO 303 IM=1,NEQ
AA(IL,IM)=0.00
303 CONTINUE

C
C NON-ZERO MATRIX ELEMENTS
C
X0(1)=1.00

AA(1,1)=-GAMAA
AA(1,6)=2.00*VAC1
AA(1,8)=2.00*VAC2

AA(2,2)=-GAMAC
AA(2,6)=-2.00*VAC1
AA(2,14)=-2.00*VBC1

AA(3,1)=GAMAA
AA(3,2)=GAMAC
AA(3,4)=GAMAC
AA(3,14)=2.00*VBC1
AA(3,16)=2.00*VBC2

```

```

AA(4,4)=-GAMAC
AA(4,8)=-2.00*VAC2
AA(4,16)=-2.00*VBC2

AA(5,5)=- (GAMAA+GAMAC)/2.00
AA(5,6)=-WAC1
AA(5,12)=-VAC2
AA(5,10)=-VBC1

AA(6,6)=AA(5,5)
AA(6,5)=-AA(5,6)
AA(6,2)=VAC1
AA(6,1)=-VAC1
AA(6,11)=VAC2
AA(6,9)=-VBC1

AA(7,7)=AA(5,5)
AA(7,8)=-WAC2
AA(7,12)=VAC1
AA(7,10)=-VBC2

AA(8,8)=AA(7,7)
AA(8,7)=-AA(7,8)
AA(8,4)=VAC2
AA(8,1)=-VAC2
AA(8,11)=VAC1
AA(8,9)=-VBC2

AA(9,9)=-GAMAA/2.00
AA(9,10)=WAB
AA(9,14)=VAC1
AA(9,16)=VAC2
AA(9,6)=VBC1
AA(9,8)=VBC2

AA(10,10)=-GAMAA/2.00
AA(10,9)=-AA(9,10)
AA(10,13)=-VAC1
AA(10,15)=-VAC2
AA(10,5)=VBC1
AA(10,7)=VBC2

AA(11,11)=-GAMAC
AA(11,12)=WC1C2
AA(11,8)=-VAC1
AA(11,16)=-VBC1
AA(11,6)=-VAC2
AA(11,14)=-VBC2

```



```

AA(12,12)=-3AMAC
AA(12,11)=-WC1C2
AA(12,7)=-LAC1
AA(12,15)=-WBC1
AA(12,5)=UAC2
AA(12,13)=BC2

AA(13,13)=-3AMAC/2.00
AA(13,14)=-WBC1
AA(13,10)=LAC1
AA(13,12)=-WBC2

AA(14,14)=-3AMAC/2.00
AA(14,13)=WBC1
AA(14,9)=-LAC1
AA(14,3)=-WBC1
AA(14,2)=VEC1
AA(14,11)=BC2

AA(15,15)=-3AMAC/2.00
AA(15,16)=-WBC2
AA(15,10)=UAC2
AA(15,12)=BC1

AA(16,16)=-3AMAC/2.00
AA(16,15)=WBC2
AA(16,9)=-LAC2
AA(16,3)=-WBC2
AA(16,4)=VEC2
AA(16,11)=VBC1

C      print *, 'idel',idel
      CALL SOLVE(NEQ,1,AA,X0,ZR,ZR0,ZRINV,ZW,TA,TINCA,X,1,2,3,4)
C
C      STORE THE SOLUTION
C
      XI(IDEL)=E2
      RHOA(IDEL)=X(1,1)
      RHOC1(IDEL)=X(2,1)
      RHOC2(IDEL)=X(4,1)
      RHOB(IDEL)=X(3,1)
C
5000 CONTINUE
C
C      OUTPUT

```

C

```
      WRITE(6,54)(XI(IDEL),RHOA(IDEL),RHOB(IDEL),RHOC1(IDEL)  
1  RHOC2(IDEL),IDEL=1,NPTS)  
54 FORMAT(1X,1P5D15.6)  
55 FORMAT(1X,1P2D15.6)  
      WRITE(1,55)(XI(IDEL),RHOA(IDEL),  
1  IDEL=1,NPTS)  
      WRITE(2,55)(XI(IDEL),RHOB(IDEL),  
1  IDEL=1,NPTS)  
      WRITE(6,*)'ANOTHER RUN? Y = YES, N = NO'  
      READ(5,10)ANS  
      IF((ANS.EQ.'N').OR.(ANS.EQ.'n'))IFLG=1  
      END DO  
      STOP  
      END
```

APPENDIX K

**PROGRAM PNP
(NAME LIST AND CODE LISTING)**

APPENDIX K

PROGRAM PNP

NAME LIST

A - Parameter in determining well depth Yukawa Potential

B - Parameter in Yukawa Potential for radial scaling

BC - Parameter in Yukawa Potential for

Y(12) Array for phase space position of the three-particle system

DERY(12) Array for time derivatives of Y(12)

WORK(352) Real *8 Work Array for ODE

IWORK(5) Integer Work Array for ODE

X1, Y1, PX1, PY Positions and Momenta for Neutron in Cartesian Coordinates

X2, Y2, PX2, PY2 Positions and Momenta for 1 Proton in Cartesian Coordinates

X3, Y3, PX3, PY3 Positions and Momenta for 2nd Proton in Cartesian
Coordinates

Assignment of positions and momentum are as follows:

Y(1)	X1	Neutron
------	----	---------

Y(2)	Y1	
------	----	--

Y(3)	X2	Proton 1	Cartesian Coordinates
------	----	----------	-----------------------

Y(4)	Y2	
------	----	--

Y(5)	X3	Proton 2
------	----	----------

Y(6)	Y3	
------	----	--

Y(7)	PX1	Neutron	
Y(8)	PY1		
Y(9)	PX2	Proton 1	Cartesian Momenta
Y(10)	PY2		
Y(11)	PX3	Proton 2	
Y(12)	PY3		

URAND(IY) Random number generator with seed IY in range [0,1]

DX - Range of X,Y Box for initial coordinates

DP - Range of Px, Py Box for initial momenta

PX - Total X momentum

PY - Total Y momentum

ETOT - Subroutine to Compute

Kinetic energy - EK

Potential energy - EPOT

Total energy - ET

Angular Momentum - XL

from phase space configuration Y(12)

ODE - Name for differential equation solver

FCT - external function containing set of equations

T - time variable (current)

TOUT - target time for ODE

Relerr - Relative Error

Abserr - Absolute Error

IFLAG - Communication Variable

IFLAG = 1 on 1st Step

IFLAG = 2 on normal return

R1 - Distance of Neutron to Proton 1

R2 - Distance of Neutron to Proton 2

R3 - Distance of Proton 1 to Proton 2

FCT Subroutine for set of Hamilton's equations to be solved. The 1st set of 6 equations are for the calculation of particle momenta.

$$\text{DERY (1)} = \frac{\text{DY (1)}}{\text{DT}} = \frac{\partial \text{H}}{\partial \text{Y (1)}} = \frac{\partial \text{H}}{\partial \text{X}_1} = \text{PX1}$$

$$\text{DERY (2)} = \frac{\text{DY (2)}}{\text{DT}} = \frac{\partial \text{H}}{\partial \text{Y (2)}} = \frac{\partial \text{H}}{\partial \text{Y}_1} = \text{PX2}$$

$$\text{DERY (3)} = \frac{\text{DY (3)}}{\text{DT}} = \frac{\partial \text{H}}{\partial \text{Y (3)}} = \frac{\partial \text{H}}{\partial \text{X}_2} = \text{PX2}$$

$$\text{DERY (4)} = \frac{\text{DY (4)}}{\text{DT}} = \frac{\partial \text{H}}{\partial \text{Y (4)}} = \frac{\partial \text{H}}{\partial \text{Y}_2} = \text{PY2}$$

$$\text{DERY (5)} = \frac{\text{DY (5)}}{\text{DT}} = \frac{\partial \text{H}}{\partial \text{Y (5)}} = \frac{\partial \text{H}}{\partial \text{Y}_3} = \text{PX3}$$

$$\text{DERY (6)} = \frac{\text{DY (6)}}{\text{DT}} = \frac{\partial \text{H}}{\partial \text{Y (6)}} = \frac{\partial \text{H}}{\partial \text{Y}_3} = \text{PY3}$$

The second set of six equations are for the calculation of particle coordinates.

$$\text{DERY (7)} = \frac{\text{DY(7)}}{\text{DT}} = \frac{-\partial \text{H}}{\partial \text{X}_1} = \frac{-\partial \text{V}}{\partial \text{R}_1} \frac{\partial \text{R}_1}{\partial \text{X}_1} - \frac{\partial \text{V}}{\partial \text{R}_2} \frac{\partial \text{R}_2}{\partial \text{X}_1}$$

$$\text{DERY (8)} = \frac{\text{DY(8)}}{\text{DT}} = \frac{-\partial \text{H}}{\partial \text{Y}_1} = \frac{-\partial \text{V}}{\partial \text{R}_1} \frac{\partial \text{R}_1}{\partial \text{Y}_1} - \frac{\partial \text{V}}{\partial \text{R}_2} \frac{\partial \text{R}_2}{\partial \text{Y}_1}$$

$$\text{DERY (9)} = \frac{\text{DY(9)}}{\text{DT}} = \frac{-\partial \text{H}}{\partial \text{X}_2} = \frac{-\partial \text{V}}{\partial \text{R}_1} \frac{\partial \text{R}_1}{\partial \text{X}_2} - \frac{\partial \text{V}}{\partial \text{R}_3}$$

$$\text{DERY (10)} = \frac{\text{DY(10)}}{\text{DT}} = \frac{-\partial \text{H}}{\partial \text{Y}_2} = \frac{-\partial \text{V}}{\partial \text{R}_1} \frac{\partial \text{R}_1}{\partial \text{Y}_2} - \frac{\partial \text{V}}{\partial \text{R}_3} \frac{\partial \text{R}_3}{\partial \text{Y}_2}$$

$$\text{DERY (11)} = \frac{\text{DY(11)}}{\text{DT}} = \frac{-\partial \text{H}}{\partial \text{X}_3} = \frac{-\partial \text{V}}{\partial \text{R}_2} \frac{\partial \text{R}_2}{\partial \text{X}_3} - \frac{\partial \text{V}}{\partial \text{R}_3} \frac{\partial \text{R}_3}{\partial \text{X}_3}$$

$$\text{DERY (12)} = \frac{\text{DY(12)}}{\text{DT}} = \frac{-\partial \text{H}}{\partial \text{Y}_3} = \frac{-\partial \text{V}}{\partial \text{R}_2} \frac{\partial \text{R}_2}{\partial \text{Y}_3} - \frac{\partial \text{V}}{\partial \text{R}_3} \frac{\partial \text{R}_3}{\partial \text{Y}_3}$$

For this set of equations the following code names are used in the computer program.

$$\text{DVR1} \equiv \partial \text{V} / \partial \text{R1}$$

$$\text{DVR2} \equiv \partial \text{V} / \partial \text{R2}$$

$$\text{DVR3} \equiv \partial \text{V} / \partial \text{R3}$$

$$\text{DR1X1} \equiv \partial \text{R1} / \partial \text{X1}$$

$$\text{DR1Y1} \equiv \partial \text{R1} / \partial \text{Y1}$$

$$\text{DR1X2} \equiv \partial \text{R1} / \partial \text{X2}$$

$$\text{DR1Y2} \equiv \partial \text{R1} / \partial \text{Y2}$$

$$\text{DR2X1} \equiv \partial \text{R2} / \partial \text{X1}$$

$$\text{DR2Y1} \equiv \partial \text{R2} / \partial \text{Y1}$$

$$DR2X3 \equiv \partial R2 / \partial X3$$

$$DR2Y3 \equiv \partial R2 / \partial Y3$$

$$DR3X2 \equiv \partial R3 / \partial X2$$

$$DR3Y2 \equiv \partial R3 / \partial Y2$$

$$DR3X3 \equiv \partial R3 / \partial X3$$

$$DR3Y3 \equiv \partial R3 / \partial Y3$$

List of parameters used in ETOT, subroutine used to compute energy and angular momenta.

EKN - Kinetic energy of neutron

EKP1 - Kinetic energy of proton 1

EKP2 - Kinetic energy of proton 2

VR1 - Potential energy of neutron - proton 1

VR2 - Potential energy of neutron - proton 2

VR3 - Potential energy of proton 1 - proton 2

EK - Total kinetic energy

EPOT - Total potential energy

ET - Sum of total kinetic and potential energy

XC - X Cartesian position of center of mass

YC - Y Cartesian position of center of mass

XL1 - Angular momentum of neutron about (Xc, Yc)

XL2 - Angular momentum of proton 1 about (Xc, Yc)

XL3 - Angular momentum of proton 2 about (Xc, Yc)

XL - Total angular momentum

PNP ELECTRON NUCLEAR COUPLING CODES

```

IMPLICIT REAL*8(A-H,O-Z)
COMMON /AAA/ A,BC,B,XMN
REAL*8 Y(12),DERY(12)
DIMENSION WORK(352),IWORK(5)
EXTERNAL FCT

```

```

PROGRAM FOR P,N,P (HE 3) V2
BY D W NOID
SEPT 1985

```

```

      N
      *
      *
      *
      +-----+
P*****P

```

```

MOTION CONFINED TO X--Y SPACE
N X1,Y1,PX1,PY1 Q(1,2),P(7,8)
P1 X2,Y2,PX2,PY2 Q(3,4),P(9,10)
P2 X3,Y3,PX3,PY3 Q(5,6),P(11,12)

```

```

UNITS
1 TIME UNIT = ?
1 ENERGY UNIT = 1 MEV
1 DISTANCE UNIT = 1 FM (10**-13CM)

```

```

INPUT OFF PARAMETERS
A = 22.7D0
B = 0.858D0
BC = 2.47D0
XMN = 1000.0D0

```

```

INPUT INITIAL CONDITIONS
*****

```

```

CODE RUNS 100 TRAJECTORIES
FOR -30 < E < -10 MEV
AND 4 < L < 10

```

```

DO 1001 II=1,100
IY = 7
DX = 8.0D0
DP = 100.0D0
X1 = 0.0D0
Y1 = 0.0D0

```

```

DO 1 J=1,1000
X2 = DX*(URAND(IY)-0.5D0)
Y2 = DX*(URAND(IY)-0.5D0)
X3 = DX*(URAND(IY)-0.5D0)
Y3 = DX*(URAND(IY)-0.5D0)

```

```

PX1 = DP*(URAND(IY) -0.5D0)
PY1 = DP*(URAND(IY) -0.5D0)
PX2 = DP*(URAND(IY) -0.5D0)
PY2 = DP*(URAND(IY) -0.5D0)
PX3 = -(PX1 + PX2)
PY3 = -(PY1 + PY2)

```

```

C
C      MOMENTUM CHECK
      PX = PX1 + PX2 + PX3
      PY = PY1 + PY2 + PY3
      Y(1) = X1
      Y(2) = Y1
      Y(3) = X2
      Y(4) = Y2
      Y(5) = X3
      Y(6) = Y3
      Y(7) = PX1
      Y(8) = PY1
      Y(9) = PX2
      Y(10) = PY2
      Y(11) = PX3
      Y(12) = PY3
C
      CALL ETOT(Y,EK,EPOT,ET,XL)
      IF (ET.GT.-30.000.AND.ET.LT.-10.000.AND.
$      DABS(XL).GT.4.000.AND.DABS(XL).LT.10.000) GO TO 2
1 CONTINUE
2 CONTINUE
      WRITE(6,106) PX,PY
106 FORMAT(' ','PXT,PYT',2D20.10)
      WRITE(6,101) X1,Y1,PX1,PY1
      WRITE(6,102) X2,Y2,PX2,PY2
      WRITE(6,103) X3,Y3,PX3,PY3
101 FORMAT(' ','111',4D20.10)
102 FORMAT(' ','222',4D20.10)
103 FORMAT(' ','333',4D20.10)
      WRITE(6,104) ET,EK,EPOT,XL
104 FORMAT(' ','ET,EK,EPOT,LT',4D20.10)

      NPTS = 8000
      T = 0.000
      ABSERR = 1.00-12
      RELERR = 0.000
      IFLAG = 1
      NDIM = 12
      TSTEP = 1.00000
C
      R1 = (Y(1)-Y(3))**2 + (Y(2)-Y(4))**2
      R2 = (Y(1)-Y(5))**2 + (Y(2)-Y(6))**2
      R3 = (Y(3)-Y(5))**2 + (Y(4)-Y(6))**2
      R1 = DSQRT(R1)
      R2 = DSQRT(R2)
      R3 = DSQRT(R3)
C
      DO 7 I=1,NPTS
      TOUT = TSTEP*DFLOAT(I)
C
      CALL ODE(FCT,NDIM,Y,T,TOUT,RELERR,ABSERR,IFLAG,WORK,IWORK)
C
      CALL ETOT(Y,EK,EPOT,ET,XL)
C
      R1 = (Y(1)-Y(3))**2 + (Y(2)-Y(4))**2
      R2 = (Y(1)-Y(5))**2 + (Y(2)-Y(6))**2
      R3 = (Y(3)-Y(5))**2 + (Y(4)-Y(6))**2
      R1 = DSQRT(R1)
      R2 = DSQRT(R2)
      R3 = DSQRT(R3)

```

```

C      OUTPUT TO PLOTTER Y(1-6)
      WRITE(6,135) R1,R2,R3,ET,XL,T
105  FORMAT('  'X,Y',6D20.10)
      7  CONTINUE
C      WRITE(6,135) P1,R2,R3,ET,T
1001  CONTINUE
      STOP
      END

C
C
      SUBROUTINE FCT(X,Y,DERY)
      IMPLICIT REAL*8(A-H,O-Z)
      COMMON /AAA/ A,B,C,B,XMN
      REAL*8 Y(12),DERY(12)

C
      R1 = (Y(1)-Y(3))**2 + (Y(2)-Y(4))**2
      R2 = (Y(1)-Y(5))**2 + (Y(2)-Y(6))**2
      R3 = (Y(3)-Y(5))**2 + (Y(4)-Y(6))**2
      R1 = DSQRT(R1)
      R2 = DSQRT(R2)
      R3 = DSQRT(R3)

C
C      DV/R1
      LVR1= A*B*C*(1.0D0+B*R1)*DEXP(-H*R1)/R1**2
      LVR2= A*B*C*(1.0D0+B*R2)*DEXP(-P*R2)/R2**2
      LVR3= A*B*C*(1.0D0+B*R3)*DEXP(-B*R3)/R3**2 -1.44D0/R3**2

C
C
      DR1/DG
      DR1X1 = (Y(1)-Y(3))/R1
      DR1X2 = (Y(3)-Y(1))/R1
      DR1Y1 = (Y(2)-Y(4))/R1
      DR1Y2 = (Y(4)-Y(2))/R1

C
C      DR2/DG
      DR2X1 = (Y(1)-Y(5))/R2
      DR2X3 = (Y(5)-Y(1))/R2
      DR2Y1 = (Y(2)-Y(6))/R2
      DR2Y3 = (Y(6)-Y(2))/R2

C
C      DR3/DG
      DR3X2 = (Y(3)-Y(5))/R3
      DR3X3 = (Y(5)-Y(3))/R3
      DR3Y2 = (Y(4)-Y(6))/R3
      DR3Y3 = (Y(6)-Y(4))/R3

C
C      P EQUATIONS
      DERY(1) = Y(7)/XMN
      DERY(2) = Y(8)/XMN
      DERY(3) = Y(9)/XMN
      DERY(4) = Y(10)/XMN
      DERY(5) = Y(11)/XMN
      DERY(6) = Y(12)/XMN

C
C      Q EQUATIONS
      DERY(7) = -DVR1*DR1X1 - DVR2*DR2X1
      DERY(8) = -DVR1*DR1Y1 - DVR2*DR2Y1
      DERY(9) = -DVR1*DR1X2 - DVR3*DR3X2
      DERY(10) = -DVR1*DR1Y2 - DVR3*DR3Y2
      DERY(11) = -DVR2*DR2X3 - DVR3*DR3X3

```

```

DERY(12) = -DVR2*DR2Y3 - DVR3*DR3Y3
RETURN
END

C
C
SUBROUTINE STOT(Y,EK,EPOT,ET,XL)
IMPLICIT REAL*8(A-H,O-Z)
COMMON /AAA/ A,HC,B,XMN
REAL*8 Y(12)

C
C   KINETIC ENERGY
EKN = 0.500*(Y(7)**2 + Y(8)**2)/XMN
EKP1 = 0.500*(Y(9)**2 + Y(10)**2)/XMN
EKP2 = 0.500*(Y(11)**2 + Y(12)**2)/XMN

C
C   POTENTIAL ENERGY
R1 = (Y(1)-Y(3))**2 + (Y(2)-Y(4))**2
R2 = (Y(1)-Y(5))**2 + (Y(2)-Y(6))**2
R3 = (Y(3)-Y(5))**2 + (Y(4)-Y(6))**2
R1 = DSQRT(R1)
R2 = DSQRT(R2)
R3 = DSQRT(R3)

C
VR1 = -A*HC*DEXP(-B*R1)/R1
VR2 = -A*HC*DEXP(-B*R2)/R2
VR3 = -A*HC*DEXP(-B*R3)/R3 + 1.4400/R3

C
C   TOTAL ENERGY
EK = EKN + EKP1 + EKP2
EPOT = VR1 + VR2 + VR3
ET = EK + EPOT

C
C   ANGULAR MOMENTUM
XC = Y(1) + Y(3) + Y(5)
YC = Y(2) + Y(4) + Y(6)
LZ = X*PY - Y*PX
XL1 = (Y(1) - XC)*Y(3) - (Y(2) - YC)*Y(7)
XL2 = (Y(3) - XC)*Y(10) - (Y(4) - YC)*Y(9)
XL3 = (Y(5) - XC)*Y(12) - (Y(6) - YC)*Y(11)
XL = XL1 + XL2 + XL3
XL = XL/197.300

C
RETURN
END

```

APPENDIX L

**PROGRAM NP2
(NAME LIST AND CODE LISTING)**

NP2 ELECTRON NUCLEAR COUPLING CODE

```

IMPLICIT REAL*8(A-H,O-Z)
COMMON /AAA/ A,RC,B,XMN
REAL*8 Y(16),DERY(16)
DIMENSION WORK(436),IWORK(5)
EXTERNAL FCT

```

PROGRAM FOR P⁺ N⁺ P⁺ N (HE 4) V2
BY D W NNOID
OCTOBER 1935

```

MOTION CONFINED TO X--Y SPACE
N1  X1,Y1,PX1,PY1  Q(1,2),P(9,10)
P1  X2,Y2,PX2,PY2  Q(3,4),P(11,12)
P2  X3,Y3,PX3,PY3  Q(5,6),P(13,14)
N2  X4,Y4,PX4,PY4  Q(7,8),P(15,16)

```

R1	N1*P1
R2	N1*P2
R3	P1*P2
R4	N1*N2
R5	N2*P1
R6	N2*P2

```

UNITS
1 TIME UNIT = ?
1 ENERGY UNIT = 1 MEV
1 DISTANCE UNIT = 1 FM (10**-13CM)

```

INPUT OFF PARAMETERS

```
A = 22.700
B = 0.85800
BC = 2.4700
XMN = 1000.000
```

INPUT INITIAL CONDITIONS

```

IY = 7
DX = 8.000
DP = 18.000
X1 = 0.000
Y1 = 0.000

```

```

D0 1 J=1,1000
X2 = DX*(URAND(IY)-0.500)
Y2 = DY*(URAND(IY)-0.500)
X2 = 2.000
Y2 = 0.000
X3 = DX*(URAND(IY)-0.500)
Y3 = DY*(URAND(IY)-0.500)

```

```

X3 = 0.000
Y3 = -2.000
X4 = DX*(URAND(IY)-0.500)
Y4 = DY*(URAND(IY)-0.500)
X4 = 2.000
Y4 = -2.000

```

```

C
PX1 = DP*(UPAND(IY) -0.500)
PY1 = DP*(URAND(IY) -0.500)
PX1 = 0.000
PY1 = -2.000
PX2 = DP*(UPAND(IY) -0.500)
PY2 = DP*(URAND(IY) -0.500)
PX2 = -2.000
PY2 = 0.000
PX3 = DP*(UPAND(IY) -0.500)
PY3 = DP*(URAND(IY) -0.500)
PX3 = 2.000
PY3 = 0.000
PX4 = -(PX1 + PX2 + PX3)
PY4 = -(PY1 + PY2 + PY3)

```

```

C
C      MOMENTUM CHECK
C      PX = PX1 + PX2 + PX3 + PX4
C      PY = PY1 + PY2 + PY3 + PY4

```

```

C
Y(1) = X1
Y(2) = Y1
Y(3) = X2
Y(4) = Y2
Y(5) = X3
Y(6) = Y3
Y(7) = X4
Y(8) = Y4
Y(9) = PX1
Y(10) = PY1
Y(11) = PX2
Y(12) = PY2
Y(13) = PX3
Y(14) = PY3
Y(15) = PX4
Y(16) = PY4

```

```

C      CALL ETOT(Y,EK,EPOT,ET,XL)
C      IF (ET.GT.-30.000.AND.ET.LT.-10.000.AND.
C      $      DABS(XL).GT.4.000.AND.DABS(XL).LT.10.000) GO TO 2
1 CONTINUE
2 CONTINUE

```

```

C
WRITE(6,106) PX,PY
106 FORMAT(' ', 'PXT,PYT',2020.10)
WRITE(6,101) X1,Y1,PX1,PY1
WRITE(6,102) X2,Y2,PX2,PY2
WRITE(6,103) X3,Y3,PX3,PY3
WRITE(6,104) X4,Y4,PX4,PY4
101 FORMAT(' ', '111',4D20.10)
102 FORMAT(' ', '222',4D20.10)
103 FORMAT(' ', '333',4D20.10)
104 FORMAT(' ', '444',4D20.10)
WRITE(6,105) ET,EK,EPOT,XL

```

```

105 FORMAT(' ',*ET,EK,EPOT,LT',4D20.10)
C
NPTS = 8000
T = 0.0D0
ABSERR = 1.0D-12
RELERR = 0.000
IFLAG = 1
NDIM = 16
TSTEP = 1.000D0
C
R1 = (Y(1)-Y(3))**2 + (Y(2)-Y(4))**2
R2 = (Y(1)-Y(5))**2 + (Y(2)-Y(6))**2
R3 = (Y(3)-Y(5))**2 + (Y(4)-Y(6))**2
R4 = (Y(7)-Y(1))**2 + (Y(8)-Y(2))**2
R5 = (Y(7)-Y(3))**2 + (Y(8)-Y(4))**2
R6 = (Y(7)-Y(5))**2 + (Y(8)-Y(6))**2
C
R1 = DSQRT(R1)
R2 = DSQRT(R2)
R3 = DSQRT(R3)
R4 = DSQRT(R4)
R5 = DSQRT(R5)
R6 = DSQRT(R6)
C
DO 7 I=1,NPTS
TOUT = TSTEP*DFLOAT(I)
C
CALL ODE(FCT,NDIM,Y,T,TOUT,RELERR,ABSERR,IFLAG,WORK,IWORK)
CALL ETOT(Y,EK,EPOT,ET,XL)
C
R1 = (Y(1)-Y(3))**2 + (Y(2)-Y(4))**2
R2 = (Y(1)-Y(5))**2 + (Y(2)-Y(6))**2
R3 = (Y(3)-Y(5))**2 + (Y(4)-Y(6))**2
R4 = (Y(7)-Y(1))**2 + (Y(8)-Y(2))**2
R5 = (Y(7)-Y(3))**2 + (Y(8)-Y(4))**2
R6 = (Y(7)-Y(5))**2 + (Y(8)-Y(6))**2
C
R1 = DSQRT(R1)
R2 = DSQRT(R2)
R3 = DSQRT(R3)
R4 = DSQRT(R4)
R5 = DSQRT(R5)
R6 = DSQRT(R6)
C
WRITE(6,107) R1,R2,R3,R4,ET,XL,T
107 FORMAT(' ',*X,Y',4D14.5,2D20.10,012.4)
7 CONTINUE
C
STOP
END
C
C
SUBROUTINE FCT(X,Y,DERY)
IMPLICIT REAL*8(A-H,O-Z)
COMMON /AAA/ A,BC,B,XMN
REAL*8 Y(16),DERY(16)
C
R1 = (Y(1)-Y(3))**2 + (Y(2)-Y(4))**2
R2 = (Y(1)-Y(5))**2 + (Y(2)-Y(6))**2
R3 = (Y(3)-Y(5))**2 + (Y(4)-Y(6))**2

```



```

R4 = (Y(7)-Y(1))**2 + (Y(8)-Y(2))**2
R5 = (Y(7)-Y(3))**2 + (Y(8)-Y(4))**2
R6 = (Y(7)-Y(5))**2 + (Y(8)-Y(6))**2

```

```

C
R1 = DSQRT(R1)
R2 = DSQRT(R2)
R3 = DSQRT(R3)
R4 = DSQRT(R4)
R5 = DSQRT(R5)
R6 = DSQRT(R6)

```

```

C
C      DV/R1
DVR1= A*HC*(1.000+B*R1)*DEXP(-B*R1)/R1**2
DVR2= A*HC*(1.000+B*R2)*DEXP(-B*R2)/R2**2
DVR3= A*HC*(1.000+B*R3)*DEXP(-B*R3)/R3**2 -1.4400/R3**2
DVR4= A*HC*(1.000+B*R4)*DEXP(-B*R4)/R4**2
DVR5= A*HC*(1.000+B*R5)*DEXP(-B*R5)/R5**2
DVR6= A*HC*(1.000+B*R6)*DEXP(-B*R6)/R6**2

```

```

C
C      DR1/D8
DR1X1 = (Y(1)-Y(3))/R1
DR1X2 = (Y(3)-Y(1))/R1
DR1Y1 = (Y(2)-Y(4))/R1
DR1Y2 = (Y(4)-Y(2))/R1

```

```

C
C      DR2/D4
DR2X1 = (Y(1)-Y(5))/R2
DR2X3 = (Y(5)-Y(1))/R2
DR2Y1 = (Y(2)-Y(6))/R2
DR2Y3 = (Y(6)-Y(2))/R2

```

```

C
C      DR3/D8
DR3X2 = (Y(3)-Y(5))/R3
DR3X3 = (Y(5)-Y(3))/R3
DR3Y2 = (Y(4)-Y(6))/R3
DR3Y3 = (Y(6)-Y(4))/R3

```

```

C
C      DR4/D8
DR4X1 = (Y(1)-Y(7))/R4
DR4X4 = (Y(7)-Y(1))/R4
DR4Y1 = (Y(2)-Y(8))/R4
DR4Y4 = (Y(8)-Y(2))/R4

```

```

C
C      DR5/D8
DR5X2 = (Y(3)-Y(7))/R5
DR5X4 = (Y(7)-Y(3))/R5
DR5Y2 = (Y(4)-Y(8))/R5
DR5Y4 = (Y(8)-Y(4))/R5

```

```

C
C      DR6/D8
DR6X3 = (Y(5)-Y(7))/R6
DR6X4 = (Y(7)-Y(5))/R6
DR6Y3 = (Y(6)-Y(8))/R6
DR6Y4 = (Y(8)-Y(6))/R6

```

```

C
C      P EQUATIONS
DERY(1) = Y(9)/XMN
DERY(2) = Y(10)/XMN

```

```

DERY(3) = Y(11)/XMN
DERY(4) = Y(12)/XMN
DERY(5) = Y(13)/XMN
DERY(6) = Y(14)/XMN
DERY(7) = Y(15)/XMN
DERY(8) = Y(16)/XMN

C
C      W EQUATIONS
DERY(9) = -DVR1*DR1X1 - DVR2*DR2X1 - DVR4*DR4X1
DERY(10) = -DVR1*DR1Y1 - DVR2*DR2Y1 - DVR4*DR4Y1
DERY(11) = -DVR1*DR1X2 - DVR3*DR3X2 - DVR5*DR5X2
DERY(12) = -DVR1*DR1Y2 - DVR3*DR3Y2 - DVR5*DR5Y2
DERY(13) = -DVR2*DR2X3 - DVR3*DR3X3 - DVR6*DR6X3
DERY(14) = -DVR2*DR2Y3 - DVR3*DR3Y3 - DVR6*DR6Y3
DERY(15) = -DVR4*DR4X4 - DVR5*DR5X4 - DVR6*DR6X4
DERY(16) = -DVR4*DR4Y4 - DVR5*DR5Y4 - DVR6*DR6Y4

C
RETURN
END

C
C      SUBROUTINE ETOT(Y,EK,EPOT,ET,XL)
      IMPLICIT REAL*8(A-H,O-Z)
      COMMON /AAA/ A,B,C,B,XMN
      REAL*8 Y(16)

      KINETIC ENERGY
      EKN1 = 0.5D0*(Y(9)**2 + Y(10)**2)/XMN
      EKP1 = 0.5D0*(Y(11)**2 + Y(12)**2)/XMN
      EKP2 = 0.5D0*(Y(13)**2 + Y(14)**2)/XMN
      EKN2 = 0.5D0*(Y(15)**2 + Y(16)**2)/XMN

      POTENTIAL ENERGY
      R1 = (Y(1)-Y(3))**2 + (Y(2)-Y(4))**2
      R2 = (Y(1)-Y(5))**2 + (Y(2)-Y(6))**2
      R3 = (Y(3)-Y(5))**2 + (Y(4)-Y(6))**2
      R4 = (Y(7)-Y(1))**2 + (Y(8)-Y(2))**2
      R5 = (Y(7)-Y(3))**2 + (Y(8)-Y(4))**2
      R6 = (Y(7)-Y(5))**2 + (Y(8)-Y(6))**2

      P1 = DSQRT(R1)
      R2 = DSQRT(R2)
      R3 = DSQRT(R3)
      R4 = DSQRT(R4)
      R5 = DSQRT(R5)
      R6 = DSQRT(R6)

      VR1 = -A*BC*DEXP(-B*R1)/R1
      VR2 = -A*BC*DEXP(-B*R2)/R2
      VR3 = -A*BC*DEXP(-B*R3)/R3 + 1.44D0/R3
      VR4 = -A*BC*DEXP(-B*R4)/R4
      VR5 = -A*BC*DEXP(-B*R5)/R5
      VR6 = -A*BC*DEXP(-B*R6)/R6

      TOTAL ENERGY
      EK = EKN1 + EKP1 + EKP2 + EKN2
      EPOT = VR1 + VR2 + VR3 + VR4 + VR5 + VR6
      ET = EK + EPOT

      ANGULAR MOMENTUM

```

```

      XC = Y(1) + Y(3) + Y(5) + Y(7)
      YC = Y(2) + Y(4) + Y(6) + Y(8)
C
C      LZ = λ*FY - Y*PX
      XL1 = (Y(1) - XC)*Y(10) - (Y(2) - YC)*Y(9)
      XL2 = (Y(3) - XC)*Y(12) - (Y(4) - YC)*Y(11)
      XL3 = (Y(5) - XC)*Y(14) - (Y(6) - YC)*Y(13)
      XL4 = (Y(7) - XC)*Y(16) - (Y(8) - YC)*Y(15)
      XL = XL1 + XL2 + XL3 + XL4
C      XL = XL/107.3100
      RETURN
      END

```

APPENDIX M

PROGRAM NEC
(NAME LIST AND CODE LISTING)

APPENDIX M

PROGRAM NEC (NAME LIST AND CODE LISTING)

XNTO - R Value of Turning Point for Proton
XLN - Proton Angular Momentum
XETO - r Value of Outer Turning Point for Electron
XLE - Electron Angular Momentum
XMN - Mass of Proton in MEV
VO - Well Depth Wood-Saxons Potential
RN - Radial Scale Parameter
AN - For Wood-Saxons Potential
Z - Nuclear Charge
XME - Mass of Electron in MEV
S - Coupling Parameter
 S = 0 - No Coupling
 S = 1 - Coupled System
Y(1) - X Cartesian Coordinate of P^+
Y(2) - Y Cartesian Coordinate of P^+
Y(3) - X Momenta of P^+ PXN
Y(4) - Y Momenta of P^+ PYN
Y(5) - X Cartesian Coordinate of e^-
Y(6) - Y Cartesian Coordinate of e^-
Y(7) - X Momenta of e^- PX_e
Y(8) - Y Momenta of e^- PY_e

XK - Nuclear Charge in MEV FM Units
 DPX - e^- - P^+ X Dipole Cartesian Component
 DPY - e^- - P^+ Y Dipole Cartesian Component
 DPNX - P^+ - X Cartesian Coordinate
 DPEX - e^- - X Cartesian Coordinate
 DPT - e^- - Proton - Coupling Term

$$= \frac{1.44}{\sqrt{(Y(1) - Y(5))^2 + (Y(2) - Y(6))^2}} = \frac{1.44}{r_{e^- P^+}}$$

ABSERR Error Parameters for ODE
 RELERR Relative Error
 IFLAG Control Parameter for ODE
 NDIM - Number of Equations
 NPTS - Number of Time Steps to be Propagated
 T - Time Variable
 TSTRP - Integration Time Step Output in Increments of TSTEP
 TOUT - Output Time
 EPOT - Total Potential Energy
 EKG - Total Kinetic Energy
 KET - Total Energy H
 CVEP - Current Value of DPT
 AVEP - Largest Value of DPT
 CORR4 - Subroutine to Fourier Analyze Correlation Functions
 TSP - Subroutine to Subtract Spectra
 POT - Function Subroutine to Compute Potential Energy
 RP - Radius of P^+ from Origin
 RE - Radius of e^- from Origin

- REP - $P^+ - e^-$ Distance
- VE - Coulomb Potential for E^-
- VN - Nuclear Potential Energy
- VEP - Nucleon - Electron - Potential Energy
- FCT - Subroutine Containing Differential Equations to be Solved (Hamilton's equations)

$$\text{DERY}(1) = \frac{DY(1)}{DT} = \frac{\partial H}{\partial P_X} = \dot{X}_N \quad \text{Nucleon equation}$$

$$\text{DERY}(2) = \frac{DY(2)}{DT} = \frac{\partial H}{\partial P_Y} = \dot{Y}_N \quad \text{Nucleon equation}$$

$$\text{DERY}(3) = \frac{DY(3)}{DT} = \frac{-\partial H}{\partial X_N} = \dot{P}_{X_N} \quad \text{Nucleon equation}$$

$$\text{DERY}(4) = \frac{DY(4)}{DT} = \frac{-\partial H}{\partial Y_N} = \dot{P}_{Y_N} \quad \text{Nucleon equation}$$

$$\text{DERY}(5) = \frac{DY(5)}{DT} = \frac{\partial H}{\partial X_e} = \dot{X}_e \quad \text{Electron equation}$$

$$\text{DERY}(6) = \frac{DY(6)}{DT} = \frac{\partial H}{\partial P_{Y_e}} = \dot{P}_{Y_e} \quad \text{Electron equation}$$

$$\text{DERY}(7) = \frac{DY(7)}{DT} = \frac{\partial H}{\partial X_e} = \dot{P}_{X_e} \quad \text{Electron equation}$$

$$\text{DERY}(8) = \frac{DY(8)}{DT} = \frac{\partial H}{\partial Y_e} = \dot{P}_{Y_e} \quad \text{Electron equation}$$

- CORR4 - Subroutine to Fourier Transform Various Dipole Operators
- DP - Array of Dipole Operators
- FFTSC - Sin/Cos Transform Subroutine in IMSL
- WA - Amplitude Function of Sin Transform
- WB - Amplitude Function of Cos Transform

TP - Signal Observation Time

FREQ - Frequency Increment in MEV

Subroutine TSP - Subtracts Various Spectral Components

NEC ELECTRON NUCLEAR COUPLING CODE

```

C      .TYPE NEC
C      IMPLICIT REAL*8(A-H,O-Z)
C      COMMON /AAA/XMN,V0,RN,AN
C      COMMON /BBB/ XME,XK,S
C      DIMENSION WORK(268),IWORK(5)
C      EXTERNAL FCT
C      REAL*8 Y(8),DERY(8)

C      PROGRAM FOR ELECTRON-FRCTION COUPLING
C
C      IN HEAVY NUCLEII
C
C      WRITTEN BY D. W. NCID
C      DECEMBER 1985
C      (JAN 6,1986)
C
C      *****
C      UNITS
C      ENERGY MEV
C      TIME 1/3*10**-23
C      DISTANCE FM 10**-13
C
C      *****
C      INPUT OF DATA
C      Z = 83   XLE = 1/2   RG = 1188
C      Z = 51   XLE = 1/2   RG = 1936
C      Z = 29   XLE = 1/2   RG = 3400
C
C      XNTO = 9.400
C      XLN = 3.000
C      XETO = 1188.000
C      XLE = 0.500
C
C      *****
C      INPUT OF PARAMETERS
C      XMN = 938.000
C      V0 = -50.000
C      RN = 7.400
C      AN = 0.6500
C      Z = 83.000
C      XME = 0.51100
C
C      *****
C      OUTPUT OF RESULTS
C
C      UN COUPLED      COUPLED      OPERATOR
C      IN      OUT      IN      OUT      < OP >/FT<OP>
C      10      11      15      16      XN - XE
C      20      21      25      26      YN - YE
C      30      31      35      36      XN
C      40      41      45      46      XE
C      50      51      55      56      1.44/REP
C      17      18      X,Y TRAJECTORY
C
C      *****
C      NUCLEON PART
C
C      Y(1) = X
C      Y(2) = Y
C      Y(3) = PX
    
```

```

C          Y(4) = PY
C
C      DO 1 IJK=1,2
C          SET S TO 1 FOR E-P COUPLE
C          S = DFLOAT(IJK - 1)
C
C          Y(1) = XMT0
C          Y(2) = 0.000
C          Y(3) = 0.000
C          Y(4) = 197.3100*XLN/Y(1)
C
C          ELECTRON PART
C
C          Y(5) = X
C          Y(6) = Y
C          Y(7) = PX
C          Y(8) = PY
C
C      Z = Z - S
C
C      XK = Z*1.4400
C      Y(5) = XET0
C      Y(6) = 0.000
C      Y(7) = 0.000
C      Y(8) = 197.3100*XLE/Y(5)
C
C
C      FIRST POINT
C      *****P15700
C      INPUT DIPOLE MOMENTS
C
C      DPX = Y(1) - Y(5)
C      I1 = 10 + 5*(IJK-1)
C      WRITE(I1) DPX
C
C      DPY = Y(2) - Y(6)
C      I2 = 20 + 5*(IJK-1)
C      WRITE(I2) DPY
C
C      DPNX = Y(1)
C      I3 = 30 + 5*(IJK-1)
C      WRITE(I3) DPNX
C
C      DPEX = Y(5)
C      I4 = 40 + 5*(IJK-1)
C      WRITE(I4) DPEX
C
C      DPT = 1.4400/DSQRT(DPX**2 + DPY**2)
C      I5 = 50 + 5*(IJK-1)
C      WRITE(I5) DPT
C
C      LOOP
C      *****
C      INPUT OF INT DATA
C
C      ABSERR = 1.00-12
C      RELERR = 0.000
C      IFLAG = 1
C      NDIM = 8
C      NPTS = 8192

```

```

      T = 0.000
      TSTEP= 25.000
      AVEP = 0.000
      IT = 16 + 1JK
C
      DO 7 I=1,NPTS
      TOUT = T + TSTEP
457 CONTINUE
C
      CALL ODE(FCT,NDIM,Y,T,TOUT,RELERR,ABSERR,IFLAG,WORK,IWORK)
C
      WRITE(IT) Y(1),Y(2),Y(5),Y(6)
      IF (T.NE.TOUT) GO TO 457
      EPOT = POT(Y(1),Y(2),Y(5),Y(6))
      EK = 0.500*(Y(3)**2 + Y(4)**2) /XMN
      $    + 0.500*(Y(7)**2 + Y(8)**2)/XME
      ET = EK + EPOT
C
C*****
C      INPUT DIPOLE MOMENTS
C
      DPX = Y(1) - Y(5)
      WRITE(I1) DPX
C
      DPY = Y(2) - Y(6)
      WRITE(I2) DPY
C
      DPNX = Y(1)
      WRITE(I3) DPNX
C
      DPEX = Y(5)
      WRITE(I4) DPEX
C
      DPT = 1.4400/DSQRT(DPX**2 + DPY**2)
      WRITE(I5) DPT
C*****
C
      CVEP = DPT
      IF (CVEP.GT.AVEP) AVEP = CVEP
      IF (10*(I/10).NE.I) GO TO 7
C      WRITE(6,498) Y(1),Y(2),ET,Y(5),Y(6),T
498  FORMAT(' ', 'A', 6D20.10)
      7 CONTINUE
      888 CONTINUE
      999 CONTINUE
      WRITE(6,598) AVEP
598  FORMAT(' ', 'MAX E-P COUPLING =', D20.10)
      1 CONTINUE
C
      DO 46 JK=1,5
      IN = 10*JK
      IOUT = IN + 1
C
      CALL CORR4(TSTEP,NPTS,IN,IOUT)
C
      IN = IN + 5
      IOUT = IOUT + 5
C
      CALL CORR4(TSTEP,NPTS,IN,IOUT)
C

```

```

C 46 CONTINUE
C      CALL TSP(NPTS)
C
C      STOP
C      END
C
C      FUNCTION POT(XN,YN,XE,YE)
C      *****
C      POTENTIAL FUNCTION FOR NUCLEON-ELECTRON MODEL
C      *****
C      IMPLICIT REAL*8(A-H,O-Z)
C      COMMON /AAA/XMN,V0,RN,AN
C      COMMON /BBB/ XME,XK,S
C
C      RP = DSQRT(XN**2 + YN**2)
C      RE = DSQRT(XE**2 + YE**2)
C      REP = DSQRT((XN-XE)**2 + (YN-YE)**2)
C      VE = -XK/RE
C      VN = V0/(1.000 + DEXP((RP-RN)/AN))
C      VEP = -1.4400/REP
C      POT = VN + VE + S*VEP
C
C      RETURN
C      END
C
C      SUBROUTINE FCT(X,Y,DERY)
C      *****
C      HAMILTONIAN EQUATION'S FOR NUCLEON-ELECTRON MODEL
C      *****
C      *****
C      IMPLICIT REAL*8(A-H,O-Z)
C      COMMON /AAA/XMN,V0,RN,AN
C      COMMON /BBB/ XME,XK,S
C      REAL*8 Y(8),DERY(8)
C
C      RP = DSQRT(Y(1)**2 + Y(2)**2)
C      RE = DSQRT(Y(5)**2 + Y(6)**2)
C      REP = DSQRT((Y(1)-Y(5))**2 + (Y(2)-Y(6))**2)
C      FRP = DEXP((RP-RN)/AN)
C      DVRP = -(V0/AN)*FRP/(1.000+FRP)**2
C
C      NUCLEON EQUATIONS
C      DERY(1) = Y(3)/XMN
C      DERY(2) = Y(4)/XMN
C      DERY(3) = -DVRP*Y(1)/RP
C      $ - S*1.4400*(Y(1)-Y(5))/REP**3
C      DERY(4) = -DVRP*Y(2)/RP
C      $ - S*1.4400*(Y(2)-Y(6))/REP**3
C
C      ELECTRON EQUATIONS
C      DERY(5) = Y(7)/XME
C      DERY(6) = Y(8)/XME
C      DERY(7) = -XK*Y(5)/RE**3
C      $ - S*1.4400*(Y(5)-Y(1))/REP**3
C      DERY(8) = -XK*Y(6)/RE**3
C      $ - S*1.4400*(Y(6)-Y(2))/REP**3
C

```

```

      RETURN
      END

C
C
      SUBROUTINE CORR4(TSTEP,N,IN,IOUT)
C*****
C      SPE
C      CTRA GENERATION FROM CORRELATION FUNCTIONS
C*****
      IMPLICIT REAL*8(A-H,O-Z)
      DIMENSION DP(16384)
      COMPLEX*16 CWK(8193)
      DIMENSION IWK(99),WA(8193),WR(8193)
      DATA T0PI/6.283185307179586D0/

C
      REWIND IN

C
      DO 1 I=1,N
      READ (IN) DP(I)
1 CONTINUE

C
      WRITE(5,88)
88 FORMAT(' ',*FREQUENCIES')

C
      CALL FFTSC(DP,N,WA,WB,IWK,WK,CWK)

C
      NN = N/2 + 1

C
      PLOT THE TRANSFORM
      SET THE ZERO FREQUENCY TERM

C
      WA(1) = 0.0D0
      WAM = 0.0D0
      WBM = 0.0D0

C
      CALCULATE FREQUENCY

C
      TP = DFLOAT(N-1)*TSTEP
      FREQ = 1.0D0/TP
      FREQ = FREQ*197.31D0

C
      DO 12 I=1,NN
      FAA= DFLOAT(I-1)*FREQ
      RESCALE FOR POSITIVE WA
      SWA = WA(I)
      WA(I) = DSQRT(SWA**2 + WR(I)**2)/DFLOAT(NN)
      WRITE(IOUT) WA(I),WR(I),FAA
12 CONTINUE

C
      RETURN
      END

C
C
      SUBROUTINE TSP(NPTS)
C
      IMPLICIT REAL*8(A-H,O-Z)

C
      REWIND 16
      REWIND 26
      REWIND 36

```

```

REWIND 46
REWIND 56
REWIND 11
REWIND 21
REWIND 31
REWIND 41
REWIND 51
C
  NN = NPTS/2
C
  DO 1 I=1,NN
    READ(16) XA1,XB1,W1
    READ(26) XA2,XB2,W2
    READ(36) XA3,XB3,W3
    READ(46) XA4,XB4,W4
    READ(56) XA5,XB5,W5
    READ(11) YA1,YB1,F1
    READ(21) YA2,YB2,F2
    READ(31) YA3,YB3,F3
    READ(41) YA4,YB4,F4
    READ(51) YA5,YB5,F5
C
    DA1 = YA1 - XA1
    DA2 = YA2 - XA2
    DA3 = YA3 - XA3
    DA4 = YA4 - XA4
    DA5 = YA5 - XA5
C
    WRITE(6,100) XA1,YA1,XA2,YA2,DA1,W1
100  FORMAT(' ',6D20.10)
    1 CONTINUE
C
    RETURN
  END

```